MITOCHONDRIAL AND SKELETAL LIMB EVOLUTION IN THE NORTH AMERICAN PINE MARTEN, *MARTES*

By

LEIGHA M LYNCH

Bachelor of Science in Geology
Bowling Green State University
Bowling Green, Ohio
2009

Master of Science in Geosciences
East Tennessee State University
Johnson City, Tennessee
2012

Submitted to the Faculty of the
Graduate College of the
Oklahoma State University
in partial fulfillment of
the requirements for
the Degree of
DOCTOR OF PHILOSOPHY
May, 2018

MITOCHONDRIAL AND SKELETAL LIMB

EVOLUTION IN THE NORTH AMERICAN

PINE MARTEN, *MARTES*

Dissertation Approved:

Dr. Anne Weil

Dissertation Adviser

Dr. Haley O'Brien

Dr. Nedra Wilson

Dr. Warren Booth

Dr. Tracy Quan

.

ACKNOWLEDGEMENTS

Thank you to Eric Lynch for your never-ending support and encouragement, which truly made my work possible. Thank you to my parents and sister for never discouraging me from a career in fossils. Thanks to Anne Weil for all your time and investment and for assistance in developing, funding, and writing this research. Thank you to my committee, Haley O'Brien, Warren Booth, Nedra Wilson, and Tracy Quan for assistance in project design and for access to lab equipment and materials. Thanks to John Dudgeon for lab training. Thank you to Merriam Belmaker, Aki Watanabe, Ian Browne, and Holly Ballard for access to digitizers, surface scanners, and photogrammetry. Thanks to Jocelyn Colella for mitochondrial sequences and Kristine Pilgrim at the National Genomics Center for Wildlife and Fish Conservation for tissue samples. Finally, thanks to Steven Wallace, Jon Dunnum, Cody Thompson, Joseph Bopp, Brandi Coyner, Aren Gunderson, Kyndall Hildebrandt, Suzanne Peurach, Sharon Birks, and Jeff Bradley for access to museum specimens, without which this research would not have been possible.

Name: LEIGHA M. LYNCH

Date of Degree: JULY, 2018

Title of Study: MITOCHONDRIAL AND SKELETAL LIMB EVOLUTION IN THE NORTH AMERICAN PINE MARTEN, *MARTES*

Major Field: BIOMEDICAL SCIENCES

Abstract: The vertebrate fossil record is comprised almost entirely of skeletal and dental elements. Skeletal morphology can be influenced by genetic evolution, climate, biome, and behavior. Because of this, paleontologists often use the skeleton to construct phylogenetic relationships, interpret past biomes and climate, and infer behavior. The interaction of genetics, climate, biome, and behavior can be complex and difficult to construct from extinct taxa alone. Many paleontologists, therefore, use extant species as a framework for determining how skeletal morphology evolves in response to these variables. Because many living species are represented in the Pleistocene fossil record, it is also possible to quantifying their morphological evolution through time. This dissertation seeks to understand how skeletal limb morphology evolves in response to climate and biome using North American pine martens, *Martes*, species commonly included in phylogenetic and ecomorphological studies, as a model.

Using linear measurements and morphometric shape data, I found that the skeletal morphology of *M. americana* and *M. caurina* differs among biomes and in correlation with climate. By time calibrating a Bayesian phylogeny constructed from mitochondrial genes from these same specimens, I found that *M. americana* and *M. caurina* likely underwent genetic divergence during the Late Pleistocene while isolated in different habitats by glaciers. This suggests that the morphology of these species evolved as an adaptation to climate and biome. Through phylogenetic comparative methods, I found limb shape did not evolve as an adaptation, but instead likely arose in conjunction with genetic drift in these isolated Pleistocene populations. A similar mode of evolution has occurred in recent history, resulting in *M. americana* having undergone no appendicular morphological evolution despite recent climate change.

These results suggest that the survival of North American *Martes* through past and current climate change may be because they are ecological generalists. Generalists have the advantage when faced with changes in climate and biome that they can shift their geographic range or alternate food sources. This supports the notion that the ecology of a species can influence its phenotypic evolution and should be considered when using extant species to infer the evolutionary history of extinct taxa.

TABLE OF CONTENTS

Chapter Page

I. INTRODUCTION 1

II. SKELETAL LIMB MORPHOLOGY OF NORTH AMERICAN PINE MARTENS, *MARTES AMERICANA* AND *M. CAURINA*, CORRELATES WITH BIOME AND CLIMATE 8

Introduction 8
Taxonomic Nomenclature 11
Institutional Abbreviations 12
Materials and Methods 12
Specimens 12
Allen's Rule 13
Climate 14
Biome 15
Results 17
Allen's Rule 17
Climate 18
Biome 18
Discussion 19
Conclusions 21

III. DETERMINING THE LENGTH OF DNA NECESSARY TO PRODUCE ACCURATE PHYLOGENETIC RELATIONSHIPS IN EXTINCT TAXA 34

Introduction 34
Taxonomic Nomenclature 36
Institutional Abbreviations 36
Materials and Methods 36
Genetic Sequences 36
DNA Extraction, Amplification, and Sequencing 37
Alignment 38
Required Gene Length 39
Required Gene in a Concatenated Sequence 39
Results 40
Genetic Sequences 40

Chapter Page

Required Gene Length 41
Required Gene in a Concatenated Sequence 43
Discussion 43
Conclusions 47

IV. MITOCHONDRIAL PHYLOGENETIC RELATIONSHIPS OF NORTH AMERICAN PINE MARTENS, *MARTES*, CONSTRUCTED FROM MULTIPLE MITOCHONDRIAL GENES SUPPORT PLEISTOCENE DIVERSIFICATION OF *M. AMERICANA* AND *M. CAURINA* 89

Introduction 89
Institutional Abbreviations 91
Materials and Methods 91
Specimens 91
DNA Extractions, Amplification, and Sequencing 91
Sequence Alignment and Nucleotide Substitution Models 93
Maximum Likelihood Phylogeny 94
Bayesian Phylogeny 95
Lineage Diversification 97
Genetic Distances 97
Results 98
Maximum Likelihood Phylogeny 98
Bayesian Phylogeny 98
Lineage Diversification 99
Genetic Distances 99
Discussion 100
Conclusions 104

V. APPENDICULAR SKELETAL MORPHOLOGY OF NORTH AMERICAN PINE MARTENS, M. AMERICANA AND M. CAURINA, IS NOT AN ADAPTATION TO BIOME 113

Introduction 113
Taxonomic Nomenclature 115
Institutional Abbreviations 116
Materials and Methods 116
Specimens 116
Bayesian Phylogeny 117
Skeletal Limb Morphology 117
Phylogenetic Signal 118
Evolutionary Rate 120
Morphological Disparity 120
Results 121
Phylogenetic Signal 121

Evolutionary Rate 122
Morphological Disparity....122
Discussion....123
Conclusions....125

VI. STASIS IN APPENDICULAR SKELETAL MORPHOLOGY OF THE NORTH AMERICAN PINE MARTEN, M. AMERICANA, ACROSS CLIMATE CHANGE IN ALASKA 134

Introduction....134
Institutional Abbreviations....137
Materials and Methods....137
Specimens 137
Morphological Change....138
Morphological Adaptation....140
Results....145
Morphological Change....145
Morphological Adaptation....146
Discussion....147
Conclusions....149

REFERENCES 158

APPENDICES 174
Appendix I. Chapter 2 Supplemental Files....174
Appendix II. Chapter 3 Supplemental Files....226
Appendix III. Chapter 4 Supplemental Files 228
Appendix IV. Chapter 5 Supplemental Files....259
Appendix V. Chapter 6 Supplemental Files 283
Appendix VI. DNA Extraction and Concentration Quantification Protocol .360
Appendix VII. Simplex PCR Amplification of DNA Protocol 368
Appendix VIII. PCR Cleaning and Sanger Sequencing Protocol....374

LIST OF TABLES

Table Page

Chapter 2
Table 1 Results of the PLS regression of limb proportions and climatic variables reported for the first two latent vectors 22
Table 2 Results of the PERMANOVA and Bonferroni α corrected post-hoc test on PC scores 23
Table 3 Results of Procrustes ANOVA/regression between Procrustes aligned landmarks and bone centroid size 23
Table 4 Results of Procrustes ANOVA/regression between Procrustes aligned landmarks and skull length....24

Chapter 3
Table 1 Gene primer sequences and annealing temperatures 48
Table 2 Polymorphic sites in 12S 49-51
Table 3 Polymorphic sites in 16S 52-58
Table 4 Polymorphic sites in Dloop.... 59-65
Table 5 Polymorphic sites in cytochrome b.... 65-76
Table 6 12S best-fit nucleotide substitution model....77
Table 7 16S best-fit nucleotide substitution model....78
Table 8 Dloop best-fit nucleotide substitution model....79
Table 9 Cytochrome b nucleotide substitution model 79
Table 10 Results of SH test for single gene sequences....80
Table 11 Concatenated sequence best-fit nucleotide substitution model 81
Table 12 Results of SH test for concatenated gene sequences 81

Chapter 4
Table 1 Gene primer sequences and annealing temperatures 106
Table 2 Best-fit nucleotide substitution models for each gene 107
Table 3 Phylogenetic priors for model parameters and statistics 107
Table 4 Fossil calibration data 108

Table Page

Chapter 5
Table 1 Phylogenetic signal 127
Table 2 Limb element shape tempo by biome 127
Table 3 Morphological disparity index 127

Chapter 6
Table 1 Gene primer sequences and annealing temperatures 151
Table 2 Best-fit nucleotide substitution models for each gene 152
Table 3 Phylogenetic priors for model parameters and statistics 152
Table 4 Results of PERMANOVA on PC scores 152
Table 5 Phylogenetic signal 153
Table 3 Limb element shape tempo by time bin 153

LIST OF FIGURES

Figure Page

Chapter 2
Figure 1 Geographic distribution of *M. americana* and *M. caurina* 25
Figure 2 Linear length measurements 26
Figure 3 Geometric morphometric landmarks 27
Figure 4 Results of PLS regression 28-29
Figure 5 Principal component analysis plot for first two PC axes 30
Figure 6 Mean shape of the radius and ulna of specimens from each biome 31
Figure 7 Mean shape of femur, tibia, and fibula of specimens from each biome32-33

Chapter 3
Figure 1 Primer design overlap in 12S, 16S, Dloop, and cytb 82-83
Figure 2 Methods used to determine the sequence length necessary 84
Figure 3 Phylogenetic tree topologies from 12S, 16S, Dloop, and cytb that were significantly different from the best-fit topology 85-86
Figure 4 Phylogenetic tree topologies from concatenated sequences 87-88

Chapter 4
Figure 1 Geographic distribution *M. americana* and *M. caurina* 109
Figure 2 Maximum likelihood phylogeny of *M. americana* and *M. caurina* 110
Figure 3 Bayesian phylogeny of *M. americana* and *M. caurina* 111-112
Figure 4 Log lineage through time plot 112

Chapter 5
Figure 1 Geographic distribution of *M. americana* and *M. caurina* 128
Figure 2 Bayesian phylogeny of *M. americana* and *M. caurina* 129
Figure 3 Geometric morphometric landmarks 130
Figure 4 Estimated disparity through time plots 131
Figure 5 Bayesian phylogeny and estimated disparity through time plots 132-133

Chapter 6
Figure 1 Geographic distribution of specimens included in the study 154
Figure 2 Geometric morphometric landmarks 155
Figure 3 Principal component analysis plots for the first two PC axes 156
Figure 4 Bayesian phylogeny of *M. americana* specimens 157

CHAPTER I

INTRODUCTION

The vertebrate fossil record is comprised almost entirely of skeletal and dental elements. Paleontologists, therefore, rely on these elements to reconstruct the complex evolutionary histories of extinct taxa. Skeletal morphology can be influenced by genetic evolution, climate, biome, and behavior. Because of this, researchers often use the skeleton to construct phylogenetic relationships (e.g., Brochu, 2012; King and Wallace, 2014; Wang et al., 1999), interpret past biomes and climate (e.g., Meachen et al., 2015; Meloro et al., 2013; Polly, 2010), and infer behavior (e.g., Meachen-Samuels and Van Valkenburgh, 2009; Samuels and Van Valkenburgh, 2008; Van Valkenburgh, 1987). But the interaction effect of each of these variables can be quite difficult to interpret in the fossil record, making these studies particularly challenging. Extant species provide an excellent framework for determining how skeletal morphology evolves in response to genetics, climate, biome, and behavior because each of these variables can be measured directly. Further, many living species are represented in the Pleistocene fossil record, providing a means of quantifying morphological evolution through time. This dissertation seeks to understand how skeletal limb morphology evolves in response to biome, climate, and genetics using North American pine martens, *Martes*, as a model. This taxon is ideal for such a study because it occupies three biomes and experiences a wide range of climate (Banfield, 1974; Clark et al., 1987, Nowak, 1999), its genetics have been studies across portions of its range

(Dawson et al., 2017; Kyle et al., 2000; Kyle and Strobeck, 2003; Small et al., 2003; Stone et al., 2002a), and it is well represented in the fossil record (Bell, 1995; Eshelman and Grady, 1986; Grady, 1984; Guilday and Hamilton, 1978; Long, 1971; Mead and Mead, 1989; Sinclair, 1907; Tankersley, 1997; Wetmore, 1962).

North American pine martens, *Martes*, are within the order Carnivora and the family Mustelidae and are most closely related to the Japanese marten, *Martes melampus*, and the beech marten, *M. foina* (Sato et al., 2012). Although initially separated into two species, *M. americana* and *M. caurina*, based on skeletal characters (Merriam, 1890), this classification was not adopted due to the high degree of morphological variation seen across their geographic range. This variation resulted in the recognition of eight subspecies (Clark et al., 1987). Researchers studying the mitochondrial DNA of *Martes* found two distinct genetic clades, which were designated as the *M. americana americana* and *M. americana caurina* groups (Stone et al., 2002a). Recent nuclear DNA (Dawson and Cook, 2012) and parasitological evidence (Hoberg et al., 2012), however, has resulted in the elevation of the taxonomic status of these groups, and North American *Martes* are now recognized as two species, *M. americana* and *M. caurina.*

Pleistocene glacial cycles are thought to have played a primary role in the speciation of North American martens. The common ancestor of both species is hypothesized to have entered North America via the Bering land bridge during the early Pleistocene and then spread across North America throughout the many glacial interglacial periods of this time (Stone and Cook, 2002; Stone et al., 2002a). The North American marten fossil record is comprised of three distinct morphotypes of martens during the Late Pleistocene. Two of these morphotypes have been assigned to either *M. americana* or *M. caurina*. The third morphotype, which is now extinct, remains contended and has been assigned as a unique species, *M. nobilis*, a subspecies of *M. americana*, or synonymous with *M. caurina* (Anderson, 1994; Hughes, 2009; Meyers, 2007; Youngman and Schueler, 1991). The fossil record indicates that martens were present in isolated

regions of the Appalachian and Rocky Mountains during the Late Pleistocene, coinciding with the Wisconsinan glaciation. This isolation is hypothesized to have resulted in the genetic divergence of *M. americana* and *M. caurina* (Brace et al., 2012; Stone and Cook, 2002; Stone et al., 2002a), and culminating in the morphological variation seen among living populations of these two species.

Today, *M. americana* and *M. caurina* are distributed across northern portions of North America in three different biomes, where they exhibit a wide range of behaviors. *M. americana* is distributed across Canada, Alaska, New England, and the Great Lakes region, while *M. caurina* is restricted to the western U.S. and Canada as well as some Alaskan islands (Banfield, 1974; Clark et al., 1987; Nowak, 1999). Within this distribution, *M. americana* occupies both temperate broadleaf deciduous forest and boreal forest biomes (Banfield, 1974; Clark et al., 1987; Nowak, 1999). *M. caurina* is found only in coniferous forest biomes (Banfield, 1974; Clark et al., 1987; Nowak, 1999). Within each biome, these species prefer habitats with 70% canopy cover (Clark et al., 1987), although researchers have found they will occupy meadows, riparian regions, and recently disturbed forests (Banfield, 1974; Spencer et al., 1983; Steventon and Major, 1982). These species also experience a wide variety of climates with temperatures ranging from -35.8° C to 29.4° C between seasons and by geographic region and annual precipitation between 19.6 cm and 200.8 cm depending on the region (U.S. Department of Commerce National Oceanic and Atmospheric Administration). These species exhibit a diverse range of locomotor and hunting behaviors. *M. americana* and *M. caurina* are both capable of climbing, swimming, running, and digging (Banfield, 1974; Clark et al., 1987; Nowak, 1999). They also have a broad diet, which includes voles, rabbits, squirrels, amphibians, birds, insects, and fruit (Zhou et al., 2011; Zielinski and Duncan, 2004). These species are particularly well suited for navigating and hunting within the tunnels of the subnivium (Nowak, 1999). Such variation in biome, climate, and behavior could have contributed to the morphology of extant populations.

Living populations have been subject to many anthropogenic influences as well. Recent anthropogenically-induced changes in climate, particularly across northern latitudes, have resulted in increased annual temperatures (Serreze et al., 2000) and non-snow precipitation (Knowles et al., 2006), as well as longer growing seasons (Myneni et al., 1997; Smith et al., 2004; Stone et al., 2002b). The combination of these factors have resulted in shifts in biomes (Euskirchen et al., 2009; Klein et al., 2005; Lloyd and Fastie, 2002; Myneni et al., 1997). The fur trade also effected marten populations, peaking in the 1940's with nearly 180,000 martens trapped yearly (Banfield, 1974). While these numbers have declined, they still remain a primary fur species and continue to be trapped (Wiebe et al., 2013). Selective pressures placed by these anthropogenic factors may also be influencing the morphology of *M. americana* and *M. caurina.*

Overall, this project seeks to determine how the skeletal limb morphology of *M. americana* and *M. caurina* evolved by answering the following questions:

1. Does the skeletal limb morphology of *M. americana* and *M. caurina* differ between biomes and does it correlate with climate?

   Using 3D geometric morphometric (GM) landmark data collected from six skeletal limb elements of contemporaneous *M. americana* and *M. caurina*, I sought to determine whether limb bone shape differed between specimens collected from different biomes. I also collected limb proportion data from the same specimens and tested for a correlation between limb length and climate. I compared forelimb and hindlimb proportions to mean, minimum, and maximum annual temperatures, as well as annual non-snow precipitation and annual snowfall.

2. How long of a DNA sequence is necessary to produce accurate phylogenetic relationships?

DNA degrades over time and at differing rates depending on tissue type and preservation (Allentoft, 2012; Campos, 2012). This can make it challenging to amplify and sequence entire genes. Because many of the specimens used in this study were historic, collected after 2000, and were bone tissue, I sought to determine how long of a gene sequence would be necessary to produce accurate phylogenetic relationships among specimens. I tested this on four mitochondrial genes commonly used in phylogenetic studies: 12S, 16S, cytochrome b (cytb), and Dloop. I subsampled complete sequences of each gene and tested the resulting tree topologies against a complete gene topology using an SH test. Those gene lengths whose topologies significantly differed from the complete gene were interpreted as insufficient in length to produce accurate phylogenetic relationships.

3. What are the phylogenetic relationships of extant *M. americana* and *M. caurina* and when did these species diverge?

Applying the results of the previous analysis, I constructed a maximum likelihood and a Bayesian phylogeny from a concatenated sequence of the 12S, 16S, cytb and Dloop mitochondrial genes from *M. americana* and *M. caurina.* The Bayesian phylogeny was node calibrated using the fossil record of *M. americana* and *M. caurina.* This allowed me to estimate when these species diverged and whether lineage diversification coincided with Pleistocene glaciation, as has been previously hypothesized (Stone and Cook, 2002; Stone et al., 2002a).

4. Was the skeletal limb morphology of *M. americana* and *M. caurina* influenced by genetic diversification or biome during the Pleistocene?

Using the constructed Bayesian phylogeny as a framework, I tested whether skeletal limb morphology of *M. americana* and *M. caurina* evolved in response to biome or genetic divergence during the Pleistocene. I collected GM landmark data from the limb elements of the same specimens included in the phylogeny. I then tested whether the landmark data and centroid size reflected underlying phylogenetic relationships using K_{mult} (Adams, 2014a), Blomberg's K (Blomberg et al., 2003), and Pagel's λ (Pagel, 1999). I also tested whether limb bone shape evolved at different rates between biomes (Adams, 2014b). Finally, to determine whether the potential disparity of these species changed through time in correlation with genetic divergence or Pleistocene glacial cycles, and thus novel biomes, I calculated disparity through time (Harmon et al., 2003).

5. Is *M. americana* undergoing changes in skeletal limb morphology in response to Alaska's recent climate change?

Recent anthropogenically induced climate change has resulted in extreme changes in Alaska's biomes and climate (Dye, 2002; Euskirchen et al., 2009; Klein et al., 2005; Myneni et al., 1997; Serreze et al., 2000; Stone et al., 2002b). I sought to determine whether the limb morphology of Alaskan *M. americana* has evolved in response to these changes. I first tested whether the limb morphology, quantified using 3D GM landmark data, of specimens collected before and after 1970 differed. I then created a Bayesian phylogeny of the 12S, cytb, and Dloop mitochondrial genes sequenced from the same specimens whose morphologies were measured. This phylogeny provided a framework to test for underlying phylogenetic signal and evolutionary rates in limb morphology. I tested whether limb morphology reflected underlying phylogenetic relationships using K_{mult} (Adams, 2014a), Blomberg's K (Blomberg et al., 2003), and Pagel's λ (Pagel, 1999). I then compared rates of morphological evolution between specimens collected

before and after 1970 to determine whether climate change influenced rates of evolution (Adams, 2014b).

This study is unique in that it compares the morphology, genetics, climate, and biome of the exact same specimens. This allows for a level of precision that can be lacking in other studies focusing on phenotypic evolution (e.g., Law et al., 2018; Rüber and Adams, 2001; Slater et al., 2010). In addition, this research will provide the first phylogeny of *M. americana* and *M. caurina* that includes specimens from the eastern U.S. and from this phylogeny the first estimate of genetic divergence between the two species. This study will also expand our understanding of how the morphology of North American *Martes* evolved, which can be compared and applied to other extant and extinct species.

CHAPTER II

SKELETAL LIMB MORPHOLOGY OF NORTH AMERICAN PINE MARTENS, *MARTES AMERICANA* AND *M. CAURINA*, CORRELATES WITH BIOME AND CLIMATE

Introduction

Animals respond to variation in habitat and climate through changes in behavior and phenotype. Skeletal limb proportions and morphology have been shown to correlate with biome, habitat, and climatic variables (Klein et al., 1987; Lindsay, 1987; Meloro et al., 2013; Polly, 2010; Schellhorn and Sanmugaraja, 2014; Weaver and Ingram, 1969). Many of these relationships were measured in mammals that do not have an elongated body. Mustelids, however, have proportionally shortened limbs and elongated bodies compared to many other mammals. Does the skeletal morphology of mustelids respond to variation in climate and biome in the same predictable ways as other mammals? I addressed this question in the North American pine marten, *Martes,* which has a wide geographic distribution across North America and inhabits a variety of climates and biomes. Using linear and morphometric data, I sought to determine whether the limb proportions and limb bone shapes of *M. americana* and *M. caurina* correlated with their respective climates and biomes.

Body size and limb proportions have been shown to correlate with temperature as a result of epigenetic effects on bone growth early in postnatal development (Serrat, 2013). These relationships have been summarized in climatic rules such as Bergmann's and Allen's Rules.

Bergmann's Rule states that animals living in a colder environment will be larger than that same species found in a warmer environment (Bergmann, 1847). Allen's Rule states that animals living in colder environments will have proportionally shorter appendages than in warmer regions (Allen, 1877). These rules are based on the understanding that animals with a high surface area to volume ratio will lose heat and thus energy more rapidly and, therefore, have a higher metabolism (Bergmann, 1847; Mayr, 1956; McNab, 1980; Tilkens et al., 2007). In colder climates, the resources needed to maintain a high metabolism might not be present year-round. It is, therefore, advantageous to be larger, with a lower surface area to volume ratio, and thus a lower metabolism to counter this shortage of resources. Bergmann's Rule holds true in several mammals including *Lepus americanus, Vulpes vulpes, Canis lupus, Lynx rufus, Puma concolor,* and several species of murid rodents (e.g., Baker et al., 1978; McNab, 1971; Meiri and Dayan, 2003; Meiri et al., 2004; Nagorsen, 1985). Allen's Rule has been tested and confirmed in mammals including *Sus scrofa domesticus, Rangifer tarandus,* and *Tamiasciurus hudsonicus* (Klein et al., 1987; Lindsay, 1987; Weaver and Ingram, 1969). Limb proportions and shape can also differ among taxa as a result of selective pressures imposed on non-physiological traits.

Skeletal limb shape may differ among taxa as a result of differing selective pressures imposed by climate and biome. These variables are not mutually exclusive as temperature and precipitation influence vegetation type and density, which are used for biome classification (Smith and Smith, 2001). Within each biome, species often adopt differing locomotor behaviors. For example, animals living in more openly vegetated biomes tend to exhibit cursorial modes of locomotion while those living in dense forests are more often arboreal. An animal's posture, body mass, and gait can influence bone curvature, robusticity, and epiphyseal size (Biewener, 1983; 2005; Lieberman et al., 2003). There is often, then, a correlation between limb morphology and biome. Felids, for example, have proportionally shorter humeral heads and more gracile radius and ulna (Meloro et al., 2013; Schellhorn and Sanmugaraja, 2014) in habitats with denser vegetation.

Calcaneal morphology of several carnivoran species also correlates with vegetation density (Polly, 2010).

Mustelids have a wide geographic distribution and inhabit a variety of climates and, therefore, biomes (Nowak, 1999). Mustelids also have an elongated bauplan (body plan), which creates a greater surface area to volume ratio than other mammals of equal mass and thus a higher metabolism (Brown and Lasiewski, 1972). Despite the expectation that they would follow ecogeographic rules, researchers have shown that most mustelid species do not follow Bergmann's Rule (Lynch, 2016; McNab, 1971; Meiri and Dayan, 2003; Meiri et al., 2004) and that, instead, body size often correlates with local prey size (McNab, 1971). Allen's Rule, however, remains to be tested in most mustelid species. In their respective biomes, mustelids exhibit a diverse range of behaviors and predation strategies. Considering the relationship between morphology, climate, and biome seen in other mammals, it may be expected that the skeletal morphology of mustelids would also correlate with climate and biome.

M. americana and *M. caurina* are two species in which a correlation between limb morphology and climate may be expected. Across their North American range, *M. americana* occupies two biomes: temperate broadleaf and mixed forest (Broadleaf) in the northeastern US and Canada; and boreal forest and taiga (Boreal) in central Alaska (Figure 1) (Banfield, 1974; Clark et al., 1987; Nowak, 1999). *M caurina* is restricted to a single biome, temperate coniferous forest (Coniferous) in central and northern Pacific US and Canada (Figure 1) (Banfield, 1974; Clark et al., 1987; Nowak, 1999). Each of these biomes differ greatly in dominant species, both plant and animal, annual precipitation, and temperature (Smith and Smith, 2001). In addition, each forest has undergone anthropogenic changes in association with industry and fire management (Martin et al., 2012). Although they prefer dense forested habitats with 70% canopy cover (Clark et al., 1987), these species have also begun to occupy meadows, riparian regions (Banfield, 1974; Spencer et al., 1983), and recently disturbed forests (Steventon and Major, 1982). This variety of

habitats, then, requires an equally diverse range of locomotor behaviors such as climbing, swimming, half-bound gait, pouncing, and digging (Banfield, 1974; Harris and Steudel, 1997). In addition, *M. americana* and *M. caurina* have a higher rate of heat loss than other mammals of similar mass (Worthen and Kilgore, 1981). This suggests that they may not adapt to extremes in temperature the same way as other mammals. All of these factors suggest that habitat influences the behaviors of North American martens and that this may be reflected in the skeleton.

This study focuses on the interspecific skeletal limb morphology of *M. americana* and *M. caurina* across their U.S. geographic range, testing three hypotheses: 1) limb proportions differ between individuals living in colder and warmer climates; 2) limb proportions correlate with climatic variables; and 3) skeletal limb bone shape differs among specimens from the three biomes occupied by these species. If *Martes* follows Allen's Rule, then limb proportions of individuals living in colder climates will be proportionally shorter and limb proportions will correlate with temperature. I tested these hypotheses by collecting linear measurements and 3D geometric morphometric landmark data of the skull, humerus, radius, ulna, femur, tibia, and fibula of 86 specimens of *M. americana* and *M. caurina* from across their U.S. range.

Taxonomic Nomenclature

North American pine martens, *M. americana* and *M. caurina*, were recently proposed as unique species based on mitochondrial, nuclear, morphological, and parasitic evidence (Dawson et al., 2017; Dawson and Cook, 2012; Hoberg et al., 2012; Merriam, 1890), but have not yet been recognized by the International Commission on Zoological Nomenclature. I have adopted these specific titles to retain consistency with recent literature.

Institutional Abbreviations

East Tennessee State Museum of Natural History (ETMNH), Sam Noble Oklahoma Museum of Natural History (SNOMNH), New York State Museum (NYSM), Florida Museum of Natural History (FLMNH), Museum of Southwestern Biology (MSB), Burke Museum of Natural History and Culture (BMUW), University of Alaska Museum of the North (UAMN), Smithsonian Institution National Museum of Natural History (USNM), and University of Michigan Museum of Zoology (UMMZ).

Materials and Methods

Specimens

I measured skeletal elements from a total of 70 individuals, some of which were incomplete, identified as *M. americana* and *M. caurina* including: 62 skulls, 70 femora, 38 fibulae, 67 humeri, 61 radii, 68 tibiae, and 38 ulnae (Appendix I, Section A). This dataset comprised 56 specimens of *M. americana* and 14 specimens of *M. caurina.* Specimens were collected across the U.S. range of these species between 1940 and 2013. Specimens were not included from Canada due to a limited availability of postcranial elements within museum collections. I identified all specimens as adults based on full epiphyseal fusion, and both sexes were included in this study. Sexes were determined through museum identification and the presence of a baculum. The measured specimens are housed in the collections at ETMNH, SNOMNH, NYSM, FLMNH, MSB, BMUW, UAMN, USNM, and UMMZ.

Allen's Rule

To test for Allen's Rule, I measured the length of 62 skulls, 53 humeri and radii, and 60 femora and tibiae (Figure 2) from 62 individuals. This dataset comprised 51 specimens of *M. americana* and 11 specimens of *M. caurina.* Skull length acted as a proxy for body mass (Van Valkenburgh, 1990). I collected minimum temperature data for the county and year each specimen was collected from the U.S. Department of Commerce National Oceanic and Atmospheric Administration using the National Center for Environmental Information database.

I calculated forelimb length as the combined length of the humerus and radius and hindlimb length as the combined length of the femur and tibia (Samuels et al., 2013). I conducted all statistical analyses in R (R Core Team, 2015). Prior to testing for Allen's Rule, I tested for normality in both the forelimb and hindlimb datasets using a Shapiro-Wilk's test and for equal variance between the two temperature bins using a Bartlett test for homogeneity. The hindlimb dataset did not have a normal distribution; however, due to the large sample size and near equal group sizes it is robust to this violation in a parametric t-test (Edgell and Noon, 1984; Havlicek and Peterson, 1976).

Because this dataset consists of proportions it is inappropriate to test for a relationship between minimum temperature and limb proportions using a linear correlation as proportion data violates the assumptions of this analysis and can return incorrectly high correlation coefficients (Kuh and Meyer, 1955; Tu et al., 2004; Yule, 1910). I therefore determined whether North American martens follow Allen's Rule by testing whether limb proportions differed between specimens assigned to two minimum temperature bins using a two-tailed, two-sample t-test. I assigned each specimen to one of two minimum temperature bins, $\leq$ -21˚C and > -21˚C, based on the minimum temperature data collected for each individual. I chose -21˚C as the threshold for binning because

it is the mean minimum temperature associated with all specimens. This resulted in 34 specimens in the ≤ -21˚C bin and 28 in the > -21˚C bin.

Climate

To determine whether limb proportions correlate with climate, I measured the length of 57 skulls, 50 humeri and radii, and 56 femora and tibiae (Figure 2) from 57 individuals. This analysis included 46 specimens of *M. americana* and 11 specimens of *M. caurina.* These specimen numbers differ from those measured in the Allen's Rule test due to a lack of available climate data for some specimens. I calculated limb to skull length proportions using the same length measurements and ratios used in the Allen's Rule test. I collected climate data from the U.S. Department of Commerce National Oceanic and Atmospheric Administration using the National Center for Environmental Information database. I collected the minimum, maximum, and mean annual temperatures, as well as the annual non-snow precipitation and annual snowfall for the county and year each specimen was collected.

I tested for a correlation between forelimb and hindlimb proportions and climate using a partial least squares (PLS) regression. This analysis is ideal for datasets in which there is covariance in the dependent variable, as seen here in the limb proportions (Abdi, 2010). A PLS regression produces a series of latent vectors which best explain the correlation between the dependent and independent variables. The results of this analysis area correlation coefficient for each latent vector, the percent of variance explained in both the independent and dependent variables by each vector, and a vector coefficient. This coefficient indicates which of the independent variables has the greatest weight in each vector and, therefore, which have the greatest influence on the variation seen in the dependent variable.

Biome

I collected 3D shape data from the humerus, radius, ulna, tibia, and fibula of 39 specimens collected between 2000 and 2013. I chose specimens collected within a limited timeframe to avoid the confounding effect of accumulated shape variation that could develop over longer time periods. This dataset included 27 specimens of *M. americana* and 12 of *M. caurina.* I assigned each specimen to one of three biomes based on the geographic location from which it was collected: 1) Temperate broadleaf and mixed forest (Broadleaf); 2) Temperate coniferous forest (Coniferous); and 3) Boreal forest and taiga (Boreal) (Olson et al., 2001).

I collected 3D geometric morphometric landmark data from each bone using a MicroScribe G2LX digitizer. This digitizer records the X, Y, and Z coordinates of a single point/landmark in space. All measured landmarks were homologous among specimens. I chose landmarks that would best capture the length and width of each element because size has been shown to change in mammals over time (e.g., Fabre et al., 2013b; Kolska Horwitz and Ducos, 1997; Meachen et al., 2014; Meachen and Samuels, 2012). I also chose landmarks that represented morphological characters frequently used in phylogenetic studies of carnivorans (Leach, 1977; Morlo and Peigné, 2010; Zrzavý and Řičánková, 2004) as these should reflect an underlying phylogenetic signal (Figure 3). I also chose landmarks previously used in ecomorphological studies (Fabre et al., 2013a; Fabre et al., 2015; Fabre et al., 2013b) to reflect locomotor variation. Where possible, I avoided landmarks associated with muscle attachments as these are highly plastic and are modified throughout an individual's life (Currey, 2002; Wei and Messner, 1996) (Appendix 1, Section B).

In addition, I tested landmarks for accuracy and repeatability. I collected all landmarks ten times on three different specimens, ETMNH 600, ETMNH 603, and ETMNH 607. I aligned landmarks using a generalized Procrustes analysis (GPA) and plotted these using a principal component

analysis (PCA). I then visually checked for greater interspecimen morphospace occupation within the first two principal components than intraspecimen. I then systematically removed one landmark from the dataset and reran the PCA for each iteration. If intraspecimen variation decreased but interspecimen variation remained the same, I interpreted the removed landmark to be inconsistent and removed it from the final dataset. Those landmarks included in this study were interpreted, therefore, as accurate and reproducible. I repeated this test for each limb element and all tests were conducted using the geomorph package (Adams and Otarola-Castillo, 2013) in R (R Core Team, 2015).

I tested for difference in limb shape in each limb element independently. First, I aligned landmarks using a GPA. I then calculated principal component (PC) scores from the aligned landmarks using a PCA. I ran these analyses using the geomorph package (Adams and Otarola-Castillo, 2013) in R (R Core Team, 2015) (Appendix I, Section E). I then tested for morphological differences between biomes using the highest ranking PC scores, those explaining 95% of the morphological variance (Zelditch et al., 2012). PC scores are commonly used in morphometric analyses as a proxy for shape and a means of reducing the number of variables in a statistical analysis (Carden et al., 2012; Fabre et al., 2013a; Meachen et al., 2016; Rychlik et al., 2006). I tested for statistical differences in these scores among specimens collected from each of the three biomes using a PERMANOVA (α=0.05, permutation 9,999) (Polly, 2008; Rychlik et al., 2006).This non-parametric analysis is robust to violations of multivariate normality and allows for more variables than specimens per group (Anderson, 2001), which occur in several of the datasets. In those elements with significant differences ($p \leq 0.05$) between biomes, I tested which biome bins were different from one another using a Bonferroni post-hoc test with corrected alpha values ($\alpha/6$). Both the PERMANOVA and Bonferroni post hoc analyses were conducted in PAST3 (Hammer et al., 2001). I qualitatively evaluated which regions of the elements differed between specimens collected from the three biomes using both thin plate splines and 3D surface

models. First, I generated the mean shape of specimens from each biome. I then compared these mean shapes using thin-plate spline visualizations of both X, Y and Y, Z dimensions. Then, to visualize variation in shape in three dimensions, I created 3D surface models of each element using either a NextEngine HD 3D laser surface scanner or photogrammetry. I created surface models of each element for a single specimen, ETMNH 609, whose morphology was the closest to the mean shape of all of the measured specimens. I then warped each element's surface into the mean shape of specimens from each biome. I also used these element surfaces to generate shape along PC axes.

Bone size can have a tremendous effect on bone morphology (Bertram and Biewener, 1990; 1992). Outomuro and Johansson (2017) found 88% of morphometric studies published in 2015 could attribute morphological variation to allometry. Because *M. americana* and *M. caurina* exhibit sexual size dimorphism (Banfield, 1974; Clark et al., 1987; Nowak, 1999), I tested whether the morphological variation seen between biomes was a result of bone size using a Procrustes ANOVA/regression (Adams and Nistri, 2010; Bookstein, 1991; Drake and Klingenberg, 2008; Mitteroecker et al., 2004) between Procrustes aligned landmarks and bone centroid size. I also tested whether there was an allometric effect on bone shape using a Procrustes ANOVA/regression between Procrustes aligned landmarks and skull length, a proxy for body mass (Van Valkenburgh, 1990).

Results

Allen's Rule

A significant difference was present in the proportional length of the forelimb (p=0.003, δ=0.08, 1-β=0.88) and hindlimb (p=0.012, δ=0.11, 1-β=0.73) between specimens from the two temperature bins. Specimens in colder environments, however, have proportionally longer limbs than those in warm environments (Figure 4B and C). This is the inverse relationship to that proposed by Allen's Rule.

Climate

I found a moderate correlation between forelimb and hindlimb to body size proportions and climate (Table 1). The correlation coefficient of the first latent vector was 0.43. The first latent vector explained 61.9% of the variance in climate and 17.8% of limb proportion variation. The vector coefficients indicated minimum and mean annual temperature as well as annual non-snow precipitation were the variables of greatest importance within the first vector (Figure 4A). There was a negative correlation between temperature and limb proportions for both the forelimb and hindlimb, with individuals living in colder regions having proportionally longer limbs (Figure 4B and C). There was also a negative correlation between annual non-snow precipitation and limb proportions such that individuals living in regions with higher annual rainfall had proportionally shorter limbs. (Figure 4D). Annual maximum temperature and snowfall were of little importance in the first vector (Table 1).

Biome

The number of PC scores composing 95% of the variance differs by bone: 18 humeral, 14 radial, 16 ulnar, 18 femoral, 15 tibial and 11 fibular (Appendix 1, Section C). The results of the PERMANOVA and Bonferroni alpha-corrected post-hoc test indicate a significant difference in

morphology between specimens from Coniferous and Broadleaf forests in all the measured bones, except the humerus ($p<0.05$) (Table 2). In addition, significant morphological differences are found in the ulna, femur, tibia, and fibula between specimens from Boreal and Coniferous forests ($p<0.01$). Specimens from Coniferous forests consistently have the most robust bones, particularly in the forelimb, while specimens from Broadleaf forests are the most gracile (Figures 5, 6, and 7; Appendix I, Section D). The radius of specimens from Coniferous forests have a longer distal epiphysis between the ulnar notch and styloid process, and the ulna has the largest, tallest, and widest olecranon process proportionally of the three groups (Figures 5 and 6). The femur of specimens from Coniferous forests has a slightly longer anatomical neck and slight anterior curvature in the distal shaft compared to those from both Broadleaf and Boreal forests (Figures 5 and 7). The tibia of specimens from Coniferous forests has a wider lateral condyle, a more proximal fibular notch, and greater lateral curvature in the distal shaft (Figures 5 and 7). Finally, the fibula of specimens from Coniferous forests has a very robust, boxy head compared to those from the other two biomes (Figures 5 and 7).

There is a correlation between centroid size and shape in the femur, with approximately 9% of the variation explained by bone size (Table 3). There is also a correlation between bone shape and skull length in the femur and fibula, with between 6-9% of shape variation attributable to body size (Table 4). This indicates that limb shape is independent of the size differences exhibited between sexes and among specimens from different biomes.

Discussion

The limb proportions of North American *Martes* do moderately correlate with climate, particularly with minimum and mean annual temperature and annual non-snow precipitation.

Individuals living in regions with warmer annual minimum and mean temperatures, as well as higher annual non-snow precipitation have proportionally shorter limbs (Figure 4). *Martes*, then, exhibit the inverse relationship of that proposed by Allen's Rule. This suggests that the metabolism of these species is not being influenced by temperature. Instead, climate may be influencing other aspects of behavior that are reflected through limb proportions. Regions with higher annual rainfall tend to have denser vegetation, often in the form of complex forests (Smith and Smith, 2001). Of the forest biomes considered here, Broadleaf forests have the warmest temperatures and greatest annual rainfall and also exhibit the greatest degree of understory complexity (Smith and Smith, 2001). Many mammals species that live in closed forest biomes have proportionally shorter appendages as a result of locomotor and predation strategies (Polly, 2010; Samuels et al., 2013; Samuels and Van Valkenburgh, 2008; Van Valkenburgh, 1985). Researchers have found that *M. americana* and *M. caurina* will exhibit different behaviors among forest patches of varying complexity within a single biome (Andruskiw et al., 2008; Fuller et al., 2005; Moriarty et al., 2015; Steventon and Major, 1982). It is, therefore, possible that the limb proportion variation seen here in *M. americana* and *M. caurina* correlate with climate as a result of differing modes of locomotion within each biome.

Limb robusticity and epiphyseal size were the greatest differences between specimens from each biome, particularly between Broadleaf and Coniferous forests (Figures 6 and 7). Previous studies have shown that increases in limb robusticity correlate with an increase in body mass, (Martin-Serra et al., 2014; Martín-Serra et al., 2014); however, there is no allometric relationship between forelimb bone shape and body mass in the specimens used in this study. These traits in the forelimbs of other mustelid species have been shown to correlate with degrees of arboreality, with more arboreal species having gracile bones while more fossorial species have robust (Fabre et al., 2015; Iwaniuk et al., 1999; Samuels et al., 2013). In North American *Martes*, the most robust bones and largest epiphyses were in specimens from Coniferous forests. This

biome has been reduced in forest complexity and undergrowth density as a preventative measure against forest fires (Stephens et al., 2013; Stephens et al., 2012). This suggests that individuals living in Coniferous forests may be exhibiting fewer arboreal behaviors in response to decreased vegetation density, resulting in more robust limb morphologies. As with limb proportions, limb shape appears to be reflecting differences in behavior in association with vegetation density.

Conclusions

Limb morphology of North American pine martens differs in correlation with both climate and biome. Despite their elongated bauplan and high surface area to volume ratio, North American pine martens do not follow Allen's Rule. Instead, vegetation density, which varies in response to temperature and non-snow precipitation, may be driving the locomotor behaviors of these species. This, in turn, results in differing skeletal limb morphologies among biomes. The morphological variation seen among specimens from each of the forest biomes also correlates with the distribution of *M. americana* and *M. caurina.* This suggests that biome may have acted as a selective pressure on limb shape, resulting in the genetic speciation and morphological differentiation of these two species. Future research on the mode of evolution in these species may shed light on how morphology has been influenced by climate through time. The skeletal limb morphology of *M. americana* and *M. caurina* appears to reflect similar ecomorphological signals as other carnivorans. If this pattern holds true in other mustelid species with wide geographic distributions, it is possible that mustelids may be good predictors of climate and biome in paleoenvironmental studies.

Tables

Table 1. Results of PLS regression of limb proportions and climatic variables reported for the first two latent vectors. Climate values within each vector represent with importance of each variable to the vector.

Variable	Vector 1	Vector 2
Mean temperature	1.16	1.09
Maximum temperature	0.15	0.70
Minimum temperature	1.33	1.25
Non-snow precipitation	1.19	1.14
Snow	0.66	0.69
Correlation coefficient	0.43	0.22
% variation in X	0.62	0.17
% variation in Y	0.18	0.03

Table 2. Results of the PERMANOVA and Bonferroni α corrected post-hoc test on PC scores

Element	**Biome**	**Biome**	***p***
Humerus	Broadleaf	Coniferous	0.07
		Boreal	0.66
	Boreal	Coniferous	0.11
Radius	Broadleaf	Coniferous	*<0.01*
		Boreal	1
	Boreal	Coniferous	0.08
Ulna	Broadleaf	Coniferous	*<0.01*
		Boreal	0.07
	Boreal	Coniferous	*<0.01*
Femur	Broadleaf	Coniferous	*<0.01*
		Boreal	0.32
	Boreal	Coniferous	*<0.01*
Tibia	Broadleaf	Coniferous	*<0.01*
		Boreal	1
	Boreal	Coniferous	*0.02*
Fibula	Broadleaf	Coniferous	*<0.01*
		Boreal	0.45
	Boreal	Coniferous	*<0.01*

Table 3. Results of Procrustes ANOVA/regression between Procrustes aligned landmarks and bone centroid size

Element	**r^2**	**F**	***p***
Humerus	0.04	0.96	0.12
Radius	0.02	1.18	0.52
Ulna	0.03	0.89	0.28
Femur	0.06	2.24	*<0.01*
Tibia	0.03	1.44	0.19
Fibula	0.02	1.05	0.36

Table 4. Results of Procrustes ANOVA/regression between Procrustes aligned landmarks and skull length

Element	**r^2**	**F**	***p***
Humerus	0.02	1.63	0.38
Radius	0.03	0.87	0.22
Ulna	0.02	1.15	0.54
Femur	0.06	2.73	*<0.01*
Tibia	0.04	1.30	0.13
Fibula	0.06	2.07	*0.02*

Figures

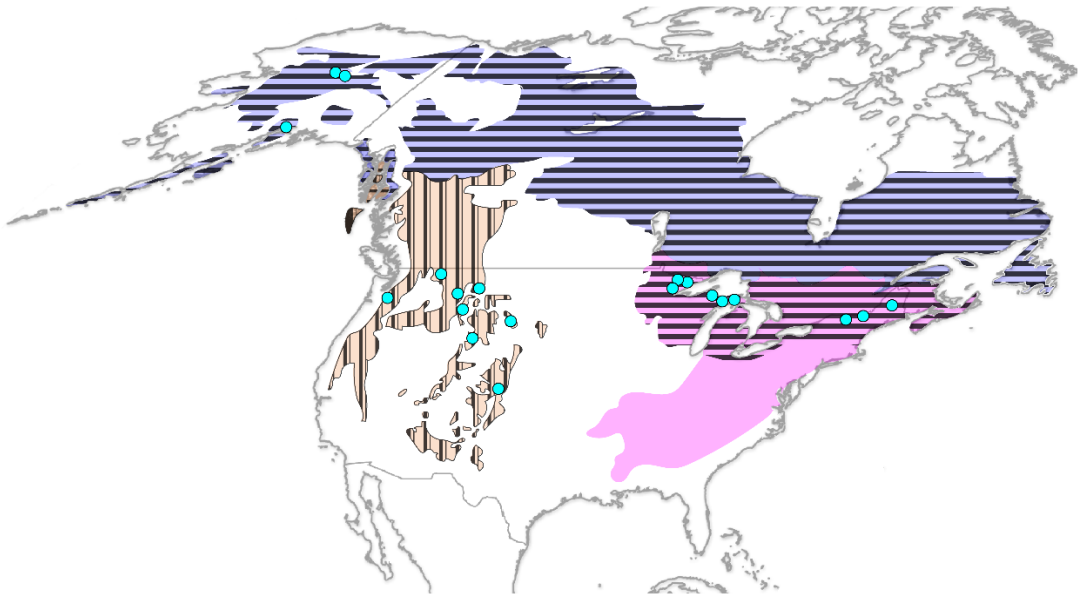

Figure 1. Geographic distribution of *Martes americana* and *Martes caurina*. Points represent location of specimens measured. Horizontal lines indicate the geographic distribution of *M. americana* and vertical lines indicate the geographic distribution of *M. caurina* (Clark et al., 1987; Nowak, 1999). Forest biome ranges are designated by purple for Boreal, orange for Coniferous, and pink for Broadleaf forests (Olson et al., 2001). Note that *M. americana* does not occupy the entire Broadleaf forest biome.

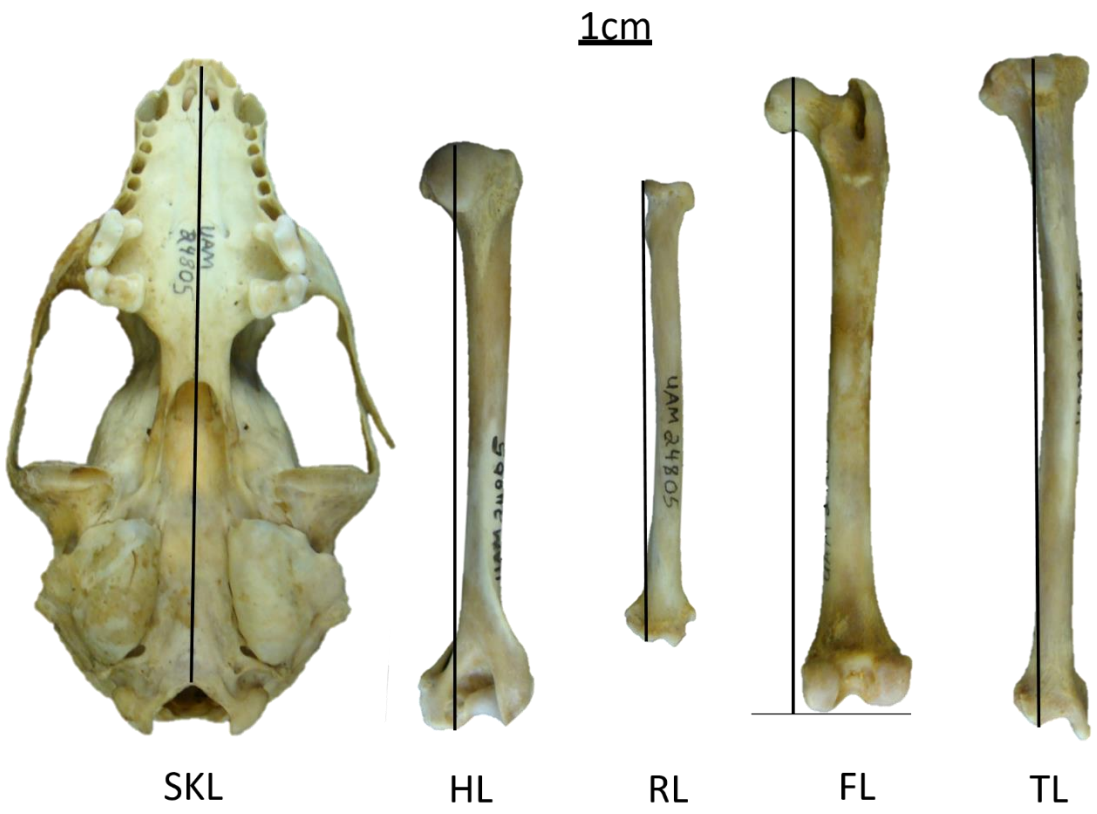

Figure 2. Linear length measurements taken on the skull, humerus, radius, femur, and tibia of each specimen to test for Allen's Rule. Length measurements based on Samuels et al. (2013).

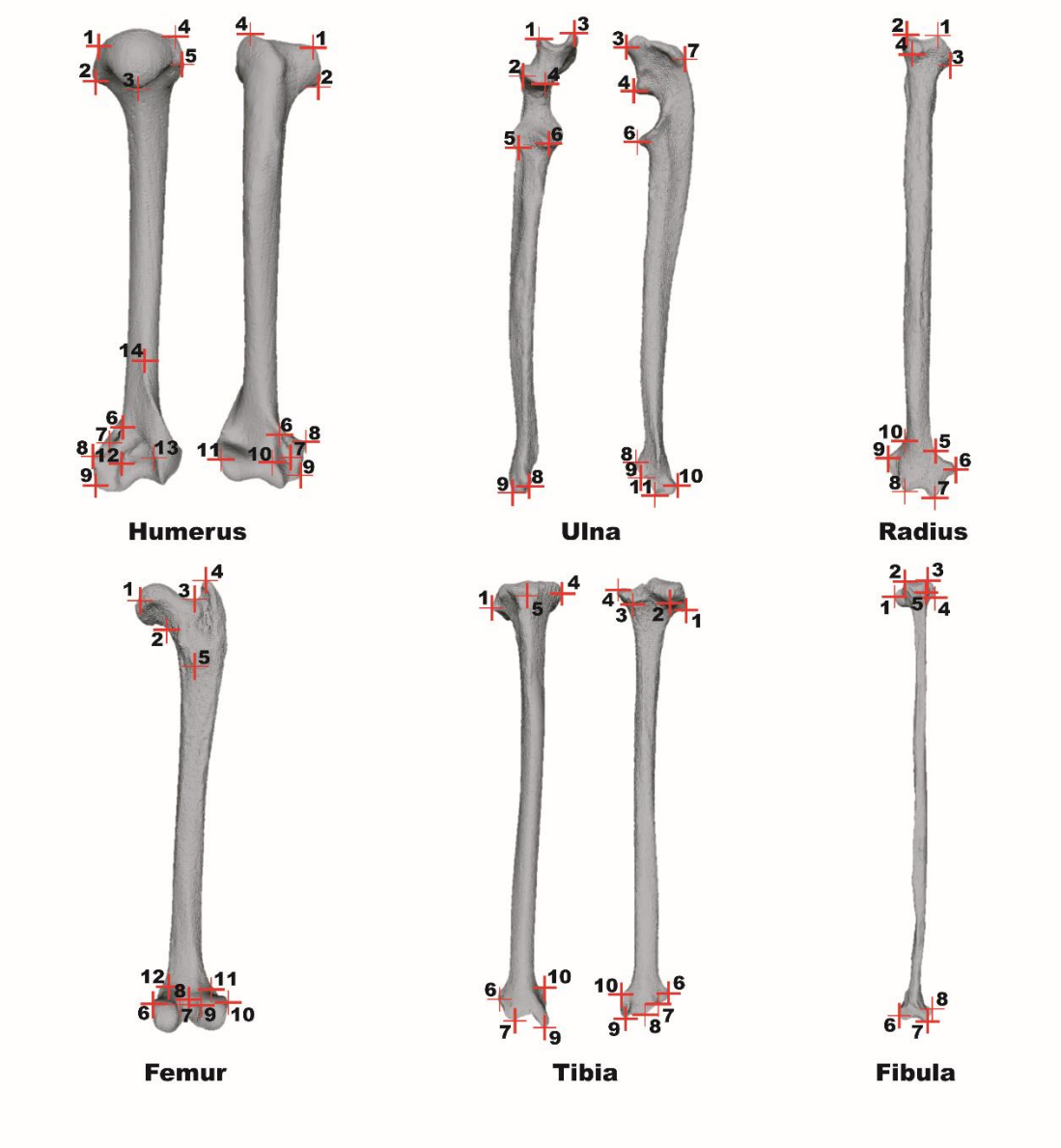

Figure 3. Geometric morphometric landmarks on the humerus, radius, ulna, femur, tibia, and fibula used to test for morphological differences between specimens from the three biomes.

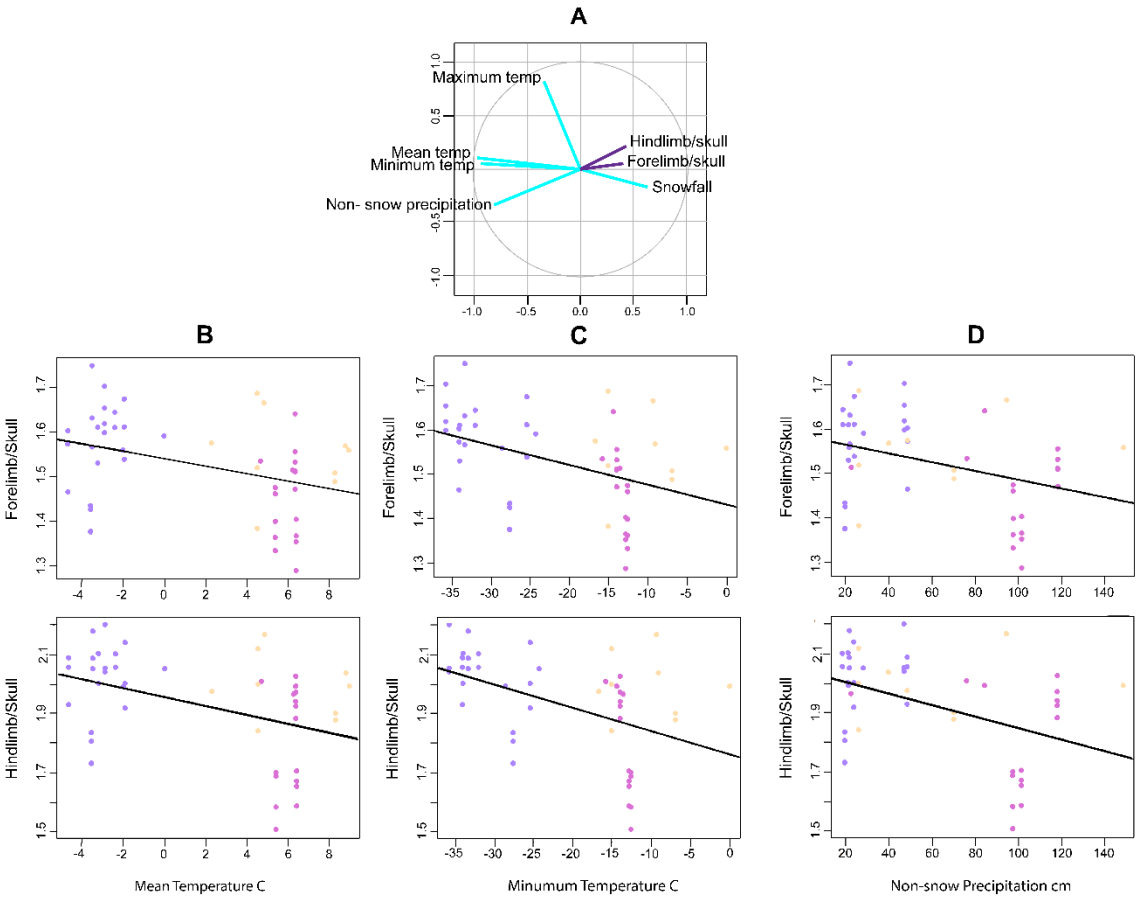

Figure 4. Results of the partial least squares (PLS) regression between limb proportions and climatic variables. A) Circle of correlations produced from PLS. Purple lines indicate the limb to skull length proportions and teal lines represent the climatic variables. Line length indicates the strength the of correlation. Variables whose lines are closest to forming a 180°angle with the line representing either forelimb or hindlimb proportions have the greatest importance in the first latent vector. Here, the most important variables within the first vector are mean and minimum annual temperature and annual non-snow precipitation. B) Scatterplots of mean annual temperature to forelimb proportions and hindlimb proportions. C) Scatterplots of minimum annual temperature to forelimb proportions and hindlimb proportions. D) Scatterplots of annual non-snow precipitation to forelimb proportions and hindlimb proportions. Points in each scatterplot represent specimens and are colored according to the biome from which each was collected. Purple represents individuals from Boreal forests. Orange are specimens from

Coniferous forests, and pink are from Broadleaf forests. The lines on each scatterplot denote a general linear trend within the data.

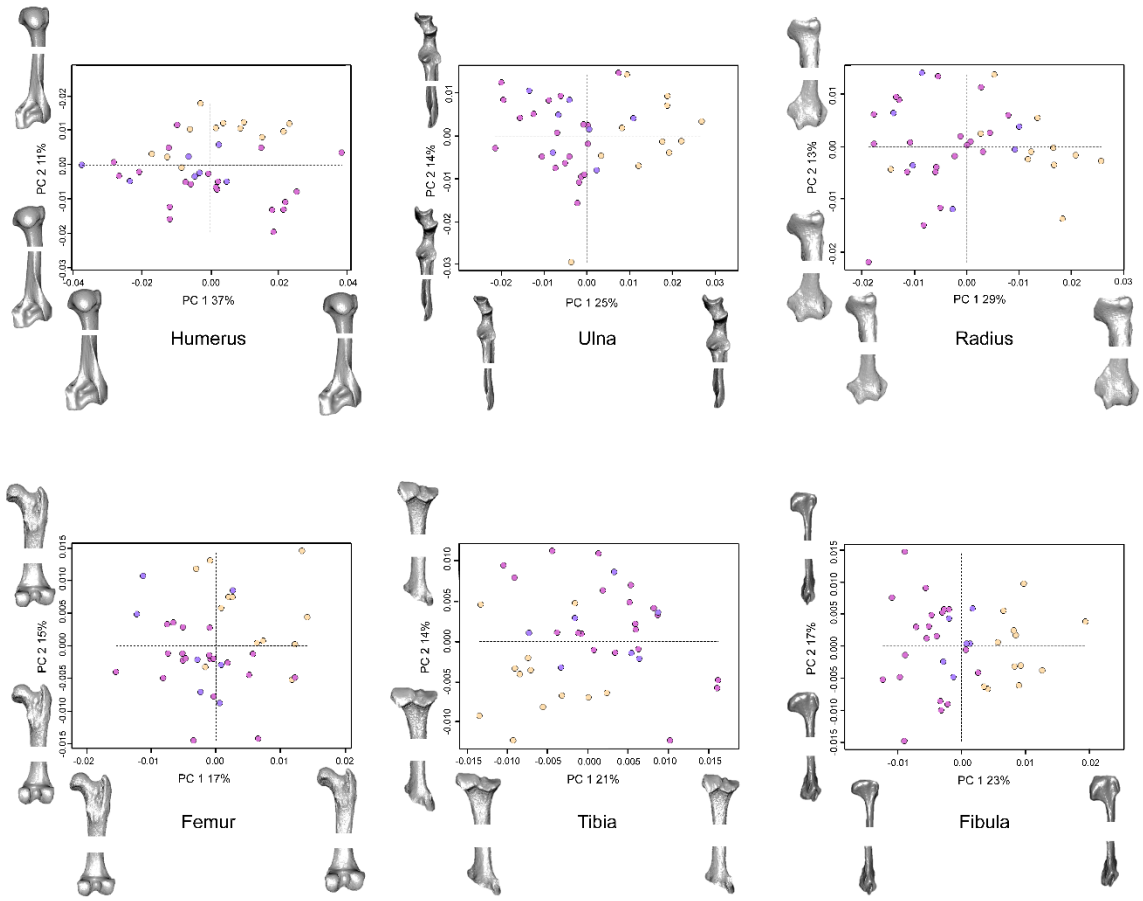

Figure 5. Principal component analysis (PCA) plots for the first two PC axes for the humerus, radius, ulna, femur, tibia, and fibula. Points are colored according to the biome from which each specimen was collected. Purple represents individuals from Boreal forests. Orange are specimens from Coniferous forests, and pink are from Broadleaf forests. The percent variance explained by each PC axis is indicated in the axis label. Bone images represent the morphology of each element at the extremes of each PC axis. In all of the bones except the humerus, the morphology of specimens from Coniferous forests (orange) significantly differed from specimens from Broadleaf (pink) and Boreal (purple) forests.

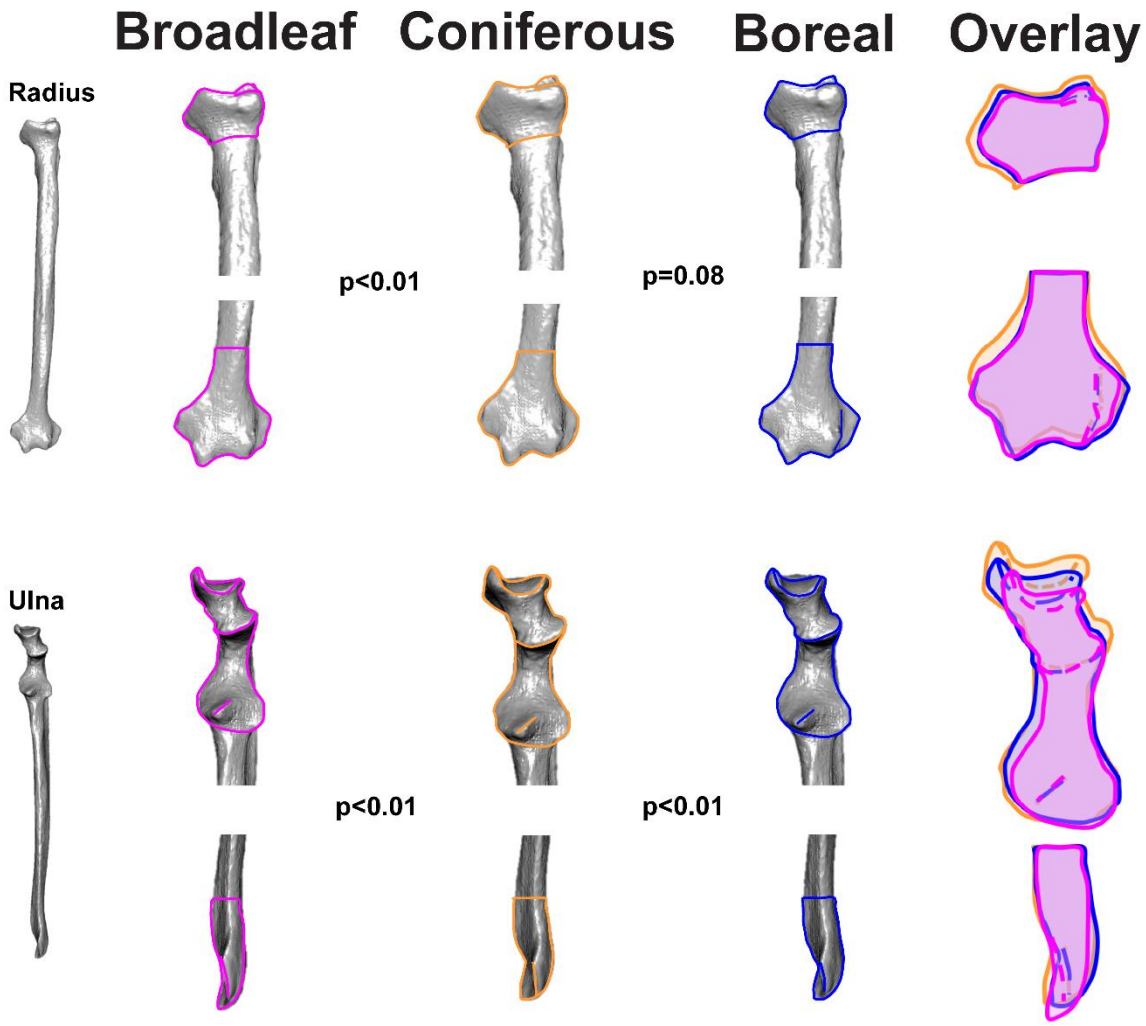

Figure 6. Mean shape of the radius and ulna of specimens from each biome. P-values indicate statistical differences in morphology between specimens from Broadleaf and Coniferous forests and specimens from Coniferous and Boreal forests, as there were no statistical differences between Broadleaf and Boreal specimens. Overlay depicts the mean epiphyseal morphology from all three biomes overlain. Biomes are designated by purple) Boreal, orange) Coniferous, and pink) Broadleaf forests. Note the overall increase in robusticity in specimens from Coniferous forests and more gracile nature of those from Broadleaf forests.

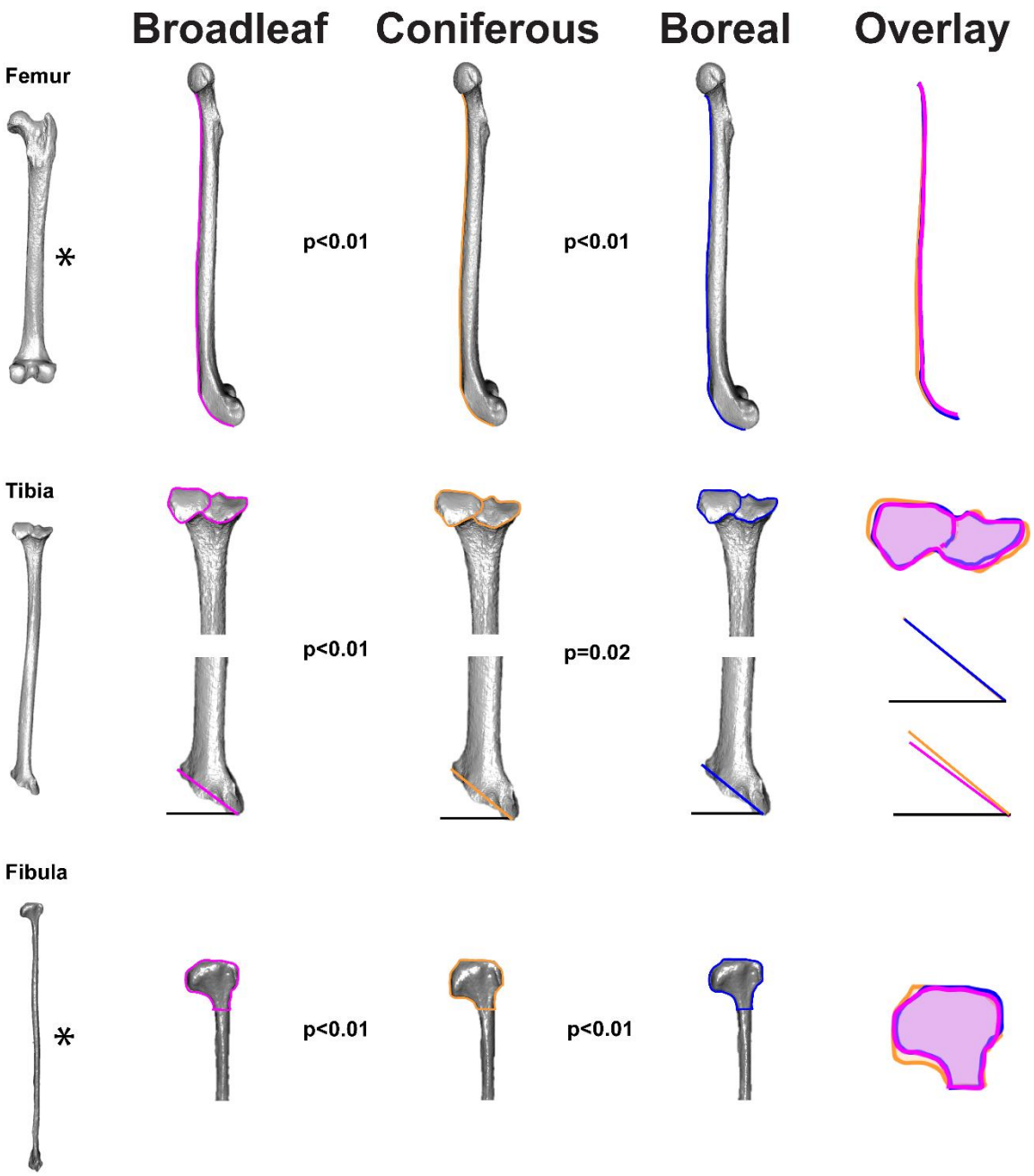

Figure 7. Mean shape of the femur, tibia, and fibula of specimens from each biome. P-values indicate statistical differences in morphology between specimens from Broadleaf and Coniferous forests and specimens from Coniferous and Boreal forests, as there were no statistical differences between Broadleaf and Boreal specimens. Overlay depicts the mean epiphyseal morphology from all three biomes overlain. Biomes are designated by: purple- Boreal; orange- Coniferous; and pink- Broadleaf forests. Note the overall increase in robusticity in specimens from Coniferous

forests and more gracile nature of specimens from Broadleaf forests. Asterisk on the femur and fibula indicates the morphology of these bones has an allometric relationship with body size; however, no more than 9% of the morphology is correlated with size.

CHAPTER III

DETERMINING THE LENGTH OF DNA NECESSARY TO PRODUCE ACCURATE PHYLOGENETIC RELATIONSHIPS IN EXTINCT TAXA

Introduction

Many living species are diagnosed from complete genetic sequences. Since the 1980s the use of ancient DNA (aDNA) to determine phylogenetic relationships between living and extinct taxa has become more common. Due to taphonomic processes, however, aDNA is often degraded and fragmentary, and as a result, many aDNA studies rely on partial gene sequences. These partial sequences could lack phylogenetically informative regions, which may result in phylogenetic analyses that construct inaccurate evolutionary relationships. It is crucial, therefore, to determine how much of a gene is required to produce accurate phylogenetic relationships. I tested whether partial mitochondrial DNA sequences recovered from specimens of extant *Martes americana* and *M. caurina* produce phylogenetic relationships significantly different from those produced from complete and nearly complete genes.

Studies using aDNA face challenges in sequencing complete genes due to the way in which DNA degrades. Increases in time, temperature, and moisture in the surrounding environment result in faster rates of denaturization and more fragmentary strands of DNA (Allentoft, 2012; Farrell et al., 2000; Murphy et al., 2007). For example, DNA preserved at 25°C will remain in only 2bp fragments after 10 ky, but if it is preserved at -5°C the strands of DNA average 683bp

(Allentoft, 2012). In addition, the secondary and tertiary structure of DNA cause regions with high mutation rates to be more susceptible to damage (Gilbert et al., 2005; Gilbert et al., 2003b). These taphonomic processes result in DNA strands that are short and that potentially lack the most phylogenetically informative regions. Consequently, the phylogenetic relationships hypothesized from these sequences may not be accurate.

Phylogenetic relationships can depend heavily on the gene(s) from which they are constructed. Mitochondrial genes are often used in aDNA studies because they evolve at faster rates than nuclear DNA and can, therefore, provide a more long-term evolutionary history (Avise, 2000; Brown et al., 1979). These faster evolutionary rates are attributed to relaxed functional constraints, poor DNA repair mechanisms, and a lack of histones, which often constrain rates of evolution (Gillespie, 1986; Nedbal and Flynn, 1998; Richter, 1992; Wilson et al., 1985). But different mitochondrial genes evolve at differing rates and can, therefore, produce differing evolutionary histories among taxa. For example, cytochrome b (cytb) and control region (Dloop) genes are fast evolving and contain several mutation sites (Nabholz et al., 2008; Parsons et al., 1997). These genes are frequently chosen by researchers for aDNA studies because this variation allows for detection of recent speciation events (Debruyne et al., 2008; Germonpre, 2009; Ozawa et al., 1997; Shapiro et al., 2004). The 12S and 16S mitochondrial genes are more conserved and evolve at slower rates than cytb and Dloop (Springer et al., 1995; Vences et al., 2005). By combining sequences from fast and slow evolving genes it is possible to obtain a more accurate depiction of mitochondrial and taxonomic evolution.

In this study, I sought to determine the accuracy of phylogenetic relationships produced from fragmentary DNA by testing two null hypotheses: 1) that there is no difference between the phylogenetic tree topologies produced from the same gene at varying lengths; and 2) that tree topologies produced from concatenated gene sequences will not differ regardless of the genes included in the concatenation. I tested these hypotheses using sequences from the mitochondrial

12S, 16S, Dloop, and cytb genes of *M. americana* and *M. caurina.* These species are well represented in living populations (Banfield, 1974; Clark et al., 1987; Nowak, 1999), allowing for study of complete genes. They are also common in the fossil record of North America (Clark et al., 1987; Hall, 1926; Hall, 1981; Hughes, 2009), permitting future application of this study to aDNA.

Taxonomic Nomenclature

North American pine martens, *M. americana* and *M. caurina,* were recently proposed as unique species based on mitochondrial, nuclear, morphological, and parasitic evidence (Dawson et al., 2017; Dawson and Cook, 2012; Hoberg et al., 2012; Merriam, 1890), but have not yet been recognized by the International Commission on Zoological Nomenclature. I have adopted these specific titles to retain consistency with recent literature.

Institutional Abbreviations

New York State Museum (NYSM), Florida Museum of Natural History (FLMNH), Burke Museum of Natural History and Culture (BMUW), University of Alaska Museum of the North (UAMN), and Smithsonian Institution National Museum of Natural History (USNM)

Materials and Methods

Genetic Sequences

Complete cytb sequences for *M. americana* and *M. caurina* were sourced from those published to GenBank (NCBI), comprising of 57 individuals (Appendix II, Section A). Sequences of 12S, 16S, and Dloop for these species were either unavailable or partial on GenBank. I, therefore, sequenced these genes from a total of 29 specimens of *M. americana* and *M. caurina* (Appendix II, Section B), housed in the collections at NYSM, FLMNH, BMUW, UAMN, and USNM. These specimens were collected across the U.S. range of both species between 1990 and 2013. This temporal range allowed me to extract DNA from recent specimens with soft tissue, which is relatively unaltered by degradation. In order to create a concatenated sequence of 12S, 16S, Dloop, and cytb, I also sequenced cytb from seven of these 29 specimens. In addition, I received sequences of 12S, 16S, cytb, and Dloop from two specimens of *M. caurina* from researchers at the Museum of Southwestern Biology (MSB) (Appendix II, Section C). To act as a reference genome and phylogenetic outgroup, I included complete 12S, 16S, Dloop, and cytb sequences from *Martes foina* published to GenBank (NCBI).

DNA Extraction, Amplification, and Sequencing

I collected soft tissue samples from all 29 specimens. DNA extractions were performed in batches of eight with one negative control per batch. I extracted genomic DNA from soft tissue using a phenol:chloroform:isoamyl (25:24:1) extraction protocol (for detailed protocol see Appendix VI). I quantified the amount of DNA present in all extractions using a ThermoFisher™ Qubit (Appendix II, Section D, Table 1).

Using a polymerase chain reaction (PCR), I amplified DNA in overlapping fragments ranging from 139-1,012bp, depending on the DNA quality of each specimen. The 12S, 16S, cytb, and Dloop mitochondrial genes were targeted using primers designed to span the entirety of each gene (Table 1, Figure 1). I designed 12S, 16S, and Dloop primers to amplify approximately 250bp

regions with 50bp of overlap (Figure 1). I designed primers to have similar annealing temperatures, within 1°C, and with GC content of at least 60%. In some cases, the GC content criterion resulted in targeted priming sites that had less than 50bp of overlap (Figure 1). Primers for cytb were taken from (Stone and Cook, 2002). For all PCRs, I used a negative and positive control. I performed PCR amplifications in 20 µL volumes and amplified each gene using 1X PCR buffer, 2 mM $MgCl_2$, 200 µM dNTP, 1 mg/ml BSA, 1.25 U Apex™ Taq, and 0.4 µM of each primer. The PCR was conducted on a Labnet International Inc., Multigene Optimax thermocycler and cycling conditions were as follows: 95°C for 10 min; 35 cycles of 95°C for 15 s, 52-60°C for 90 s, 72°C for 30 s; 72°C for 5 min. I evaluated the success of each amplification by running 5 µL of dyed PCR product on a 2% agarose gel and imaging using a BioRad Gel Doc XR system (for detailed protocol see Appendix VII).

I cleaned all PCR products using an Exo-Sap cleaning procedure and Sanger sequenced all forward and reverse strands on an Applied Biosystems 3130xl Genetic Analyzer (for detailed protocol see Appendix VIII). DNA sequences were then edited using CLC Main Workbench (Qiagen Bioinformatics).

Alignment

Sequences obtained for 12S, 16S, Dloop, and cytb were initially short amplicons which had to be assembled against a reference genome. Here, I used the mitochondrial genome of *M. foina* (HM106325.1) as a reference. I assembled all sequences using CLC Main Workbench (Qiagen Bioinformatics). Once assembled, I aligned the sequences for 12S, 16S, and Dloop independently against the mitochondrial genome of *Martes foina* (HM106325.1), which then acted as an outgroup in later phylogenetic analyses. I aligned all sequences using MEGA7 (Kumar et al., 2016). I aligned the cytb genes obtained from GenBank without a reference genome as these

sequences had already been assembled prior to publication. I chose the ClustalW algorithm with the default parameters for all alignments and manually corrected any misalignments.

Required Gene Length

To determine the sequence length necessary to produce accurate phylogenetic relationships, I compared the topology and best-fit nucleotide substitution models of subsampled sequences. I did this for 12S, 16S, Dloop, and cytb independently. First, I subsampled each gene alignment in 100bp increments from the 3' end and saved each subsample as a new sequence (Figure 2A). This was done in each gene until approximately 100bp remained. I then determined the best-fit nucleotide substitution model for each subsampled sequence using a Neighbor-Joining (NJ) tree and Maximum Likelihood (ML) statistical method with complete site deletion. I chose the best-fit nucleotide substitution model as those with the lowest Akaike information criterion (AIC). Next, I ran a ML phylogeny for each subsampled sequence using the best-fit nucleotide substitution model with complete site deletion and 500 bootstrap replicates to determine nodal support (Figure 2B). All analyses were run in MEGA7 (Kumar et al., 2016). Finally, I tested for statistical differences between tree topologies created from the complete and subsampled sequences using an SH test (Shimodaira, 1998; Shimodaira and Hasegawa, 1999) in PAUP*4.0b (Swofford, 2002). This analysis treats each phylogeny as a model whose goodness of fit is tested against the full gene alignment by calculating a natural log-likelihood value. The natural log-likelihood values are then ranked and those topologies with values significantly different from the best-fit topology are assigned a significant *p*-value ($\alpha \leq 0.05$) (Figure 2C). I then repeated each of these steps with sequences subsampled from the 5' end.

Required Gene in Concatenated Sequence

To determine which of the four genes was required in a concatenated sequence to produce accurate phylogenetic relationships, I concatenated 12S, 16S, Dloop, and cytb sequences from eight specimens of *M. americana* and *M. caurina*, with *M. foina* as an outgroup. I then subsampled this sequence four times, removing one gene each time, resulting in a concatenated sequence of three genes for each analysis (Figure 2A). I tested each subsampled concatenated sequence for the best-fit nucleotide substitution model using a NJ tree method and again chose the model with the lowest AIC. I then ran a ML phylogeny for each new sequence using the best-fit nucleotide substitution model with complete site deletion and 500 bootstrap replicates (Figure 2B). These analyses were run in MEGA7 (Kumar et al., 2016). Finally, I compared the tree topologies of each subsampled concatenated sequence to that produced from the full sequence using an SH test (Shimodaira, 1998; Shimodaira and Hasegawa, 1999) (Figure 2C). Again this analysis was conducted in PAUP*4.0b (Swofford, 2002).

Results

Genetic Sequences

From the 29 sampled specimens, I successfully sequenced 12S in 19 individuals, 16S in 9 individuals, and Dloop in 23 individuals. The published complete mitochondrial genome of *M. americana* indicates the length of these genes is as follows: 12S=959bp; 16S=1572bp; and Dloop approximately 500bp within the 1068bp of control region. I experienced difficulty in binding primers outside each gene that would amplify the beginning and end nucleotides. This is likely due to a high amount of genetic variation in the tRNA regions surrounding these genes. In addition, in some specimens there was no overlap in primer sets due to poor sequence quality at the beginning and end of reads. This resulted in some missing base pairs within the sequences. In

total, I sequenced all but approximately 200bp of each gene. While these missing sites remained in the gene alignments, missing sites were not considered in the ML phylogenetic analyses because I assigned a complete site deletion criterion. The final sequenced gene lengths were 691bp of 12S, 1335bp of 16S, and 540bp of Dloop/control region. Cytb sequences were complete and were 1140bp in length. GC content within each gene was as follows: 46% in 12S; 40% in 16S; 44% in Dloop; and 46% in cytb.

As expected, each gene had a different amount of variation among specimens. There were 36 polymorphic sites in 12S (Table 2), 93 in 16S (Table 3), 82 in Dloop (Table 4), and 51 in cytb (Table 5). Sites of variation were predominantly single nucleotide polymorphisms (SNPs) and were relatively evenly distributed throughout each gene. The genes averaged the following number of polymorphic sites per 100bp: 12S had 5; 16S had 7; Dloop had 13; and cytb had 4. In 12S, 16S, and Dloop most of the polymorphic sites were between *M. foina* and the two American marten species. If these polymorphic sites are not considered, then between *M. americana* and *M. caurina* variation averaged 2 polymorphic sites in 12S, 4 sites in 16S, and 11 sites in Dloop per 100bp. Some of the polymorphic sites contained ambiguous nucleotides. These may indicate heteroplasmy in an individual, which has been reported in other taxa (e.g., Chinnery et al., 2000; Magnacca and Brown, 2010; Paduan and Ribolla, 2008; Robison et al., 2015; Rokas et al., 2003), or they may be a result of poor sequence quality.

Required Gene Length

The best-fit genetic nucleotide substitution models for each gene differed as the gene was subsampled. In 12S, the best-fit nucleotide substitution model for both the 3' and 5' subsamples was TN93. This model changed, however, once the subsampled gene lengths decreased to 191bp in the 3' cut and 291bp in the 5' cut (Table 6). The 3' subsamples of 16S transitioned from one

best-fit nucleotide substitution model to another after approximately one-half of the gene was removed. This transition was between TN93+G and HKY+G. The 5' subsamples of 16S were much more variable in their best-fit nucleotide substitution models, transitioning between TN93+G, GTR+G, TN93, HKY, and TN92 (Table7). Dloop 3' and 5'subsamples had a HKY+G best-fit nucleotide substitution model until the gene length decreased to 140bp. At this point, the model transitioned to TN93+I (Table 8). Finally, cytb 3' subsamples had five best-fit nucleotide substitution models, HKY+G, TN93+G, TN93, HKY+Y, and HKY. These models transitioned frequently once the sequence length was approximately half of the original length. Once the gene length of the 5' subsamples was ≤740bp the best-fit nucleotide substitution model transitioned from HKY+G to TN93 (Table 9).

The SH test indicated that the required gene length to achieve a topology that did not differ from the best-fit topology varied widely between each gene (Figure 3). In 12S, the best-fit tree topology was at 591bp of the original 691bp for both the 3' and 5' cuts. In the 3' cut none of the topologies differed significantly, while in the 5' cut the topology produced from 491bp differed (Table 10). This topology had longer branch lengths and fewer nodes than the best-fit phylogeny (Figure 3). In 16S, the best-fit topology varied between the 3' and 5' cuts, with 735bp of the original 1335bp as the best-fit model in the 3' cut and 535bp in the 5' cut. There was no topology that significantly differed from the best-fit tree in the 3' subsamples. In the 5' subsamples, however, the topology produced from 135bp did significantly differ (Table 10), with incorrect placement of the outgroup (Figure 3). The 3' and 5' subsamples of Dloop both had a best-fit tree topology produced from 340bp of the original 540bp and significantly different topologies produced from ≤140bp (Table 10). Many of the nodes that were present in the best-fit topology were collapsed once the sequence length reached 140bp (Figure 3). Finally, analysis of cytb indicated the best-fit topology resulted from the entire gene, 1140bp. Those topologies produced from ≤340bp in the 3' cut or ≤440bp in the 5' cut significantly differed from the full gene

topology (Table 10). In both significantly different topologies, nodes were collapsed and branch lengths within some clades increased relative to the best-fit topology (Figure 3).

Required Genes in Concatenated Sequence

The best-fit nucleotide substitution model differed depending on which gene was removed from the concatenated sequence. When all four genes were present, the best-fit nucleotide substitution model was TN93+G. This model remained after cytb was removed from the concatenated sequence. The removal of either 12S or Dloop resulted in GTR+G and the removal of 16S resulted in HKY+G as the best-fit nucleotide substitution models (Table 11).

The SH test indicated the removal of some genes from the concatenated sequence did alter the resulting topology. The best-fit tree topology was constructed using the complete concatenated sequence (Table 12). The topologies constructed from sequences missing 16S or cytb were significantly different from the best-fit topology. These topologies both differed in branch lengths and had a reduced number of clades compared to the best-fit tree (Figure 4). The removal of 12S and Dloop did not change the topology significantly (Table 12).

Discussion

The results of this study indicate that accurate phylogenetic relationships can be recovered from minimal lengths of the 12S, 16S, Dloop, and cytb mitochondrial genes. Tree topologies constructed from subsamples of 12S, 16S, and Dloop do not significantly differ in sequences exceeding 140bp in length, with the exception of 12S when cut from the 5’ end (Table 10). This

suggests short fragments of these genes are phylogenetically informative and that the evolutionary relationships hypothesized from partial aDNA sequences of these genes may be accurate. Cytb, however, required a greater sequence length, with sequences >340bp producing statistically similar topologies (Table 10). The genetic variation within cytb is similar to that in 12S and 16S, averaging five SNPs per 100bp. The longer required gene length in cytb may be because this alignment lacked *M. foina* as an outgroup. It is possible the increased genetic variation introduced by *M. foina* in the 12S, 16S, and Dloop alignments resulted in statistically similar tree topologies at smaller sequence lengths. Future analyses including *M. foina* in the cytb alignment may result in shorter required gene lengths. If so, it suggests that the required gene lengths differ between interspecific and intraspecific datasets.

Whether a sequence was sampled from the 3' or 5' end influenced which tree topologies were determined to be the best-fit and which significantly different from the best-fit. Most of the variation seen between individuals were SNPs. While these sites were fairly evenly distributed in each gene, there were some regions with higher variation. By subsampling each gene from both the 3' and 5' end, I removed these phylogenetically informative regions at different stages. This in turn resulted in differing required lengths within a single gene. For example, in 16S the best-fit tree topology was constructed from 735bp when subsampled from the 3' end and 535bp when cropped from the 5' end. In addition, 12S and cytb required longer sequences to produce accurate phylogenetic relationships when subsampled from the 5' end. This is because there is a higher concentration of SNPs at the 3' end of each of these genes. These SNPs are removed in the 3' subsamples but not the 5' subsamples, making 5' subsamples more phylogenetically informative.

The results of this study indicate that accurate phylogenetic relationships can be constructed when some genes are missing from specimens in a concatenated genetic sequence. The removal of 16S and cytb from the concatenated sequence resulted in significantly different tree topologies while the removal of 12S and Dloop did not. This suggests 16S and cytb are the most phylogenetically

informative of the sampled genes in *M. americana* and *M. caurina.* Because genes degrade at differing rates under different conditions (Gilbert et al., 2005; Gilbert et al., 2003b) it is often difficult to amplify the same genes consistently across many specimens. As a result, many specimens are removed from studies because they lack one or more of the targeted genes. The results found here, however, suggest that this removal may be unnecessary and that as long as the most informative genes are present at appropriate lengths, the evolutionary relationships of these specimens can still be recovered. This would allow for the inclusion of more specimens with less ideal DNA quality in aDNA studies.

The topologies found to be significantly different from the best-fit tree had several collapsed nodes and variable branch lengths (Figures 3 and 4). Many researchers rely on aDNA sequences to determine the taxonomic status of extinct species, particularly of those thought to have recently diverged (e.g., Barnett et al., 2009; Orlando et al., 2013; Ozawa et al., 1997; Rohland et al., 2010; Willerslev et al., 2009), and to determine rates and timing of molecular and morphological evolution (e.g., Debruyne et al., 2008; Germonpré et al., 2009; Haile et al., 2010; Orlando et al., 2013; Orlando et al., 2009). These studies rely on accurate node placement and branch lengths within a topology. The results of this study suggest that both accurate node placement and branch lengths can be recovered from minimal sequence lengths. This is again promising for aDNA studies and the potential inclusion of specimens with poor DNA quality.

The required genes and gene lengths calculated here can be applied to aDNA studies in both initial gene targeting and in the post-sequencing pipeline. This study suggests primers and baits can be designed to capture portions rather than entire genes. This is advantageous because successfully targeting and capturing complete genes in degraded aDNA can be challenging despite recent advances in Next-Generation (Next-Gen) sequencing methods (Carpenter et al., 2013; Horn, 2012; Rizzi et al., 2012). Instead, researchers can target regions that have less variation at binding sites, increasing the likelihood of successful amplification. Next-Gen

sequencing produces reads of multiple short fragments per sample, which are then concatenated to produce a more complete sequence (Gogol-Döring and Chen, 2012; Kircher, 2012; Magi et al., 2010). Including a step in the post-sequencing pipeline that targets the required genes and removes all concatenated sequences that do not meet minimum length requirements may increase analytical accuracy.

The effects of aDNA degradation on the accuracy of results has been recognized by other researchers (e.g., Axelsson et al., 2008; Ho et al., 2007; Ho et al., 2011; Rambaut et al., 2009). DNA degradation often results in the loss of amino groups, transforming one nucleotide into another. This process, called deamination, transforms cytosine (C) into uracil (U) and adenine (A) into guanine (G) (Gilbert et al., 2003a; Gilbert et al., 2005; Gilbert et al., 2003b; Hofreiter et al., 2001). These transformations can appear as false variation between specimens, resulting in inaccurate interpretations of population size, evolutionary rate, genetic diversity, and phylogenetic relationships. To account for this, researchers have begun to implement both lab methods, such as sequence replication (Rambaut et al., 2009; Shapiro et al., 2004), and post-sequencing priors that recognize and account for these potential errors (Ho et al., 2007; Mateiu and Rannala, 2008; Rambaut et al., 2009). Applying analyses such as these to sequences of appropriate lengths will result in more accurate interpretations of the evolution of ancient populations and species.

While the required gene lengths calculated here are specific to *M. americana* and *M. caurina,* they may still be informative for other mammalian taxa. For example, within the cyt b gene of two closely related species of *Martes*, the Japanese marten (*M. zibellina*) and the sable (*M. melampus*), there are 72 polymorphic sites (Kurose et al., 1999). In another mustelid species, the Eurasian badger (*Meles meles*), cytb has 97 polymorphic sites among populations (Kurose et al., 2001). In more distantly related species such as the Siberian chipmunk (*Tamias sibiricus*), populations exhibit 213 polymorphic sites in cytb (Lee et al., 2008). These examples suggest that

the number of cytb polymorphic sites seen in North American *Martes* (51), and perhaps in the other mitochondrial genes of these species, are conservative. Because accurate phylogenetic relationships can be produced from >340bp of cytb in *M. americana* and *M. caurina,* then even shorter sequences may be successful in taxa with more genetic variation. Future analysis of required sequence lengths across taxa with higher amounts of genetic variation will aid in determining whether *Martes* reflects a more conservative required gene length.

Conclusions

The results of this study suggest that the most commonly used mitochondrial genes in aDNA studies can produce accurate phylogenetic relationships from minimal sequence lengths. In North American *Martes* only about a quarter of the 12S, 16S, Dloop, and cytb genes are required. In addition, accurate phylogenetic relationships can be constructed from concatenated sequences that are missing genes, provided that the most informative genes are present. This is beneficial for aDNA studies, where DNA is often so fragmented it is difficult to amplify and sequence an entire gene. As Next-Gen full genome sequencing becomes more common, expansion of this type of study into other commonly used mitochondrial and nuclear genes may be beneficial. This will allow researchers to target shorter amplicons and place required length criteria within their post-sequencing pipelines, ensuring only samples with the most phylogenetically informative genes at appropriate lengths are included in final analyses. Furthermore, by combining these methods with those used to correct for aDNA damage, it will be possible to produce more accurate phylogenetic relationships in extinct taxa.

Tables

Table 1. Gene Primer Sequences and Annealing Temperatures

Gene	Primer	Forward Sequence	Reverse Sequence	Annealing Temp C
12S	1	GCCTAGAAGAGTCACAAGAC	CACTGCTGTATCCCGTGG	60
	2	GAGCGGGCATCAGG	CGCCGTGAGCCTATTAATTC	52
	3	CGTGCCAGCCACC	GGCTGGGCATAGTGG	52
	4	CTCCAACAACACGATAGCTG	CGATTACAGAACAGGCTCC	60
	5	GGACTTGGCGGTGC	CATGGCCCTATTCAACTAAGC	58
	6	GGTCAAGGTGTAACCCATG	GGTGTAAGCCAGGTGC	58
16S	1	GCACCTGGCTTACACC	CATCATTCCCTTGCGGTAC	52
	2	CCAACTACCACGACATCC	CATAGGTAGCTCGTCTGG	50
	3	GCTACCTATGAGCAATCCAC	CTAAGCAAGGTTGTTTCCTTG	50
	4	CCTAACGTATCACTGGGC	CAGTGCCTCCAATACTGAG	52
	5	GCACAAGCTTATAACAGTCAACG	GGCCGTTAAACTAATGTCACTG	52
	6	CACAGGCGTGCAGTAAG	GTTAGACCTGGTTGGTGG	52
	7	GACGAGAAGACCCTATGGAG	GATAGCTGCTGCACCATC	54
	8	GACCTCGATGTTGGATCAG	CAATTACTGGGCTCTGCC	54
Dloop	1	CAACAGCCCCGCCATC	GTGRGGTGCACGGATGC	58
	2	CGTGCATTAATGGCTTGCC	GGATTGAGGACTTCCATGGC	58
	3	CGTGTACCTCTTCTCGCTC	GAAGGATAAGCCCAGCTACAAG	58
Cytb	1	CGAYYTACCTGCYCCATC	YAGGAACAGGCAGATGAAG	60
	2	YTCTTCATCTGCCTGTTCCTG	GCGAAGAATCGYGTTAGGGTAG	60
	3	CTGAGGAGGATTCTCGGTAGACAAGG	GGATTAGGAATAGGGCGCCTAGG	60
	4	CTAGGCGCCCTATTCCTAATC	CTGAGTGGGCGGAATATCAT	60
	5	CAATTRTCCCATTVCTYCATAC	RATGGCTGGCATRAGGAYTAG	60

Table 2. Polymorphic Sites in 12S

Specimen	**2**	**4**	**5**	**6**	**9**	**10**	**11**	**33**	**34**	**35**	**36**	**79**	**99**	**162**	**177**
M. foina	A	T	A	G	T	A	C	C	C	C	A	C	C	A	C
UAM101819	G	A	G	C	–	·	T	·	·	·	·	T	T	·	·
UAM24805	G	A	G	C	C	·	·	Y	Y	·	·	T	T	·	·
UAM59579	G	A	G	C	–	·	·	·	·	·	·	T	T	·	·
UAM101851	–	–	–	–	–	–	–	–	–	–	–	T	T	·	·
UAM22680	–	A	G	C	–	·	·	·	·	·	·	T	T	·	·
UAM22736	G	A	G	C	–	·	·	·	·	·	·	T	T	·	·
UAM101828	G	A	G	C	C	·	·	·	·	·	·	T	T	·	·
UWBM81064	–	–	–	–	–	–	–	–	–	–	–	–	–	W	Y
UWBM81688	G	A	G	C	C	·	M	·	Y	·	·	T	T	·	·
UWBM81025	G	A	G	C	–	·	·	·	·	·	·	T	T	·	·
UF31328	G	A	G	C	–	·	·	·	·	·	·	T	T	·	·
NY14242	G	A	G	C	–	·	·	·	·	·	·	T	T	·	·
USNM600580	–	–	–	–	–	–	–	–	–	·	·	T	T	·	·
USNM600583	–	A	G	C	–	·	·	·	·	·	·	T	T	·	·
USNM592896	–	A	G	C	–	–	–	·	T	K	K	T	T	·	·
USNM592895	G	A	G	C	C	·	·	·	·	·	·	T	T	·	·
USNM600579	G	A	G	C	–	M	M	·	T	·	·	T	T	·	·
USNM592316	G	A	G	C	C	·	·	·	·	·	·	T	T	·	·
USNM600581	G	A	G	C	–	·	·	·	·	·	·	T	T	·	·

*– indicates no nucleotide at that position, · indicates no difference from *M. foina*

* some nucleotides are ambiguous and are represented by M (A or C), K (G or T), W (A or T), Y (C or T), R (A or G), or D (A, G, or T) based on IUPAC designations

Table 2 continued

Specimen	188	190	219	232	238	265	268	338	345	356	357	414	438	480	482	499
M. foina	A	A	T	T	C	T	C	T	T	T	A	C	A	T	A	C
UAM101819	·	G	·	·	T	C	C	·	C	·	G	T	G	C	·	·
UAM24805	·	G	·	·	T	C	C	·	C	·	G	T	G	C	M	·
UAM59579	·	G	·	·	T	C	C	·	C	·	G	T	G	C	·	·
UAM101851	·	G	·	·	T	C	C	·	C	·	G	T	G	C	·	M
UAM22680	·	G	·	·	T	C	C	·	C	·	G	T	G	C	·	·
UAM22736	·	G	·	·	T	C	C	·	C	·	G	T	G	C	·	·
UAM101828	·	G	·	·	T	C	C	·	C	·	G	T	G	C	·	·
UWBM81064	R	G	·	Y	T	C	C	·	C	Y	G	·	G	C	M	Y
UWBM81688	·	G	·	·	T	C	C	·	C	·	G	·	G	C	·	·
UWBM81025	·	G	·	·	T	C	C	·	C	·	G	·	G	C	·	·
UF31328	·	G	·	·	T	C	C	·	C	·	G	T	G	C	·	·
NY14242	·	G	D	·	T	C	C	·	C	·	G	T	G	C	·	·
USNM600580	·	G	·	·	T	C	C	·	C	·	G	T	G	C	M	Y
USNM600583	·	G	·	·	T	C	C	C	C	·	G	T	G	C	·	·
USNM592896	·	G	·	·	T	C	C	·	C	·	G	T	G	C	·	·
USNM592895	·	G	·	·	T	C	C	·	C	·	G	T	G	C	·	·
USNM600579	·	G	·	·	T	C	C	·	C	·	G	T	G	C	·	·
USNM592316	·	G	·	·	T	C	C	·	C	·	G	T	G	C	·	·
USNM600581	·	G	·	·	T	C	C	·	C	·	G	T	G	C	·	·

*– indicates no nucleotide at that position, · indicates no difference from *M. foina*

* some nucleotides are ambiguous and are represented by M (A or C), K (G or T), W (A or T), Y (C or T), R (A or G), or D (A, G, or T) based on IUPAC designations

Table 2 continued

Specimen	542	628	631	639	654	688
M. foina	T	C	T	G	C	A
UAM101819	C	T	·	A	T	G
UAM24805	C	T	–	·	–	–
UAM59579	C	T	·	·	–	–
UAM101851	C	T	·	·	–	–
UAM22680	C	–	–	–	–	–
UAM22736	C	T	·	A	T	G
UAM101828	C	T	·	A	T	G
UWBM81064	·	–	–	–	–	–
UWBM81688	·	T	·	A	T	G
UWBM81025	·	T	·	A	T	G
UF31328	C	T	·	A	T	G
NY14242	C	T	–	A	T	–
USNM600580	C	–	–	–	–	–
USNM600583	C	T	·	A	–	–
USNM592896	C	T	·	A	T	G
USNM592895	C	T	·	A	T	G
USNM600579	C	T	·	A	T	G
USNM592316	C	T	·	A	T	G
USNM600581	C	T	·	A	T	G

*– indicates no nucleotide at that position, · indicates no difference from *M. foina*

* some nucleotides are ambiguous and are represented by M (A or C), K (G or T), W (A or T), Y (C or T), R (A or G), or D (A, G, or T) based on IUPAC designations

Table 3. Polymorphic Sites in 16S

Specimen	**10**	**13**	**17**	**25**	**43**	**49**	**116**	**119**	**139**	**149**	**178**	**187**	**188**	**198**	**205**
M. foina	T	A	A	–	C	C	G	T	C	G	C	G	A	G	A
UAM101828	C	G	T	·	G	A	A	C	A	A	T	·	·	A	C
UAM24794	C	G	C	·	G	A	A	C	A	A	T	·	·	A	C
NY14241	C	G	T	·	G	A	A	C	A	A	T	·	·	A	C
UWBM81688	C	G	T	A	A	·	A	C	T	A	T	·	·	A	C
USNM592316	C	G	T	·	G	A	A	C	A	A	T	·	T	A	C
UF31427	C	–	–	A	A	·	A	C	T	A	T	·	·	A	C
UAM101819	C	G	T	·	G	A	A	C	A	A	T	A	·	A	C
MSB 197115	C	G	C	·	G	A	A	C	A	A	T	·	·	A	C
MSB 196581	C	G	T	A	A	·	A	C	T	A	T	·	·	A	C

*– indicates no nucleotide at that position, · indicates no difference from *M. foina*

* some nucleotides are ambiguous and are represented by M (A or C), K (G or T), W (A or T), Y (C or T), R (A or G), or D (A, G, or T) based on IUPAC designations

Table 3 continued

Specimen	**207**	**222**	**223**	**233**	**234**	**235**	**276**	**285**	**286**	**287**	**291**	**292**	**294**	**303**	**305**
M. foina	C	G	A	G	A	G	A	G	C	A	G	T	A	C	T
UAM101828	T	·	G	·	·	·	·	·	·	·	·	·	·	·	·
UAM24794	T	·	·	·	·	·	·	·	·	·	·	·	·	·	·
NY14241	T	·	·	·	·	·	·	·	·	·	·	·	·	·	·
UWBM81688	·	·	G	·	·	T	·	·	·	·	·	·	·	·	·
USNM592316	T	·	·	·	G	·	·	·	·	·	·	·	·	·	·
UF31427	·	–	·	–	–	–	W	K	Y	R	R	K	W	M	Y
UAM101819	T	A	·	K	·	·	·	·	·	·	·	·	·	·	·
MSB 197115	T	·	·	·	·	·	·	·	·	·	·	·	·	·	·
MSB 196581	·	·	·	·	·	·	·	·	·	·	·	·	·	·	·

*– indicates no nucleotide at that position, · indicates no difference from *M. foina*

* some nucleotides are ambiguous and are represented by M (A or C), K (G or T), W (A or T), Y (C or T), R (A or G), or D (A, G, or T) based on IUPAC designations

Table 3 continued

Specimen	**319**	**343**	**345**	**351**	**368**	**380**	**381**	**390**	**396**	**405**	**432**	**438**	**447**	**449**	**451**
M. foina	A	C	C	G	G	A	A	T	T	G	G	A	C	T	T
UAM101828	·	T	T	A	A	–	–	·	·	A	A	·	·	·	·
UAM24794	·	T	T	A	A	–	–	·	·	A	A	·	·	·	K
NY14241	·	T	T	A	A	–	–	·	·	·	A	·	·	·	·
UWBM81688	·	T	T	A	A	·	–	·	·	·	A	·	·	·	·
USNM592316	·	T	T	A	A	–	–	·	·	·	A	T	G	A	·
UF31427	R	T	T	A	A	–	–	K	–	–	–	–	–	–	·
UAM101819	·	T	T	A	A	–	–	·	·	·	A	·	·	·	·
MSB 197115	·	T	T	A	A	–	–	·	·	·	A	·	·	·	·
MSB 196581	·	T	T	A	A	–	–	·	·	·	A	·	·	·	·

*– indicates no nucleotide at that position, · indicates no difference from *M. foina*

* some nucleotides are ambiguous and are represented by M (A or C), K (G or T), W (A or T), Y (C or T), R (A or G), or D (A, G, or T) based on IUPAC designations

Table 3 continued

Specimen	460	465	469	471	477	478	497	511	513	514	516	526	535	557	564
M. foina	T	A	T	G	T	A	T	T	A	C	–	C	T	T	C
UAM101828	·	·	T	A	·	G	C	A	C	A	T	T	C	C	T
UAM24794	·	R	T	A	·	G	C	A	C	A	T	T	C	C	T
NY14241	C	·	T	A	·	G	C	A	C	A	T	T	C	C	T
UWBM81688	·	·	T	A	Y	G	C	A	C	A	T	T	C	C	T
USNM592316	·	·	T	A	·	Y	C	A	C	A	T	T	C	C	T
UF31427	·	·	T	A	·	G	C	A	C	A	T	T	C	C	T
UAM101819	·	·	T	A	–	G	C	A	C	A	T	T	C	C	T
MSB 197115	·	·	T	A	·	G	C	A	C	A	T	T	C	C	T
MSB 196581	·	·	T	A	·	G	C	A	C	A	T	T	C	C	T

*– indicates no nucleotide at that position, · indicates no difference from *M. foina*

* some nucleotides are ambiguous and are represented by M (A or C), K (G or T), W (A or T), Y (C or T), R (A or G), or D (A, G, or T) based on IUPAC designations

Table 3 continued

Specimen	**645**	**677**	**754**	**805**	**824**	**827**	**829**	**859**	**880**	**881**	**898**	**899**	**903**	**909**	**910**
M. foina	C	C	C	T	G	T	C	C	A	T	C	A	T	G	A
UAM101828	T	T	T	C	A	G	T	T	G	A	·	·	C	A	G
UAM24794	T	T	T	C	A	G	T	T	G	A	·	·	C	A	G
NY14241	T	T	T	C	A	G	T	T	G	A	·	·	C	A	G
UWBM81688	T	T	T	C	A	A	T	T	G	A	·	·	C	A	G
USNM592316	T	T	T	C	A	G	T	T	G	A	·	·	C	A	G
UF31427	T	T	T	C	A	A	T	T	G	A	A	G	C	A	G
UAM101819	T	T	T	C	A	G	T	T	G	A	·	·	C	A	G
MSB 197115	T	T	T	C	A	G	T	T	G	A	·	·	C	A	G
MSB 196581	T	T	T	C	A	A	T	T	G	A	·	·	C	A	G

*– indicates no nucleotide at that position, · indicates no difference from *M. foina*

* some nucleotides are ambiguous and are represented by M (A or C), K (G or T), W (A or T), Y (C or T), R (A or G), or D (A, G, or T) based on IUPAC designations

Table 3 continued

Specimen	**923**	**924**	**984**	**990**	**1014**	**1131**	**1205**	**1233**	**1234**	**1263**	**1264**	**1278**	**1279**	**1284**	**1285**
M. foina	A	G	T	A	C	C	C	A	C	A	A	T	A	A	A
UAM101828	G	A	C	·	T	T	T	·	·	M	M	Y	M	C	T
UAM24794	G	A	C	·	T	T	T	·	·	·	·	·	·	·	·
NY14241	G	A	C	·	T	T	T	·	·	·	·	·	·	·	·
UWBM81688	G	G	C	T	T	·	T	G	T	·	·	·	·	·	·
USNM592316	G	A	C	·	T	T	T	·	·	·	·	·	·	·	·
UF31427	G	G	C	T	T	·	T	G	T	·	·	·	·	·	·
UAM101819	G	A	C	·	T	T	T	·	·	·	·	·	·	·	·
MSB 197115	G	A	C	·	T	T	T	·	·	·	·	·	·	·	·
MSB 196581	G	G	C	T	T	·	T	G	T	·	·	·	·	·	·

*– indicates no nucleotide at that position, · indicates no difference from *M. foina*

* some nucleotides are ambiguous and are represented by M (A or C), K (G or T), W (A or T), Y (C or T), R (A or G), or D (A, G, or T) based on IUPAC designations

Table 3 continued

Specimen	1286	1290	1329
M. foina	T	T	C
UAM101828	·	S	·
UAM24794	·	·	·
NY14241	·	·	·
UWBM81688	W	·	T
USNM592316	·	·	·
UF31427	W	·	T
UAM101819	·	·	·
MSB 197115	·	·	·
MSB 196581	·	·	T

*– indicates no nucleotide at that position, · indicates no difference from *M. foina*

* some nucleotides are ambiguous and are represented by M (A or C), K (G or T), W (A or T), Y (C or T), R (A or G), or D (A, G, or T) based on IUPAC designations

Table 4. Polymorphic Sites in Dloop

Specimen	**45**	**51**	**52**	**56**	**58**	**59**	**61**	**65**	**68**	**77**	**81**	**85**	**88**	**93**	**95**
M. foina	C	T	C	–	C	A	T	A	C	A	A	C	A	G	T
UAM24805	T	·	T	·	T	G	C	·	·	·	·	T	C	C	·
UAM101819	·	·	T	·	T	G	C	·	·	·	·	T	C	C	·
UAM22680	T	·	T	·	T	G	C	·	·	·	·	T	C	C	A
UAM22736	T	·	T	·	T	G	C	·	·	·	·	T	C	C	·
UAM101828	T	·	T	·	T	G	C	·	·	·	·	T	C	C	C
UAM47308	T	·	T	·	T	G	C	·	·	·	·	T	C	C	·
UAM24794	T	·	T	·	T	G	C	·	·	·	·	T	C	C	·
UAM24808	T	·	T	·	T	G	C	·	·	·	·	T	C	C	·
UAM22678	T	·	T	·	T	G	C	·	·	·	·	T	C	C	·
UAM59579	T	·	T	·	T	G	C	·	·	·	·	T	C	C	·
UWBM81064	T	C	T	C	T	·	C	·	·	·	·	T	C	C	·
UWBM81688	T	C	T	C	T	·	C	·	·	·	·	T	C	C	·
UWBM81059	T	C	T	C	T	·	C	·	·	·	G	T	C	C	·
UF31427	T	C	T	C	T	·	C	·	·	·	·	T	C	C	·
NY14388	T	·	T	·	T	G	C	V	·	·	·	T	C	C	·
NY14242	T	·	T	·	T	G	C	·	·	·	·	T	C	C	·
NY14387	T	·	T	·	T	G	C	·	·	·	·	T	C	C	·
NY14241	T	·	T	·	T	G	C	·	·	·	·	T	C	C	·
USNM600583	T	·	T	·	T	G	C	·	·	·	·	T	C	C	·
USNM592896	T	·	T	·	T	G	C	·	·	·	·	T	C	C	·
USNM592316	T	·	T	·	T	G	C	·	·	·	·	T	C	C	·
USNM600581	T	·	T	·	T	G	C	·	·	·	·	T	C	C	·
USNM600584	T	·	T	·	W	G	Y	·	Y	W	·	T	M	C	·

*– indicates no nucleotide at that position, · indicates no difference from *M. foina*

* some nucleotides are ambiguous and are represented by M (A or C), K (G or T), W (A or T), Y (C or T), R (A or G), or D (A, G, or T) based on IUPAC designations

Table 4 continued

Specimen	97	100	101	102	117	133	138	141	145	149	177	178	183	189	192
M. foina	C	–	–	–	–	C	T	A	A	T	A	C	C	T	A
UAM24805	·	·	·	·	C	T	·	·	·	C	·	·	·	C	G
UAM101819	·	·	·	·	·	T	·	·	·	C	·	T	·	C	G
UAM22680	·	·	·	·	·	T	·	·	·	C	·	T	·	C	G
UAM22736	·	·	·	·	·	T	·	·	R	C	·	T	·	C	G
UAM101828	·	·	·	·	·	T	·	·	·	C	G	T	·	C	G
UAM47308	·	·	·	·	·	T	A	·	·	C	·	T	·	C	G
UAM24794	·	·	·	·	·	T	·	·	·	C	·	T	·	C	G
UAM24808	·	·	·	·	·	T	·	·	G	C	·	T	·	C	G
UAM22678	·	·	·	·	·	T	·	·	·	C	·	T	·	C	G
UAM59579	·	·	·	·	·	T	·	·	·	C	·	T	·	C	G
UWBM81064	·	·	·	·	·	T	·	·	·	C	·	·	·	C	G
UWBM81688	·	·	·	·	·	T	·	·	·	C	·	T	·	C	G
UWBM81059	·	·	·	·	·	T	·	M	·	·	·	T	·	C	G
UF31427	·	·	·	·	·	T	·	·	·	C	·	T	·	C	G
NY14388	A	C	A	G	T	T	·	·	·	C	·	T	T	C	G
NY14242	·	·	·	·	·	T	·	·	·	C	·	T	·	C	G
NY14387	·	·	·	·	·	T	·	·	G	C	·	T	·	C	G
NY14241	·	·	·	·	·	T	·	·	·	C	·	T	·	C	G
USNM600583	·	·	·	·	·	T	·	·	·	C	·	T	·	C	G
USNM592896	·	·	·	·	·	T	·	·	·	C	·	T	·	C	G
USNM592316	·	·	·	·	·	T	·	·	·	C	·	·	·	C	G
USNM600581	·	·	·	·	·	T	·	·	·	C	·	·	·	C	G
USNM600584	·	·	·	·	·	T	·	·	·	C	·	·	·	C	G

*– indicates no nucleotide at that position, · indicates no difference from *M. foina*

* some nucleotides are ambiguous and are represented by M (A or C), K (G or T), W (A or T), Y (C or T), R (A or G), or D (A, G, or T) based on IUPAC designations

Table 4 continued

Specimen	196	197	198	203	204	211	214	216	236	251	258	259	262	265	288
M. foina	C	C	A	T	C	A	T	A	T	C	T	A	C	G	A
UAM24805	T	A	G	·	T	G	C	·	·	·	C	C	·	·	·
UAM101819	T	A	G	·	·	G	C	·	·	·	C	C	T	·	·
UAM22680	T	G	G	·	·	G		·	·	·	C	C	·	·	·
UAM22736	T	A	G	·	·	G	C	·	·	·	C	C	T	·	·
UAM101828	T	A	G	C	·	G	C	·	·	·	C	C	T	·	·
UAM47308	T	A	G	·	·	G	C	·	·	·	C	C	T	·	·
UAM24794	T	A	G	C	·	G	C	·	·	·	C	C	T	·	·
UAM24808	T	A	G	·	·	G	C	·	·	·	C	C	T	·	·
UAM22678	T	A	G	C	·	G	C	·	·	·	C	C	T	·	·
UAM59579	T	A	G	C	·	G	C	·	·	·	C	C	·	·	·
UWBM81064	T	·	G	C	T	G	·	G	·	·	C	C	·	·	·
UWBM81688	·	·	G	C	·	G	·	G	·	·	C	C	·	·	·
UWBM81059	·	·	G	C	·	G	·	G	·	·	C	C	·	A	·
UF31427	·	·	G	C	·	G	·	·	·	·	C	C	·	·	·
NY14388	T	A	G	·	·	G	C	·	C	·	C	C	·	·	·
NY14242	T	A	G	·	·	G	C	·	·	·	C	C	·	·	M
NY14387	T	A	G	C	·	G	C	·	·	·	C	C	·	·	·
NY14241	T	A	G	·	·	R	C	·	·	·	C	C	·	·	·
USNM600583	T	A	G	C	·	G	C	·	·	T	C	C	·	·	·
USNM592896	T	A	G	·	·	G	C	·	·	·	C	T	·	·	·
USNM592316	T	A	G	·	·	G	C	·	·	·	C	C	·	·	·
USNM600581	T	A	G	C	·	G	C	·	·	·	C	C	·	·	·
USNM600584	T	A	G	C	·	G	C	·	·	·	C	C	·	·	·

*– indicates no nucleotide at that position, · indicates no difference from *M. foina*

* some nucleotides are ambiguous and are represented by M (A or C), K (G or T), W (A or T), Y (C or T), R (A or G), or D (A, G, or T) based on IUPAC designations

Table 4 continued

Specimen	290	291	292	294	304	309	340	352	379	380	445	449	450	458	469
M. foina	A	G	C	T	T	C	T	A	T	C	A	A	T	T	T
UAM24805	G	A	T	·	·	A	C	·	C	T	·	·	·	C	G
UAM101819	G	A	T	·	·	A	C	·	C	T	·	·	·	C	G
UAM22680	G	A	T	·	·	A	C	·	C	T	·	·	·	C	G
UAM22736	G	A	T	·	·	A	C	·	C	T	·	·	·	C	G
UAM101828	G	A	T	·	·	A	C	·	C	T	·	·	·	C	G
UAM47308	G	A	T	·	·	A	·	·	C	T	·	·	·	C	G
UAM24794	G	A	T	·	·	A	C	·	C	T	·	·	·	C	G
UAM24808	G	A	T	·	·	A	C	·	C	T	·	·	·	C	G
UAM22678	G	A	T	·	·	A	C	·	C	T	·	·	·	C	G
UAM59579	G	A	T	C	·	A	C	·	C	T	·	·	·	C	G
UWBM81064	·	A	·	·	·	A	·	G	C	T	·	·	·	C	G
UWBM81688	·	A	·	·	·	A	·	G	C	T	·	·	·	C	G
UWBM81059	·	A	·	·	·	A	·	G	C	T	·	·	·	C	G
UF31427	·	A	·	·	·	A	·	·	C	T	·	M	W	Y	G
NY14388	G	A	T	·	·	A	C	·	C	T	W	·	·	C	G
NY14242	G	A	T	·	·	A	C	·	C	T	·	–	–	–	–
NY14387	G	A	·	·	C	A	·	·	C	T	·	·	·	C	G
NY14241	G	A	T	·	·	A	C	·	C	T	·	·	·	C	G
USNM600583	G	A	T	C	·	A	C	·	C	T	·	·	·	C	G
USNM592896	G	A	T	·	·	A	C	·	C	T	·	·	·	C	G
USNM592316	G	A	T	·	·	A	C	·	C	T	·	·	·	C	G
USNM600581	G	A	T	C	·	A	C	·	C	T	·	·	·	C	G
USNM600584	G	A	T	C	·	A	C	·	C	T	·	·	·	C	G

*– indicates no nucleotide at that position, · indicates no difference from *M. foina*

* some nucleotides are ambiguous and are represented by M (A or C), K (G or T), W (A or T), Y (C or T), R (A or G), or D (A, G, or T) based on IUPAC designations

Table 4 continued

Specimen	470	477	479	480	482	498	504	508	510	511	512	513	514	518	519
M. foina	A	G	G	G	C	A	G	A	G	C	C	T	C	G	C
UAM24805	G	A	A	A	T	G	A	·	·	·	·	·	·	·	·
UAM101819	G	A	A	A	T	G	A	·	·	·	·	·	·	·	·
UAM22680	G	A	A	A	T	G	A	·	·	·	·	·	·	·	·
UAM22736	G	A	A	A	T	G	A	·	·	·	·	·	·	·	·
UAM101828	G	A	A	A	T	G	A	·	·	·	·	·	·	·	·
UAM47308	G	A	A	A	T	G	A	·	·	·	·	K	S	R	·
UAM24794	G	A	A	A	T	G	A	·	·	·	·	·	·	·	·
UAM24808	G	A	A	A	T	G	A	·	·	·	·	·	·	·	·
UAM22678	G	A	A	A	T	G	A	·	·	·	·	·	·	·	·
UAM59579	G	A	A	A	T	G	A	·	·	·	·	·	·	·	·
UWBM81064	G	A	A	A	T	G	·	·	·	·	·	·	·	·	·
UWBM81688	G	A	A	A	T	G	·	·	·	·	·	·	·	·	·
UWBM81059	G	A	A	A	T	G	A	·	C	·	T	–	–	–	–
UF31427	G	A	A	A	T	G	G	·	C	T	–	–	–	–	–
NY14388	G	A	A	A	T	G	A	·	A	·	–	–	–	–	–
NY14242	–	–	–	–	–	–	–	–	–	–	–	–	–	–	–
NY14387	G	A	A	A	T	G	A	·	·	·	·	·	·	S	·
NY14241	G	A	A	A	T	G	A	·	·	·	·	·	·	·	·
USNM600583	G	A	A	A	T	G	A	R	·	·	·	·	·	N	–
USNM592896	G	A	A	A	T	G	A	·	·	·	·	·	·	·	·
USNM592316	G	A	A	A	T	G	A	·	·	·	·	·	·	R	·
USNM600581	G	A	A	A	T	G	A	·	·	·	·	·	·	S	M
USNM600584	G	A	A	A	T	G	A	·	·	·	·	·	·	–	–

*– indicates no nucleotide at that position, · indicates no difference from *M. foina*

* some nucleotides are ambiguous and are represented by M (A or C), K (G or T), W (A or T), Y (C or T), R (A or G), or D (A, G, or T) based on IUPAC designations

Table 4 continued

Specimen	**521**	**522**	**523**	**525**	**527**	**531**	**539**
M. foina	G	T	C	G	T	T	G
UAM24805	R	·	·	A	·	·	·
UAM101819	R	·	·	A	·	·	·
UAM22680	·	·	·	A	·	·	·
UAM22736	·	·	·	A	W	·	·
UAM101828	·	·	·	A	·	·	·
UAM47308	S	·	W	A	W	W	·
UAM24794	·	–	–	–	–	–	–
UAM24808	R	W	M	A	·	·	·
UAM22678	R	·	·	A	·	·	·
UAM59579	R	·	M	A	W	·	·
UWBM81064	·	·	·	A	·	·	·
UWBM81688	·	·	·	A	·	–	–
UWBM81059	–	–	–	–	–	–	–
UF31427	–	–	–	–	–	–	–
NY14388	–	–	–	–	–	–	–
NY14242	–	–	–	–	–	–	–
NY14387	S	M	·	A	·	·	·
NY14241	S	·	·	A	·	·	·
USNM600583	–	–	–	–	–	–	–
USNM592896	T	W	·	A	·	·	·
USNM592316	A	·	·	A	·	·	·
USNM600581	A	·	·	A	·	·	N
USNM600584	–	–	–	–	–	–	–

*– indicates no nucleotide at that position, · indicates no difference from *M. foina*

* some nucleotides are ambiguous and are represented by M (A or C), K (G or T), W (A or T), Y (C or T), R (A or G), or D (A, G, or T) based on IUPAC designations

Table 5. Polymorphic Sites in Cytochrome b

Specimen	**48**	**60**	**61**	**69**	**82**	**156**	**198**	**243**	**268**	**294**	**300**	**318**	**330**	**345**	**438**
AF154974.1	T	C	C	C	T	C	T	C	T	C	A	T	C	T	T
AF154973.1	·	·	·	·	·	·	·	·	·	·	·	·	·	·	·
AF154972.1	·	·	·	·	·	·	·	·	·	·	·	·	·	·	·
AF154971.1	C	·	T	T	·	T	·	·	·	T	G	·	T	·	·
AF154970.1	·	·	·	·	·	·	C	·	·	·	·	·	·	·	·
AF154969.1	·	·	T	T	·	·	·	·	·	T	G	·	T	·	·
AF154968.1	·	·	T	T	·	·	·	·	·	T	G	·	T	·	·
AF154967.1	·	·	T	T	·	·	·	·	·	T	G	·	T	·	·
AF154966.1	·	·	T	T	·	·	·	·	·	T	G	·	T	·	·
AF154965.1	·	·	T	T	·	·	·	·	·	T	G	·	T	·	·
AF154964.1	·	·	T	T	·	·	·	·	·	T	G	·	T	·	·
NC020642.1	·	·	T	T	·	·	·	·	·	T	G	·	T	·	·
AF057130.1	·	·	T	T	·	·	·	·	·	T	G	·	T	·	·
HM106324.1	·	·	T	T	·	·	·	·	·	T	G	·	T	·	·
AY121352.1	·	·	T	T	·	·	·	·	·	T	G	·	T	·	·
AY121344.1	·	·	T	T	·	·	·	·	·	T	G	·	T	·	·
AY121341.1	·	·	T	T	·	·	·	·	·	T	G	·	T	·	·
AY121321.1	·	·	T	T	·	·	·	·	·	T	G	·	T	·	·
AY121318.1	·	·	T	T	·	·	·	·	·	T	G	·	T	·	·
AY121280.1	·	·	T	T	·	·	·	·	·	T	G	·	T	·	·

*– indicates no nucleotide at that position, · indicates no difference from *M. foina*

* some nucleotides are ambiguous and are represented by M (A or C), K (G or T), W (A or T), Y (C or T), R (A or G), or D (A, G, or T) based on IUPAC designations

Table 5 continued

Specimen	48	60	61	69	82	156	198	243	268	294	300	318	330	345	438
AY121279.1	·	·	T	T	·	·	·	·	·	T	G	·	T	·	·
AY121277.1	·	·	T	T	·	·	·	·	·	T	G	·	T	·	·
AY121275.1	·	·	T	T	·	·	·	·	·	T	G	·	T	·	·
AY121273.1	·	·	T	T	·	·	·	·	·	T	G	·	T	·	·
AY121250.1	C	·	T	T	·	·	·	·	·	T	G	·	T	·	·
AY121249.1	C	·	T	T	·	·	·	·	·	T	G	·	T	·	·
AY121193.1	C	·	T	T	·	·	·	·	·	T	G	·	T	·	·
AY121187.1	C	·	T	T	A	·	·	·	·	T	G	·	T	·	·
EU873311.1	C	·	T	T	A	·	·	·	·	T	G	·	T	·	·
EU873310.1	·	·	·	·	·	·	·	·	·	·	·	·	·	·	·
EU873309.1	·	·	·	·	·	·	·	T	·	·	·	·	·	·	·
EU873308.1	·	·	·	·	·	·	·	·	·	·	·	·	·	·	·
EU873307.1	·	·	·	·	·	·	·	·	·	·	·	·	·	·	·
EU873304.1	·	·	·	·	·	·	C	·	·	·	·	·	·	·	·
EU873303.1	·	·	·	·	·	·	·	·	·	·	·	·	·	C	·
EU873302.1	·	·	·	·	·	·	·	·	·	·	·	·	·	C	·
EU873301.1	·	·	·	·	·	·	·	·	·	·	·	·	·	·	·
EU873300.1	·	·	·	·	·	·	·	·	·	·	·	·	·	·	·
EU873299.1	C	·	T	T	·	T	·	·	·	T	G	·	T	·	·
EU873298.1	C	·	T	T	·	·	·	·	·	T	G	·	T	·	·

*– indicates no nucleotide at that position, · indicates no difference from *M. foina*

* some nucleotides are ambiguous and are represented by M (A or C), K (G or T), W (A or T), Y (C or T), R (A or G), or D (A, G, or T) based on IUPAC designations

Table 5 continued

Specimen	48	60	61	69	82	156	198	243	268	294	300	318	330	345	438
EU873297.1	C	·	T	T	·	·	·	·	·	T	G	·	T	·	·
EU873296.1	C	·	T	T	·	·	·	·	C	T	G	·	T	·	·
EU873295.1	·	·	T	T	·	·	·	·	·	T	G	·	T	·	·
EU873294.1	C	·	T	T	·	·	·	·	·	T	G	·	T	·	·
EU873293.1	·	·	T	T	·	·	·	·	·	T	G	·	T	·	C
EU873292.1	C	·	T	T	·	·	·	·	·	T	G	·	T	·	·
EU873291.1	·	·	·	·	·	·	·	·	·	·	·	·	·	·	·
EU873290.1	·	·	·	·	·	·	·	·	·	·	·	·	·	·	·
EU873289.1	·	·	·	·	·	·	·	·	·	·	·	·	·	·	·
EU873288.1	·	·	·	·	·	·	·	·	·	·	·	C	·	·	·
EU873287.1	C	·	T	T	·	·	·	·	·	T	G	·	T	·	
AF448238.1	C	·	T	T	·	·	·	·	·	T	G	·	T	·	
AF448237.1	C	·	T	T	·	·	·	·	C	T	G	·	T	·	
AF268274.1	C	T	T	T	·	·	·	·	·	T	G	·	T	·	
AF268273.1	·	·	T	T	·	·	·	·	·	T	G	·	T	·	
AF268272.1	·	·	T	T	·	·	·	·	·	T	G	·	T	·	
AB051234.1	·	·	T	T	·	·	·	·	·	T	G	·	T	·	

*– indicates no nucleotide at that position, · indicates no difference from *M. foina*

* some nucleotides are ambiguous and are represented by M (A or C), K (G or T), W (A or T), Y (C or T), R (A or G), or D (A, G, or T) based on IUPAC designations

Table 5 continued

Specimen	445	447	468	477	480	528	549	565	567	569	576	585	603	618	713
AF154974.1	T	G	C	T	T	G	C	A	C	C	A	T	C	T	T
AF154973.1	·	·	·	·	·	·	T	·	·	·	·	·	·	·	·
AF154972.1	·	·	·	·	·	·	T	·	·	·	·	·	·	·	·
AF154971.1	C	A	·	C	C	·	T	·	·	T	G	A	T	·	C
AF154970.1	·	·	·	·	·	·	T	·	·	·	·	·	·	·	·
AF154969.1	C	A	·	·	C	A	T	G	·	T	G	A	T	·	C
AF154968.1	C	A	·	·	C	A	T	G	·	T	G	A	T	·	C
AF154967.1	C	A	·	·	C	A	T	G	·	T	G	A	T	·	C
AF154966.1	C	A	·	·	C	A	T	G	·	T	G	A	T	·	C
AF154965.1	C	A	·	·	C	A	T	G	·	T	G	A	T	·	C
AF154964.1	C	A	·	·	C	A	T	G	·	T	G	A	T	·	C
NC020642.1	C	A	·	·	C	A	T	G	·	T	G	A	T	·	C
AF057130.1	C	A	·	·	C	A	T	G	·	T	G	A	T	·	C
HM106324.1	C	A	·	·	C	A	T	G	·	T	G	A	T	·	C
AY121352.1	C	A	·	·	C	A	T	G	·	T	G	A	T	·	C
AY121344.1	C	A	·	·	C	A	T	G	·	T	G	A	T	·	C
AY121341.1	C	A	·	·	C	A	T	G	T	T	G	A	T	·	C
AY121321.1	C	A	·	·	C	A	T	G	·	T	G	A	T	·	C
AY121318.1	C	A	·	·	C	A	T	G	·	T	G	A	T	·	C
AY121280.1	C	A	·	·	C	A	T	G	·	T	G	A	T	·	C

*– indicates no nucleotide at that position, · indicates no difference from *M. foina*

* some nucleotides are ambiguous and are represented by M (A or C), K (G or T), W (A or T), Y (C or T), R (A or G), or D (A, G, or T) based on IUPAC designations

Table 5 continued

Specimen	445	447	468	477	480	528	549	565	567	569	576	585	603	618	713
AY121279.1	C	A	·	·	C	A	T	G	·	T	G	A	T	·	C
AY121277.1	C	A	·	·	C	A	T	G	·	T	G	A	T	·	C
AY121275.1	C	A	·	·	C	A	T	G	·	T	G	A	T	·	C
AY121273.1	C	A	·	·	C	A	T	G	·	T	G	A	T	·	C
AY121250.1	C	A	·	·	C	·	T	·	·	T	G	A	T	·	C
AY121249.1	C	A	·	·	C	·	T	·	·	T	G	A	T	·	C
AY121193.1	C	A	·	·	C	·	T	·	·	T	G	A	T	·	C
AY121187.1	C	A	·	·	C	·	T	·	·	T	G	A	T	·	C
EU873311.1	C	A	·	·	C	·	T	·	·	T	G	A	T	·	C
EU873310.1	·	·	·	·	·	·	T	·	·	·	·	·	·	·	·
EU873309.1	·	·	·	·	·	·	T	·	·	·	·	·	·	·	·
EU873308.1	·	·	·	C	·	·	T	·	·	·	·	·	·	·	·
EU873307.1	·	·	·	C	·	·	T	·	·	·	·	·	·	·	·
EU873304.1	·	·	·	·	·	·	T	·	·	·	·	·	·	·	·
EU873303.1	·	·	·	·	·	·	T	·	·	·	·	·	·	·	·
EU873302.1	·	·	·	·	·	·	T	·	·	·	·	·	·	·	·
EU873301.1	·	·	·	·	·	·	T	·	·	·	·	·	·	·	·
EU873300.1	·	·	·	·	·	·	T	·	·	·	·	·	·	·	·
EU873299.1	C	A	·	C	C	·	T	·	·	T	G	A	T	·	C
EU873298.1	C	A	T	·	C	·	T	·	·	T	G	A	T	·	C

*– indicates no nucleotide at that position, · indicates no difference from *M. foina*

* some nucleotides are ambiguous and are represented by M (A or C), K (G or T), W (A or T), Y (C or T), R (A or G), or D (A, G, or T) based on IUPAC designations

Table 5 continued

Specimen	445	447	468	477	480	528	549	565	567	569	576	585	603	618	713
EU873297.1	C	A	·	·	C	·	T	·	·	T	G	A	T	·	C
EU873296.1	C	A	·	·	C	·	T	·	·	T	G	A	T	·	C
EU873295.1	C	A	·	·	C	A	T	G	·	T	G	A	T	C	C
EU873294.1	C	A	·	·	C	·	T	·	·	T	G	A	T	·	C
EU873293.1	C	A	·	·	C	A	T	G	·	T	G	A	T	·	C
EU873292.1	C	A	·	·	C	·	T	·	·	T	G	A	T	·	C
EU873291.1	·	·	·	·	·	·	T	·	·	·	·	·	·	·	·
EU873290.1	·	·	·	·	·	·	T	·	·	·	·	·	·	·	·
EU873289.1	·	·	·	·	·	·	T	·	·	·	·	·	·	·	·
EU873288.1	·	·	·	·	·	·	T	·	·	·	·	·	·	·	·
EU873287.1	C	A	T	·	C	·	T	·	·	T	G	A	T	·	C
AF448238.1	C	A	·	·	C	·	T	·	·	T	G	A	T	·	C
AF448237.1	C	A	·	·	C	·	T	·	·	T	G	A	T	·	C
AF268274.1	C	A	·	·	C	·	T	·	·	T	G	A	T	·	C
AF268273.1	C	A	·	·	C	A	T	G	·	T	G	A	T	·	C
AF268272.1	C	A	·	·	C	A	T	G	·	T	G	A	T	·	C
AB051234.1	C	A	·	·	C	A	T	G	·	T	G	A	T	·	C

*– indicates no nucleotide at that position, · indicates no difference from *M. foina*

* some nucleotides are ambiguous and are represented by M (A or C), K (G or T), W (A or T), Y (C or T), R (A or G), or D (A, G, or T) based on IUPAC designations

Table 5 continued

Specimen	722	732	770	783	792	810	813	841	843	897	898	910	918	921	987
AF154974.1	C	A	T	A	G	C	A	T	A	G	G	A	G	T	A
AF154973.1	T	·	·	·	·	·	·	·	·	·	·	·	·	·	·
AF154972.1	T	·	·	·	·	·	·	·	·	·	A		A	·	·
AF154971.1	T	·	·	G	A	T	G	C	G	A	·	G	·	C	G
AF154970.1	T	·	·	·	·	·	·	·	·	·	·	·	·	·	·
AF154969.1	T	·	·	G	A	T	G	C	G	A	·	G	·	C	·
AF154968.1	T	·	·	G	A	T	G	C	G	A	·	G	C	C	·
AF154967.1	T	·	·	G	A	T	G	C	G	A	·	G	C	C	·
AF154966.1	T	·	·	G	A	T	G	C	G	A	·	G	C	C	·
AF154965.1	T	·	·	G	A	T	G	C	G	A	·	G	C	C	·
AF154964.1	T	·	·	G	A	T	G	C	G	A	·	G	C	C	·
NC020642.1	T	·	·	G	A	T	G	C	G	A	·	G	C	C	·
AF057130.1	T	·	·	G	A	T	G	C	G	A	·	G	C	C	·
HM106324.1	T	·	·	G	A	T	G	C	G	A	·	G	C	C	·
AY121352.1	T	·	·	G	A	T	G	C	G	A	·	G	C	C	·
AY121344.1	T	·	·	G	A	T	G	C	G	A	·	G	C	C	·
AY121341.1	T	·	·	G	A	T		C	G	A	·	G	·	C	·
AY121321.1	T	·	·	G	A	T	G	C	G	A	·	G	C	C	·
AY121318.1	T	·	·	G	A	T	G	C	G	A	·	G	C	C	·
AY121280.1	T	·	·	G	A	T	G	C	G	A	·	G	C	C	·

*– indicates no nucleotide at that position, · indicates no difference from *M. foina*

* some nucleotides are ambiguous and are represented by M (A or C), K (G or T), W (A or T), Y (C or T), R (A or G), or D (A, G, or T) based on IUPAC designations

Table 5 continued

Specimen	722	732	770	783	792	810	813	841	843	897	898	910	918	921	987
AY121279.1	T	·	·	G	A	T	G	C	G	A	·	G	C	C	·
AY121277.1	T	·	·	G	A	T	G	C	G	A	·	G	C	C	·
AY121275.1	T	·	·	G	A	T	G	C	G	A	·	G	C	C	·
AY121273.1	T	·	·	G	A	T	G	C	G	A	·	G	C	C	·
AY121250.1	T	·	·	G	A	T	G	C	G	A	·	G	·	C	G
AY121249.1	T	·	·	G	A	T	G	C	G	A	·	G	·	C	G
AY121193.1	T	·	·	G	A	T	G	C	G	A	·	G	·	C	G
AY121187.1	T	·	·	G	A	T	G	C	G	A	·	G	·	C	G
EU873311.1	T	·	·	G	A	T	G	C	G	A	·	G	·	C	G
EU873310.1	T	·	·	·	·	·	·	·	·	·	·	·	·	·	·
EU873309.1	T	·	·	·	·	·	·	·	·	·	A	·	A	·	·
EU873308.1	T	·	·	·	·	·	·	·	·	·	·	·	·	·	·
EU873307.1	T	·	·	·	·	·	·	·	·	·	·	·	·	·	·
EU873304.1	T	·	·	·	·	·	·	·	·	·	·	·	·	·	·
EU873303.1	T	·	C	·	·	·	·	·	·	·	·	·	·	·	·
EU873302.1	T	·	C	·	·	·	·	·	·	·	·	·	·	·	·
EU873301.1	T	·	C	·	·	·	·	·	·	·	·	·	·	·	·
EU873300.1	T	·	C	·	·	·	·	·	·	·	·	·	·	·	·
EU873299.1	T	·	·	G	A	T	G	C	G	A	·	G	·	C	G
EU873298.1	T	·	·	G	A	T	G	C	G	A	·	G	·	C	G

*– indicates no nucleotide at that position, · indicates no difference from *M. foina*

* some nucleotides are ambiguous and are represented by M (A or C), K (G or T), W (A or T), Y (C or T), R (A or G), or D (A, G, or T) based on IUPAC designations

Table 5 continued

Specimen	722	732	770	783	792	810	813	841	843	897	898	910	918	921	987
EU873297.1	T	·	C	G	A	T	G	C	G	A	·	G	·	C	G
EU873296.1	T	·	·	G	A	T	G	C	G	A	·	G	·	C	G
EU873295.1	T	·	·	G	A	T	G	C	G	A	·	G	·	C	·
EU873294.1	T	·	C	G	A	T	G	C	G	A	·	G	·	C	G
EU873293.1	T	·	·	G	A	T	G	C	G	A	·	G	·	C	·
EU873292.1	T	·	C	G	A	T	G	C	G	A	·	G	·	C	G
EU873291.1	T	·	C	·	·	·	·	·	·	·	·	·	·	·	·
EU873290.1	T	·	C	·	·	·	·	·	·	·	·	·	·	·	·
EU873289.1	T	·	·	·	·	·	·	·	·	·	·	·	·	·	·
EU873288.1	T	·	C	·	·	·	·	·	·	·	·	·	·	·	·
EU873287.1	T	·	·	G	A	T	G	C	G	A	·	G	·	C	G
AF448238.1	T	·	C	G	A	T	G	C	G	A	·	G	·	C	G
AF448237.1	T	·	·	G	A	T	G	C	G	A	·	G	·	C	G
AF268274.1	T	·	·	G	A	T	G	C	G	A	·	G	·	C	G
AF268273.1	T	·	·	G	A	T	G	C	G	A	·	G	·	C	·
AF268272.1	T	G	·	G	A	T	G	C	G	A	·	G	·	C	·
AB051234.1	T	·	·	G	A	T	G	C	G	A	·	G	·	C	·

*– indicates no nucleotide at that position, · indicates no difference from *M. foina*

* some nucleotides are ambiguous and are represented by M (A or C), K (G or T), W (A or T), Y (C or T), R (A or G), or D (A, G, or T) based on IUPAC designations

Table 5 continued

Specimen	999	1065	1090	1095	1107	1129
AF154974.1	C	G	G	C	C	C
AF154973.1	·	·	A	·	·	·
AF154972.1	·	·	A	·	·	·
AF154971.1	T	A	A	T	T	T
AF154970.1	·	·	·	·	·	·
AF154969.1	T	A	A	T	T	T
AF154968.1	T	A	A	T	T	T
AF154967.1	T	A	A	T	T	T
AF154966.1	T	A	A	T	T	T
AF154965.1	T	A	A	T	T	T
AF154964.1	T	A	A	T	T	T
NC020642.1	T	A	A	T	T	T
AF057130.1	T	A	A	T	T	T
HM106324.1	T	A	A	T	T	T
AY121352.1	T	A	A	T	T	T
AY121344.1	T	A	A	T	T	T
AY121341.1	T	A	A	T	T	T
AY121321.1	T	A	A	T	T	T
AY121318.1	T	A	A	T	T	T
AY121280.1	T	A	A	T	T	T

*– indicates no nucleotide at that position, · indicates no difference from *M. foina*

* some nucleotides are ambiguous and are represented by M (A or C), K (G or T), W (A or T), Y (C or T), R (A or G), or D (A, G, or T) based on IUPAC designations

Table 5 continued

Specimen	999	1065	1090	1095	1107	1129
AY121279.1	T	A	A	T	T	T
AY121277.1	T	A	A	T	T	T
AY121275.1	T	A	A	T	T	T
AY121273.1	T	A	A	T	T	T
AY121250.1	T	A	A	T	T	T
AY121249.1	T	A	A	T	T	T
AY121193.1	T	A	A	T	T	T
AY121187.1	T	A	A	T	T	T
EU873311.1	T	A	A	T	T	T
EU873310.1	·	·	A	·	·	·
EU873309.1	·	·	A	·	·	·
EU873308.1	·	·	A	·	·	·
EU873307.1	·	·	A	·	·	·
EU873304.1	·	·	·	·	·	·
EU873303.1	·	·	A	·	·	·
EU873302.1	·	·	A	·	·	·
EU873301.1	·	·	A	·	·	·
EU873300.1	·	·	A	·	·	·
EU873299.1	T	A	A	T	T	T
EU873298.1	T	A	A	T	T	T

*– indicates no nucleotide at that position, · indicates no difference from *M. foina*

* some nucleotides are ambiguous and are represented by M (A or C), K (G or T), W (A or T), Y (C or T), R (A or G), or D (A, G, or T) based on IUPAC designations

Table 5 continued

Specimen	999	1065	1090	1095	1107	1129
EU873297.1	T	A	A	T	T	T
EU873296.1	T	A	A	T	T	T
EU873295.1	T	A	A	T	T	T
EU873294.1	T	A	A	T	T	T
EU873293.1	T	A	A	T	T	T
EU873292.1	T	A	A	T	T	T
EU873291.1	·	·	A	·	·	·
EU873290.1	·	·	A	·	·	·
EU873289.1	·	·	A	·	·	·
EU873288.1	·	·	A	·	·	·
EU873287.1	T	A	A	T	T	T
AF448238.1	T	A	A	T	T	T
AF448237.1	T	A	A	T	T	T
AF268274.1	T	A	A	T	T	T
AF268273.1	T	A	A	T	T	T
AF268272.1	T	A	A	T	T	T
AB051234.1	T	A	A	T	T	T

*– indicates no nucleotide at that position, · indicates no difference from *M. foina*

* some nucleotides are ambiguous and are represented by M (A or C), K (G or T), W (A or T), Y (C or T), R (A or G), or D (A, G, or T) based on IUPAC designations

Table 6. 12S Best-fit Nucleotide Substitution Model

Cut	Sequence Length (bp)	Best-fit Model	AIC
3’	691	TN93	1931.61
	591	TN93	1226.52
	491	TN93	1072.75
	391	TN93	769.40
	291	TN93	478.19
	191	K2	190.19
5’	691	TN93	1931.61
	591	TN93	1687.09
	491	TN93	1393.98
	391	TN93	1110.52
	291	HKY	816.16
	191	TN93	511.59

Table 7. 16S Best-fit Nucleotide Substitution Model

Cut	Sequence Length	Best-fit Model	AIC
3’	1335	TN93+G	1375.11
	1235	TN93+G	3611.77
	1135	TN93+G	3290.53
	1035	TN93+G	2991.87
	935	HKY+G	2677.59
	835	TN93+G	2303.95
	735	TN93+G	1969.15
	635	TN93+G	1656.42
	535	HKY+G	1365.91
	435	HKY+G	1071.35
	335	HKY+G	884.72
	235	HKY+G	715.93
	135	HKY+G	392.41
5’	1335	TN93+G	1375.11
	1235	TN93+G	3681.41
	1135	GTR+G	3313.30
	1035	TN93	3169.57
	935	TN93	2888.03
	835	TN93	2734.23
	735	HKY	2400.58
	635	HKY	2102.10
	535	HKY	1812.66
	435	HKY	1460.90
	335	TN92	1080.27
	235	TN92	793.07
	135	TN92	499.22

Table 8. Dloop Best-fit Nucleotide Substitution Model

Cut	Sequence Length	Best-fit Model	AIC
3’	540	HKY+G+I	1754.32
	440	HKY+G	1738.12
	340	HKY+G	1410.62
	240	HKY+G+I	945.15
	140	TN93+I	449.83
5’	540	HKY+G+I	1754.32
	440	HKY+G	1738.12
	340	HKY+G	1410.62
	240	HKY+G+I	945.15
	140	TN93+I	449.83

Table 9. Cytochrome b Best-fit Nucleotide Substitution Model

Cut	Sequence Length	Best-fit Model	AIC
3’	1140	HKY+G	4029.16
	1040	HKY+G	3688.20
	940	HKY+G	3372.14
	840	HKY+G	3036.91
	740	HKY+G	2711.23
	640	TN93+G	2336.18
	540	TN93+G	1974.60
	440	TN93+G	1682.03
	340	TN93	1336.52
	240	HKY+I	1003.40
	140	HKY	659.28
5’	1140	HKY+G	4029.16
	1040	HKY+G	3693.48
	940	HKY+G	3386.47
	840	HKY+G	3019.89
	740	TN93	2668.47
	640	TN93	2360.89
	540	TN93	1986.27
	440	TN93	1621.35
	340	TN93	1312.23
	240	TN93	959.76
	140	TN93	658.85

Table 10. Results of SH Test for Single Gene Sequences

Gene	3’				5’			
	Best-fit	**ln Log**	**Significantly Different (p<0.05)**	**ln Log**	**Best-fit**	**ln Log**	**Significantly Different (p<0.05)**	**ln Log**
12S	591bp	1105.86	NA	NA	591bp	1105.86	491bp	1126.34
16S	735bp	2280.57	NA	NA	535bp	2287.96	≤135bp	2306.60
Dloop	340bp	1230.44	≤140bp	1317.83	340bp	1230.44	≤140bp	1317.83
Cytb	1140bp	1915.32	≤340bp	≥2005.98	1140bp	1915.32	≤440bp	≥2011.31

Table 11. Concatenated Sequence Best-fit Nucleotide Substitution Model

Removed Gene	**Best-fit Model**	**AIC**
None	TN93+G	10265.09
12S	GTR+G	8125.24
16S	HKY+G	7106.24
Dloop	GTR+G	8396.03
Cytb	TN93+G	7141.73

Table 12. Results of SH Test for Concatenated Gene Sequence

Removed Gene	**ln Log**	***p***
None	6217.79	Best-fit
12S	6217.79	0.77
16S	6246.05	*0.02*
Dloop	6229.06	0.10
Cytb	6246.05	*0.02*

Figures

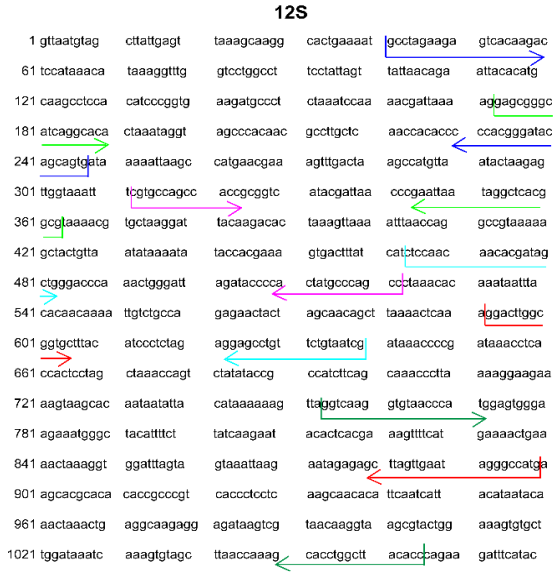
12S
1 gttaatgtag cttattgagt taaagcaagg cactgaaaat gcctagaaga gtcacaagac
61 tccataaaca taaaggtttg gtcctggcct tcctattagt tattaacaga attacacatg
121 caagcctcca catcccggtg aagatgccct ctaaatccaa aacgattaaa aggagcgggc
181 atcaggcaca ctaaataggt agcccacaac gccttgctc aaccacaccc ccacgggatac
241 agcagtgata aaaattaagc catgaacgaa agtttgacta agccatgtta atactaagag
301 ttggtaaatt tcgtgccagcc accgcggtc atacgattaa cccgaattaa taggctcacg
361 gcgtaaaacg tgctaaggat tacaagacac taaagttaaa atttaaccag gccgtaaaaa
421 gctactgtta atataaaata taccacgaaa gtgactttat catctccaac aacacgatag
481 ctgggaccca aactgggatt agataccccc ctatgcccag cctaaacac aaataattta
541 cacaacaaaa ttgtctgcca gagaactact agcaacagct taaaactcaa aggacttggc
601 ggtgctttac atcctctag aggagcctgt tctgtaatcg ataaaccccg ataaacctca
661 ccatcctag ctaaaccagt ctatataccg ccatcttcag caaacctta aaaggaagaa
721 aagtaagcac aataatatta cataaaaaag ttaggtcaag gtgtaaccca tggagtggga
781 agaaatgggc tacattttct tatcaagaat acactcacga aagttttcat gaaaactgaa
841 aactaaaggt ggatttagta gtaaattaag aatagagagc ttagttgaat agggccatga
901 agcacgcaca caccgcccgt caccctcctc aagcaacaca ttcaatcatt acataataca
961 aactaaactg aggcaagagg agataagtcg taacaaggta agcgtactgg aaagtgtgct
1021 tggataaatc aaagtgtagc ttaaccaaag cacctggctt acacccagaa gatttcatac


16S
1 tggataaatc aaagtgtagc ttaaccaaag cacctggctt acacccagaa gatttcatac
61 gacatgacca ctttgaacta aagctagccc aaccacccac taaccaact accacgacat
121 ccctcaaatc aaaacattta accacacatt acagtatagg agatagaaat tctacttgga
181 gctatagaga aagtaccgca agggaatgat gaaagaaaat tcaaagtaat aaacagcaaa
241 gtctacccct tatacctttt gcataatgag ctagctagaa taatttagcg aagagacctt
301 aagctaactc ccccgaaacc agacgagcta cctatgagca atccacaggg ataaactcat
361 ctatgtcgca aaatagtgag aagacttgca ggtagaggtg aaaagcctaa cgagcctggt
421 gatagctggt tgcccagaat agaattttag ttcaacttta aatttaccta aaaacccaaa
481 aaattataat gtaaatttaa aatatagtct aaaaaggtac agcttttttag aacaaggaaa
541 caaccttgct taagagagtaa aattaaacaa aaccatagta ggcctaaaag cagccaccaa
601 ttaagaaagc gttcaagctc aacaatataa ccccttaat cccaaaaaac cctaaccaac
661 tcctaacgta tcactgggct aatctattta acaatagaag caataatgct agtatgagta
721 acaagaagta cttctccttg cacaagctta taacagtcaa cgaatgccca ctgatagtta
781 acaacacgat aaaaataaac cactaataaa acatctatca aaccaattgt tagcccaaca
841 caggcgtgca gtaaggaaag attaaaagaa gtaaaaggaa ctcggcaaac acaaaccccg
901 cctgtttacc aaaaacatca cctccagcat actcagtatt ggaggcactg cctgccagt
961 gacattagtt taacggccgc ggtatcctg accgtgcaaag gtagcataat catttgttct
1021 ctaaataagg acttgtatga atggccacac gagggtttaa ctgtctctta cttccaatca
1081 gtgaaattga ccccccgtg aagaggcggg gataaattaa taagacgaga agaccctatg
1141 gagctttaat taactaaccc atagtaagaa cacttaacca ccaaccaggt ctaacaagac
1201 cttactaatg ggttagcaat ttaggttggg gtgacctcgg agaataaaac aacctccgag
1261 tgatacaagc acagacatac cagtcaaagc atcctatcat ttattgatcc aataacttga
1321 tcaacggaac aagttaccct agggataaca gcgcaatcct atttgagagt ccatatcaac
1381 aataggttt atgacctcga tgttggatca ggacatcccg atggtgcagc agctatcaag
1441 ggttcgtttg ttcaacgatt aaagtcctac gtgatctgag ttcagaccgg agtaatccag
1501 gtcggtttct atctattaca gtaacttctc ccagtacgaa aggacaagag aagtaaggcc
1561 cactctactg gaatgcctta ggactaatag atgatataat cttaatctag ccagtctatc
1621 taattccata accctagaga tagggtttgt tagggtggca gagcccagta attgtgtaaa

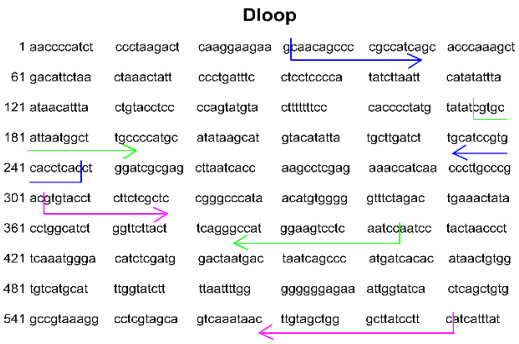
Dloop
1 aaccccatct ccctaagact caaggaagaa gcaacagccc cgccatcagc acccaaagct
61 gacattctaa ctaaactatt ccctgatttc ctcctcccca tatcttaatt catatattta
121 ataacattta ctgtacctcc ccagtatgta ctttttttcc caccctatg tatatcgtgc
181 attaatggct tgccccatgc atataagcat gtacatatta tgcttgatct tgcatccgtg
241 cacctcagct ggatcgcgag cttaatcacc aagcctcgag aaaccatcaa ccctgcccg
301 atgtgtacct cttctcgctc cgggcccata acatgtgggg gtttctagac tgaaactata
361 cctggcatct ggttcttact tcagggccat ggaagtcctc aatccaatcc tactaaccct
421 tcaaatggga catctcgatg gactaatgac taatcagccc atgatcacac ataactgtgg
481 tgtcatgcat ttggtatctt ttaattttgg gggggagaa attggtatca ctcagctgtg
541 gccgtaaagg cctcgtagca gtcaaataac ttgtagctgg gcttatcctt catcatttat


Cytochrome b
1 ataagaacat taatgaccaa cattcgtaaa acccacccac tagctaaaat cattaaca
61 tcatttattcg acttacctgc tccatcaaac atttcogcat gatgaaacti cggctcoctc
121 cttggaatct gcctaatcct acagattctt acaggtttat ttctagccat acactacaca
181 tcagatacag ccacagcctt ctcatcagtt acccacattt gccgagatgt caactacggc
241 tgaattatcc gatacataca tgccaatggg gcttccatat tcttcatctg cctgttcctg
301 cacgttggac ggggcctata ctatggatct tatatatacc ctgaaacatg gaatattggc
361 atcatcctat tattcgcagt tatagcaaca gcattcatag gttacgttct gccatgagga
421 caaatatcct tttgaggtgc gaccgtaatt accaacctac tgtcagccat cccctacatc
481 ggaaccagtc tcgtagaatg aatctgagga ggattctcgg tagacaaggc taccctaacg
541 cgattcttcg ccttccactt tatcctgcca ttcatcatct tagcattggc agcagtacac
601 cttctattcc tccatgaaac aggatccaat aaccctcag gaatccoctc cgattctgac
661 aaaatcccat tccacccata ctacaccatc aaagacatcc taggcgccct attcctaatc
721 ctagccctca taatactagt actattctca cccgaccttc tgggagaccc agacaactac
781 acccccgcca acccgctcaa cacaccaccc catattaaac ctgagtgata cttcctgttc
841 gcatatgcaa tcctgcgatc catccccaac aaactaggag gagtactagc cctagtcttc
901 tccatcctag tcctggcaat tgtcccattg ctccatactt caaaacaacg aggcatgata
961 ttccgcccac tcagccaatg cctattctga ctattagtgg ctgacctcct taccttaacc
1021 tggattggag gacagcccgt agaacaccca ttcatcacta tcggtcaact agcctcaatc
1081 ctctacttcg caatccttct aatccttatg ccagccatta gcattattga aaataaccta
1141 ttaaaatgaa gagtctttgt agtatattga ttacctggt ctgtaaacc aaaaatggag

Figure 1. Primer design overlap in 12S, 16S, Dloop, and cytb. Arrows indicate the region of each gene targeted by a primer set. Arrows pointing right represent forward primers and those pointing left are reverse primers. The length of the arrow represents the primer sequence length. Matching arrow colors within a gene represent primer pairs.

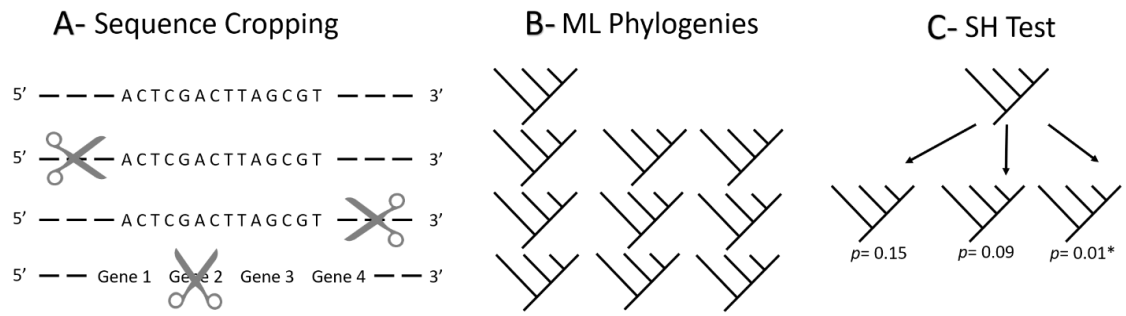

Figure 2. Methods used to determine the sequence length necessary in the 12S, 16S, Dloop, and cytb genes and a concatenated sequence of the four genes to produce accurate phylogenetic relationships. A) Complete or nearly complete gene sequences were subsampled in 100bp increments from the 3' and 5' ends independently. In addition, the concatenated sequence was subsampled by entirely removing one gene. B) I then ran a ML phylogeny for each complete gene and each subsample using their best-fit nucleotide substitution model. C) The resulting tree topologies were fit to the full gene sequence alignment and the goodness of fit for each topology was determined from natural log-likelihood values. Those trees that significantly differed in topology from the best-fit tree were interpreted as being too short or not containing the most phylogenetically informative genes to produce accurate phylogenetic relationships.

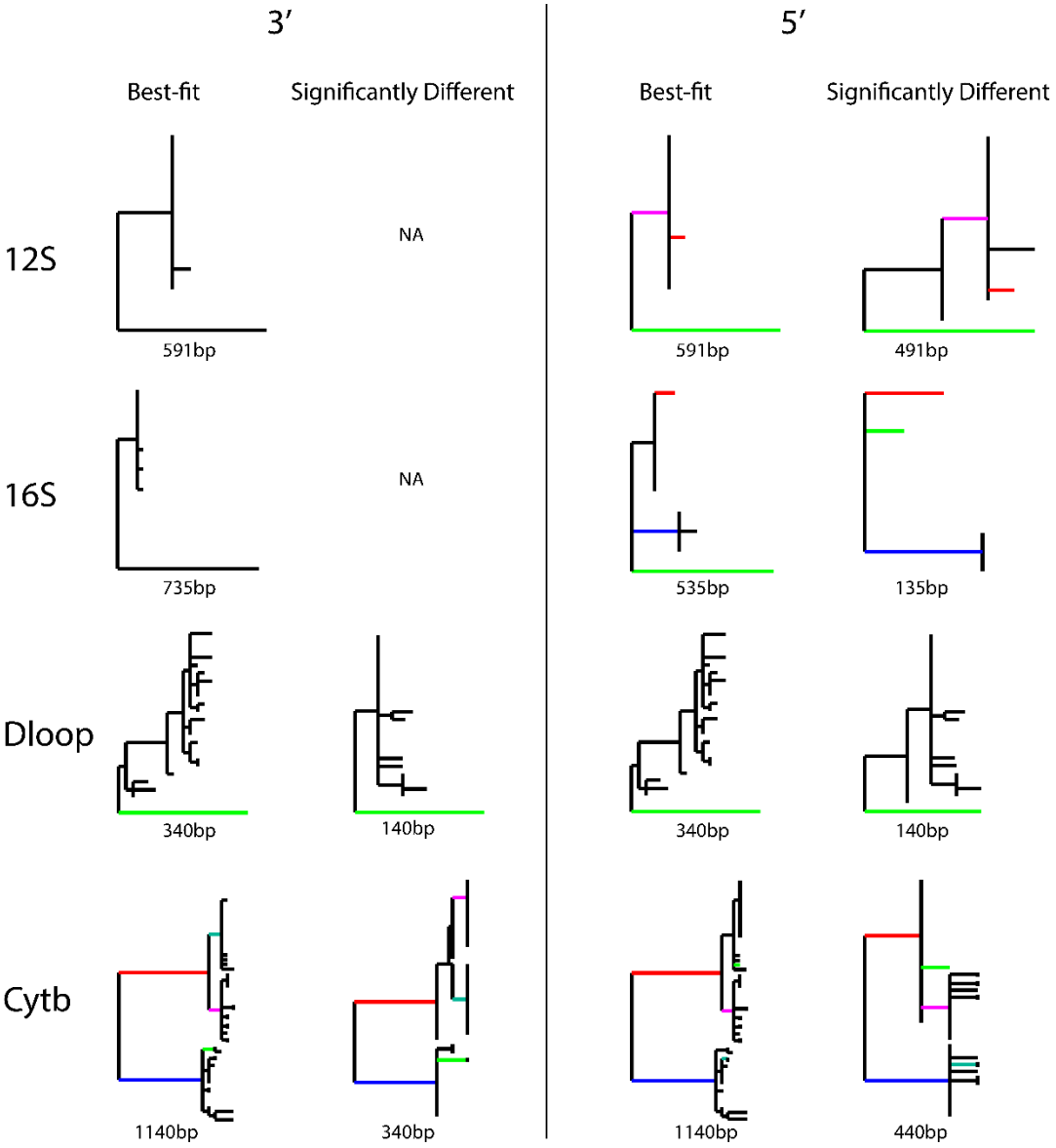

Figure 3. Phylogenetic tree topologies from 12S, 16S, Dloop, and cytb that were found by the SH test to be the best-fit for the complete sequence data and significantly different from the best-fit topology. The topologies on the left are those created from subsampling from the 3' end and those on the right were created by subsampling from the 5' end. NA indicates no topologies were found to be significantly different. Numbers beneath each topology indicate the number of base pairs used to construct the phylogeny. Branch colors that are the same in each gene between the best-fit and significantly different topologies represent nodes that contain the same specimens and

are, therefore, equivalent between the two topologies. Black branches indicate no similarity is present.

Full Sequence

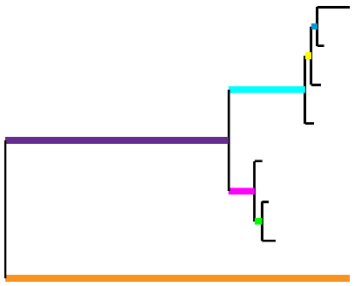

Best-fit

12S Removed

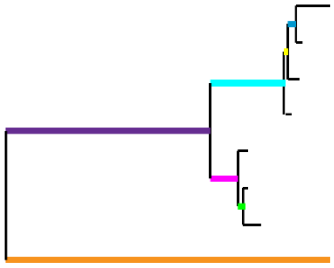

p=0.77

16S Removed

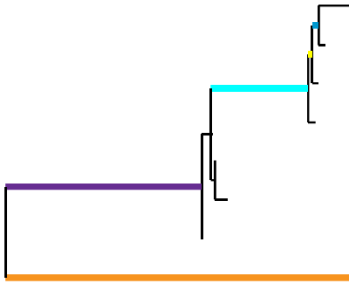

p=0.02

Cytb Removed

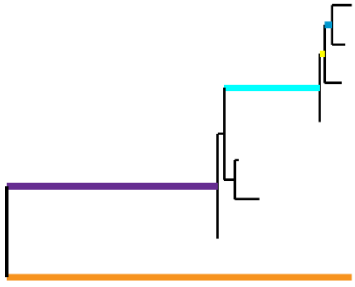

p=0.02

Dloop Removed

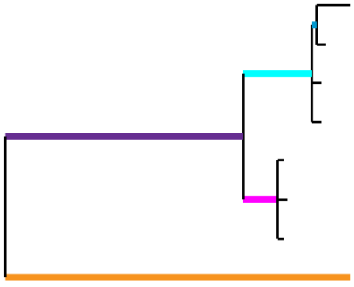

p=0.10

Figure 4. Phylogenetic tree topologies from the concatenated 12S, 16S, cytb, and Dloop gene sequences. The topology to the left was created from the entire concatenated sequence and was found to be the best-fit to the dataset. The remaining four trees were created from concatenated sequences where 12S, 16S, cytb, and Dloop were each removed independently. Significant *p*-values indicate the topology was found to significantly differ from the best-fit topology by the SH test. Branch colors that are the same in each subsample between the best-fit and significantly different topologies represent nodes that contain the same specimens.

CHAPTER IV

MITOCHONDRIAL PHYLOGENETIC RELATIONSHIPS OF NORTH AMERICAN PINE MARTENS, *MARTES*, CONSTRUCTED FROM MULTIPLE MITOCHONDRIAL GENES SUPPORT PLEISTOCENE DIVERSIFICATION OF *M. AMERICANA* AND *M. CAURINA*

Introduction

The taxonomic status of North American pine martens (*Martes)* has been debated since the late 1800s (Merriam, 1890). The diverse morphology and pelage of these animals have resulted in the recognition of as many as 14 subspecies across their geographic range (Banfield, 1974; Clark et al., 1987; Dawson and Cook, 2012). Recently, the evolutionary relationships within living North American *Martes* have been studied using mitochondrial and nuclear DNA. These studies support the presence of two clades with distinct geographic ranges (Figure 1). Initially, based on cytochrome b (cytb) sequences, these clades were assigned a subspecific status. The geographic distribution of these subspecies comprised *M. americana americana* across the eastern U.S., Canada, and Alaska and *M. americana caurina* found in the western U.S. and Canada, as well as Alaskan islands (Cook et al., 2001; Stone et al., 2002). A genetic distance of 2.5-3.0% between these two clades was interpreted to be within the range of genetic distances commonly accepted for the delineation of mammalian subspecies (Bradley and Baker, 2001; Hoisington-Lopez et al., 2012; Nava-García et al., 2016; Sackett et al., 2014), further supporting this status. Since these studies were conducted, however, researchers have proposed that these

two subspecies should be elevated to the status of individual species based on relationships recovered from nuclear and mitochondrial DNA (Carr and Hicks, 1997; Dawson et al., 2017; Dawson and Cook, 2012). These new taxonomic statuses have not yet been recognized by the International Commission on Zoological Nomenclature. While these studies have provided much insight into the evolution of North American *Martes*, none have included populations from the eastern U.S. This is because recent genetic research has focused on the distribution and diversification of interacting populations of *M. caurina* and *M. americana* in western North America. A lack of Eastern populations in these studies may in turn have resulted in incomplete phylogenetic relationships and reduced genetic distance estimates.

Researchers have proposed that North American *Martes* underwent allopatric speciation during the Late Pleistocene (Dawson et al., 2017; Dawson and Cook, 2012; Stone et al., 2002). This speciation would have resulted from the isolation of marten populations into two glacial refugia, one in the eastern U.S. and the other in the western U.S. Fossil evidence supports the presence of *Martes* in these regions of North America during the Late Pleistocene (Bell, 1995; Eshelman and Grady, 1986; Grady, 1984; Guilday and Hamilton, 1978; Long, 1971; Mead and Mead, 1989; Sinclair, 1907; Tankersley, 1997; Wetmore, 1962). While a history of allopatric speciation is plausible, to date no studies have inferred when North American *Martes* last shared a common ancestor or underwent lineage diversification. In order to understand the climatic and ecological contexts under which *Martes* evolved, it is essential that their evolution be placed in a temporal context.

I sought to expand upon previous phylogenetic studies of North American *Martes* by studying specimens morphologically identified as *M. americana* and *M. caurina* from across their geographic range, including for the first time populations from the eastern U.S. Using sequences from four mitochondrial genes, I tested for the phylogenetic relationships between sampled specimens and sought to infer when these relationships arose. In addition, I compared genetic

distances between *M. americana* and *M. caurina* calculated from multiple mitochondrial genes to those previously reported values produced from cytb.

Institutional Abbreviations

East Tennessee State Museum of Natural History (ETMNH), New York State Museum (NYSM), Florida Museum of Natural History (FLMNH), Museum of Southwestern Biology (MSB), Burke Museum of Natural History and Culture (BMUW), University of Alaska Museum of the North (UAMN), University of Michigan Museum of Zoology (UMMZ), and Smithsonian Institution National Museum of Natural History (USNM).

Material and Methods

Specimens

I included a total of 31 individuals morphologically identified as *M. americana* (N= 25) or *M. caurina* (N=6) (Appendix III, Section A). Specimens were collected across the U.S. range of these species between 2000 and 2013 (Figure 1). Contemporaneous specimens from Canada were unavailable. I used specimens housed in the collections at ETMNH, NYSM, FLMNH, MSB, BMUW, UAMN, UMMZ, and USNM. DNA sequences for one specimen of *M. caurina* were provided by J. Colella from MSB (Appendix III, Section B). In addition, I included complete mitochondrial gene sequences for the 12S, 16S, cytb, and Dloop genes for *Martes foina* from GenBank (NCBI) to be used as an outgroup (Appendix III, Section C).

DNA Extraction, Amplification, and Sequencing

From 30 specimens, I collected samples from a rib bone or soft tissue. I extracted genomic DNA from soft tissue using the following protocol: approximately 0.025 g of soft tissue was incubated at 55°C for 24 hours while rotating in 125 µL lysis buffer (Bello et al., 2001), 8.75 µL 20 mg/mL proteinase K, 5 µL 1 mg/mL RNase A, and 10 µL 5 mM DTT followed by a phenol:chloroform:isoamyl (25:24:1) extraction protocol (see detailed protocol in Appendix VI). I extracted genomic DNA from bone tissue using the silica binding protocol of Rohland (2012) (see detailed protocol in Appendix VI). Prior to sampling, all bones were cleaned in a 2-4% bleach solution, then rinsed and allowed to air dry. I then powdered the entire rib using a SPEX® Cryogenic Grinder. This yielded between 0.05 g and 0.1 g of powder (Appendix III, Section D, Table 1). I eluted all samples in 40-65 µL of 86°C elution buffer (10 mM Tris and 0.1mM EDTA). I quantified the amount of DNA present in all extractions using a ThermoFisher™ Qubit® (Appendix III, Section D, Table 1). Because bone tissue is often more degraded than soft tissue, DNA quantity was lower in extractions from bone tissue.

I amplified DNA in overlapping fragments ranging from 139-1,012bp, depending on the DNA quality of each specimen, using a polymerase chain reaction (PCR) (see detailed protocol in Appendix VII). The 12S, 16S, cytochrome b (cytb), and Dloop mitochondrial genes were all targeted using primers that I designed to span the entirety of each gene (Table 1; Appendix III, Section E, Figure S1). I designed 12S, 16S, and Dloop primers to amplify approximately 250bp regions with 50bp of overlap (Appendix III, Section E, Figure S1). I designed primers to have similar annealing temperatures, within 1°C, and with GC content of at least 60%. In some cases, the GC content criterion resulted in targeted priming sites that had less than 50bp of overlap (Figure 1). Primers for cytb were taken from (Stone and Cook, 2002). For all PCRs, I used a negative and positive control. I performed PCR amplifications in 20 µL volumes using separate protocols for bone and soft tissue extractions. For samples extracted from bone tissue, I amplified each gene using the following reagents: 1X PCR buffer, 2 mM $MgCl_2$, 200 µM dNTP, 1 mg/ml

BSA, 1.25 U ThermoFisher™ AmpliTaq Gold, and 0.4 µM of each primer. The PCR was conducted on a Labnet International, Inc. MultiGene Optimax thermocycler and cycling conditions were as follows: 95°C for 15 min; 35 cycles of 95°C for 15 s, 52-60°C for 30 s, 72°C for 30 s; 72°C for 5 min. For samples extracted from soft tissue, I amplified each gene using 1X PCR buffer, 2 mM $MgCl_2$, 200 µM dNTP, 1 mg/ml BSA, 1.25U Apex™ Taq, and 0.4 µM of each primer. The PCR cycling conditions were as follows: 95°C for 10 min; 35 cycles of 95°C for 15 s, 52-60°C for 90 s, 72°C for 30 s; 72°C for 5 min. I evaluated the success of each amplification by running 5 µL of dyed PCR product on a 2% agarose gel and imaging using a BioRad Gel Doc XR system.

I cleaned all PCR products using an Exo-Sap cleaning procedure and Sanger sequenced all forward and reverse strands on an Applied Biosystems 3130xl Genetic Analyzer (see detailed protocol in Appendix VIII) I edited all DNA sequences using CLC Main Workbench (Qiagen Bioinformatics).

Sequence Alignment and Nucleotide Substitution Modeling

Sequences obtained for 12S, 16S, Dloop, and cytb were initially short amplicons which had to be assembled against a reference genome. Here, I used the mitochondrial genome of *M. foina* (HM106325.1) as a reference. I assembled all sequences using CLC Main Workbench (Qiagen Bioinformatics). Using MEGA7 (Kumar et al., 2016), I then aligned the assembled sequences for each gene independently against the mitochondrial genome of *Martes foina* (HM106325.1), which acted as an outgroup. I used the ClustalW algorithm with the default parameters for all alignments and corrected any misalignments by hand. Because some sequences were partial, I trimmed all alignments to reduce the amount of missing data. This resulted in the following length ranges for each gene: 12S = 0-690bp; 16S = 224-1334bp; cytb = 235-934bp; Dloop = 0-

464bp. Previous analyses (Chapter 2) indicated that accurate phylogenetic relationships can only be constructed using sequence lengths of 0bp of 12S, >135bp of 16S, >340bp of cytb, and 0bp of Dloop in a concatenated sequence. I, therefore, removed all specimens from the final analysis that did not meet these thresholds. This resulted in 5 specimens of *M. caurina* and 14 specimens of *M. americana* as well as a single specimen of *M. foina* as an outgroup. I then concatenated the four genes into a single sequence of 3,425bp, allowing me to test phylogenetic relationships from all four genes simultaneously (Appendix III, Section D, Table 2).

I tested for the best-fit nucleotide substitution model for each gene independently and for the concatenated sequence in MEGA7 (Kumar et al., 2016) using a maximum likelihood model and an 85% site coverage cutoff because some specimens had missing data. I chose this cutoff because it allowed for some missing data while still more heavily considering the sites with full coverage. I chose the best-fit nucleotide substitution models as those with the lowest Akaike information criterion (AIC) (Table 2).

Maximum Likelihood Phylogeny

I tested for phylogenetic relationships between the 19 specimens included in the final concatenated sequence using a Maximum Likelihood (ML) analysis. This allowed me to determine evolutionary relationships under a heuristic model. I assigned the best-fit nucleotide substitution model for the concatenated sequence, which was GTR+G (AIC=5328.04) with four possible gamma states. The phylogeny was run using a Nearest-Neighbor-Interchange (NNI) heuristic method. Due to the partial nature of some sequences, I again allowed for an 85% site cutoff. To determine branch support, I ran 500 bootstrap replicates.

Bayesian Phylogeny

I also tested for phylogenetic relationships between specimens using a Bayesian Markov Chain Monte Carlo (MCMC) phylogenetic analysis. I ran this analysis using Beast 1.8.4 (Drummond et al., 2012). I unlinked the nucleotide substitution models for each gene and assigned the best-fit model to each: 12S = TN93; 16S = GTR; cytb = HKY; Dloop = GTR+G (Table 2). I chose a relaxed lognormal molecular clock (Drummond et al., 2006). Under simulated datasets, this clock model had the highest power for data evolving under both clocklike and non-clocklike conditions when compared to other strict and autocorrelated clock models (Drummond et al., 2006). I also assumed coalescence with a constant population size because this null is the most appropriate when testing for intraspecific evolutionary relationships (Kingman, 1982). A single MCMC chain was run for 100,000,000 iterations with parameters written every 1,000 generations (Table 3). I discarded the first 20% of trees as burn-in.

I time calibrated the phylogeny using three fossil calibration points: the divergence between the ingroup and outgroup clades; the node for crown *M. americana;* and the node for crown *M. caurina*. The first time calibration was for the last common ancestor of *M. americana, M. caurina,* and *M. foina*. Here I constrained the node using date records of *Martes vetus*, a European marten whose morphology suggests it was ancestral to the *Martes* subgenus (Anderson, 1970; 1994; Baryshnikov and Batyrov, 1994; Wiszniowska, 1989; Wolsan, 1989; 1990; 1993a). *M. vetus* is dated between 1.75 Ma and 2.0 Ma based on the chronological ranges of associated arvicoline rodents (Maul and Markova, 2007). I chose an upper bound of 5.33 Ma, or the Mio-Pliocene boundary, following the methods of Li et al. (2014) and the 95% confidence range of this node obtained in previous phylogenetic analysis of Mustelidae (Koepfli et al., 2008; Law et al., 2018). The chosen date range for this node was then 5.33-1.75 Ma (Table 3, 4) with a mean age of 3.54 Ma. The prior distribution for this node was a uniform distribution, which places equal probability of the node age spanning the interval between the two bounds (Table 3). It is an

appropriate distribution for calibrations defined by both a fossil age and previously calculated node age estimates (Heath, 2018).

Next, I time calibrated the nodes for crown *M. americana* and crown *M. caurina*. I assigned specimens to one of the two clades based on their placement in the ML phylogeny (Figure 2). I calibrated the nodes of each of these clades using the ages of fossils identified as *M. americana* from the fossilworks database (Behrensmeyer and Turner, 2013; Bell, 1995; Eshelman and Grady, 1986; Grady, 1984; Guilday and Hamilton, 1978; Long, 1971; Mead and Mead, 1989; Sinclair, 1907; Tankersley, 1997; Wetmore, 1962). The age of fossil specimens within the current and ancient geographic range of *M. caurina* were used to calibrate the *M. caurina* clade node and those within the current and ancient range of *M. americana* calibrated that clade's node. I assigned each node a range based on the first and last appearance of fossils within each geographic region. For the *M. caurina* clade, the date range was 1.8 Ma -117 ka (Bell, 1995; Long, 1971; Mead and Mead, 1989; Sinclair, 1907) with a mean of 905 ka and a standard deviation of 1.6 (Table 3, 4). The *M. americana* clade had a date range of 126-11.7 ka (Eshelman and Grady, 1986; Grady, 1984; Guilday and Hamilton, 1978; Tankersley, 1997; Wetmore, 1962) with a mean of 68.9 ka and standard deviation of 0.76 (Table 3, 4). These age ranges were interpreted as minimum ages under the assumption that these extinct populations lived after the divergence of each species. I assigned a lognormal prior distribution for each of these nodes (Table 3). This distribution is most appropriate when the node age is interpreted to be older than the fossils because this distribution curve places a higher probability on older age values (Bibi, 2013; Heath, 2018).

Tracer 1.6 (Rambaut et al., 2014) was used to check for convergence between runs and I checked Effective Sample Size (ESS) values for each prior to determine whether the posterior distributions of all parameters were well estimated. Finally, using TreeAnnotator 1.8.2 (Drummond et al., 2012), I compiled the maximum credibility tree from the post burn-in sample.

Lineage Diversification

To determine the rate at which pine marten lineages diversified, I first plotted log lineages through time using the constructed Bayesian phylogeny. I then calculated the gamma (γ) statistic (Pybus and Harvey, 2000), which is a measure of the relative position of nodes within the phylogeny. I then ran a constant-rates test using a Pure Birth null model of speciation, where the rates of lineage extinction are zero and lineages speciate at a constant rate or log-linearly through time (Yule, 1925). I did this using the ltt function in the ape package (Paradis et al., 2004) in R (R Core Team, 2015), which tests γ using a two-tailed test (Appendix III, Section F). A significantly positive γ value indicates that nodes are skewed toward the tips of the tree and that rates of diversification are increasing or remaining constant. Significantly negative γ values indicate that the majority of nodes are near the tree root and that rates of diversification are decreasing. It should be noted that while γ has high power when detecting recent decreases in diversification rates (Fordyce, 2010), its power is low when detecting rate acceleration (Fordyce, 2010; Pybus and Harvey, 2000).

Genetic Distances

To determine molecular divergence between *M. americana* and *M. caurina,* I calculated inter- and intraclade genetic distances. I used the concatenated sequence data and assigned specimens to the *M. americana* or *M. caurina* clade based on their position within the constructed phylogenies. I calculated uncorrected *p*, which is a ratio of the number of nucleotide matches between clades to the total number of nucleotides. This method allowed for comparison to previous studies (Stone et al., 2002). While informative, uncorrected *p* does not correct for multiple substitutions at a single locus. I, therefore, also calculated *p* using the best-fit nucleotide substitution model,

Tamura92+G (Tamura, 1992). This model allows for a difference in substitution rates between nucleotides, which are modeled from a gamma distribution (Tamura, 1992). For all analyses, standard error was calculated using 500 bootstrap replicates and I allowed for a site coverage cutoff of 85% due to the partial nature of some sequences.

Results

Maximum Likelihood Phylogeny

The ML phylogeny assigned each specimen to two major clades, with *M. foina* as the outgroup (Figure 2). The first clade contained specimens that were collected in Alaska, New Hampshire, Minnesota, New York, and Alaska and represents exclusively specimens of the *M. americana* clade. The second clade contained specimens from Idaho, Wyoming, and Washington and represents the *M. caurina* clade. These clade designations are based on both museum specimen identification and the geographic location from which specimens were collected. Bootstrap support for these clades was high, with 87% for *americana* and 97% for *M. caurina.* There were three bootstrap supported clades within *M. americana*: 1) specimens from Alaska and New Hampshire; 2) specimens from Minnesota; and 3) specimens from New Hampshire. The remaining *M. americana* specimens fell within a polytomy. *M. caurina* specimens were well differentiated by geographic location with the youngest branches from Washington and the oldest from Wyoming.

Bayesian Phylogeny

The Bayesian phylogeny comprises two major clades with 100% posterior probability support, one containing *M. americana* specimens and the other *M. caurina* specimens, with *M. foina* as the outgroup (Figure 3). Within the *M. americana* clade, specimens further subdivided into geographic regions (New York, New Hampshire, and Minnesota). These geographic divisions were not perfect, however, and specimens from Alaska, Minnesota, and New Hampshire were polyphyletic. In the *M. americana* clade, the youngest branches are specimens from New York, while branches with specimens from Washington were the youngest in the *M. caurina* clade. Because the phylogeny was time calibrated, the times at which clades originated were estimated. The outgroup node age was estimated at 2.12 Ma +/- 0.37 Ma, which fits previous age estimates of this divergence (Koepfli et al., 2008; Li et al., 2014). The last common ancestor of the *M. americana* and *M. caurina* clades is estimated to have existed 234 kya +/- 168 ka. Intraclade diversifications are inferred to have begun around 132 kya +/- 92 ka for the *M. americana* clade and 83 kya +/- 69 ka for the *M. caurina* clade.

Lineage Diversification

By plotting log lineages through time, I found diversity was relatively low and remained stable until 234 kya +/- 168 ka. Log lineage diversity then increased slightly, followed again by a period of stabilization until 132 kya +/- 92 ka. There was then a rapid increase, with diversity more than doubling between 132 kya +/- 92 ka and the Present (Figure 4). Gamma values were positive (γ=4.61) and significantly differed from the Pure Birth null model (p<0.01).

Genetic Distances

I found molecular distances between the *M. americana* and *M. caurina* clades was 2.2% (SE=0.004) when *p* was uncorrected and 2.3% (SE= 0.004) under a Tamura92+G nucleotide

substitution model. The *M. americana* clade had greater intraclade distances under both the uncorrected (*p*=0.46%, SE= 0.0009) and Tamura92+G (*p*=0.46%, SE=0.0007) models. Intraclade distances in the *M. caurina* clade were 0.38% under the uncorrected model (SE=0.001) and Tamura92+G (SE=0.001). The reduced distances in the *M. caurina* clade may be due to the smaller number of specimens assigned to this clade.

Discussion

The evolutionary relationships produced here from both the ML and Bayesian phylogenies support those found by previous researchers using single mitochondrial and nuclear genes (Dawson et al., 2017; Dawson and Cook, 2012; Small et al., 2003; Stone and Cook, 2002; Stone et al., 2002). Dawson and Cook (2012) and Dawson et al. (2017) recently designated living North American martens as two unique species, assigning populations across the eastern U.S., Canada, and Alaska to *M. americana* and those from the western U.S., western Canada, and Alaskan islands to *M. caurina* on the basis of skeletal morphology (Merriam, 1890), genetic variation (Carr and Hicks, 1997; Dawson and Cook, 2012), and parasitological evidence (Hoberg et al., 2012; Koehler et al., 2009). Both phylogenies produced here further support the genetic separation of populations from the eastern U.S. and Alaska from those collected in the western U.S. (Figure 2, 3). These phylogenetic relationships, however, provide neither evidence for nor against their taxonomic status as unique species.

The genetic distances calculated from the 12S, 16S, cytb, and Dloop concatenated sequence are consistent with previous values used to support the subspecific status of *M. americana* and *M. caurina* (Stone et al., 2002). Stone et al. (2002) reported that interclade divergence between these two populations was 2.5-3.0% based on cytb. This is slightly higher than the 2.2-2.3% calculated

here. Many mammal species have an interspecific divergence averaging 8.13% and an intersubspecific divergence averaging 0.0-4.21% (e.g., Aliabadian et al., 2009; Ambriz-Morales et al., 2016; Bradley and Baker, 2001; Brower, 1994; Clare et al., 2007; Mayer et al., 2007; Oshida et al., 2015; Rosel et al., 2017; Vences et al., 2005). This suggests that the taxonomic rank of subspecies may be more appropriate for the *M. americana* and *M. caurina* clades. Use of divergence values when assigning a taxonomic status, however, can be arbitrary as these ranges can vary widely across taxa (e.g., Aliabadian et al., 2009; Ambriz-Morales et al., 2016; Bradley and Baker, 2001; Brower, 1994; Clare et al., 2007; Mayer et al., 2007; Oshida et al., 2015; Rosel et al., 2017; Vences et al., 2005). As a result, other methods such as Bayesian species delimitation have been developed to more accurately designate species (see review in Rannala, 2015). It should be noted that *M. americana* and *M. caurina* do fit a form of the Phylogenetic Species Concept (Mayden, 1997; McKitrick and Zink, 1988) because they form monophyletic clades and are diagnosable using both molecular (Dawson et al., 2017; Slauson et al., 2009; Stone and Cook, 2002) and morphological characters (Anderson, 1970; 1994; Graham and Graham, 1994; Merriam, 1890; Meyers, 2007). This definition, however, can be problematic in taxa with high geographic, morphological, and molecular variation (Gutiérrez and Garbino, 2018; Tattersall, 2007), such as that exhibited by the North American marten (Chapter 1; Banfield, 1974; Clark et al., 1987; Giannico and Nagorsen, 1989; Hagmeier, 1958; Meyers, 2007; Nowak, 1999). Future application of species delimitation methods using multiple genes may aid in determining the taxonomic status of North American martens.

The subclades recovered in the *M. americana* clade may reflect a complex history of recent reintroduction, high gene flow, and/or ancient dispersal. Due to habitat loss and the fur trade, North American marten populations were extirpated or drastically reduced across the eastern U.S. (Banfield, 1974; Clark et al., 1987). In an effort to revive the species, many individuals were introduced from thriving populations in Canada, Maine, and New York into historic ranges (Kelly

et al., 2009; Proulx et al., 2005). Of the individuals studied here, only those from New Hampshire represent reintroduced populations, having been taken from Maine during the 1970s (Kelly et al., 2009; Proulx et al., 2005). While individuals from this region are polyphyletic, so too are specimens from Alaska and Minnesota, which represent original, thriving populations. Little genetic structure is present in microsatellite data from *M. americana* collected across Canada (Kyle et al., 2000), suggesting there are few barriers to gene flow across their wide geographic range. It is possible that the mitochondrial DNA of this species is reflecting a similar lack of structure, resulting in specimens from geographically isolated regions being closely related. In addition, it has been hypothesized that martens from the eastern U.S. expanded across Canada and into Alaska at the end of the Wisconsinan glaciation (Dawson et al., 2017; Stone et al., 2002). The phylogenetic placement of specimens from Alaska may be reflecting an origin from these ancient eastern populations. To date, however, no studies comparing genetic structure between populations in Alaska, Canada, and the eastern U.S. have been conducted to test these hypotheses.

By applying a molecular clock and time calibrations at nodes within the Bayesian phylogeny, I was able to estimate the timing and rate of lineage divergence in North American martens. Stone and Cook (2002) hypothesized that the last common ancestor of *M. americana* and *M. caurina* came into North America via the Bering land bridge and then dispersed across North America during an interglacial period. No dates, however, were provided to support this hypothesis. I inferred that the *M. americana* and *M. caurina* clades share a last common ancestor 243 kya +/- 168 ky (Figure 3). This is during the pre-Illinoian episode, which consists of multiple glacial interglacial cycles (2.4 Mya – 160 kya) (Rovey and Balco, 2011). Researchers have also hypothesized that North American martens underwent allopatric speciation because of glacial isolation during the Wisconsinan glaciation (Stone and Cook, 2002; Stone et al., 2002), although no specific dates of clade origination have been proposed. The results of the present study suggest

that the *M. americana* clade began to diversify 132 kya +/- 92 ky and that the *M. caurina* clade diversified beginning 83 kya +/-69 ky (Figure 3 and 4). The error on these dates places the diversification of these clades during either the Sangamonian interglacial period (130-155 kya) (Edwards et al., 1997; Shackleton et al., 2003; Stirling et al., 1998) or during the Wisconsinan glaciation (80-18 kya) (Clark et al., 2009; Dyke, 2004). Because fossil evidence places these clades within separate refugia during the Wisconsinan glaciation, I propose that these clades most likely diversified while isolated by glaciers. The diversification pattern seen here significantly differed from what would be predicted under a Pure Birth model. This indicates that nodes within the phylogeny are skewed toward the tree tips (present) and that rates of diversification increased through time. This could indicate that marten lineages: 1) have undergone exponential growth (Quental and Marshall, 2010); 2) are in the early stages of logistic growth (Liow et al., 2010); 3) are undergoing logistic growth with a low ratio of initial speciation to extinction rate (Quental and Marshall, 2009; Rabosky and Lovette, 2008) or; 4) have constant diversity and are experiencing a species turnover (Liow et al., 2010). The variety of possible interpretations is because γ has low power when detecting acceleration in phylogenies with recent diversification. While the log lineage through time plot suggests an increase in diversification rates, interpretations of how this pattern of diversification arose may be inaccurate.

This is not the first evidence of genetic divergence in a North American species during the Pleistocene. Many species of mammals, reptiles, amphibians, birds, fish, and insects are thought to have diversified as a result of isolation in novel habitats as Pleistocene glaciers expanded (see review in Shafer et al., 2010). Of particular interest for this study are the evolutionary histories of tree squirrels (*Tamiasciurus* sp.), voles (Arvicolinae), and small songbirds (Passeriformes) as they are some of the common prey items of North American pine martens (Banfield, 1974; Clark et al., 1987; Nowak, 1999; Zielinski and Duncan, 2004). Tree squirrels are interpreted to have been isolated by glaciers in the eastern, western, and southwestern U.S., which in turn resulted in the

speciation of *T. douglassi, T. mearnsi,* and *T. hudsonicus* (Arbogast et al., 2001). The genetic divergence of these species ranges between 1.0% and 2.4% (Arbogast et al., 2001). A similar pattern of glacial isolation in the eastern and western U.S. has been reported in red-back voles, *Clethrionomys gapperi* (Runck and Cook, 2005). The genetic divergence among populations of this species ranges from 1.2% to 5.2%. In yellow-rumped warblers, *Dendroica* sp., additional species thought to have been influenced by Pleistocene glaciation, interspecific genetic divergence in Dloop ranges from 0.16% to 6.28% and intraspecific divergence ranges from 0.05% to 1.45% (Milá et al., 2007). These divergence values among prey species are comparable to the divergence values obtained between (2.2-2.3%) and within (0.38-0.46%) the *M. americana* and *M. caurina* clades. It is possible that these similar divergence values resulted from shared evolutionary histories among these species. Today and during the Pleistocene, the geographic ranges of these species overlapped (Banfield, 1974; Milá et al., 2007; Nowak, 1999), subjecting them to similar selective pressures, which would have influenced their genetic evolution. These pressures may have been novel habitats and climatic conditions imposed by expanding and contracting glaciers (Koch et al., 2004; Rahmstorf, 2002; Seierstad et al., 2014; Williams and Jackson, 2007; Williams et al., 2001; Wolff et al., 2010) and/or predator prey relationships (see review in Schoener, 2011). By combining studies such as these with climatic and biome data it may be possible to gain insight into Pleistocene community structure.

Conclusions

The results of this study support previously reported phylogenetic relationships separating living North American martens into two clades (Dawson et al., 2017; Dawson and Cook, 2012; Small et al., 2003; Stone and Cook, 2002; Stone et al., 2002). The time calibrated Bayesian phylogeny

constructed here suggests North American martens shared a last common ancestor 243 kya +/- 168 ky and that both clades underwent increases in lineage diversity around 125 kya. This supports previous hypotheses that these clades diverged as a result of glacial isolation during the Wisconsinan glaciation (80-18 kya) (Clark et al., 2009; Dyke, 2004; Stone and Cook, 2002; Stone et al., 2002). The genetic divergence of these clades was 2.2-2.3%, which is slightly lower than previous estimates (Stone et al., 2002). While these values are within the range of genetic distances commonly accepted for the delineation of mammalian subspecies, they are similar to those seen among other species thought to have undergone divergence as a result of Pleistocene glaciation in North America. These low divergence values across multiple species may be a reflection of similar selective pressures imposed by changing climate and predator prey interactions. This suggests that North American *Martes* may, in fact, be two species, as was previously proposed (Dawson et al., 2017; Dawson and Cook, 2012). Additional research focusing on the tempo and mode of morphological evolution may indicate whether lineage diversification coincides with increases in morphological variation in response to novel Pleistocene biomes, and, therefore, whether climate and biome acted as selective pressures during these species' divergence.

Tables

Table 1. Gene Primer Sequences and Annealing Temperatures

Gene	Primer	Forward Sequence	Reverse Sequence	Annealing Temp C
12S	1	GCCTAGAAGAGTCACAAGAC	CACTGCTGTATCCCGTGG	60
	2	GAGCGGGCATCAGG	CGCCGTGAGCCTATTAATTC	52
	3	CGTGCCAGCCACC	GGCTGGGCATAGTGG	52
	4	CTCCAACAACACGATAGCTG	CGATTACAGAACAGGCTCC	60
	5	GGACTTGGCGGTGC	CATGGCCCTATTCAACTAAGC	58
	6	GGTCAAGGTGTAACCCATG	GGTGTAAGCCAGGTGC	58
16S	1	GCACCTGGCTTACACC	CATCATTCCCTTGCGGTAC	52
	2	CCAACTACCACGACATCC	CATAGGTAGCTCGTCTGG	50
	3	GCTACCTATGAGCAATCCAC	CTAAGCAAGGTTGTTTCCTTG	50
	4	CCTAACGTATCACTGGGC	CAGTGCCTCCAATACTGAG	52
	5	GCACAAGCTTATAACAGTCAACG	GGCCGTTAAACTAATGTCACTG	52
	6	CACAGGCGTGCAGTAAG	GTTAGACCTGGTTGGTGG	52
	7	GACGAGAAGACCCTATGGAG	GATAGCTGCTGCACCATC	54
	8	GACCTCGATGTTGGATCAG	CAATTACTGGGCTCTGCC	54
Dloop	1	CAACAGCCCCGCCATC	GTGRGGTGCACGGATGC	58
	2	CGTGCATTAATGGCTTGCC	GGATTGAGGACTTCCATGGC	58
	3	CGTGTACCTCTTCTCGCTC	GAAGGATAAGCCCAGCTACAAG	58
Cytb	1	CGAYYTACCTGCYCCATC	YAGGAACAGGCAGATGAAG	60
	2	YTCTTCATCTGCCTGTTCCTG	GCGAAGAATCGYGTTAGGGTAG	60
	3	CTGAGGAGGATTCTCGGTAGACAAGG	GGATTAGGAATAGGGCGCCTAGG	60
	4	CTAGGCGCCCTATTCCTAATC	CTGAGTGGGCGGAATATCAT	60
	5	CAATTRTCCCATTVCTYCATAC	RATGGCTGGCATRAGGAYTAG	60

Table 2. Best Fit Substitution Models for Each Gene

Gene	Evolutionary Model	AIC
12S	TN93	1919.62
16S	GTR	1223.50
Cytb	HKY	1233.02
Dloop	GTR+G	1792.78

Table 3. Phylogenetic Priors for Model Parameters and Statistics

Parameter	Prior	Bound
tmrca(*americana*)	LogNormal [R0.06885, 0.76], initial=?	n/a
tmrca(*caurina*)	LogNormal [R0.90585, 1.6], initial=?	n/a
12S kappa 1	LogNormal [1,1.25], initial=2	0,∞
12S kappa 2	LogNormal [1,1.25], initial=2	0,∞
12S frequencies	Uniform [0,1], initial=0.25	0,1
16S. ac	Gamma [0.05,10], initial=1	0,∞
16S.ag	Gamma [0.05,20], initial=1	0,∞
16S.at	Gamma [0.05,10], initial=1	0,∞
16S.cg	Gamma [0.05,10], initial=1	0,∞
16S.gt	Gamma [0.05,10], initial=1	0,∞
16S frequencies	Uniform [0,1], initial=0.25	0,1
Cytb kappa	LogNormal [1,1.25], initial=2	0,∞
Cytb frequencies	Uniform [0,1], initial=0.25	0,1
Dloop.ac	Gamma [0.05,10], initial=1	0,∞
Dloop.ag	Gamma [0.05,20], initial=1	0,∞
Dloop.at	Gamma [0.05,10], initial=1	0,∞
Dloop.cg	Gamma [0.05,10], initial=1	0,∞
Dloop.gt	Gamma [0.05,10], initial=1	0,∞
Dloop frequencies	Uniform [0,1], initial=0.25	0,1
Dloop alpha	Exponential [0.5], initial=0.5	0,∞
allmus	Gamma [0.001,1000], initial=1	0,∞
ucld stdev	Exponential [0.333333], initial=0.333333	0,∞
ucld mean	Exponential [1], initial=1	0,∞
treeModel rootHeight	Uniform [1.75, 5.33], initial=?	1.75,5.33
Constant popSize	1/x, initial=1	0,∞

Table 4. Fossil Calibration Data

Calibrated Node	**Age Ma**	**Age Type**	**95% Range**	**Fossil Taxon**	**Reference**
LCA with *M. foina*	1.75	Minimum	1.75-5.33	*Martes vetus*	Methods of Li et al. (2014) Fossil ages of Wolsan (1987; 1989; 1990; 1993a); Wolsan (1993b)
Crown *M. americana*	0.0117	Minimum	0.126-0.0117	*M. americana* in Eastern U.S.	Fossil ages of Eshelman and Grady (1986); Grady (1984); Guilday and Hamilton (1978); Tankersley (1997); Wetmore (1962)
Crown M. *caurina*	0.0117	Minimum	1.8-0.0117	*M. caurina* in western U.S.	Fossil ages of Bell (1995); Long (1971); Mead and Mead (1989); Sinclair (1907)

Figures

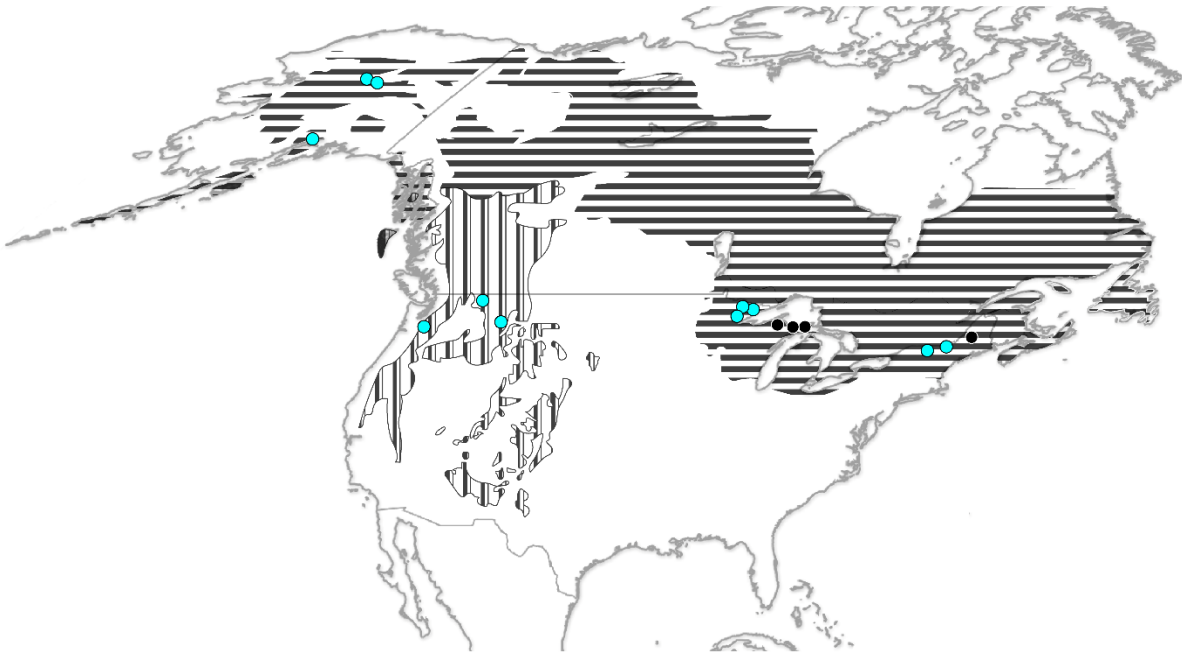

Figure 1. Geographic distribution of *M. americana* (horizontal lines) and *M. caurina* (vertical lines) (Nowak, 1999). Points on the map indicate the geographic location from which specimens were collected. Teal points present the collection location of specimens that were sequenced and included in the phylogenetic analysis while black points are sequenced specimens that were excluded due to inadequate DNA lengths.

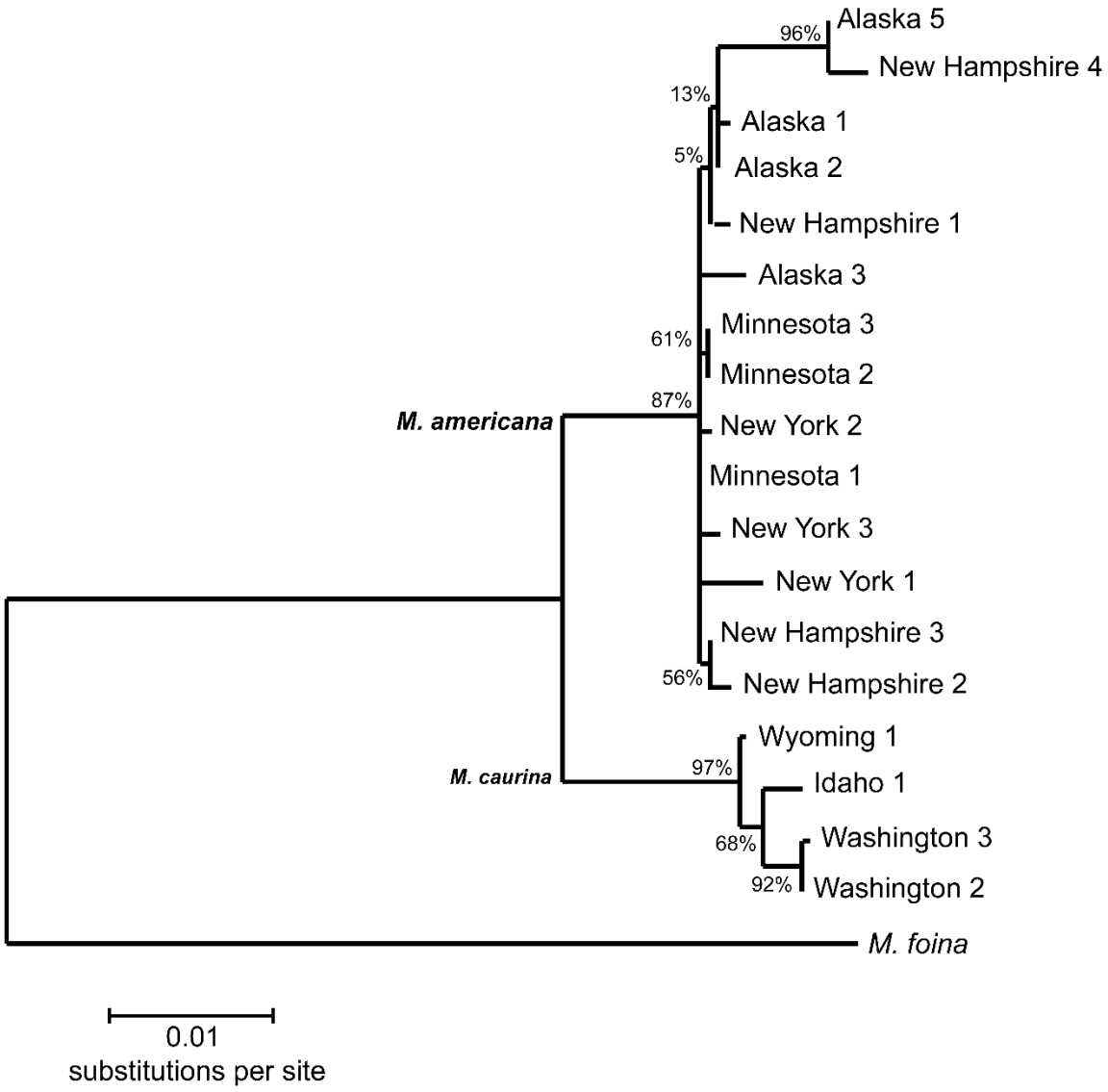

Figure 2. Maximum likelihood phylogeny of *M. americana* and *M. caurina* specimens constructed from a concatenated sequence of 12S, 16S, cytb, and Dloop mitochondrial genes. Branch lengths represent the number of nucleotide substitutions per site as denoted by the scale bar. Node values indicated the bootstrap support after 500 replicates. Tip labels indicate the state from which specimens were collected followed by an individual specimen number. See Appendix III (Section D, Table 3) for the collection number associated with each tip label.

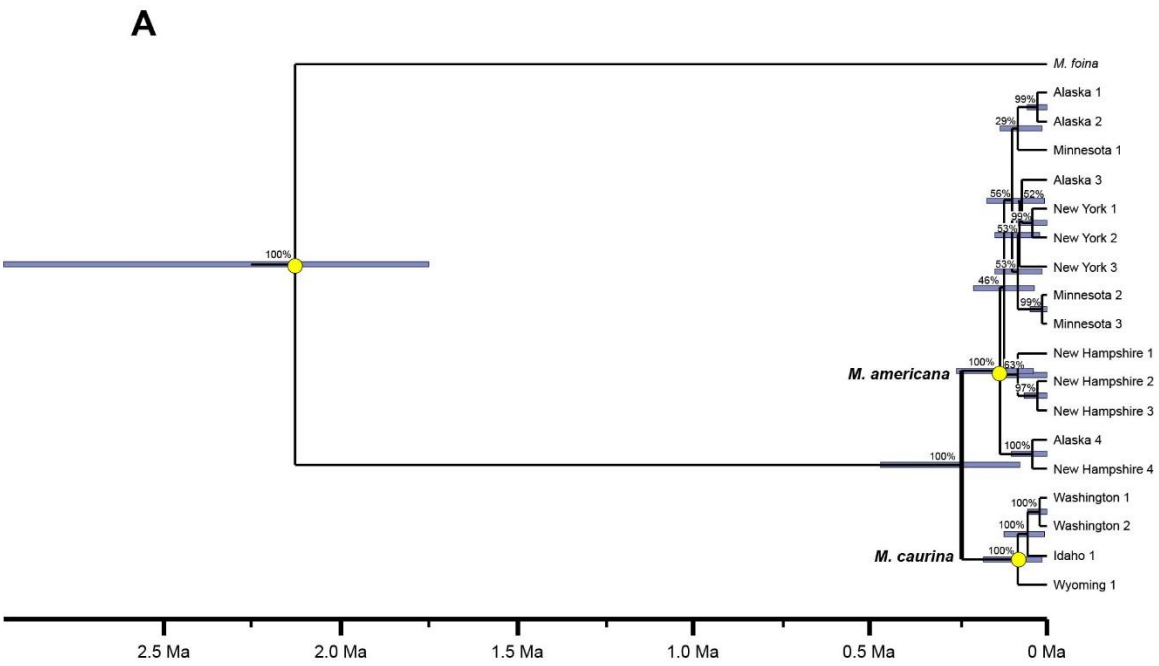
A
M. foina
Alaska 1
Alaska 2
Minnesota 1
Alaska 3
New York 1
New York 2
New York 3
Minnesota 2
Minnesota 3
New Hampshire 1
New Hampshire 2
New Hampshire 3
Alaska 4
New Hampshire 4
Washington 1
Washington 2
Idaho 1
Wyoming 1
M. americana
M. caurina
100%
99%
29%
56%
52%
53%
46%
63%
97%
2.5 Ma
2.0 Ma
1.5 Ma
1.0 Ma
0.5 Ma
0 Ma

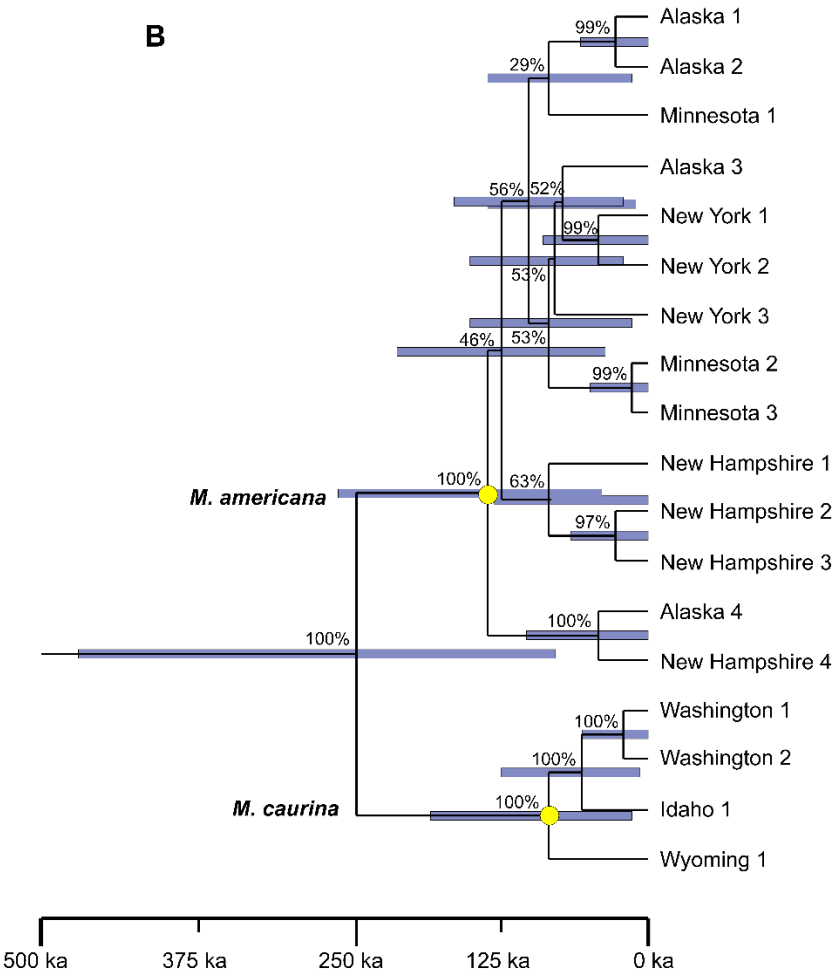
B
Alaska 1
Alaska 2
Minnesota 1
Alaska 3
New York 1
New York 2
New York 3
Minnesota 2
Minnesota 3
New Hampshire 1
New Hampshire 2
New Hampshire 3
Alaska 4
New Hampshire 4
Washington 1
Washington 2
Idaho 1
Wyoming 1
M. americana
M. caurina
99%
29%
56%
52%
53%
46%
63%
97%
500 ka
375 ka
250 ka
125 ka
0 ka

Figure 3. Bayesian phylogeny of *M. americana* and *M. caurina* specimens constructed from a concatenated sequence of 12S, 16S, cytb, and Dloop mitochondrial genes. Branch lengths represent time and node values indicate posterior probability support. Yellow circles denote nodes that were fossil calibrated (Table 3, 4). Purple bars on nodes represent the 95% confidence interval on node ages. Tip labels indicate the state from which specimens were collected followed by an individual specimen number. See Appendix III (Section D, Table 3) for the collection number associated with each tip label. A) depicts the full phylogeny and B) depicts the nodes that originated in the most recent 500 ka.

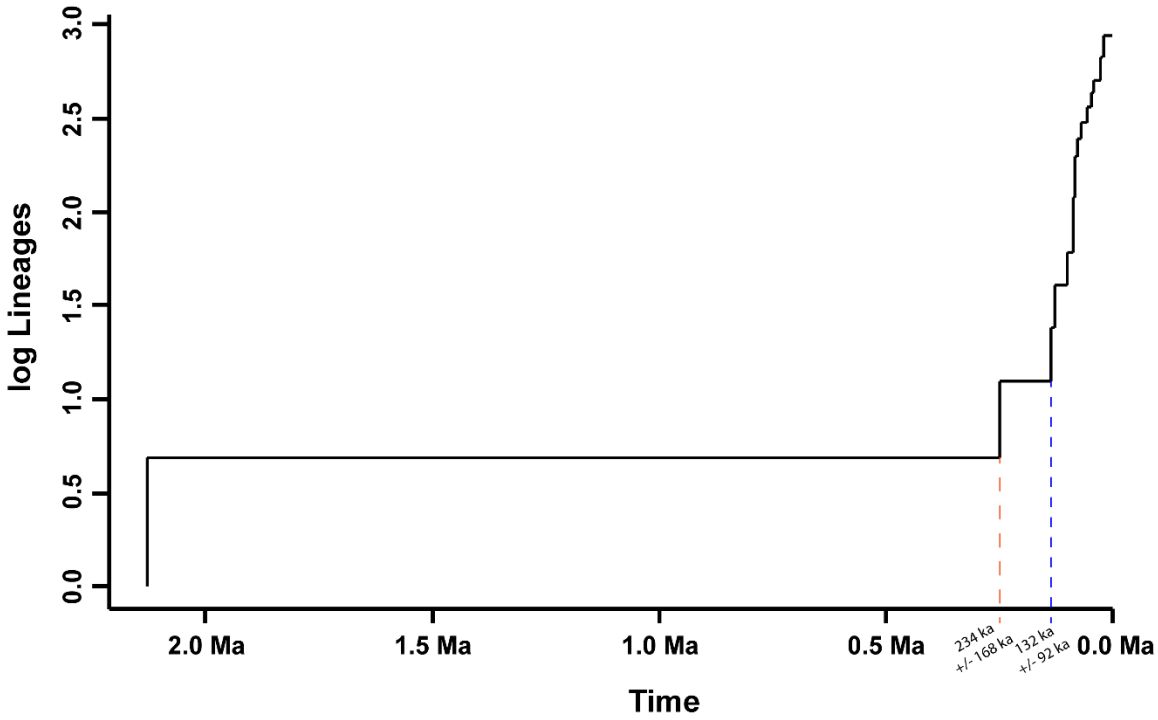

Figure 4. log lineage through time plot. X-axis indicates millions of years since present. Rates of log lineage diversification did significantly differ from those predicted under a Pure Birth null model (p<0.01). The pink dashed line denotes the first increase in lineage diversity 234 kya +/- 168 ka and the blue dashed line indicates the initial point of rapid increase in lineage diversity 132 kya +/- 92 ka. Error in these dates was determined from the 95% confidence interval of the node ages in the Bayesian phylogeny.

CHAPTER V

APPENDICULAR SKELETAL MORPHOLOGY OF NORTH AMERICAN PINE MARTENS, *M. AMERICANA* AND *M. CAURINA*, IS NOT AN ADAPTATION TO BIOME

Introduction

Recent changes in climate have exposed many living species to novel biomes and selective pressures. Our ability to infer how species will survive relies, in part, on our understanding of the evolutionary history of each species. Determining how the phenotypes of living species have evolved can be particularly challenging, however, because they can be influenced by several intrinsic and environmental variables. North American pine martens, *Martes americana* and *M. caurina*, are two species whose biomes are currently being affected by anthropogenically induced climate change (Dye, 2002; Euskirchen et al., 2007; Knowles et al., 2006; Rahmstorf et al., 2007; Serreze et al., 2000; Stone et al., 2002b). These species are thought to have undergone genetic and phenotypic divergence during the Pleistocene as a result of isolation in differing biomes (Chapter 3; Dawson et al., 2017; Dawson and Cook, 2012; Stone et al., 2002a). Given the relationships among climate, biome, and limb morphology in these species, it is possible that their limb morphology evolved as an adaptation to selective pressures imposed by Pleistocene and Recent climate and biomes. Determining how the phenotypes of these species evolved in the past may allow for predictions of adaptability to future climates.

Intrinsic and environmental selective pressures, such as genetics, climate, and biome, can

influence the phenotypes of populations through several evolutionary processes. These processes may include genetic drift, phenotypic plasticity, and adaptation through natural selection (Andrews, 2010; Pigliucci, 2001; Reznick and Travis, 2001). Through genetic drift, populations accumulate random genetic mutations through time which can lead to random increases in phenotypic variation (Andrews, 2010; Harmon, 2018; Lande, 1976). If genetic drift occurs in isolated populations, it can result in the genotypic and phenotypic divergence of these populations. Species that are phenotypic plastic are capable of exhibiting multiple phenotypes from a single genotype (Pigliucci, 2001). This can manifest as two phenotypically divergent populations with few genotypic differences (e.g., Dodson, 1989; Hoch, 2009; Marchinko and Geary, 2003). Populations that are adapting to different environmental selective pressures may also become phenotypically divergent (Reznick and Travis, 2001; Reznick and Ghalambor, 2001). In this process, phenotypic traits that improve performance and in turn increase an individual's fitness become more prevalent in a population. This process is often recognized through changes in evolutionary rates and decreases in intraclade morphological disparity (Foote, 1997; Hendry et al., 2008; Kinnison and Hendry, 2001; Schluter, 2000; Slater et al., 2010). Using a phylogenetic framework as a model of genotypic evolution, it is possible to test for these evolutionary processes and infer the phenotypic evolutionary history of extant and extinct species (Cornwell and Nakagawa, 2017; Garamszegi, 2014; O'Meara, 2012)

M. americana and *M. caurina* (Dawson et al., 2017; Dawson and Cook, 2012) are two species whose skeletal phenotypes may have evolved in response to selective pressures associated with climate and biome. These species are thought to have genetically diverged during the Wisconsinan glaciation as a result of geographic isolation (Chapter 3; Dawson et al., 2017; Dawson and Cook, 2012; Stone et al., 2002a). The skeletal morphologies of *M. americana* and *M. caurina* differ, suggesting they may have experience phenotypic divergence during this same period. Limb morphologies of these species also differ between biomes, with *M. caurina* in

coniferous forests being significantly more robust than *M. americana* in boreal and broadleaf forests (Chapter 1). Because the morphology of *M. americana* does not differ between boreal and broadleaf forests, it suggests that these species are not exhibiting phenotypic plasticity. Limb phenotypes may have evolved, then, through genetic drift in isolated populations or as an adaptation to the different biomes occupied by these species.

In this study, I sought to determine whether the skeletal limb morphology of *M. americana* and *M. caurina* evolved as an adaptation to biome. Using a phylogeny constructed from mitochondrial genes from multiple specimens of *M. americana* and *M. caurina* as a framework, I tested the following hypotheses:

H_0- Limb morphology evolved randomly under a Brownian motion mode of evolution.

H_1-Limb morphology evolved as an adaption to biome.

To test these hypotheses, I tested for evolutionary tempo and mode and modelled the morphological disparity through time of skeletal limb morphology. I quantified limb shape using 3D geometric morphometric landmark data from 17 specimens of *M. americana* and *M. caurina* that had been included in the mitochondrial phylogeny.

Taxonomic Nomenclature

North American pine martens, *M. americana* and *M. caurina*, were recently proposed as unique species based on mitochondrial, nuclear, morphological, and parasitological evidence (Dawson et al., 2017; Dawson and Cook, 2012; Hoberg et al., 2012; Merriam, 1890), but have not yet been recognized by the International Commission on Zoological Nomenclature. My research has further supported this status, as genetic distances between these species are similar to those seen

in other species thought to have diverged during the late Pleistocene. I, therefore, have adopted these specific titles throughout this chapter.

Institutional Abbreviations

New York State Museum (NYSM), Florida Museum of Natural History (FLMNH), Museum of Southwestern Biology (MSB), Burke Museum of Natural History and Culture (BMUW), University of Alaska Museum of the North (UAMN), Smithsonian Institution National Museum of Natural History (USNM)

Materials and Methods

Specimens

I included a total of 17 individuals morphologically identified as *M. americana* and *M. caurina* (Appendix IV, Section A). This dataset comprised 13 specimens of *M. americana* and 4 specimens of *M. caurina.* These individuals represent 17 of the 18 specimens included in the previously constructed Bayesian phylogeny (Chapter 3). USNM 592895 was excluded from morphological analysis because it was a juvenile, as determined by lack of epiphyseal fusion. All other specimens were adults. Both sexes, as determined by museum identification and the presence of a baculum, were included in this study. Specimens were collected across the U.S. range of these species between 2000 and 2013 (Figure 1). I chose specimens collected within a limited timeframe to capture morphological variation at a single point in these species' evolutionary history. I assigned each specimen to one of three biomes based on the geographic

location from which it was collected: 1) temperate broadleaf and mixed forest ; 2) temperate coniferous forest; and 3) boreal forest and taiga (Olson et al., 2001). These specimens are housed in the collections at NYSM, FLMNH, MSB, BMUW, UAMN, USNM.

Bayesian Phylogeny

To provide a phylogenetic framework for comparative analysis, I used a previously constructed phylogeny (Chapter 3) composed of the same individuals whose skeletal limb morphologies were measured. The phylogeny was created using a concatenated sequence of 12S, 16S, cytochrome b (cytb), and Dloop mitochondrial genes. I assigned each gene its best-fit nucleotide substitution model as determined by Akaike Information Criteria (AIC). The phylogeny was time calibrated using three fossil occurrence date ranges at 3 nodes: the divergence between the ingroup and outgroup clades (5.33-1.75 Ma); the node for crown *M. americana* (126-11.7 ka)*;* and the node for crown *M. caurina* (1.8 Ma- 11.7 ka). The phylogeny had a relaxed lognormal molecular clock and was assumed to coalesce under a constant population size.

The phylogeny comprises two major clades with 100% posterior probability support, one containing *M. americana* and the other *M. caurina,* with *M. foina* as the outgroup (Figure 2, Chapter 3). The *M. foina* node age was estimated at 2.12 Ma +/- 0.37 Ma, which fits previous age estimates of this divergence (Koepfli et al., 2008; Li et al., 2014). The last common ancestor of *M. americana* and *M. caurina* is estimated at 234 kya +/- 168 ka. The diversification of *M. americana* is inferred to have begun 132 kya +/- 92 ka, and that of *M. caurina* diversification around 83 kya +/- 69 ka.

Skeletal Limb Morphology

I collected shape data from appendicular skeletal elements (humerus, radius, ulna, femur, tibia, and fibula) of 17 individuals, of which only the fibula was not represented in all individuals (N=11). I collected 3D geometric morphometric landmark data from each bone using a MicroScribe G2LX digitizer. This digitizer records the X, Y, and Z coordinates of a single point/landmark in space. I chose landmarks that would best capture the length and width of each element because size evolves in mammals through time (e.g., Fabre et al., 2013; Kolska Horwitz and Ducos, 1997; Meachen et al., 2014; Meachen and Samuels, 2012). I also chose landmarks that represented morphological characters frequently used in phylogenetic studies of carnivorans (Leach, 1977; Meachen-Samuels, 2012; Morlo and Peigné, 2010; Zrzavý and Řičánková, 2004). This allowed me to use previously identified traits that are thought to contain phylogenetic signal (Figure 3, Appendix IV, Section B). Where possible, I avoided landmarks associated with muscle attachments, as these are modified throughout an individual's life (Currey, 2002; Wei and Messner, 1996). In addition, I tested all landmarks for accuracy and repeatability (Chapter 1). I aligned landmarks for each bone independently using a series of generalized Procrustes analyses (GPA), one for each limb element, and then calculated the centroid size of each element in every specimen (Appendix IV, Section C, Table 2). I ran these analyses using the geomorph package (Adams and Otarola-Castillo, 2013) in R (R Core Team, 2015) (Appendix IV, Section D).

Phylogenetic Signal

To determine whether appendicular skeletal morphology varies in correlation with the underlying phylogenetic relationships of *M. americana* and *M. caurina*, I tested for phylogenetic signal in limb bone shape in each element independently. I measured phylogenetic signal using a generalization of Blomberg's K (Blomberg et al., 2003) that is appropriate for multivariate data (K_{mult}) (Adams, 2014b; Adams and Collyer, 2018). This model is ideal for geometric

morphometric data because it has high power and appropriate Type I error despite trait dimensionality and covariance (Adams, 2014a; Adams and Collyer, 2018). To evaluate the significance of K_{mult} I tested it against a Brownian Motion (BM) null model of evolution using a permutation method for 999 iterations ($\alpha \leq 0.05$). BM is an appropriate null model for phenotypic evolution because it assumes phenotypes shift randomly and proportionally with time, and, therefore, form a normal distribution (Felsenstein, 1973; Felsenstein, 2004). I ran this analysis in R (R Core Team, 2015) using the geomorph package (Adams and Otarola-Castillo, 2013) (Appendix IV, Section D).

Second, I tested for phylogenetic signal using centroid size as a measure of shape. I chose a univariate trait because there are currently no accurate methods for interpreting evolutionary mode in multivariate data (Adams and Collyer, 2018). I measured phylogenetic signal using two indices: Blomberg's K (Blomberg et al., 2003) and Pagel's λ (Pagel, 1999). Blomberg's K values that are significant and positive indicate there is a greater phylogenetic signal in the data than would be expected at random. Blomberg's K calculates phylogenetic signal as a ratio of the mean squared error (MSE) of the tip data around a phylogenetically corrected mean and the MSE of the given phylogeny under a BM null model of evolution. The significance of this index is then determined by comparing the ratios produced under a BM null model of evolution to those produced at random through a permutation method (Blomberg et al., 2003). Here I tested for significance using 999 iterations. Pagel's λ values close to one indicate a strong phylogenetic signal in the data. To calculate Pagel's λ the phylogeny is transformed under a BM null model of evolution. λ is then the coefficient required to scale the resulting covariance matrix to match that from the original, untransformed phylogeny (Pagel, 1999). I calculated both indices as a means of comparing to the results of the K_{mult} analysis, and because Pagel's λ is a more accurate measure of phylogenetic signal in phylogenies with few tips (Münkemüller et al., 2012). I ran these analyses in R (R Core Team, 2015) using the phytools package (Revell, 2012).

Evolutionary Rate

Because skeletal morphology differs among specimens from the three different biomes occupied by North American *Martes* (Chapter 1), I sought to determine whether differences in selective pressures among biomes influenced the tempo of appendicular morphological evolution. I tested for differences in evolutionary tempo among specimens from the three biomes occupied by North American *Martes*: 1) temperate broadleaf and mixed forest; 2) temperate coniferous forest; and 3) boreal forest and taiga (Olson et al., 2001). For this analysis I quantified limb bone shape using the GPA aligned landmark data for each element. I tested for evolutionary rates in each limb element independently. Evolutionary rates were calculated by phylogenetically transforming the shape data under a BM null model of evolution and then calculating the resulting between-specimen Euclidian distances. Rate was quantified as the sum of squared distances between the phylogenetically transformed data and the origin of the phylogeny (Adams, 2014b). To determine whether rates significantly differed among specimens from each biome, I compared ratios of rates between each biome to ratios of rates produced from simulated data with rates that do not significantly differ. I did this using a permutation method for 999 iterations (Denton and Adams, 2015). This method produces appropriate Type I error and high power, despite small rate differences between groups (Adams and Collyer, 2018). I ran all analyses in R (R Core Team, 2015) using the geomorph package (Adams and Otarola-Castillo, 2013) (Appendix IV, Section D).

Morphological Disparity

I estimated morphological disparity in *Martes* from the Pleistocene to Present to infer trends in disparity through time. I quantified bone shape using the centroid size of each bone. I estimated

morphological disparity through time using the dtt function in GEIGER (Harmon et al., 2008) (Appendix IV, Section E). In the dtt function, the average disparity of the entire phylogeny is first calculated using the assigned tip values. Then, moving up the phylogeny from the root to the tips, mean relative disparity is calculated for each node. The mean relative disparity is a ratio of the average disparity of each subclade whose ancestral lineage was present at that point in time relative to the average disparity of the entire phylogeny (Foote, 1997; Harmon et al., 2003). The greater the relative mean disparity (≥1), the greater a volume of morphospace is occupied by each subclade. For this analysis I chose an average squared Euclidian distance disparity index because it is the most commonly used distance when quantifying morphospace in geometric morphometric analyses (Zelditch et al., 2012) and because this distance is the least sensitive to small sample sizes (Ciampaglio et al., 2001). I then compared the estimated disparity through time to that expected under a BM null model of evolution using the morphological disparity index (MDI). The MDI represents the difference in relative disparity between the observed and simulated data (Harmon et al., 2003). To calculate MDI, I simulated centroid size evolution under a BM null model of evolution 1,000 times and then from this simulated data generated the mean relative disparity at each node.

Results

Phylogenetic Signal

I found a significant phylogenetic signal ($p \leq 0.05$) in the landmark data from only the ulna (K_{mult}= 0.44) (Table 1). A significant K_{mult} result with a value less than one indicates that morphology is less similar between specimens than expected under a BM null model (Adams, 2014a; Adams and Collyer, 2018). K_{mult} did not significantly differ, however, from that expected under a BM

null model in the landmark data of the remaining five elements and ranged from 0.36-0.43 (Table 1). I found no phylogenetic signal in the centroid size of all six measured elements ($K > 0.05$, $\lambda \leq 0.04$; Table 1). These results suggest that the appendicular morphology of *M. americana* and *M. caurina* has evolved independent of phylogenetic relationships and reflects a stochastic, BM model of evolution.

Evolutionary Rate

There was a significant difference in the rate of evolution among the femora of specimens collected from the three different biomes ($p<0.05$) (Table 2). Specimens from boreal forests were evolving at the fastest rate (2.68×10^{-4}) and those from broadleaf forests evolved under the slowest rate (9.4×10^{-5}). Evolutionary rates did not significantly differ in the other limb elements ($p>0.05$, Table 2). This suggests that biome has had little influence on the rate of appendicular morphological evolution in *M. americana* and *M. caurina.*

Morphological Disparity

In all six elements, morphological disparity was estimated to have reached an initial peak early in the evolution of *M. americana* and *M. caurina* (Figure 4). This peak was then followed by a declining trend, marked by two slight increases (Figure 4). While the disparity through time analysis does not provide age ranges at each measured node, it was possible to correlate age ranges from the underlying phylogeny (Chapter 3). The initial peak in estimated disparity then occurred approximately 132 kya +/- 92 ka, when *M. americana* underwent lineage diversification. The second peak coincides with the diversification of *M. caurina* 83 kya +/- 69 ka. The final increase in disparity then occurred around 24 kya +/- 6 ka (Figure 4, 5). The MDI indicated that

the overall relative disparity of the measured data did not significantly differ from that expected under a BM model of evolution (Table 3). This suggests that the morphological disparity seen in *M. americana* and *M. caurina* developed through the accumulation of random trait changes through time.

Discussion

The results of this study indicate that the skeletal limb morphology of North American *Martes* has not evolved as an adaptation to biome. Populations undergoing phenotypic adaptation in response to selective pressures often exhibit phylogenetic signal in the phenotype, differing rates of evolution, and low within-clade disparity (Foote, 1997; Hendry et al., 2008; Kinnison and Hendry, 2001; Schluter, 2000; Slater et al., 2010). In North American pine martens, neither measure of limb shape had an underlying phylogenetic signal (Table 1). There was also no significant difference in evolutionary rates among specimens from different biomes (Table 2). Estimates of relative clade disparity through time were ≥ 1 for the majority of the evolutionary history of these species, suggesting that they were not undergoing adaptation. Each of these analyses indicated that limb element shape has evolved under a BM mode of evolution, meaning that limb shape variation has accumulated randomly in proportion to time. The simplest way to obtain this mode of phenotypic evolution is through genetic drift (Harmon, 2018; Lande, 1976). Genetic drift in geographically isolated populations may result in divergent phenotypes.

M. americana and *M. caurina* may have differing phenotypes as a result of genetic drift occurring in isolated populations during the Pleistocene. Fluctuations in climate during the Pleistocene (Bond et al., 1993) resulted in multiple glacial interglacial cycles (Lang et al., 1999; Rahmstorf, 2002; Seierstad et al., 2014; Wolff et al., 2010) (Figure 5). During the last of these glacial

periods, the Wisconsinan glaciation (80-18 kya) (Clark et al., 2009; Dyke, 2004), North American pine martens likely became isolated in different biomes in the eastern and western U.S. (Chapter 3; Dawson et al., 2017; Stone and Cook, 2002; Stone et al., 2002a). This hypothesis is supported by the presence of fossils in these regions during this glacial period (Behrensmeyer and Turner, 2013; Bell, 1995; Eshelman and Grady, 1986; Grady, 1984; Guilday and Hamilton, 1978; Long, 1971; Mead and Mead, 1989; Sinclair, 1907; Tankersley, 1997; Wetmore, 1962) and the estimated node ages constructed in the phylogenetic analysis (Figure 2 and 5). Relative disparity is modeled to have increased in conjunction with the initial lineage diversification of *M. americana* (132 kya +/- 92 ka) and then again with the diversification of *M. caurina* (83 kya +/- 69 ka) (Figure 4 and 5). This increase in disparity may coincide with the Wisconsinan glaciation (80-18 kya) (Clark et al., 2009; Dyke, 2004), suggesting that both genotypic and phenotypic diversification occurred in these species while they were geographically isolated (Figure 5).

M. americana and *M. caurina* may have survived fluctuations in climate and biome without undergoing phenotypic adaptation because they are behaviorally plastic. Researchers have shown that *M. americana* and *M. caurina* will vary both their hunting and nesting behaviors seasonally and by habitat quality (Andruskiw et al., 2008; Ben-David et al., 1997; Fuller et al., 2005; Moriarty et al., 2015; Steventon and Major, 1982; Zielinski and Duncan, 2004). In addition, these species are capable of several locomotor behaviors including climbing, swimming, pouncing, digging, and a half-bound gate (Banfield, 1974; Harris and Steudel, 1997). This variety of locomotor behaviors is also reflected in their hunting strategies as these species have a wide dietary range that includes hares, voles, birds, insects, and fruit (Banfield, 1974; Clark et al., 1987; Nowak, 1999). If this wide range of behaviors has been exhibited by *M. americana* and *M. caurina* from the Pleistocene to Present, they may have been advantageous when facing past climate change.

North American *Martes* are not the only species hypothesized to have undergone phenotypic divergence as a result of glacial isolation during the Pleistocene. Similar evolutionary histories have been reported in several species of insects, amphibians, reptiles, birds, and mammals (see review in Shafer et al., 2010). For example, both yellow-rumped warblers, *Dendoica* sp., and song sparrows, *Melospiza melodia*, are thought to have undergone phenotypic divergence in plumage patterns while isolated in glacial refugia and during later range expansion after glacial retreat (Milá et al., 2007; Zink and Dittmann, 1993). Species of North American tree squirrels, *Tamisciurus* sp., are also thought to have undergone phenotypic divergence in glacial refugia (Arbogast et al., 2001). By determining the modes of phenotypic evolution in these and other species that were isolated during the Pleistocene, it may be possible to begin reconstructing how Pleistocene communities were influenced by past climate and biomes.

Conclusions

The results of this study suggest that the appendicular skeletal morphology of North American pine martens, *M. americana* and *M. caurina*, evolved through genetic drift in geographically isolated populations during the Late Pleistocene. Despite changes in both climate and biome from the Pleistocene to Present, these species were able to survive without undergoing phenotypic adaptation. Their survival through these extrinsic fluctuations may be attributed to their behavioral plasticity. The changes in morphology studied here occurred over nearly two hundred thousand years. Today, living populations of *Martes* are experiencing rapid changes in climate and habitat (Rahmstorf et al., 2007) that may, in turn, influence their behavior and likelihood of survival. If these species can survive climate change by being behaviorally plastic, as

hypothesized here, it may provide them with an advantage when facing future climatic shifts across their geographic ranges.

Tables

Table 1. Phylogenetic Signal

Element	**Kmult**	**Kmult *p***	**K**	**K *p***	**λ**
Humerus	0.37	0.22	0.36	0.52	0.04
Radius	0.39	0.08	0.28	0.80	<0.01
Ulna	*0.44*	*<0.01*	0.30	0.77	<0.01
Femur	0.36	0.24	0.35	0.51	<0.01
Tibia	0.39	0.06	0.30	0.77	<0.01
Fibula	0.38	0.09	0.28	0.79	<0.01

Table 2. Limb Element Shape Tempo by Biome

Element	***p***	**Evolutionary Rates by Biome**		
		Boreal Forest	Broadleaf Forest	Coniferous Forest
Humerus	0.85	2.31×10^{-4}	2.74×10^{-4}	2.84×10^{-4}
Radius	0.67	2.24×10^{-4}	2.19×10^{-4}	2.84×10^{-4}
Ulna	0.24	2.16×10^{-4}	1.88×10^{-5}	3.52×10^{-4}
Femur	*<0.01*	*2.68×10^{-4}*	*9.40×10^{-5}*	*1.30×10^{-4}*
Tibia	0.68	1.69×10^{-4}	1.28×10^{-4}	1.31×10^{-4}
Fibula	0.95	1.02×10^{-4}	9.40×10^{-5}	1.30×10^{-4}

Table 3. Morphological Disparity Index

Element	**MDI**	***p***
Humerus	0.84	1.0
Radius	1.19	1.0
Ulna	1.13	1.0
Femur	0.87	1.0
Tibia	1.15	1.0
Fibula	1.28	1.0

Figures

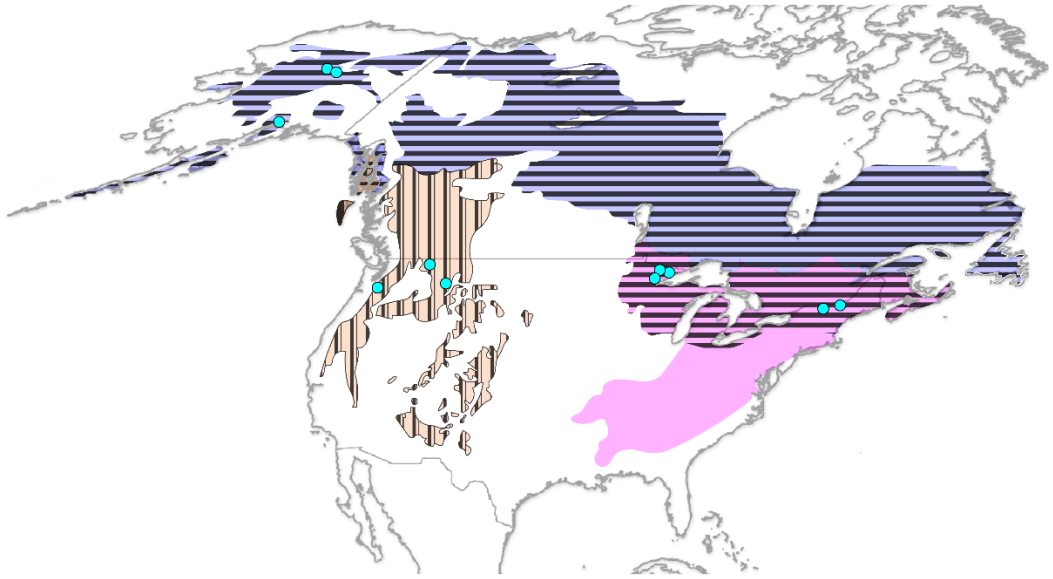

Figure 1. Geographic distribution of *M. americana* (horizontal lines) and *M. caurina* (vertical lines). Colors indicate the biome distributions. Blue are boreal forests. Orange are coniferous forests, and pink are broadleaf forests. Teal points on the map indicate the geographic location from which specimens were collected.

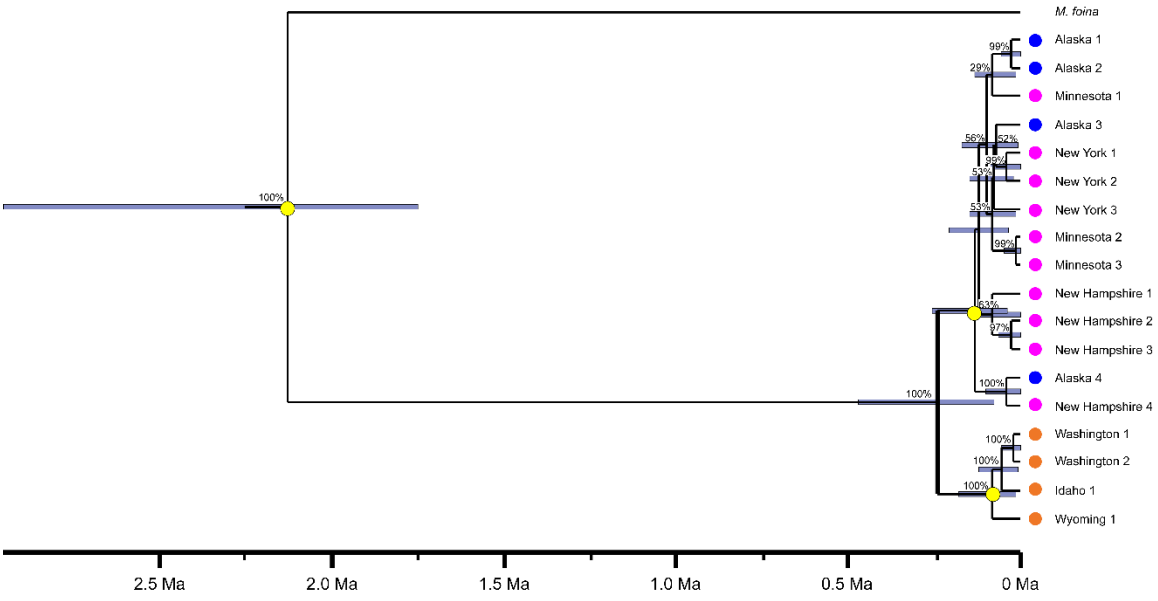

Figure 2. Bayesian phylogeny of *M. americana* and *M. caurina* specimens constructed from a concatenated sequence of 12S, 16S, cytb, and Dloop mitochondrial genes. Branch lengths represent time and node values indicate posterior probability support. Yellow circles denote nodes that were fossil calibrated (Chapter 3; Table 3 and 4). Purple bars on nodes represent the 95% confidence interval on node ages. Blue, orange, and pink circles at tips represent the biome from which specimens were collected, as indicated by the key to the left. Tip labels indicate the state from which specimens were collected followed by an individual specimen number. See Appendix IV (Section C, Table 1) for the collection number associated with each tip label.

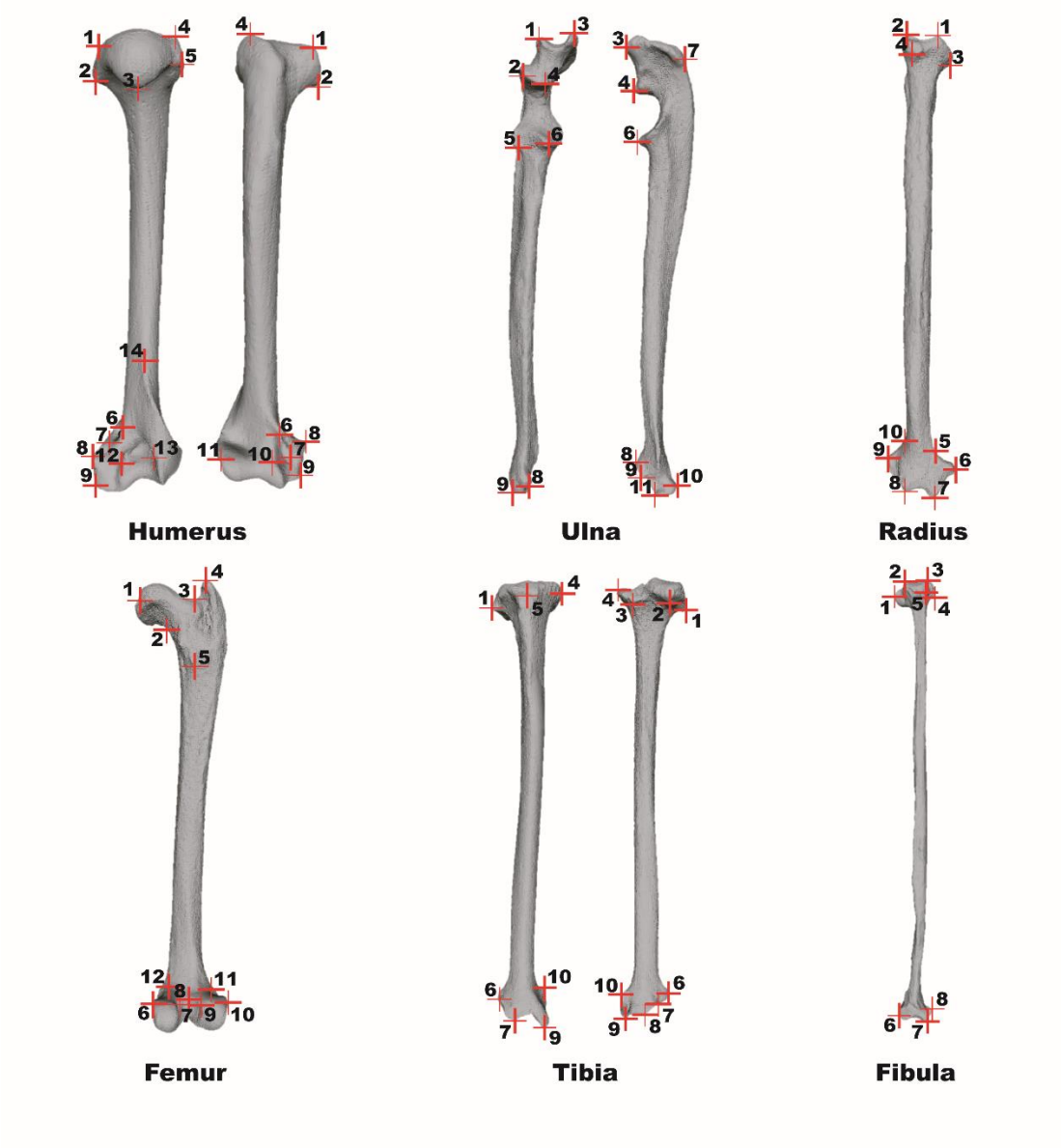

Figure 3. Geometric morphometric landmarks on the humerus, radius, ulna, femur, tibia, and fibula used to quantify bone shape of specimens.

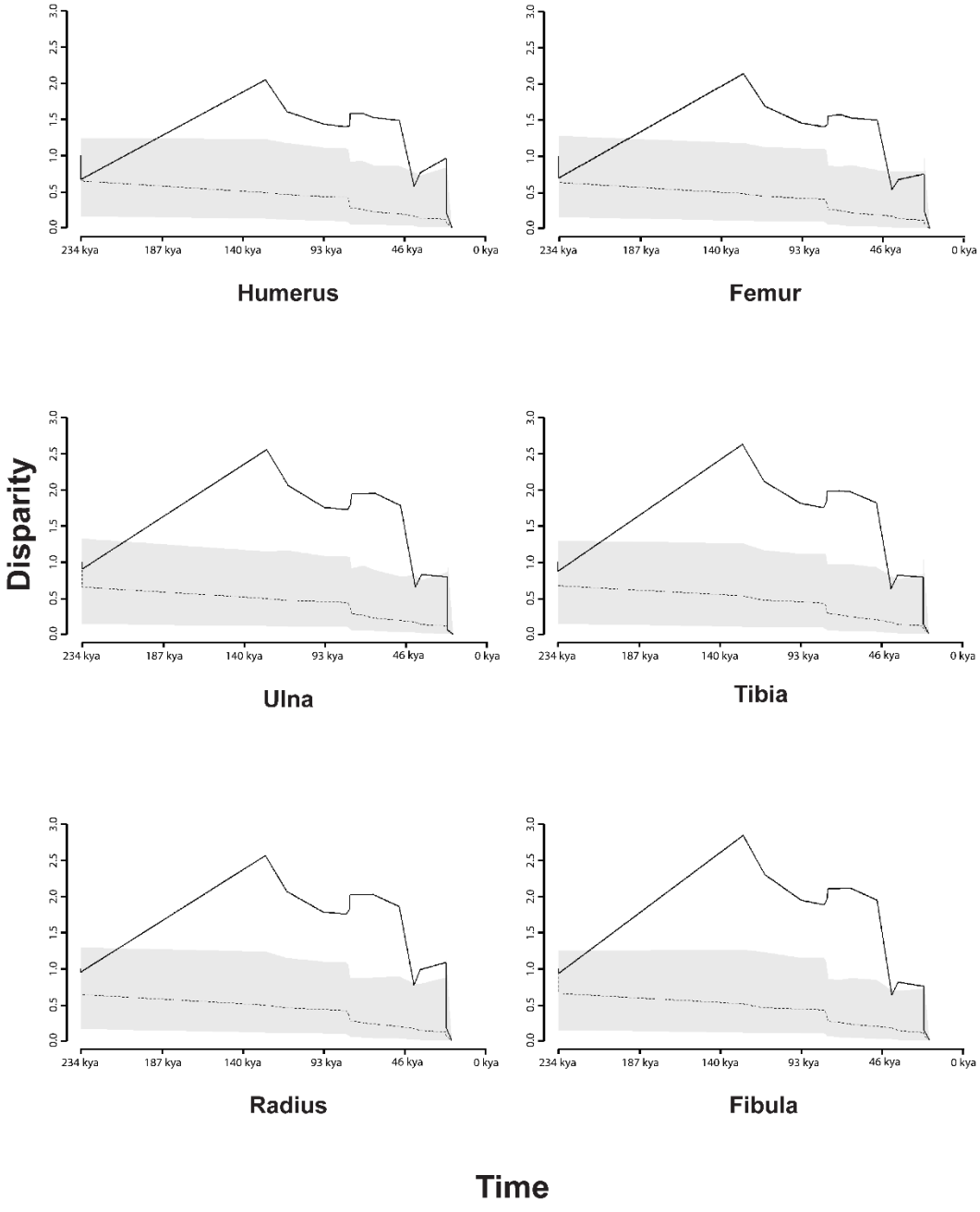

Figure 4. Estimated disparity through time plots for the humerus, ulna, radius, femur, tibia, and fibula. Solid lines on the DTT plot represent estimates of the mean subclade morphological disparity. The dotted black line is the simulated disparity calculated under a Brownian motion null model of evolution with 95% confidence intervals in grey.

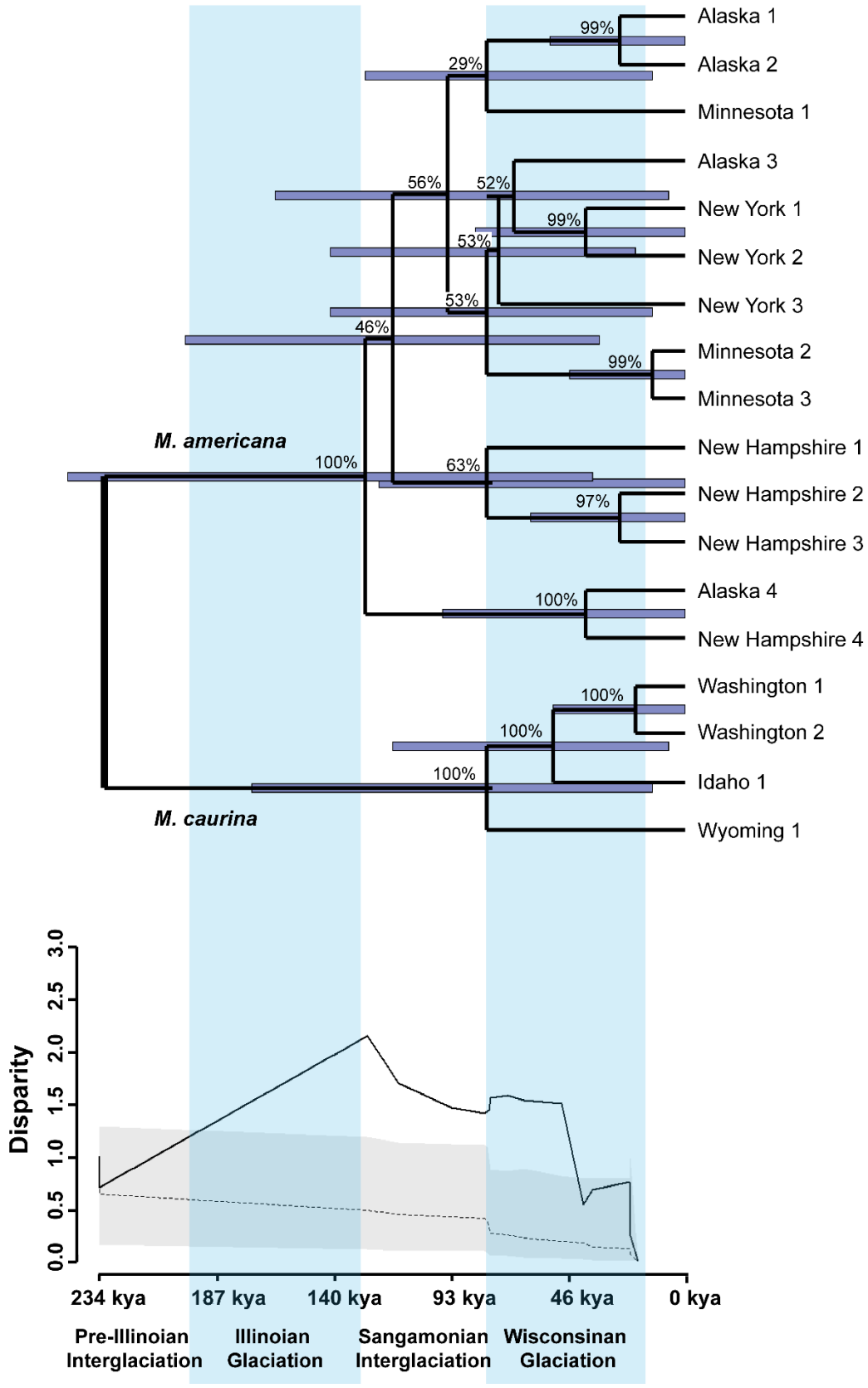
Alaska 1
Alaska 2
Minnesota 1
Alaska 3
New York 1
New York 2
New York 3
Minnesota 2
Minnesota 3
New Hampshire 1
New Hampshire 2
New Hampshire 3
Alaska 4
New Hampshire 4
Washington 1
Washington 2
Idaho 1
Wyoming 1
M. americana
M. caurina
99%
29%
56%
52%
99%
53%
53%
46%
99%
100%
63%
97%
100%
100%
100%
100%
Disparity
0.0
0.5
1.0
1.5
2.0
2.5
3.0
234 kya
187 kya
140 kya
93 kya
46 kya
0 kya
Pre-Illinoian Interglaciation
Illinoian Glaciation
Sangamonian Interglaciation
Wisconsinan Glaciation

Figure 5. Bayesian phylogeny of *M. americana* and *M. caurina* (upper) (Chapter 3) and estimated disparity through time (DTT; lower) plots. Purple bars on phylogeny nodes represent the 95% confidence interval on node ages. DTT plot was constructed from the femoral data and represents trends that are consistent in all six elements (Figure 4). Solid lines on the DTT plot represent the estimated mean subclade morphological disparity. The dotted black line is the simulated disparity calculated under a Brownian motion null model of evolution with 95% confidence intervals in grey. Blue boxes represent the Wisconsinan and Illinoian glacial periods while white boxes represent the Pre-Illinoian, Sangamonian, and current interglacial periods. Glacial cycle data was collected from Clark et al. (2009); Dyke (2004); Edwards et al. (1997); Rovey and Balco (2011); Shackleton et al. (2003); and Stirling et al. (1998).

CHAPTER VI

STASIS IN APPENDICULAR SKELETAL MORPHOLOGY OF THE NORTH AMERICAN PINE MARTEN, *M. AMERICANA,* ACROSS CLIMATE CHANGE IN ALASKA

Introduction

Climate is changing at unprecedented rates as a result of anthropogenic factors (Rahmstorf et al., 2007), and Alaska has become one of the most volatile geographic regions in the world (Dye, 2002; Euskirchen et al., 2007; Serreze et al., 2000; Stone et al., 2002). Over the past 60 years, Alaska has experienced significant shifts in annual temperature and precipitation, as well as dominant vegetation (Dye, 2002; Euskirchen et al., 2009; Klein et al., 2005; Myneni et al., 1997; Serreze et al., 2000; Stone et al., 2002). Researchers have shown that many living species from other geographic regions are undergoing phenotypic evolution on decadal scales in response to rapid global climate change (Doudna and Danielson, 2015; Franssen, 2011; Poroshin et al., 2010; Rychlik et al., 2006; Stumpp et al., 2016). It is, therefore, possible that species found in Alaska are also undergoing phenotypic evolution over brief time-scales. The North American pine marten, *Martes americana*, is distributed within boreal forests across Alaska (Clark et al., 1987; Nowak, 1999), a biome currently undergoing significant vegetational changes (Dial et al., 2016; Euskirchen et al., 2009; Klein et al., 2005; Lloyd and Fastie, 2002; Lloyd et al., 2003; Myneni et al., 1997). The morphology of *M. americana* may be evolving in response to Alaskan climate perturbation due to the species' close association with these forest habitats

(Banfield, 1974; Clark et al., 1987; Nowak, 1999). Here I sought to determine whether the morphology of *M. americana* is changing in response to Alaska's Recent climate.

Alaska's climate has undergone very pronounced changes over the past 60 years. Since the 1960s, Alaska has experienced an increase in annual temperature, gaining an average 0.5-1.0°C every ten years (Serreze et al., 2000). This has resulted in a decrease in annual snowfall (Dye, 2002; Euskirchen et al., 2007; Stone et al., 2002) and a decrease in permafrost stability (Jorgenson et al., 2001; Lloyd et al., 2003; Osterkamp and Romanovsky, 1999). Warmer annual temperatures have caused an increase in non-snow precipitation (Knowles et al., 2006) and lengthened the growing season (Myneni et al., 1997; Smith et al., 2004; Stone et al., 2002). Consequently, tundra habitats in Alaska have begun to shrink, while boreal forest tree lines and shrubbery have expanded (Euskirchen et al., 2009; Klein et al., 2005; Lloyd and Fastie, 2002; Myneni et al., 1997). While boreal forests are expanding, the composition of these forests is changing. Boreal forests are characterized by low shrub understories and are dominated by black spruce, *Picea mariana,* and jack pine, *Pinus banksania* (Smith and Smith, 2001). Recently, these forests have seen an increased density of tall shrub species (Dial et al., 2016), while spruce within these forests have decreased their annual growth (Lloyd and Fastie, 2002). Climate change in Alaska, therefore, appears to be causing shifts in weather patterns, habitat ranges, and habitat composition.

Several species found across Alaska have undergone phenotypic changes in correlation with anthropogenically induced climate change since the 1960s (Pergams and Lawler, 2009; Rode et al., 2010; Yom-Tov and Yom-Tov, 2005; Yom-Tov et al., 2007). Body size increases have been observed in the masked shrew, *Sorex cinereus*, over the past 60 years (Yom-Tov and Yom-Tov, 2005) and black footed-lemmings, *Lemmus trimucronatus nigripes*, have undergone decreases in foot and tail length within this same time span (Pergams and Lawler, 2009). Phenotypic skeletal changes have also occurred in large bodied species such as polar bears, *Ursus maritimis*, and the Canadian lynx, *Lynx canadensis* (Rode et al., 2010; Yom-Tov et al., 2007). Polar bears have

undergone a decrease in both cranial width and body length (Rode et al., 2010), while Canadian lynx have increased the zygomatic breadth of their skull (Yom-Tov et al., 2007). Researchers have attributed these skeletal changes to changes in food quality (Yom-Tov and Yom-Tov, 2005; Yom-Tov et al., 2008; Yom-Tov et al., 2007) and habitat availability (Rode et al., 2010) as Alaska's climate continues to warm and biomes shift.

M. americana may be undergoing skeletal phenotypic changes in response to shifts in Alaska's climate and boreal forest composition. This species is distributed throughout much of Alaska and predominantly occupies boreal forests in this region (Clark et al., 1987; Nowak, 1999). *M. americana* has a wide range of prey, but is particularly suited for hunting voles and other rodents within the subnivium (Buskirk, 1983; Nowak, 1999). This seasonal hunting strategy and unique mode of locomotion may make this species susceptible to changes in annual snowfall. *M. americana* has also been found to exhibit different hunting and nesting behaviors among forest patches of differing vegetation complexity (Andruskiw et al., 2008; Fuller et al., 2005; Moriarty et al., 2015; Steventon and Major, 1982). This suggests that changes in boreal forest complexity may influence the behavior of *M. americana,* which may in turn affect their skeletal limb morphology. Researchers have found that this species is undergoing phenotypic shifts in correlation with anthropogenic climate change, with body size increasing over the past 50 years (Yom-Tov et al., 2008). This body size change was attributed to a shift in diet (Yom-Tov et al., 2008). This study suggests that *M. americana* can undergo phenotypic evolution over a short time span and that it may be modifying its hunting behaviors to adapt to prey availability. Changes in hunting and locomotor behaviors which influence posture and gait can influence limb bone curvature, robusticity, and epiphyseal size (Biewener, 1983; 2005; Lieberman et al., 2003). It is, therefore, possible that these behavioral changes have resulted in differing limb phenotypes in *M. americana* since the 1960s. Previous research, however, indicates that the limb morphology of *M. americana* evolved independent of climate throughout the Pleistocene (Chapter 4). Are recent

changes in climate across Alaska drastic enough to induce appendicular phenotypic changes in *M. americana*?

In this study, I focused on the phenotypic variation in Alaskan *M. americana* to determine whether skeletal limb morphology has changed through time and whether it is evolving in response to selective pressures introduced by Alaska's changing climate. I tested two hypotheses: 1) skeletal limb morphology differs between specimens collected before and after 1970; and 2) skeletal limb morphology is adapting to Alaska's novel climate. To test these hypotheses, I analyzed geometric morphometric landmark data from specimens of *M. americana* collected from mainland Alaska between 1940 and 2007. I then tested for morphological evolutionary rate and mode using a phylogenetic framework constructed from mitochondrial DNA sequences taken from the same specimens whose morphology I measured.

Institutional Abbreviations

Sam Noble Oklahoma Museum of Natural History (SNOMNH), Florida Museum of Natural History (FMNH), University of Alaska Museum of the North (UAMN), and Smithsonian Institution National Museum of Natural History (USNM)

Materials and Methods

Specimens

I studied a total of 34 individuals morphologically identified as *M. americana.* Some specimens were incomplete, resulting in a dataset that included 31 skulls, 34 humeri, 30 radii, 30 ulnae, 34 femora, 32 tibiae, and 30 fibulae (Appendix V, Section A). Specimens were collected across

mainland Alaska between 1940 and 2007 (Figure 1A). All specimens were adults as determined by full epiphyseal fusion. The dataset also included both sexes which were determined by museum identification and presence of a baculum. I measured 15 specimens collected before and 19 collected after 1970. From 33 of these specimens I extracted DNA from bone or soft tissue. These specimens are housed in the collections at SNOMNH, FMNH, UAMN, and USNM. In addition, I included complete mitochondrial gene sequences for the 16S, cytochrome b (cytb), and Dloop genes for *Martes foina* from GenBank (NCBI) to be used as an outgroup (Appendix V, Section C).

Morphological Change

I collected shape data from appendicular skeletal elements (humerus, radius, ulna, femur, tibia, and fibula) of each specimen. I collected 3D geometric morphometric landmark data from each bone using a MicroScribe G2LX digitizer. This digitizer records the X, Y, and Z coordinates of a single point/landmark in space. I chose landmarks that would best capture the length and width of each element because size evolves in mammals through time (e.g., Fabre et al., 2013b; Kolska Horwitz and Ducos, 1997; Meachen et al., 2014; Meachen and Samuels, 2012). I also chose landmarks that represented morphological characters frequently used in phylogenetic studies of carnivorans (Leach, 1977; Morlo and Peigné, 2010; Zrzavý and Řičánková, 2004). This allowed me to use previously identified traits that are thought to contain phylogenetic signal. Where possible, I avoided landmarks associated with muscle attachments, as these are modified throughout an individual's life (Currey, 2002; Wei and Messner, 1996). In addition, I tested all landmarks for accuracy and repeatability (Chapter 1). This resulted in 14 humeral, 10 radial, 11 ulnar, 12 femoral, 10 tibial, and 8 fibular landmarks (Figure 2; Appendix V, Section D). I aligned landmarks for each element independently using a generalized Procrustes analysis (GPA) and

then calculated the centroid size of each bone from each specimen (Appendix V, Section E, Table 1). I ran these analyses using the geomorph package (Adams and Otarola-Castillo, 2013) in R (R Core Team, 2015) (Appendix V, Section G).

I assigned each specimen to one of two time-bins, those collected before 1970 and those collected after 1970. I chose 1970 as a bin cut-off because Alaska's climate began to change considerably during the 1960s (Dye, 2002; Klein et al., 2005; Serreze et al., 2000; Stone et al., 2002). *M. Americana has* an approximately ten year life-span, begin reproducing around two years of age, and can reproduce once per year there-after (Banfield, 1974; Clark et al., 1987). Given this life history, these bins then allowed me to compare the morphologies of individuals that lived entirely in Alaska's historic climate to those that were born into Alaska's recent climate.

I tested for a significant difference in limb element shape between specimens collected before (N=15) and after (N=19) 1970. To do this, I first calculated principal component (PC) scores for the aligned landmarks using a principal components analysis. I then tested for morphological differences between specimens from each time bin in each element individually using the highest ranking PC scores, those explaining 95% of the morphological variance (Zelditch et al., 2012). PC scores are commonly used in morphometric analyses as a proxy for shape and a means of reducing the number of variables in a statistical analysis (Carden et al., 2012; Fabre et al., 2013a; Meachen et al., 2016; Rychlik et al., 2006). I tested for statistical differences between the PC scores for each time bin and element using a series of PERMANOVAs (α=0.05, permutation 9,999) (Polly, 2008; Rychlik et al., 2006). PERMANOVA is robust to violations of multivariate normality and allows for more variables than specimens per group (Anderson, 2001), which occur in several of the datasets. I ran this analysis six times, once for each element.

Morphological Adaptation

DNA Extraction, Amplification, and Sequencing

I collected samples from a rib bone or soft tissue from each of the 32 specimens. I extracted genomic DNA from soft tissue using the following protocol: approximately 0.025 g of soft tissue was incubated at 55°C for 24 hours while rotating in 125 µL lysis buffer (Bello et al., 2001), 8.75 µL 20 mg/mL proteinase K, 5 µL 1 mg/mL RNase A, and 10 µL 5 mM DTT followed by a phenol:chloroform:isoamyl (25:24:1) extraction protocol (see detailed protocol in Appendix VI). I extracted cellular DNA from bone tissue using a silica binding protocol modified from Rohland (2012) (see detailed protocol in Appendix VI). Prior to sampling, all bones were cleaned in a 2-4% bleach solution, then rinsed and allowed to air dry. I then powdered the entire rib using a SPEX® Cryogenic Grinder. This yielded between 0.05 g and 0.1 g of powder (Appendix V, Section E, Table 4). I eluted all samples in 40-65 µL of 86°C elution buffer (10 mM Tris and 0.1 mM EDTA). I quantified the amount of DNA present in all extractions using a ThermoFisher™ Qubit® (Appendix V, Section E, Table 4).

I amplified DNA in overlapping fragments ranging from 139-1,012 bp, depending on the DNA quality of each specimen, using a polymerase chain reaction (PCR) (see detailed protocol in Appendix VII). The 16S, cytb, and Dloop mitochondrial genes were all targeted using primers that I designed to span the entirety of each gene (Table 1; Appendix V, Section F, Figure S1). I designed 12S, 16S, and Dloop primers to amplify approximately 250bp regions with 50bp of overlap (Appendix V, Section F, Figure S1). I designed primers to have similar annealing temperatures, within 1°C, and with GC content of at least 60%. In some cases, the GC content criterion resulted in targeted priming sites that had less than 50bp of overlap (Appendix V, Section F, Figure S1). Primers for cytb were taken from (Stone and Cook, 2002). For all PCRs, I used a negative and positive control. I performed PCR amplifications in 20 µL volumes using

separate protocols for bone and soft tissue extractions. For samples extracted from bone tissue, I amplified each gene using the following reagents: 1X PCR buffer, 2 mM $MgCl_2$, 200 µM dNTP, 1 mg/ml BSA, 1.25 U ThermoFisher^{TM} AmpliTaq Gold, and 0.4 µM of each primer. The PCR was conducted on a Labnet International, Inc. MultiGene Optimax thermocycler and cycling conditions were as follows: 95°C for 15 min; 35 cycles of 95°C for 15 s, 52-60°C for 30 s, 72°C for 30 s; 72°C for 5 min. For samples extracted from soft tissue, I amplified each gene using 1X PCR buffer, 2 mM $MgCl_2$, 200 µM dNTP, 1 mg/ml BSA, 1.25 U Apex^{TM} Taq, and 0.4 µM of each primer. The PCR cycling conditions were as follows: 95°C for 10 min; 35 cycles of 95°C for 15 s, 52-60°C for 90 s, 72°C for 30 s; 72°C for 5 min. I evaluated the success of each amplification by running 5 µL of dyed PCR product on a 2% agarose gel and imaging using a BioRad Gel Doc XR system.

I cleaned all PCR products using an Exo-Sap cleaning procedure and Sanger sequenced all forward and reverse strands on an Applied Biosystems 3130xl Genetic Analyzer (see detailed protocol in Appendix VIII) I edited all DNA sequences using CLC Main Workbench (Qiagen Bioinformatics).

Sequence Alignment and Nucleotide Substitution Modeling

Sequences obtained for 12S, 16S, Dloop, and cytb were initially short amplicons which had to be assembled against a reference genome. Here, I used the mitochondrial genome of *M. foina* (HM106325.1) as a reference. Using MEGA7 (Kumar et al., 2016), I aligned the sequences for each gene independently against the mitochondrial genome of *Martes foina* (HM106325.1), which acted as an outgroup. I used the ClustalW algorithm with the default parameters for all alignments and corrected any misalignments manually. Because some sequences were partial, I trimmed all alignments to reduce the amount of missing data. This resulted in the following

length ranges for each gene: 16S = 0-960 bp; cytb = 0-830 bp; Dloop = 274-538 bp. Previous analyses (Chapter 2) indicate that accurate phylogenetic relationships can only be constructed using sequence lengths of >135bp of 16S, >340bp of cytb, and 0bp of Dloop in a concatenated sequence. I, therefore, removed all specimens from the final analysis that did not meet these three requirements. This resulted in 16 specimens of *M. americana*, 5 collected before 1970 and 11 collected after 1970, as well as the single GenBank sequence of *M. foina* as an outgroup. Sequence lengths ranged from 219-960bp in 16S, 410-830bp in cytb, and 234-538bp Dloop (Appendix V, Section E, Table 5).

I tested for the best-fit nucleotide substitution model for each gene independently and for the concatenated sequence in MEGA7 (Kumar et al., 2016) using a maximum likelihood model and an 85% site coverage cutoff because some specimens had missing data. I chose the best-fit nucleotide substitution models as those with the lowest Akaike Information Criterion (AIC) (Akaike, 1974) (Table 2). I then concatenated the three genes into a single sequence of 2,330 bp allowing me to test phylogenetic relationships using all three genes simultaneously.

Bayesian Phylogeny

I tested for phylogenetic relationships between specimens using a Bayesian Markov Chain Monte Carlo (MCMC) phylogenetic analysis. I ran this analysis using Beast 1.8.4 (Drummond et al., 2012). I unlinked the nucleotide substitution models for each gene and assigned the best-fit model to each: 16S = TN93; cytb = HKY; Dloop = K2+I (Table 2). I chose a relaxed lognormal molecular clock (Drummond et al., 2006). Under simulated datasets, this clock model had the highest power for data evolving under both clocklike and non-clocklike conditions when compared to other strict and autocorrelated clock models (Drummond et al., 2006). I also assumed coalescence with a constant population size because this null is the most appropriate

when testing for intraspecific evolutionary relationships (Kingman, 1982). A single MCMC chain was run for 100,000,000 iterations with parameters written every 1,000 generations (Table 3). I discarded the first 20% of trees as burn-in.

Tracer 1.6 (Rambaut et al., 2014) was used to check for convergence between runs. I checked Effective Sample Size values for each prior to determine whether the posterior distributions of all parameters were well estimated. Finally, using TreeAnnotator 1.8.2 (Drummond et al., 2012), I compiled the maximum credibility tree from the post burn-in sample.

Phylogenetic Signal

To determine whether appendicular skeletal morphology reflected the underlying phylogenetic relationships of Alaskan *M. americana,* I tested for phylogenetic signal in limb bone shape in each element independently. I included the 16 specimens of *M. americana* whose phylogenetic relationships were determined and whose skeletal limb morphology was quantified using geometric morphometrics. This dataset was comprised of 5 specimens collected before 1970 and 11 specimens collected after 1970 (Figure 1B). I measured phylogenetic signal using a generalization of Blomberg's K (Blomberg et al., 2003) that is appropriate for multivariate data (K_{mult}) (Adams, 2014b; Adams and Collyer, 2018). This model is ideal for geometric morphometric data because it has high power and appropriate Type I error despite trait dimensionality and covariance (Adams, 2014a; Adams and Collyer, 2018). To evaluate the significance of K_{mult} I tested it against a Brownian Motion (BM) null model of evolution using a permutation method for 999 iterations ($\alpha \leq 0.05$). BM is an appropriate null model for phenotypic evolution because it assumes phenotypes shift randomly and proportionally with time, thereby forming a normal trait distribution (Felsenstein, 1973; Felsenstein, 2004). I ran this analysis in R

(R Core Team, 2015) using the geomorph package (Adams and Otarola-Castillo, 2013) (Appendix IV, Section G).

Second, I tested for phylogenetic signal using centroid size as a measure of shape. I chose a univariate trait because there are currently no accurate methods for interpreting evolutionary mode in multivariate data (Adams and Collyer, 2018). I measured phylogenetic signal using two indices: Blomberg's K (Blomberg et al., 2003) and Pagel's λ (Pagel, 1999). Blomberg's K values that are significant and positive indicate there is a greater phylogenetic signal in the data than would be expected at random. Blomberg's K calculates phylogenetic signal as a ratio of the mean squared error (MSE) of the tip data around a phylogenetically corrected mean and the MSE of the given phylogeny under a BM null model of evolution. The significance of this index is then determined by comparing the ratios produced under a BM null model of evolution to those produced at random through a permutation method (Blomberg et al., 2003). Here I tested for significance using 999 iterations. Pagel's λ values close to one indicate a strong phylogenetic signal in the data. To calculate Pagel's λ the phylogeny is transformed under a BM null model of evolution. λ is then the coefficient required to scale the resulting covariance matrix to match that from the original, untransformed phylogeny (Pagel, 1999). I calculated both indices as a means of comparing to the results of the K_{mult} analysis, and because Pagel's λ is a more accurate measure of phylogenetic signal in phylogenies with few tips (Münkemüller et al., 2012). I ran these analyses in R (R Core Team, 2015) using the phytools package (Revell, 2012).

Evolutionary Rate

Because Alaskan climate has changed drastically over the past 60 years, I sought to determine whether this change influenced the rate of appendicular morphological evolution in *M. americana*. I tested for differences in evolutionary rate between specimens collected before 1970

(N=5) and those collected after (N=11). For this analysis I quantified limb element shape using the GPA aligned landmark data for each element. Evolutionary rates were calculated by phylogenetically transforming the shape data under a BM null model of evolution and then calculating the resulting between-specimen Euclidian distances. Rate was quantified as the sum of squared distances between the phylogenetically transformed data and the origin of the phylogeny (Adams, 2014b). To determine whether rates significantly differed between specimens from each time bin, I compared ratios of rates between each time bin to ratios of rates produced from simulated data with rates that do not significantly differ under a BM null model of evolution. I did this using a permutation method for 999 iterations (Denton and Adams, 2015). This method produces appropriate Type I error and high power, despite small rate differences between groups (Adams and Collyer, 2018). I ran all analyses in R (R Core Team, 2015) using the geomorph package (Adams and Otarola-Castillo, 2013) (Appendix IV, Section G).

Results

Morphological Change

The number of PCs composing 95% of the variance in shape differed by element: 17 humeral, 12 radial, 15 ulnar, 17 fibular, 15 tibial, and 15 ulnar (Appendix V, Section E, Table 2). The variation explained by each PC ranged from 36% to 1% depending on the element (Appendix V, Section E, Table 3). The results of the PERMANOVA indicated that there was no significant difference in morphology between specimens collected before and after 1970 in any of the six measured elements (Table 4). This can be visualized through the PC plots, which show considerable overlap in morphospace between specimens collected before and after 1970 (Figure 3).

Morphological Adaptation

Bayesian Phylogeny

In the Bayesian phylogeny, all specimens of *M. americana* comprised a single clade with *M. foina* as the outgroup (Figure 4). This node had 100% posterior probability support. Within *M. americana* there were several subclades often containing specimens collected in the same time bin. For example, some of the oldest specimens, collected in 1940 and 1968, comprised one subclade and the youngest specimens, collected between 1990 and 2006, formed another subclade. While subclades were organized by time, the relationship was not perfect, and specimens collected in 1976 were most closely related to those collected in 2006. Posterior probability support for these subclades ranged from 29% to 96%.

Phylogenetic Signal

I found no significant phylogenetic signal in the landmark data in all six measured elements (Table 5). There was also no significant phylogenetic signal in the centroid size data and Blomberg's K and Pagel's λ ranged from <0.01 to 0.38 (Table 5). These results indicate that the skeletal limb morphology of Alaskan *M. americana* hasn't measurably evolved in conjunction with phylogenetic relationships and that instead phenotypic phenotypic variation has accrued under a BM model of evolution.

Evolutionary Rate

I found that the rates of skeletal limb evolution in Alaskan *M. americana* differed between specimens collected before and after 1970 (Table 6), with younger specimens consistently having faster rates of evolution in all six measured elements. This difference in tempo, however, did not significantly differ from that expected under a BM null model of evolution ($p>0.05$). This suggests that changes in climate and biome have not influenced rates of morphological evolution in this species.

Discussion

The results of this study suggest that changes in climate and biome in mainland Alaska since the 1960s have had little influence on the skeletal limb evolution of *M. americana.* Alaskan climate change has resulted in changes in annual snowfall, non-snow precipitation, and temperature (Dye, 2002; Euskirchen et al., 2007; Knowles et al., 2006; Serreze et al., 2000; Stone et al., 2002), which, in turn, has caused changes in boreal forest composition and complexity (Euskirchen et al., 2009; Klein et al., 2005; Lloyd and Fastie, 2002; Myneni et al., 1997). Given that the behavior of *M. americana* can vary in response to snowfall and forest complexity (Andruskiw et al., 2008; Clark et al., 1987; Fuller et al., 2005; Moriarty et al., 2015; Nowak, 1999; Steventon and Major, 1982), I predicted these factors would have acted as selective pressures on behavior, which in turn would have resulted in changes in limb morphology. In other vertebrates, climate change has been shown to influence skeletal morphology on decadal and even seasonal time-scales (Doudna and Danielson, 2015; Franssen, 2011; Poroshin et al., 2010; Rychlik et al., 2006; Stumpp et al., 2016). For many of these species, morphological evolution is directional and suggests that novel, climate-related selective pressures are influencing phenotypic adaptation toward a new fitness optimum (Doudna and Danielson, 2015; Franssen, 2011; Stumpp et al., 2016). In *M. americana*,

however, there was no difference in skeletal limb morphology between specimens collected before and after 1970. Instead, the morphology of this species has accumulated variation under a BM model of evolution. Further, species undergoing phenotypic evolution in response to changes in climate and biome often exhibit different rates of evolution than they exhibited previously (Hendry et al., 2008; Kinnison and Hendry, 2001; Salamin et al., 2010). *M. americana* does not differ in evolutionary rate between time-bins, suggesting that selective pressures imposed by Alaska's changing climate and biomes are not influencing the rate of limb evolution in this species. It is, therefore, likely that *M. americana* is responding to Alaska's recent climate change in a different manner.

Rather than undergoing phenotypic adaptation, species can also respond to changes in biome and climate by modifying their geographic distributions (Dietl and Flessa, 2011; MacLean and Beissinger, 2017). Historically, the Kenai Peninsula was uninhabited by *M. americana,* as it was hypothesized to have been suboptimal territory for the species (Baltensperger et al., 2017). Over the past 60 years, however, this region has seen a loss of tundra habitat and the expansion of tree lines and dense shrubs as a result of Alaska's increased precipitation and longer growing season (Dial et al., 2016; Klein et al., 2005; Myneni et al., 1997). While capable of occupying a range of habitats (Banfield, 1974; Steventon and Major, 1982), the preferred habitat of *M. americana* is a dense forest with 70% canopy cover (Clark et al., 1987). Researchers have found that *M. americana* has shifted its range from eastern territories to previously uninhabited regions within the western Kenai Peninsula (Baltensperger et al., 2017), suggesting that *M. americana* is responding to changes in climate and habitat in Alaska by altering its geographic range and tracking newly forested habitats. It is, therefore, possible that *M. americana* will be able to survive current climate change despite a lack of morphological limb evolution.

M. americana may be able to respond to Alaskan climate change without undergoing significant changes in limb morphology because this species is a generalist (Banfield, 1974; Clark et al.,

1987; Nowak, 1999). Generalist taxa tend to be less susceptible to climate change because they can often shift their geographic ranges to track more suitable habitat and prey (Clavel et al., 2011; Dunn et al., 2009; Futuyma and Moreno, 1988; Gilchrist, 1995; Kassen, 2002; Lurgi et al., 2012; Menéndez et al., 2006). Of the Alaskan species whose morphology has shifted in correlation with anthropogenic climate change, many are dietary specialists. For example, both polar bears and Canadian lynx are specialized hunters that feed almost exclusively on a single prey (Banfield, 1974; DeMaster and Stirling, 1981; Nowak, 1999; Poole, 2003). The masked shrew feeds predominantly on insects, the life cycles of which are dependent on ambient temperature (Bale et al., 2002; Banfield, 1974; Nowak, 1999). Changes in climate are likely to be influencing the prey of these specialized hunters, resulting in phenotypic changes in the predators as they adapt accordingly (Rode et al., 2010; Yom-Tov and Yom-Tov, 2005; Yom-Tov et al., 2007). A similar hypothesis was presented to explain the recent increase in body size seen in Alaskan martens (Yom-Tov et al., 2008). The lack of morphological changes in the limbs, however, suggests that these species are not changing hunting behaviors. Instead, their wide dietary range may be allowing them to shift preferred prey choice as necessary (Banfield, 1974; Clark et al., 1987; Nowak, 1999).

Conclusions

The North American pine marten, *M. americana*, has not undergone changes in limb morphology in correlation with anthropogenic climate change. Further, this species is not exhibiting directional evolution in response to selective pressures imposed by changes in temperature, precipitation, or forest composition. Instead, the generalist nature of *M. americana* may be allowing it to successfully shift geographic ranges and perhaps change food sources as needed. This conclusion suggests that *M. americana* and other less morphologically specialized species

may not require extensive conservation efforts to ensure their future survival. By studying of the morphology of recently established populations of *M. americana* it may be possible to expand our understanding of how this species is adapting to modern novel habitats.

Tables

Table 1. Gene Primer Sequences and Annealing Temperatures

Gene	Primer	Forward Sequence	Reverse Sequence	Annealing Temp C
16S	1	GCACCTGGCTTACACC	CATCATTCCCTTGCGGTAC	52
	2	CCAACTACCACGACATCC	CATAGGTAGCTCGTCTGG	50
	3	GCTACCTATGAGCAATCCAC	CTAAGCAAGGTTGTTTCCTTG	50
	4	CCTAACGTATCACTGGGC	CAGTGCCTCCAATACTGAG	52
	5	GCACAAGCTTATAACAGTCAACG	GGCCGTTAAACTAATGTCACTG	52
	6	CACAGGCGTGCAGTAAG	GTTAGACCTGGTTGGTGG	52
	7	GACGAGAAGACCCTATGGAG	GATAGCTGCTGCACCATC	54
	8	GACCTCGATGTTGGATCAG	CAATTACTGGGCTCTGCC	54
Dloop	1	CAACAGCCCCGCCATC	GTGRGGTGCACGGATGC	58
	2	CGTGCATTAATGGCTTGCC	GGATTGAGGACTTCCATGGC	58
	3	CGTGTACCTCTTCTCGCTC	GAAGGATAAGCCCAGCTACAAG	58
Cytb	1	CGAYYTACCTGCYCCATC	YAGGAACAGGCAGATGAAG	60
	2	YTCTTCATCTGCCTGTTCCTG	GCGAAGAATCGYGTTAGGGTAG	60
	3	CTGAGGAGGATTCTCGGTAGACAAGG	GGATTAGGAATAGGGCGCCTAGG	60
	4	CTAGGCGCCCTATTCCTAATC	CTGAGTGGGCGGAATATCAT	60
	5	CAATTRTCCCATTVCTYCATAC	RATGGCTGGCATRAGGAYTAG	60

Table 2. Best-fit Substitution Models for Each Gene

Gene	Evolutionary Model	AIC
16S	TN93	566.12
Cytb	HKY	1152.87
Dloop	K2+I	1265.14

Table 3. Phylogenetic Priors for Model Parameters and Statistics

Parameter	Prior	Bound
16S.kappa1	Lognormal [1,1.25], initial=2	0,∞
16S.kappa2	Lognormal [1,1.25], initial=2	0,∞
16S frequencies	Uniform [0,1], initial=0.25	0,1
Cytb kappa	LogNormal [1,1.25], initial=2	0,∞
Cytb frequencies	Uniform [0,1], initial=0.25	0,1
Dloop.kappa	Lognormal [1,1.25], initial=2	0,∞
ucld stdev	Exponential [0.333333], initial=0.333333	0,∞
ucld mean	Fixed value, value=1	0,∞
treeModel rootHeight	Using Tree Prior in [0, ∞]	0, ∞
Constant popSize	1/x, initial=1	0,∞

Table 4. Results of PERMANOVA on PC scores

Element	F	*p*
Humerus	0.67	0.72
Radius	0.72	0.75
Ulna	1.36	0.16
Femur	1.25	0.22
Tibia	1.36	0.16
Fibula	1.27	0.23

Table 5. Phylogenetic Signal

Element	**Kmult**	**Kmult *p***	**K**	**K *p***	**λ**
Humerus	0.41	0.68	0.52	0.23	<0.01
Radius	0.36	0.89	0.55	0.18	<0.01
Ulna	0.39	0.75	0.49	0.28	<0.01
Femur	0.44	0.26	0.53	0.22	<0.01
Tibia	0.40	0.85	0.61	0.14	0.38
Fibula	0.47	0.19	0.49	0.37	<0.01

Table 6. Limb Element Shape Tempo by Time Bin

Element	***p***	**Evolutionary Rates by Time Bin**	
		Before 1970	After 1970
Humerus	0.10	$1.8x10^{-3}$	$6.1x10^{-3}$
Radius	0.14	$1.7x10^{-3}$	$5.8x10^{-3}$
Ulna	0.07	$1.4x10^{-3}$	$5.1x10^{-3}$
Femur	0.87	$1.4x10^{-3}$	$2.3x10^{-3}$
Tibia	0.50	$1.1x10^{-3}$	$3.5x10^{-3}$
Fibula	0.49	$7.0x10^{-4}$	$2.0x10^{-3}$

Figures

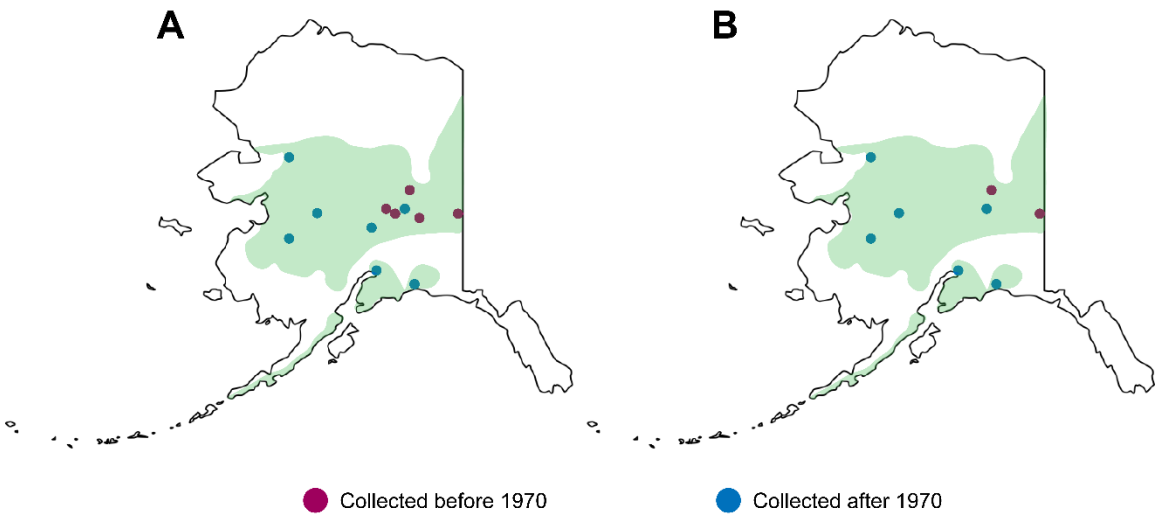

Figure 1. Geographic distribution of specimens included in the study. A) Geographic location of specimens whose skeletal morphology was measured. B) Geographic location of specimens that were included in the final phylogeny and, therefore, whose phenotypic evolution was determined. Red points on the map represent specimens collected before 1970 and blue represent those collected after 1970. The distribution of the boreal forest biome in Alaska is indicated in green (Olson et al., 2001).

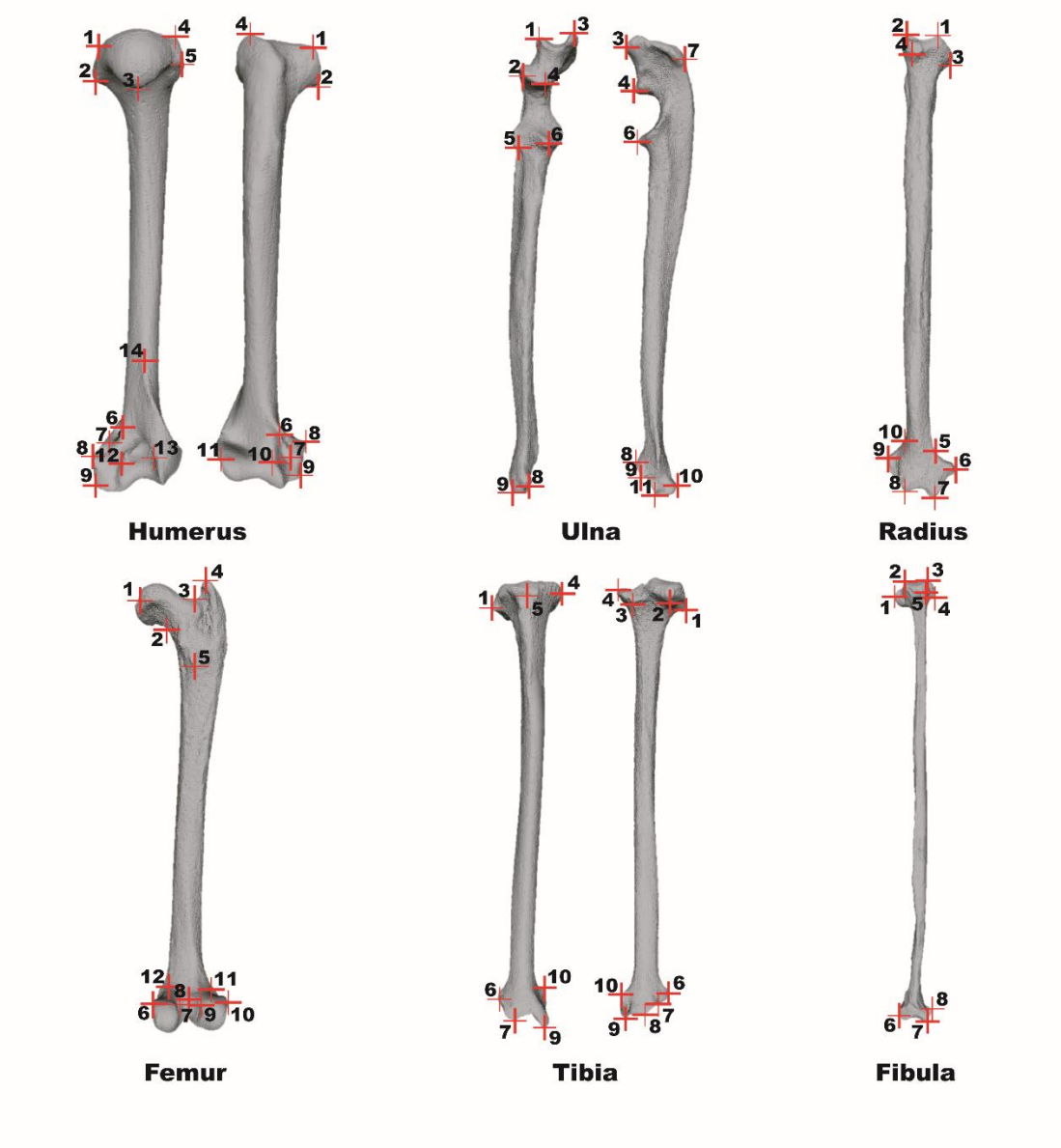

Figure 2. Geometric morphometric landmarks on the humerus, radius, ulna, femur, tibia, and fibula used to quantify bone shape.

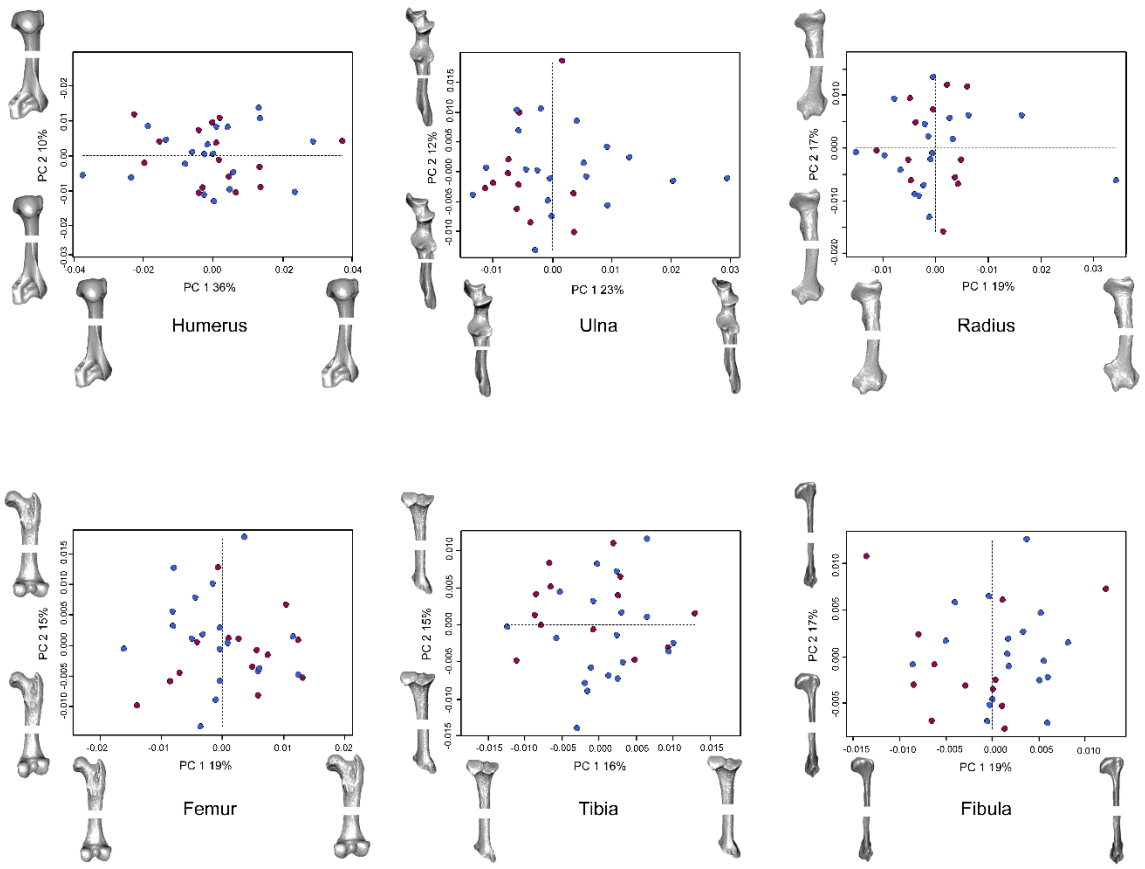

Figure 3. Principal component analysis (PCA) plots for the first two PC axes for the humerus, radius, ulna, femur, tibia, and fibula. Points are colored according to the time bin to which each specimen was assigned. Red represents individuals collected before 1970. Blue represents specimens collected after 1970. The percent variance explained by each PC axis is indicated in the axis label. Bone images represent the morphology of each element at the extremes of each PC axis. In all of the bones there was no significant difference in element morphology between specimens from the two time bins.

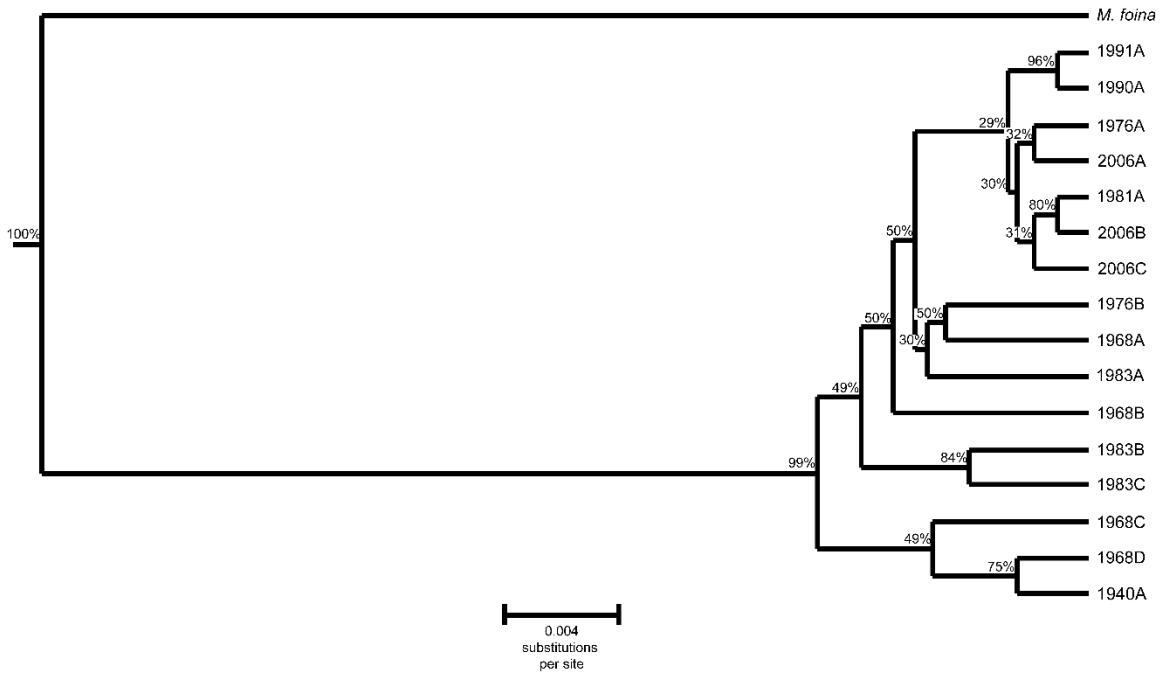

Figure 4. Bayesian phylogeny of *M. americana* specimens constructed from a concatenated sequence of 16S, cytb, and Dloop mitochondrial genes. Branch lengths represent the number of nucleotide substitutions per site as denoted by the scale bar. Node values indicate the posterior probability support. Tip labels indicate the year each specimen was collected followed by an individual specimen letter. See Appendix V (Section E, Table 6) for the collection number associated with each tip label.

REFERENCES

Abdi H. 2010. Partial least squares regression and projection on latent structure regression (PLS Regression). Wiley Interdisciplinary Reviews: Computational Statistics 2(1):97-106.

Adams DC. 2014a. A generalized K statistic for estimating phylogenetic signal from shape and other high-dimensional multivariate data. Systematic Biology 63(5):685-697.

Adams DC. 2014b. Quantifying and comparing phylogenetic evolutionary rates for shape and other high-dimensional phenotypic data. Systematic Biology 63(2):166-177.

Adams DC, Collyer ML. 2018. Multivariate phylogenetic comparative methods: evaluations, comparisons, and recommendations. Systematic Biology 67(1):14-31.

Adams DC, Nistri A. 2010. Ontogenetic convergence and evolution of foot morphology in European cave salamanders (Family: Plethodontidae). BMC Evol Biol 10:216-216.

Adams DC, Otarola-Castillo E. 2013. Geomorph: an R package for the collection and analysis of geometric morphometric shape data. Methods in Ecology and Evolution 4:393-399.

Akaike H. 1974. A new look at the statistical model identification. IEEE transactions on automatic control 19(6):716-723.

Aliabadian M, Kaboli M, Nijman V, Vences M. 2009. Molecular identification of birds: performance of distance-based DNA barcoding in three genes to delimit parapatric species. PLOS ONE 4(1):e4119.

Allen JA. 1877. The influence of physical conditions in the genesis of species. Radical Review 1:108-140.

Allentoft ME, M. Collins. D. Harker. J. Haile. C. Oskam. M. Hale. P. Campos. J. Samaneigo. M. Gilbert. E. Willerslev. G. Zhang. R. Scofield. R. Holdaway. M. Bunce. 2012. The half-life of DNA in bone: measuring decay kinetics in 158 dated fossils. Proceedings of the Royal Society in Biological Sciences 279:4724-4733.

Ambriz-Morales P, De La Rosa-Reyna XF, Sifuentes-Rincon AM, Parra-Bracamonte GM, Villa-Melchor A, Chassin-Noria O, Arellano-Vera W. 2016. The complete mitochondrial genomes of nine white-tailed deer subspecies and their genomic differences. Journal of Mammalogy 97(1):234-245.

Anderson E. 1970. Quaternary evolution of the genus *Martes* (Carnivora, Mustelidae). Acta Zoologica Fennica 130:1-132.

Anderson E. 1994. Evolution, prehistoric distribution, and systematics of *Martes*. Martens, Sables and Fishers: Biology and Conservation:13-25.

Anderson MJ. 2001. A new method for non-parametric multivariate analysis of variance. Austral Ecology 26(1):32-46.

Andrews CA. 2010. Natural selection, genetic drift, and gene flow do not act in isolation in natural populations. Nature Education and Knowledge 3(10):5.

Andruskiw M, Fryxell JM, Thompson ID, Baker JA. 2008. Habitat-mediated variation in predation risk by the American marten Ecology 89(8):2273-2280.

Abdi H. 2010. Partial least squares regression and projection on latent structure regression (PLS Regression). Wiley Interdisciplinary Reviews: Computational Statistics 2(1):97-106.
Adams DC. 2014a. A generalized K statistic for estimating phylogenetic signal from shape and other high-dimensional multivariate data. Systematic Biology 63(5):685-697.
Adams DC. 2014b. Quantifying and comparing phylogenetic evolutionary rates for shape and other high-dimensional phenotypic data. Systematic Biology 63(2):166-177.
Adams DC, Collyer ML. 2018. Multivariate phylogenetic comparative methods: evaluations, comparisons, and recommendations. Systematic Biology 67(1):14-31.
Adams DC, Nistri A. 2010. Ontogenetic convergence and evolution of foot morphology in European cave salamanders (Family: Plethodontidae). BMC Evol Biol 10:216-216.
Adams DC, Otarola-Castillo E. 2013. Geomorph: an R package for the collection and analysis of geometric morphometric shape data. Methods in Ecology and Evolution 4:393-399.
Akaike H. 1974. A new look at the statistical model identification. IEEE transactions on automatic control 19(6):716-723.
Aliabadian M, Kaboli M, Nijman V, Vences M. 2009. Molecular identification of birds: performance of distance-based DNA barcoding in three genes to delimit parapatric species. PLOS ONE 4(1):e4119.
Allen JA. 1877. The influence of physical conditions in the genesis of species. Radical Review 1:108-140.
Allentoft ME, M. Collins. D. Harker. J. Haile. C. Oskam. M. Hale. P. Campos. J. Samaneigo. M. Gilbert. E. Willerslev. G. Zhang. R. Scofield. R. Holdaway. M. Bunce. 2012. The half-life of DNA in bone: measuring decay kinetics in 158 dated fossils. Proceedings of the Royal Society in Biological Sciences 279:4724-4733.
Ambriz-Morales P, De La Rosa-Reyna XF, Sifuentes-Rincon AM, Parra-Bracamonte GM, Villa-Melchor A, Chassin-Noria O, Arellano-Vera W. 2016. The complete mitochondrial genomes of nine white-tailed deer subspecies and their genomic differences. Journal of Mammalogy 97(1):234-245.
Anderson E. 1970. Quaternary evolution of the genus *Martes* (Carnivora, Mustelidae). Acta Zoologica Fennica 130:1-132.
Anderson E. 1994. Evolution, prehistoric distribution, and systematics of *Martes*. Martens, Sables and Fishers: Biology and Conservation:13-25.
Anderson MJ. 2001. A new method for non-parametric multivariate analysis of variance. Austral Ecology 26(1):32-46.
Andrews CA. 2010. Natural selection, genetic drift, and gene flow do not act in isolation in natural populations. Nature Education and Knowledge 3(10):5.
Andruskiw M, Fryxell JM, Thompson ID, Baker JA. 2008. Habitat-mediated variation in predation risk by the American marten Ecology 89(8):2273-2280.
Arbogast BS, Browne RA, Weigl PD. 2001. Evolutionary genetics and pleistocene biogeography of North American tree squirrels (*Tamiasciurus*). Journal of Mammalogy 82(2):302-319.
Avise JC. 2000. Phylogeography: the history and formation of species. Cambridge, Massachusetts: Harvard University Press.
Axelsson E, Willerslev E, Gilbert MTP, Nielsen R. 2008. The effect of ancient DNA damage on inferences of demographic histories. Molecular Biology and Evolution 25(10):2181-2187.
Baker AJ, Peterson RL, Eger JL, Manning TH. 1978. Statistical analysis of geographic variation in the skull of the arctic hare (*Lepus arcticus*). Canadian Journal of Zoology 56(10):2067-2082.
Bale JS, Masters GJ, Hodkinson ID, Awmack C, Bezemer TM, Brown VK, Butterfield J, Buse A, Coulson JC, Farrar J, Good JEG, Harrington R, Hartley S, Jones TH, Lindroth RL, Press MC, Symrnioudis I, Watt AD, Whittaker JB. 2002. Herbivory in global climate change

research: direct effects of rising temperature on insect herbivores. Global Change Biol 8(1):1-16.
Baltensperger AP, Morton JM, Huettmann F. 2017. Expansion of American marten (*Martes americana*) distribution in response to climate and landscape change on the Kenai Peninsula, Alaska. Journal of Mammalogy 98(3):703-714.
Banfield AWF. 1974. Mammals of Canada. Toronto, Canada: University of Toronto Press.
Barnett R, Shapiro B, Barnes IAN, Ho SYW, Burger J, Yamaguchi N, Higham TFG, Wheeler HT, Rosendahl W, Sher AV, Sotnikova M, Kuznetsova T, Baryshnikov GF, Martin LD, Harington CR, Burns JA, Cooper A. 2009. Phylogeography of lions (*Panthera leo* ssp.) reveals three distinct taxa and a late Pleistocene reduction in genetic diversity. Molecular Ecology 18(8):1668-1677.
Baryshnikov G, Batyrov B. 1994. Sredneplejstocenovye hisnye mlekopitaûsie (Carnivora, Mammalia) Srednej Azii. Tr Zool Inst RAN 256:3-43.
Behrensmeyer AK, Turner A. 2013. Taxonomic occurences of *Martes americana* recorded in the Paleobiology Database. Fossilworks.
Bell C. 1995. A Middle Pleistocene (Irvingtonian) microtine rodent fauna from White Pine County, Nevada, and its implications for microtine rodent biochronology. Journal of Vertebrate Paleontology 15:18A-18A.
Bello N, Francino O, Sánchez A. 2001. Isolation of genomic DNA from feathers. Journal of Veterinary Diagnostic Investigation 13(2):162-164.
Ben-David M, Flynn R, Schell D. 1997. Annual and seasonal changes in diets of martens: evidence from stable isotope analysis. Oecologia 111(2):280-291.
Bergmann C. 1847. Ueber die Verhältnisse der Wärmeökonomie der Thiere zu ihrer Grösse. Gottinger Studien 3:595-708.
Bertram JEA, Biewener AA. 1990. Differential scaling of the long bones in the terrestrial Carnivora and other mammals. Journal of Morphology 204.
Bertram JEA, Biewener AA. 1992. Allometry and curvature in the long bones of quadrupedal mammals. Journal of Zoology 226(3):455-467.
Bibi F. 2013. A multi-calibrated mitochondrial phylogeny of extant Bovidae (Artiodactyla, Ruminantia) and the importance of the fossil record to systematics. BMC Evol Biol 13(1):166.
Biewener AA. 1983. Allometry of quadrupedal locomotion: the scaling of duty factor, bone curvature and limb orientation to body size. J Exp Biol 105(1):147-171.
Biewener AA. 2005. Biomechanical consequences of scaling. J Exp Biol 208.
Blomberg SP, Garland Jr T, Ives AR, Crespi B. 2003. Testing for phylogenetic signal in comparative data: behavioral traits are more labile. Evolution 57(4):717-745.
Bond G, Broecker W, Johnsen S, McManus J, Labeyrie L, Jouzel J, Bonani G. 1993. Correlations between climate records from North Atlantic sediments and Greenland ice. Nature 365(6442):143-147.
Bookstein F. 1991. Morphometric Tools for Landmark Analysis: Geometry and Biology. New York: New York: Cambridge Univ Press.
Brace S, Palkopoulou E, Dalén L, Lister AM, Miller R, Otte M, Germonpré M, Blockley SPE, Stewart JR, Barnes I. 2012. Serial population extinctions in a small mammal indicate Late Pleistocene ecosystem instability. Proceedings of the National Academy of Sciences 109(50):20532-20536.
Bradley RD, Baker RJ. 2001. A test of the genetic species concept: cytochrome-b sequences and mammals. Journal of Mammalogy 82(4):960-973.
Brochu CA. 2012. Phylogenetic relationships of Palaeogene ziphodont eusuchians and the status of *Pristichampsus* Gervais, 1853. Earth and Environmental Science Transactions of the Royal Society of Edinburgh 103(3-4):521-550.

Brower AV. 1994. Rapid morphological radiation and convergence among races of the butterfly *Heliconius erato* inferred from patterns of mitochondrial DNA evolution. Proceedings of the National Academy of Sciences 91(14):6491-6495.
Brown JH, Lasiewski RC. 1972. Metabolism of weasels: The cost of being long and thin. Ecology 53(5):939-943.
Brown WM, George M, Wilson AC. 1979. Rapid evolution of animal mitochondrial DNA. Proceedings of the National Academy of Sciences 76(4):1967-1971.
Buskirk SW. 1983. The ecology of marten in southcentral Alaska: University of Alaska Fairbanks, Alaska.
Campos PF, O.E. Craig. G. Turner-Walker. E. Peacock. E. Willerslev. M.T.P. Gilbert. 2012. DNA in ancient bone- where is it located and how should we extract it? Annals of Anatomy 194:7-16.
Carden RF, McDevitt AD, Zachos FE, Woodman PC, O'Toole P, Rose H, Monaghan NT, Campana MG, Bradley DG, Edwards CJ. 2012. Phylogeographic, ancient DNA, fossil and morphometric analyses reveal ancient and modern introductions of a large mammal: the complex case of red deer (*Cervus elaphus*) in Ireland. Quaternary Science Reviews 42:74-84.
Carpenter Meredith L, Buenrostro Jason D, Valdiosera C, Schroeder H, Allentoft Morten E, Sikora M, Rasmussen M, Gravel S, Guillén S, Nekhrizov G, Leshtakov K, Dimitrova D, Theodossiev N, Pettener D, Luiselli D, Sandoval K, Moreno-Estrada A, Li Y, Wang J, Gilbert M Thomas P, Willerslev E, Greenleaf William J, Bustamante Carlos D. 2013. Pulling out the 1%: Whole-genome capture for the targeted enrichment of ancient DNA sequencing libraries. American Journal of Human Genetics 93(5):852-864.
Carr SM, Hicks SA. 1997. Are there two species of marten in North America? Genetic and evolutionary relationships within *Martes*. *Martes*: Taxonomy, Ecology, Techniques, and Management:15-28.
Chinnery PF, Thorburn DR, Samuels DC, White SL, Dahl H-HM, Turnbull DM, Lightowlers RN, Howell N. 2000. The inheritance of mitochondrial DNA heteroplasmy: random drift, selection or both? Trends Genet 16(11):500-505.
Ciampaglio CN, Kemp M, McShea DW. 2001. Detecting changes in morphospace occupation patterns in the fossil record: characterization and analysis of measures of disparity. Paleobiology 27(4):695-715.
Clare EL, Lim BK, Engstrom MD, Eger JL, Hebert PD. 2007. DNA barcoding of Neotropical bats: species identification and discovery within Guyana. Molecular Ecology Notes 7(2):184-190.
Clark PU, Dyke AS, Shakun JD, Carlson AE, Clark J, Wohlfarth B, Mitrovica JX, Hostetler SW, McCabe AM. 2009. The Last Glacial Maximum. Science 325(5941):710-714.
Clark TW, Anderson E, Douglas C, Strickland M. 1987. *Martes americana*. Mammalian Species 289:1-8.
Clavel J, Julliard R, Devictor V. 2011. Worldwide decline of specialist species: toward a global functional homogenization? Front Ecol Environ 9(4):222-228.
Cook J, Bidlack A, Conroy C, Demboski J, Fleming M, Runck A, Stone K, MacDonald S. 2001. A phylogeographic perspective on endemism in the Alexander Archipelago of southeast Alaska. Biological Conservation 97(2):215-227.
Cornwell W, Nakagawa S. 2017. Phylogenetic comparative methods. Current Biology 27(9):R333-R336.
Currey JD. 2002. Bones Structure and Mechanics. New Jersey: Princeton University Press.
Dawson NG, Colella JP, Small MP, Stone KD, Talbot SL, Cook JA. 2017. Historical biogeography sets the foundation for contemporary conservation of martens (genus *Martes*) in northwestern North America. Journal of Mammalogy 98(3):715-730.

Dawson NG, Cook JA. 2012. Behind the genes. In: Aubry KB, Zielinski WJ, Raphael MG, Proulx G, Buskirk SW, editors. Biology and Conservation of Martens, Sables, and Fishers A New Synthesis. New York, USA: Cornell University Press.
Debruyne R, Chu G, King CE, Bos K, Kuch M, Schwarz C, Szpak P, Gröcke DR, Matheus P, Zazula G, Guthrie D, Froese D, Buigues B, de Marliave C, Flemming C, Poinar D, Fisher D, Southon J, Tikhonov AN, MacPhee RDE, Poinar HN. 2008. Out of America: ancient DNA evidence for a new world origin of Late Quaternary woolly mammoths. Current Biology 18(17):1320-1326.
DeMaster DP, Stirling I. 1981. *Ursus maritimus*. Mammalian Species 145:1-7.
Denton JS, Adams DC. 2015. A new phylogenetic test for comparing multiple high-dimensional evolutionary rates suggests interplay of evolutionary rates and modularity in lanternfishes (Myctophiformes; Myctophidae). Evolution.
Dial RJ, Smeltz TS, Sullivan PF, Rinas CL, Timm K, Geck JE, Tobin SC, Golden TS, Berg EC. 2016. Shrubline but not treeline advance matches climate velocity in montane ecosystems of south-central Alaska. Global Change Biol 22(5):1841-1856.
Dietl GP, Flessa KW. 2011. Conservation paleobiology: putting the dead to work. Trends in Ecology and Evolution 26(1):30-37.
Dodson SI. 1989. The ecological role of chemical stimuli for the zooplankton: predator-induced morphology in Daphnia. Oecologia 78(3):361-367.
Doudna JW, Danielson BJ. 2015. Rapid morphological change in the masticatory structures of an important ecosystem service provider. PloS one 10(6):e0127218.
Drake AG, Klingenberg CP. 2008. The pace of morphological change: historical transformation of skull shape in St Bernard dogs. Proceedings of the Royal Society Biology 275(1630):71-76.
Drummond AJ, Ho SYW, Phillips MJ, Rambaut A. 2006. Relaxed phylogenetics and dating with confidence. PLOS Biology 4(5):e88.
Drummond AJ, Suchard MA, Xie D, Rambaut A. 2012. Bayesian phylogenetics with BEAUti and the BEAST 1.7. Molecular Biology and Evolution 29(1969-1973).
Dunn RR, Harris NC, Colwell RK, Koh LP, Sodhi NS. 2009. The sixth mass coextinction: are most endangered species parasites and mutualists? Proceedings of the Royal Society B: Biological Sciences 276(1670):3037-3045.
Dye DG. 2002. Variability and trends in the annual snow-cover cycle in Northern Hemisphere land areas, 1972–2000. Hydrological Processes 16(15):3065-3077.
Dyke AS. 2004. An outline of North American deglaciation with emphasis on central and northern Canada. In: Ehlers J, Gibbard PL, editors. Developments in Quaternary Sciences: Elsevier. p 373-424.
Edgell SE, Noon SM. 1984. Effect of violation of normality on the *t* test of the correlation coefficient. Psychological Bulletin 95(3):576-583.
Edwards RL, Cheng H, Murrell MT, Goldstein SJ. 1997. Protactinium-231 dating of carbonates by thermal ionization mass spectrometry: implications for quaternary climate change. Science 276(5313):782-786.
Eshelman R, Grady F. 1986. Quaternary vertebrate localities of Virginia and their avian and mammalian fauna. The Quaternary of Virginia Department of Mines, Minerals and Energy, Division of Mineral Resources, Charlotteville, Virginia:43-70.
Euskirchen ES, McGuire AD, Chapin FS. 2007. Energy feedbacks of northern high-latitude ecosystems to the climate system due to reduced snow cover during 20th century warming. Global Change Biol 13(11):2425-2438.
Euskirchen ES, McGuire AD, Chapin FS, Yi S, Thompson CC. 2009. Changes in vegetation in northern Alaska under scenarios of climate change, 2003–2100: implications for climate feedbacks. Ecol Appl 19(4):1022-1043.

Fabre A, Cornette R, Slater G, Argot C, Peigné S, Goswami A, Pouydebat E. 2013a. Getting a grip on the evolution of grasping in musteloid carnivorans: a three-dimensional analysis of forelimb shape. Journal of Evolutionary Biology 26(7):1521-1535.
Fabre AC, Cornette R, Goswami A, Peigné S. 2015. Do constraints associated with the locomotor habitat drive the evolution of forelimb shape? A case study in musteloid carnivorans. Journal of Anatomy 226(6):596-610.
Fabre AC, Cornette R, Peigné S, Goswami A. 2013b. Influence of body mass on the shape of forelimb in musteloid carnivorans. Biological Journal of the Linnean Society 110(1):91-103.
Farrell LE, Roman J, Sunquist ME. 2000. Dietary separation of sympatric carnivores identified by molecular analysis of scats. Molecular Ecology 9(10):1583-1590.
Felsenstein J. 1973. Maximum-likelihood estimation of evolutionary trees from continuous characters. American Journal of Human Genetics 25(5):471-492.
Felsenstein J. 2004. Inferring Phylogenies. Sunderland, Massachusetts: Sinauer Associates Sunderland, MA.
Foote M. 1997. The evolution of morphological diversity. Annual Review of Ecology and Systematics 28(1):129-152.
Fordyce JA. 2010. Interpreting the γ statistic in phylogenetic diversification rate studies: a rate decrease does not necessarily indicate an early burst. PLoS ONE 5(7):e11781.
Franssen NR. 2011. Anthropogenic habitat alteration induces rapid morphological divergence in a native stream fish. Evolutionary Applications 4(6):791-804.
Fuller AK, Harrison DJ, Morrison. 2005. Influence of partial timber harvesting on American martens in North-Central Maine J Wildl Manage 69(2):710-722.
Futuyma DJ, Moreno G. 1988. The evolution of ecological specialization. Annual Review of Ecology and Systematics 19:207-233.
Garamszegi LZ. 2014. Modern Phylogenetic Comparative Methods and Their Application in Evolutionary Biology: Concepts and Practice. Heidelberg: Springer.
Germonpre M, M.V. Sablin. R.E. Stevens. R.E.M. Hedges. M. Hofreiter. M. Stiller. V.R. Despres. 2009. Fossil dogs and wolves from Paleolithic sites in Belgium, the Ukraine and Russia: osteometry, ancient DNA and stable isotopes. Journal of Archaeological Science 36:473-490.
Germonpré M, Sablin MV, Stevens RE, Hedges REM, Hofreiter M, Stiller M, Després VR. 2009. Fossil dogs and wolves from Palaeolithic sites in Belgium, the Ukraine and Russia: osteometry, ancient DNA and stable isotopes. Journal of Archaeological Science 36(2):473-490.
Giannico GR, Nagorsen DW. 1989. Geographic and sexual variation in the skull of Pacific coast marten (*Martes americana*). Canadian Journal of Zoology 67(6):1386-1393.
Gilbert MTP, Hansen AJ, Willerslev E, Rudbeck L, Barnes I, Lynnerup N, Cooper A. 2003a. Characterization of genetic miscoding lesions caused by postmortem damage. The American Journal of Human Genetics 72(1):48-61.
Gilbert MTP, Shapiro B, Drummond A, Cooper A. 2005. Post-mortem DNA damage hotspots in Bison (Bison bison) provide evidence for both damage and mutational hotspots in human mitochondrial DNA. Journal of Archaeological Science 32(7):1053-1060.
Gilbert MTP, Willerslev E, Hansen AJ, Barnes I, Rudbeck L, Lynnerup N, Cooper A. 2003b. Distribution patterns of postmortem damage in human mitochondrial DNA. The American Journal of Human Genetics 72(1):32-47.
Gilchrist GW. 1995. Specialists and generalists in changing environments. I. Fitness landscapes of thermal sensitivity. The American Naturalist 146(2):252-270.
Gillespie JH. 1986. Variability of evolutionary rates of DNA. Genetics 113(4):1077-1091.
Gogol-Döring A, Chen W. 2012. An overview of the analysis of next generation sequencing data. Next Generation Microarray Bioinformatics: Springer. p 249-257.

Grady F. 1984. A Pleistocene occurrence of *Geomys* (Rodentia: Geomyidae) in West Virginia. Contributions in Quaternary vertebrate paleontology: a volume in memorial to John E Guilday (HH Genoways and MR Dawson, eds), Carnegie Museum of Natural History Special Publications 8:1-538.
Graham R, Graham M. 1994. The late quaternary distribution of *Martes* in North America. In: Buskirk SW, Harestad AS, Raphael MG, Powell RA, editors. Martens, Sables, and Fishers: Biology and Conservation. London: Cornell University Press. p 26-58.
Guilday JE, Hamilton HW. 1978. Ecological significance of displaced boreal mammals in West Virginia caves. Journal of Mammalogy 59(1):176-181.
Gutiérrez E, Garbino G. 2018. Species delimitation based on diagnosis and monophyly, and its importance for advancing mammalian taxonomy. Zool Res 39(3):1-8.
Hagmeier EM. 1958. Inapplicability of the subspecies concept to North American marten. Systematic Zoology 7(1):1-7.
Haile J, Larson G, Owens K, Dobney K, Shapiro B. 2010. Ancient DNA typing of archaeological pig remains corroborates historical records. Journal of Archaeological Science 37:174-177.
Hall ER. 1926. A new marten from the Pleistocene cave deposits of California. Journal of Mammalogy 7(2):127-130.
Hall ER. 1981. The Mammals of North America. New York, New York: John Wiley and Sons, Inc.
Hammer O, Harper DAT, Ryan PD. 2001. PAST: Paleontological statistics software package for education and data analysis. Paleontologia Electronica 4(1):1-9.
Harmon LJ. 2018. Phylogenetic Comparative Methods: Learning from Trees.
Harmon LJ, Schulte JA, Larson A, Losos JB. 2003. Tempo and mode of evolutionary radiation in iguanian lizards. Science 301(5635):961-964.
Harmon LJ, Weir JT, Brock CD, Glor RE, Challenger W. 2008. GEIGER: investigating evolutionary radiations. Bioinformatics 24(1):129-131.
Harris MA, Steudel K. 1997. Ecological correlates of hind-limb length in the Carnivora. J Zool 241.
Havlicek LL, Peterson NL. 1976. Robustness of the Pearson Correlation against Violations of Assumptions. Percept Motor Skills 43(3_suppl):1319-1334.
Heath TA. 2018. Divergence time estimation using BEAST v.2*: dating species divergence with the fossilized birth-death process.
Hendry AP, Farrugia TJ, Kinnison MT. 2008. Human influences on rates of phenotypic change in wild animal populations. Molecular Ecology 17(1):20-29.
Ho SYW, Heupink TH, Rambaut A, Shapiro B. 2007. Bayesian estimation of sequence damage in ancient DNA. Molecular Biology and Evolution 24(6):1416-1422.
Ho SYW, Lanfear R, Phillips MJ, Barnes I, Thomas JA, Kolokotronis S-O, Shapiro B. 2011. Bayesian estimation of substitution rates from ancient DNA sequences with low information content. Systematic Biology 60(3):366-375.
Hoberg E, Koehler A, Cook J. 2012. Complex host–parasite systems in *Martes*: implications for conservation biology of endemic faunas. In: Aubry KB, Zielinski WJ, Raphael MG, Proulx G, Buskirk SW, editors. Biology and Conservation of Martens, Sables and Fishers: A New Synthesis. Ithaca, New York: Comstock Publishing Associates. p 39-57.
Hoch JM. 2009. Adaptive plasticity of the penis in a simultaneous hemarphrodite. Evolution 63(8):1946-1953.
Hofreiter M, Jaenicke V, Serre D, Haeseler Av, Pääbo S. 2001. DNA sequences from multiple amplifications reveal artifacts induced by cytosine deamination in ancient DNA. Nucleic Acids Research 29(23):4793-4799.

Hoisington-Lopez JL, Waits LP, Sullivan J. 2012. Species limits and integrated taxonomy of the Idaho ground squirrel (*Urocitellus brunneus*): genetic and ecological differentiation. Journal of Mammalogy 93(2):589-604.
Horn S. 2012. Target Enrichment via DNA Hybridization Capture. In: Shapiro B, Hofreiter M, editors. Ancient DNA Methods and Protocols. New York: Humana Press, Springer. p 177-188.
Hughes SS. 2009. Noble marten (*Martes americana nobilis*) revisited: its adaptation and extinction. Journal of Mammalogy 90(1):74-92.
Iwaniuk AN, Pellis SM, Whishaw IQ. 1999. The relationship between forelimb morphology and behaviour in North American carnivores (Carnivora). Canandian Journal of Zoolology 77.
Jorgenson MT, Racine CH, Walters JC, Osterkamp TE. 2001. Permafrost Degradation and Ecological Changes Associated with a WarmingClimate in Central Alaska. Clim Change 48(4):551-579.
Kassen R. 2002. The experimental evolution of specialists, generalists, and the maintenance of diversity. Journal of Evolutionary Biology 15(2):173-190.
Kelly JR, Fuller TK, Kanter JJ. 2009. Records of recovering American Marten, *Martes americana*, in New Hampshire. The Canadian Field-Naturalist 123(1):1-6.
King LM, Wallace SC. 2014. Phylogenetics of Panthera, including Panthera atrox, based on craniodental characters. Historical Biology 26(6):827-833.
Kingman JFC. 1982. The coalescent. Stochastic Processes and their Applications 13(3):235-248.
Kinnison MT, Hendry AP. 2001. The pace of modern life II: from rates of contemporary microevolution to pattern and process. In: Hendry AP, Kinnison MT, editors. Microevolution Rate, Pattern, Process. Dordrecht: Springer Netherlands. p 145-164.
Kircher M. 2012. Analysis of High-Throughput Ancient DNA Sequencing Data. In: Shapiro B, Hofreiter M, editors. Ancient DNA Methods and Protocols. New York: Humana Press, Springer. p 197-228.
Klein DR, Meldgaard M, Fancy SG. 1987. Factors Determining Leg Length in *Rangifer tarandus*. Journal of Mammalogy 68(3):642-655.
Klein E, Berg EE, Dial R. 2005. Wetland drying and succession across the Kenai Peninsula Lowlands, south-central Alaska. Canadian Journal of Forest Research 35(8):1931-1941.
Knowles N, Dettinger MD, Cayan DR. 2006. Trends in snowfall versus rainfall in the western United States. J Clim 19(18):4545-4559.
Koch PL, Diffenbaugh NS, Hoppe KA. 2004. The effects of late Quaternary climate and pCO 2 change on C 4 plant abundance in the south-central United States. Palaeogeography, Palaeoclimatology, Palaeoecology 207(3):331-357.
Koehler AVA, Hoberg EP, Dokuchaev NE, Tranbenkova NA, Whitman JS, Nagorsen DW, Cook JA. 2009. Phylogeography of a Holarctic nematode, *Soboliphyme baturini*, among mustelids: climate change, episodic colonization, and diversification in a complex host–parasite system. Biological Journal of the Linnean Society 96(3):651-663.
Koepfli K-P, Deere K, Slater G, Begg C, Begg K, Grassman L, Lucherini M, Veron G, Wayne R. 2008. Multigene phylogeny of the Mustelidae: resolving relationships, tempo and biogeographic history of a mammalian adaptive radiation. BMC Biology 6(1):10.
Kolska Horwitz LR, Ducos P. 1997. The influence of climate on artiodactyl size during the Late Pleistocene-Early Holocene of the Southern Levant. Paléorient 23(2):229-247.
Kuh E, Meyer JR. 1955. Correlation and Regression Estimates when the Data are Ratios. Econometrica 23(4):400-416.
Kumar S, Stetcher G, Tamura K. 2016. MEGA7: Molecular evolutionary genetics analysis version 7.0 for bigger datasets. Molecular Biology and Evolution 33:1870-1874.
Kurose N, Kaneko Y, Abramov AV, Siriaroonrat B, Masuda R. 2001. Low genetic diversity in Japanese populations of the Eurasian badger *Meles meles* (Mustelidae, Carnivora)

revealed by mitochondrial cytochrome b gene sequences. Zoological Science 18(8):1145-1151.
Kurose N, Masuda R, Siriaroonrat B, Yoshida MC. 1999. Intraspecific variation of mitochondrial cytochrome b gene sequences of the Japanese marten *Martes melampus* and the sable *Martes zibellina* (Mustelidae, Carnivora, Mammalia) in Japan. Zoological Science 16(4):693-700.
Kyle CJ, Davis CS, Strobeck C. 2000. Microsatellite analysis of North American pine marten (*Martes americana*) populations from the Yukon and Northwest Territories. Canadian Journal of Zoology 78(7):1150-1157.
Kyle CJ, Strobeck C. 2003. Genetic homogeneity of Canadian mainland marten populations underscores the distinctiveness of Newfoundland pine martens (*Martes americana atrata*). Canadian Journal of Zoology 81(1):57-66.
Lande R. 1976. Natural selection and random genetic drift in phenotypic evolution. Evolution 30(2):314-334.
Lang C, Leuenberger M, Schwander J, Johnsen S. 1999. 16°C rapid temperature variation in central Greenland 70,000 years ago. Science 286(5441):934-937.
Law CJ, Slater GJ, Mehta RS. 2018. Lineage diversity and size disparity in Musteloidea: testing patterns of adaptive radiation using molecular and fossil-based methods. Systematic Biology 67(1):127-144.
Leach D. 1977. The descriptive and comparative postcranial osteology of marten (*Martes americana* Turton) and fisher (*Martes pennanti* Erxleben): the appendicular skeleton. Canadian Journal of Zoology 55(1):199-214.
Lee M-Y, Lissovsky AA, Park S-K, Obolenskaya EV, Dokuchaev NE, Zhang Y-p, Yu L, Kim Y-J, Voloshina I, Myslenkov A, Choi T-Y, Min M-S, Lee H. 2008. Mitochondrial cytochrome b sequence variations and population structure of Siberian chipmunk (*Tamias sibiricus*) in Northeastern Asia and population substructure in South Korea.
Li B, Wolsan M, Wu D, Zhang W, Xu Y, Zeng Z. 2014. Mitochondrial genomes reveal the pattern and timing of marten (*Martes*), wolverine (*Gulo*), and fisher (*Pekania*) diversification. Molecular phylogenetics and evolution 80:156-164.
Lieberman DE, Pearson OM, Polk JD, Demes B, Crompton AW. 2003. Optimization of bone growth and remodeling in response to loading in tapered mammalian limbs. J Exp Biol 206(18):3125-3138.
Lindsay SL. 1987. Geographic size and son-size variation in Rocky Mountain *Tamiasciurus hudsonicus*: Significance in relation to Allen's Rule and vicariant biogeography. Journal of Mammalogy 68(1):39-48.
Liow LH, Quental TB, Marshall CR. 2010. When can decreasing diversification rates be detected with molecular phylogenies and the fossil record? Systematic Biology 59(6):646-659.
Lloyd AH, Fastie CL. 2002. Spatial and Temporal Variability in the Growth and Climate Response of Treeline Trees in Alaska. Clim Change 52(4):481-509.
Lloyd AH, Yoshikawa K, Fastie CL, Hinzman L, Fraver M. 2003. Effects of permafrost degradation on woody vegetation at arctic treeline on the Seward Peninsula, Alaska. Permafrost and Periglacial Processes 14(2):93-101.
Long CA. 1971. Significance of the Late Pleistocene fauna from the Little Box Elder Cave, Wyoming, to studies of zoogeography of recent mammals. The Great Basin Naturalist 31(2):93-105.
Lurgi M, López BC, Montoya JM. 2012. Novel communities from climate change. Philosophical Transactions of the Royal Society B: Biological Sciences 367(1605):2913-2922.
Lynch LM. 2016. *Martes americana* is selective in following the rules: a test of Bergmann's and Allen's rules. Journal of Vertebrate Paleontology Programs and Abstracts 179.

MacLean SA, Beissinger SR. 2017. Species' traits as predictors of range shifts under contemporary climate change: A review and meta-analysis. Global Change Biol 23(10):4094-4105.
Magi A, Benelli M, Gozzini A, Girolami F, Torricelli F, Brandi ML. 2010. Bioinformatics for next generation sequencing data. Genes 1(2):294-307.
Magnacca KN, Brown MJF. 2010. Tissue segregation of mitochondrial haplotypes in heteroplasmic Hawaiian bees: implications for DNA barcoding. Molecular Ecology Resources 10(1):60-68.
Marchinko KB, Geary D. 2003. Dramatic phenotypic plasticity in barnacle legs (*Balanus gladula darwin*): magnitude, age dependence, and speed of response. Evolution 57(6):1281-1290.
Martin-Serra A, Figueirido B, Palmqvist P. 2014. A three-dimensional analysis of morphological evolution and locomotor performance of the carnivoran forelimb. PLoS One 9.
Martín-Serra A, Figueirido B, Palmqvist P. 2014. A three-dimensional analysis of the morphological evolution and locomotor behaviour of the carnivoran hind limb. BMC Evol Biol 14(1):129.
Martin RM, Kneeland D, Brooks D, Matta R, Ball J, Brown C, Broadhead J, Carle J, Ciesla W, Durst P, El-Lakany H, Ferreira dos Santos V, Flejzor L, Gerrand A, Harcharik D, Heino J, Killmann W, Kone P, Lebedys A, MacDicken K, Muller E, Nair CTS, Paveri M, Rojas-Briales E, Steierer F, Tissari J, Whiteman A. 2012. State of the World's Forests. Obstler R, editor. Rome.
Mateiu LM, Rannala BH. 2008. Bayesian inference of errors in ancient DNA caused by postmortem degradation. Molecular Biology and Evolution 25(7):1503-1511.
Maul LC, Markova AK. 2007. Similarity and regional differences in Quaternary arvicolid evolution in Central and Eastern Europe. Quaternary International 160(1):81-99.
Mayden RL. 1997. A hierarchy of species concepts: the denouement in the saga of the species problem. In: Claridge MF, Dawah HA, Wilson MR, editors. Species: The Units of Diversity: Chapman & Hall. p 381–423.
Mayer F, Dietz C, Kiefer A. 2007. Molecular species identification boosts bat diversity. Frontiers in Zoology 4(1):4.
Mayr E. 1956. Geographical character gradients and climatic adaptation. Evolution 10(1):105-108.
McKitrick MC, Zink RM. 1988. Species concepts in ornithology. The Condor 90(1):1-14.
McNab BK. 1971. On the Ecological Significance of Bergmann's Rule. Ecology 52(5):845-854.
McNab BK. 1980. Food Habits, Energetics, and the Population Biology of Mammals. The American Naturalist 116(1):106-124.
Meachen-Samuels JA. 2012. Morphological convergence of the prey-killing arsenal of sabertooth predators. Paleobiology 38.
Meachen-Samuels JA, Van Valkenburgh B. 2009. Forelimb indicators of prey-size preference in the Felidae. J Morphol 270.
Meachen J, O'Keefe F, Sadleir R. 2014. Evolution in the sabre-tooth cat, *Smilodon fatalis*, in response to Pleistocene climate change. Journal of Evolutionary Biology 27(4):714-723.
Meachen JA, Brannick AL, Fry TJ. 2016. Extinct Beringian wolf morphotype found in the continental U.S. has implications for wolf migration and evolution. Ecology and Evolution:3430-3438.
Meachen JA, Dunn RH, Werdelin L. 2015. Carnivoran postcranial adaptations and their relationships to climate. Ecography 38:001-008.
Meachen JA, Samuels JX. 2012. Evolution in coyotes (*Canis latrans*) in response to the megafaunal extinctions. Proceedings of the National Academy of Sciences 109(11):4191-4196.
Mead EM, Mead JI. 1989. Snake Creek Burial Cave and a review of the Quaternary mustelids of the Great Basin. Western North American Naturalist 49(2):143-154.

Meiri S, Dayan T. 2003. On the validity of Bergmann's rule. Journal of biogeography 30(3):331-351.
Meiri S, Dayan T, Simberloff D. 2004. Carnivores, biases and Bergmann's rule. Biological Journal of the Linnean Society 81(4):579-588.
Meloro C, Elton S, Louys J, Bishop LC, Ditchfield P. 2013. Cats in the forest: predicting habitat adaptations from humerus morphometry in extant and fossil Felidae (Carnivora). Paleobiology 39(3):323-344.
Menéndez R, Megías AG, Hill JK, Braschler B, Willis SG, Collingham Y, Fox R, Roy DB, Thomas CD. 2006. Species richness changes lag behind climate change. Proceedings of the Royal Society B: Biological Sciences 273(1593):1465-1470.
Merriam CH. 1890. Description of a new marten (*Mustela caurina*) from the northwest coast region of the United States. North American Fauna:27-30.
Meyers JI. 2007. Basicranial analysis of *Martes* and the extinct *Martes nobilis* (Carnivora: Mustelidae) using geometric morphometrics: Northern Arizona University.
Milá B, Smith TB, Wayne RK. 2007. Speciation and rapid phenotypic differentiation in the yellow-rumped warbler Dendroica coronata complex. Molecular Ecology 16(1):159-173.
Mitteroecker P, Gunz P, Bernhard M, Schaefer K, Bookstein FL. 2004. Comparison of cranial ontogenetic trajectories among great apes and humans. Journal of Human Evolution 46(6):679-698.
Moriarty KM, Epps CW, Betts MG, Hance DJ, Bailey J, Zielinski WJ. 2015. Experimental evidence that simplified forest structure interacts with snow cover to influence functional connectivity for Pacific martens. Landscape Ecol 30(10):1865-1877.
Morlo M, Peigné S. 2010. Molecular and morphological evidence for Ailuridae and a review of its genera. In: Goswami A, Friscia AR, editors. Carnivoran Evolution: New Views on Phylogeny, Form, and Function. New York: Cambridge University Press. p 92-140.
Münkemüller T, Lavergne S, Bzeznik B, Dray S, Jombart T, Schiffers K, Thuiller W. 2012. How to measure and test phylogenetic signal. Methods in Ecology and Evolution 3(4):743-756.
Murphy MA, Kendall KC, Robinson A, Waits LP. 2007. The impact of time and field conditions on brown bear (Ursus arctos) faecal DNA amplification. Conservation Genetics 8(5):1219-1224.
Myneni RB, Keeling CD, Tucker CJ, Asrar G, Nemani RR. 1997. Increased plant growth in the northern high latitudes from 1981 to 1991. Nature 386:698.
Nabholz B, Glémin S, Galtier N. 2008. Strong variations of mitochondrial mutation rate across mammals—the Longevity Hypothesis. Molecular Biology and Evolution 25(1):120-130.
Nagorsen DW. 1985. A morphometric study of geographic variation in the snowshoe hare (*Lepus americanus*). Canadian Journal of Zoology 63(3):567-579.
Nava-García E, Guerrero-Enríquez JA, Arellano E. 2016. Molecular phylogeography of harvest mice (*Reithrodontomys megalotis*) based on cytochrome b DNA sequences. Journal of Mammalian Evolution 23(3):297-307.
Nedbal MA, Flynn JJ. 1998. Do the combined effects of the asymmetric process of replication and DNA damage from oxygen radicals produce a mutation-rate signature in the mitochondrial genome? Molecular Biology and Evolution 15(2):219-223.
Nowak RM. 1999. Walker's Mammals of the World. Baltimore, Maryland: Johns Hopkins University Press.
O'Meara BC. 2012. Evolutionary inferences from phylogenies: a review of methods. Annual Review of Ecology, Evolution, and Systematics 43(1):267-285.
Olson DM, Dinerstein E, Wikramanayake ED, Burgess ND, Powell GVN, Underwood EC, D'amico JA, Itoua I, Strand HE, Morrison JC, Loucks CJ, Allnutt TF, Ricketts TH, Kura Y, Lamoreux JF, Wettengel WW, Hedao P, Kassem KR. 2001. Terrestrial ecoregions of

the world: a new map of life on earth: a new global map of terrestrial ecoregions provides an innovative tool for conserving biodiversity. BioScience 51(11):933-938.
Orlando L, Ginolhac A, Zhang G, Froese D, Albrechtsen A, Stiller M, Schubert M, Cappellini E, Petersen B, Moltke I, Johnson PLF, Fumagalli M, Vilstrup JT, Raghavan M, Korneliussen T, Malaspinas A-S, Vogt J, Szklarczyk D, Kelstrup CD, Vinther J, Dolocan A, Stenderup J, Velazquez AMV, Cahill J, Rasmussen M, Wang X, Min J, Zazula GD, Seguin-Orlando A, Mortensen C, Magnussen K, Thompson JF, Weinstock J, Gregersen K, Roed KH, Eisenmann V, Rubin CJ, Miller DC, Antczak DF, Bertelsen MF, Brunak S, Al-Rasheid KAS, Ryder O, Andersson L, Mundy J, Krogh A, Gilbert MTP, Kjaer K, Sicheritz-Ponten T, Jensen LJ, Olsen JV, Hofreiter M, Nielsen R, Shapiro B, Wang J, Willerslev E. 2013. Recalibrating *Equus* evolution using the genome sequence of an early Middle Pleistocene horse. Nature 499(7456):74-78.
Orlando L, Metcalf JL, Alberdi MT, Telles-Antunes M, Bonjean D, Otte M, Martin F, Eisenmann V, Mashkour M, Morello F, Prado JL, Salas-Gismondi R, Shockey BJ, Wrinn PJ, Vasil'ev SK, Ovodov ND, Cherry MI, Hopwood B, Male D, Austin JJ, Hänni C, Cooper A. 2009. Revising the recent evolutionary history of equids using ancient DNA. Proceedings of the National Academy of Sciences 106(51):21754-21759.
Oshida T, Lin L-K, Chang S-W, Dang CN, Nguyen ST, Nguyen NX, Nguyen DX, Endo H, Kimura J, Sasaki M, Hayashida A, Takano A. 2015. Mitochondrial DNA evidence suggests challenge to the conspecific status of the hairy-footed flying squirrel *Belomys pearsonii* from Taiwan and Vietnam. Mammal Study 40(1):29-33.
Osterkamp TE, Romanovsky VE. 1999. Evidence for warming and thawing of discontinuous permafrost in Alaska. Permafrost and Periglacial Processes 10(1):17-37.
Outomuro D, Johansson F. 2017. A potential pitfall in studies of biological shape: does size matter? J Anim Ecol 86(6):1447-1457.
Ozawa T, Hayashi S, Mikhelson VM. 1997. Phylogenetic position of mammoth and Steller's sea cow within Tethytheria demonstrated by mitochondrial DNA sequences. J Mol Evol 44(4):406-413.
Paduan KDS, Ribolla PEM. 2008. Mitochondrial DNA polymorphism and heteroplasmy in populations of *Aedes aegypti* in Brazil. Journal of Medical Entomology 45(1):59-67.
Pagel M. 1999. Inferring the historical patterns of biological evolution. Nature 401(6756):877-884.
Paradis E, Claude J, Strimmer K. 2004. APE: analysis of phylogenetics and evolution in R language. Bioinformatics 20:289-290.
Parsons TJ, Muniec DS, Sullivan K, Woodyatt N, Alliston-Greiner R, Wilson MR, Berry DL, Holland KA, Weedn VW, Gill P. 1997. A high observed substitution rate in the human mitochondrial DNA control region. Nat Genet 15(4):363.
Pergams ORW, Lawler JJ. 2009. Recent and widespread rapid morphological change in rodents. PLOS ONE 4(7):e6452.
Pigliucci M. 2001. Phenotypic plasticity. In: Fox CW, Roff DA, Fairbairn DJ, editors. Evol Ecol. Oxford: Oxford University Press.
Polly PD. 2008. Adaptive zones and the pinniped ankle: a three-dimensional quantitative analysis of carnivoran tarsal evolution. In: Sargis EJ, Dagosto M, editors. Mammalian Evolutionary Morphology. Dordrecht: Springer. p 167-196.
Polly PD. 2010. Tiptoeing through the trophics: geographic variation in carnivoran locomotor ecomorphology in relation to environment. In: Goswami A, Friscia A, editors. Carnivoran evolution: new views on phylogeny, form, and function. Cambridge: Cambridge University Press. p 374-401.
Poole KG. 2003. A review of the Canada lynx, *Lynx canadensis*, in Canada. The Canadian Field-Naturalist 117(3):360-376.

Poroshin EA, Polly PD, Wójcik JM. 2010. Climate and morphological change on decadal scales: multiannual variation in the common shrew *Sorex araneus* in northeast Russia. Acta Theriologica 55(3):193-202.
Proulx G, Aubry K, Birks J, Buskirk S, Fortin C, Frost H, Krohn W, Mayo L, Monakhov V, Payer D. 2005. World distribution and status of the genus *Martes* in 2000. Martens and Fishers (*Martes*) in Human-altered Environments. Ney York, NY: Springer. p 21-76.
Pybus OG, Harvey PH. 2000. Testing macro–evolutionary models using incomplete molecular phylogenies. Proceedings of the Royal Society of London Series B: Biological Sciences 267(1459):2267-2272.
Quental TB, Marshall CR. 2009. Extinction during evolutionary radiations: reconciling the fossil record with molecular phylogenies. Evolution 63(12):3158-3167.
Quental TB, Marshall CR. 2010. Diversity dynamics: molecular phylogenies need the fossil record. Trends Ecol Evol 25(8):434-441.
R Core Team. 2015. R: A language and environment for statistical computing. Vienna, Austria: R Foundation for Statistical Computing.
Rabosky DL, Lovette IJ. 2008. Explosive evolutionary radiations: decreasing speciation or increasing extinction through time? Evolution 62(8):1866-1875.
Rahmstorf S. 2002. Ocean circulation and climate during the past 120,000 years. Nature 419:207.
Rahmstorf S, Cazenave A, Church JA, Hansen JE, Keeling RF, Parker DE, Somerville RCJ. 2007. Recent climate observations compared to projections. Science 316(5825):709-709.
Rambaut A, Ho SYW, Drummond AJ, Shapiro B. 2009. Accommodating the effect of ancient DNA damage on inferences of demographic histories. Molecular Biology and Evolution 26(2):245-248.
Rambaut A, Suchard MA, Xie D, Drummond AJ. 2014. Tracer v1.6. Available from http://tree.bio.ed.ac.uk/software/tracer.
Rannala B. 2015. The art and science of species delimitation. Current Zoology 61(5):846-853.
Revell LJ. 2012. phytools: an R package for phylogenetic comparative biology (and other things). Methods in Ecology and Evolution 3(2):217-223.
Reznick D, Travis J. 2001. Adaptation. In: Fox CW, Roff DA, Fairbairn DJ, editors. Evol Ecol. Oxford: Oxford University Press.
Reznick DN, Ghalambor CK. 2001. The population ecology of contemporary adaptations: What empirical studies reveal about the conditions that promote adaptive evolution. In: Hendry AP, Kinnison MT, editors. Microevolution Rate, Pattern, Process. Dordrecht: Springer Netherlands. p 183-198.
Richter C. 1992. Reactive oxygen and DNA damage in mitochondria. Mutation Research/DNAging 275(3):249-255.
Rizzi E, Lari M, Gigli E, De Bellis G, Caramelli D. 2012. Ancient DNA studies: new perspectives on old samples. Genet Sel Evol 44(1):21-29.
Robison GA, Balvin O, Schal C, Vargo EL, Booth W. 2015. Extensive mitochondrial heteroplasmy in natural populations of a resurging human pest, the bed bug (Hemiptera: Cimicidae). Journal of Medical Entomology 52(4):734-738.
Rode KD, Amstrup SC, Regehr EV. 2010. Reduced body size and cub recruitment in polar bears associated with sea ice decline. Ecol Appl 20(3):768-782.
Rohland N. 2012. DNA extraction of ancient animal hard tissue samples via adsorption to silica particles. In: Shapiro B, Hofreiter M, editors. Ancient DNA Methods and Protocols. New York: Humana Press, Springer. p 21-28.
Rohland N, Reich D, Mallick S, Meyer M, Green RE, Georgiadis NJ, Roca AL, Hofreiter M. 2010. Genomic DNA sequences from mastodon and woolly mammoth reveal deep speciation of forest and savanna elephants. PLOS Biology 8(12):e1000564.
Rokas A, Ladoukakis E, Zouros E. 2003. Animal mitochondrial DNA recombination revisited. Trends Ecol Evol 18(8):411-417.

Rosel PE, Hancock-hanser BL, Archer FI, Robertson KM, Martien KK, Leslie MS, Berta A, Cipriano F, Viricel A, Viaud-Martinez KA, Taylor BL. 2017. Examining metrics and magnitudes of molecular genetic differentiation used to delimit cetacean subspecies based on mitochondrial DNA control region sequences. Mar Mamm Sci 33(S1):76-100.
Rovey CW, Balco G. 2011. Chapter 43 - Summary of Early and Middle Pleistocene Glaciations in Northern Missouri, USA. In: Ehlers J, Gibbard PL, Hughes PD, editors. Developments in Quaternary Sciences: Elsevier. p 553-561.
Rüber L, Adams DC. 2001. Evolutionary convergence of body shape and trophic morphology in cichlids from Lake Tanganyika. Journal of Evolutionary Biology 14(2):325-332.
Runck AM, Cook JA. 2005. Postglacial expansion of the southern red-backed vole (Clethrionomys gapperi) in North America. Molecular Ecology 14(5):1445-1456.
Rychlik L, Ramalhinho G, Polly PD. 2006. Response to environmental factors and competition: skull, mandible and tooth shapes in Polish water shrews (*Neomys*, Soricidae, Mammalia). Journal of Zoological Systematics and Evolutionary Research 44(4):339-351.
Sackett LC, Seglund A, Guralnick RP, Mazzella MN, Wagner DM, Busch JD, Martin AP. 2014. Evidence for two subspecies of Gunnison's prairie dogs (*Cynomys gunnisoni*), and the general importance of the subspecies concept. Biological Conservation 174:1-11.
Salamin N, Wüest RO, Lavergne S, Thuiller W, Pearman PB. 2010. Assessing rapid evolution in a changing environment. Trends Ecol Evol 25(12):692-698.
Samuels JX, Meachen JA, Sakai SA. 2013. Postcranial morphology and the locomotor habits of living and extinct carnivorans. Journal of Morphology 274(2):121-146.
Samuels JX, Van Valkenburgh B. 2008. Skeletal indicators of locomotor adaptations in living and extinct rodents. J Morphol 269.
Sato JJ, Wolsan M, Prevosti FJ, D'Elía G, Begg C, Begg K, Hosoda T, Campbell KL, Suzuki H. 2012. Evolutionary and biogeographic history of weasel-like carnivorans (Musteloidea). Molecular Phylogenetics and evolution 63(3):745-757.
Schellhorn R, Sanmugaraja M. 2014. Habitat adaptations in the felid forearm. Paläontologische Zeitschrift 89(2):261-269.
Schluter D. 2000. The Ecology of Adaptive Radiation. Oxford: Oxford University Press.
Schoener TW. 2011. The newest synthesis: understanding the interplay of evolutionary and ecological dynamics. Science 331(6016):426-429.
Seierstad IK, Abbott PM, Bigler M, Blunier T, Bourne AJ, Brook E, Buchardt SL, Buizert C, Clausen HB, Cook E. 2014. Consistently dated records from the Greenland GRIP, GISP2 and NGRIP ice cores for the past 104 ka reveal regional millennial-scale δ 18 O gradients with possible Heinrich event imprint. Quaternary Science Reviews 106:29-46.
Serrat MA. 2013. Allen's Rule Revisited: Temperature Influences Bone Elongation During a Critical Period of Postnatal Development. The Anatomical Record 296(10):1534-1545.
Serreze MC, Walsh JE, Chapin FS, Osterkamp T, Dyurgerov M, Romanovsky V, Oechel WC, Morison J, Zhang T, Barry RG. 2000. Observational Evidence of Recent Change in the Northern High-Latitude Environment. Clim Change 46(1):159-207.
Shackleton NJ, Sánchez-Goñi MF, Pailler D, Lancelot Y. 2003. Marine isotope substage 5e and the Eemian interglacial. Global Planet Change 36(3):151-155.
Shafer ABA, Cullingham CI, CÔTÉ SD, Coltman DW. 2010. Of glaciers and refugia: a decade of study sheds new light on the phylogeography of northwestern North America. Molecular Ecology 19(21):4589-4621.
Shapiro B, Drummond AJ, Rambaut A, Wilson MC, Matheus PE, Sher AV, Pybus OG, Gilbert MTP, Barnes I, Binladen J, Willerslev E, Hansen AJ, Baryshnikov GF, Burns JA, Davydov S, Driver JC, Froese DG, Harington CR, Keddie G, Kosintsev P, Kunz ML, Martin LD, Stephenson RO, Storer J, Tedford R, Zimov S, Cooper A. 2004. Rise and fall of the Beringian steppe bison. Science 306(5701):1561-1565.

Shimodaira H. 1998. An Aapplication of multiple comparison techniques to model selection. Annals of the Institute of Statistical Mathematics 50(1):1-13.
Shimodaira H, Hasegawa M. 1999. Multiple c omparisons of log-Likelihoods with applications to phylogenetic inference. Molecular Biology and Evolution 16(8):1114.
Sinclair WJ. 1907. The Exploration of the Potter Creek Cave. Oakland, Californa: University of California Press.
Slater GJ, Price SA, Santini F, Alfaro ME. 2010. Diversity versus disparity and the radiation of modern cetaceans. Proceedings of the Royal Society B: Biological Sciences 277(1697):3097-3104.
Slauson KM, Zielinski WJ, Stone KD. 2009. Characterizing the molecular variation among American marten (*Martes americana*) subspecies from Oregon and California. Conservation Genetics 10(5):1337-1341.
Small MP, Stone KD, Cook JA. 2003. American marten (*Martes americana*) in the Pacific Northwest: population differentiation across a landscape fragmented in time and space. Molecular Ecology 12(1):89-103.
Smith NV, Saatchi SS, Randerson JT. 2004. Trends in high northern latitude soil freeze and thaw cycles from 1988 to 2002. Journal of Geophysical Research: Atmospheres 109(D12).
Smith RL, Smith TM. 2001. Ecology and Field Biology. San Francisco: Benjamin Cummings.
Spencer WD, Barrett RH, Zielinski WJ. 1983. Marten habitat preferences in the northern Sierra Nevada. The Journal of Wildlife Management:1181-1186.
Springer MS, Hollar LJ, Burk A. 1995. Compensatory substitutions and the evolution of the mitochondrial 12S rRNA gene in mammals. Molecular Biology and Evolution 12(6):1138-1150.
Stephens S, Agee JK, Fulé P, North M, Romme W, Swetnam T, Turner MG. 2013. Managing forests and fire in changing climates. Science 342(6154):41-42.
Stephens SL, McIver JD, Boerner REJ, Fettig CJ, Fontaine JB, Hartsough BR, Kennedy PL, Schwilk DW. 2012. The effects of forest fuel-reduction treatments in the United States. BioScience 62(6):549-560.
Steventon JD, Major JT. 1982. Marten use of habitat in a commercially clear-cut forest. The Journal of Wildlife Management 46(1):175-182.
Stirling CH, Esat TM, Lambeck K, McCulloch MT. 1998. Timing and duration of the Last Interglacial: evidence for a restricted interval of widespread coral reef growth. Earth and Planetary Science Letters 160(3):745-762.
Stone KD, Cook JA. 2002. Molecular evolution of Holarctic martens (genus *Martes*, Mammalia: Carnivora: Mustelidae). Molecular Phylogenetics and Evolution 24(2):169-179.
Stone KD, Flynn RW, Cook JA. 2002a. Post-glacial colonization of northwestern North America by the forest-associated American marten (*Martes americana*, Mammalia: Carnivora: Mustelidae). Molecular Ecology 11(10):2049-2063.
Stone RS, Dutton EG, Harris JM, Longenecker D. 2002b. Earlier spring snowmelt in northern Alaska as an indicator of climate change. Journal of Geophysical Research: Atmospheres 107(D10):ACL 10-11-ACL 10-13.
Stumpp R, Fuzessy L, Paglia AP. 2016. Environment drivers acting on rodent rapid morphological change. Journal of Mammalian Evolution:1-10.
Swofford DL. 2002. PAUP*. Phylogenetic Analyis Under Parsimony (*and Other Methods). Version 4. Sunderland, Massachusetts: Sinauer Associates.
Tamura K. 1992. Estimation of the number of nucleotide substitutions when there are strong transition-transversion and G+C-content biases. Molecular Biology and Evolution 9(4):678-687.
Tankersley KB. 1997. Sheriden: A Clovis cave site in eastern North America. Geoarchaeology 12(6):713-724.

Tattersall I. 2007. Madagascar's Lemurs: Cryptic diversity or taxonomic inflation? Evolutionary Anthropology: Issues, News, and Reviews 16(1):12-23.
Tilkens MJ, Wall-Scheffler C, Weaver TD, Steudel-Numbers K. 2007. The effects of body proportions on thermoregulation: an experimental assessment of Allen's rule. Journal of Human Evolution 53(3):286-291.
Tu Y-K, Clerehugh V, Gilthorpe MS. 2004. Ratio variables in regression analysis can give rise to spurious results: illustration from two studies in periodontology. Journal of Dentistry 32(2):143-151.
Van Valkenburgh B. 1985. Locomotor diversity within past and present guilds of large predatory mammals. Paleobiology 11.
Van Valkenburgh B. 1987. Skeletal indicators of locomotor behavior in living and extinct carnivores. Journal of Vertebrate Paleontology 7(2):162-182.
Van Valkenburgh B. 1990. Skeletal and dental predictors of body mass in carnivores. In: Damuth J, MacFadden B, editors. Body size in mammalian paleobiology: estimation and biological implications. Cambridge, UK: Cambridge University Press.
Vences M, Thomas M, van der Meijden A, Chiari Y, Vieites DR. 2005. Comparative performance of the 16S rRNA gene in DNA barcoding of amphibians. Frontiers in Zoology 2(1):5.
Wang X, Tedford RH, Taylor BE. 1999. Phylogenetic systematics of the Borophaginae (Carnivora, Canidae). Bulletin of the AMNH; no. 243.
Weaver ME, Ingram DL. 1969. Morphological changes in swine associated with environmental temperature. Ecology 50(4):710-713.
Wei X, Messner K. 1996. The postnatal development of the insertions of the medial collateral ligament in the rat knee. Anatomy and Embryology 193(1):53-59.
Wetmore A. 1962. Notes on fossil and subfossil birds. Smithsonian Miscellaneous Collections 145(2).
Wiebe PA, Fryxell JM, Thompson ID, Börger L, Baker JA. 2013. Do trappers understand marten habitat? The Journal of Wildlife Management 77(2):379-391.
Willerslev E, Gilbert MT, Binladen J, Ho SY, Campos PF, Ratan A, Tomsho LP, da Fonseca RR, Sher A, Kuznetsova TV, Nowak-Kemp M, Roth TL, Miller W, Schuster SC. 2009. Analysis of complete mitochondrial genomes from extinct and extant rhinoceroses reveals lack of phylogenetic resolution. Evolutionary Biology 9(95):95.
Williams JW, Jackson ST. 2007. Novel climates, no-analog communities, and ecological surprises. Front Ecol Environ 5(9):475-482.
Williams JW, Shuman BN, Webb T. 2001. Dissimilarity analyses of late-Quaternary vegetation and climate in eastern North America. Ecology 82(12):3346-3362.
Wilson AC, Cann RL, Carr SM, George M, Gyllensten UB, Helm-Bychowski KM, Higuchi RG, Palumbi SR, Prager EM, Sage RD, Stoneking M. 1985. Mitochondrial DNA and two perspectives on evolutionary genetics. Biological Journal of the Linnean Society 26(4):375-400.
Wiszniowska T. 1989. Middle Pleistocene Carnivora (Mammalia) from Kozi Grzbiet in the Swietokrzyskie Mts, Poland: Panst. wydaw. nauk Warszawa.
Wolff EW, Chappellaz J, Blunier T, Rasmussen SO, Svensson A. 2010. Millennial-scale variability during the last glacial: The ice core record. Quaternary Science Reviews 29(21):2828-2838.
Wolsan M. Quaternary carnivores of Poland; 1987; National Research Council of Canada, Ottawa. p 290.
Wolsan M. 1989. Drapie_zne—Carnivora. In: Kowalski K, editor. Historia i Ewolucja La¸dowej Fauny Polski: Folia Quat. p 177-196.
Wolsan M. 1990. Lower Pleistocene carnivores of Poland. Quartärpaläontologie 8:277-280.

Wolsan M. 1993a. Evolution des carnivores quaternaires en Europe centrale dans leur contexte stratigraphique et paleoclimatique. l'Anthropologie 97(2/3):203-222.
Wolsan M. 1993b. Phylogeny and classification of early European Mustelida (Mammalia: Carnivora). Acta Theriologica 38(4).
Worthen GL, Kilgore DL. 1981. Metabolic rate of pine marten in relation to air temperature. Journal of Mammalogy 62(3):624-628.
Yom-Tov Y, Yom-Tov J. 2005. Global warming, Bergmann's rule and body size in the masked shrew Sorex cinereus Kerr in Alaska. J Anim Ecol 74(5):803-808.
Yom-Tov Y, Yom-Tov S, Jarrell G. 2008. Recent increase in body size of the American marten *Martes americana* in Alaska. Biological Journal of the Linnean Society 93(4):701-707.
Yom-Tov Y, Yom-Tov S, MacDonald D, Yom-Tov E. 2007. Population cycles and changes in body size of the lynx in Alaska. Oecologia 152(2):239.
Youngman PM, Schueler FW. 1991. *Martes nobilis* is a synonym of *Martes americana*, not an extinct Pleistocene-Holocene species. Journal of Mammalogy 72(3):567-577.
Yule GU. 1910. On the Interpretation of Correlations between Indices or Ratios. Journal of the Royal Statistical Society 73(6/7):644-647.
Yule UG. 1925. A mathematical theory of evolution, based on the conclusions of Dr. JC Willis, FRS. Philosophical Transactions of the Royal Society of London Series B 213:21-87.
Zelditch ML, Swiderski DL, Sheets HD. 2012. Geometric Morphometrics for Biologists: A Primer. London: Academic Press.
Zhou YB, Newman C, Xu WT, Buesching CD, Zalewski A, Kaneko Y, Macdonald DW, Xie ZQ. 2011. Biogeographical variation in the diet of Holarctic martens (genus Martes, Mammalia: Carnivora: Mustelidae): adaptive foraging in generalists. Journal of Biogeography 38(1):137-147.
Zielinski WJ, Duncan NP. 2004. Diets of sympatric populations of American martens (*Martes americana*) and fishers (*Martes pennanti*) in California. Journal of Mammalogy 85(3):470-477.
Zink RM, Dittmann DL. 1993. Gene flow, refugia, and evolution of geographic variation in the song sparrow (*Melospiza melodia*). Evolution 47(3):717-729.
Zrzavý J, Řičánková V. 2004. Phylogeny of Recent Canidae (Mammalia, Carnivora): relative reliability and utility of morphological and molecular datasets. Zoologica Scripta 33(4):311-333.

APPENDICES

Appendix I- Chapter 2 Supplemental Files

A List of specimens

ETMNH 600, 603, 607, 608, 609; MSB 196536, 196578, 196581, 196582, 196583, 196981, 197115, 224027, 56692, 61713; UMMZ 177697, 177826, 177827; NYSM (NY) 14241, 14242, 14387, 14388; SNOMNH 11542, 11543, 11544, 11545, 11546, 11547, 11548, 11549, 11550, 11551; UAMN (UAM) 101819, 101828, 101851, 11236, 11237, 13542, 22678, 22680, 22736, 24794, 24805, 24808, 509, 511, 47308, 59579; FMNH (UF) 31142, 31328, 31370, 31427; USNM A07549, A07551, 265584, 265585, 266142, 546139, 546140, 546141, 592316, 592896, 592943, 600579, 600580, 600581, 600583, 600584; BMUW (UWBM) 81025, 81688

University of Alaska Museum of the North (UAMN)
Burke Museum of Natural History and Culture (BMUW)
Florida Museum of Natural History (FMNH)
New York State Museum (NYSM)
Smithsonian Institution National Museum of Natural History (USNM)
Museum of Southwestern Biology (MSB)

B Geometric Morphometric Landmark Definitions:

Humerus

1. Most superior point of the lesser tubercle
2. Most inferomedial point of the lesser tubercle
3. Most inferior point of the head
4. Most superior point of the greater tubercle
5. Most inferior and medial point on the greater tubercle
6. Most superior point within the entepicondylar foramen
7. Most inferior point within the entepicondylar foramen
8. Most superior point of the medial epicondyle
9. Most inferior point of the medial epicondyle
10. Most medial intersection of the trochlea and coronoid fossa
11. Most lateral intersection of the trochlea and coronoid fossa
12. Most medial intersection of the trochlea and olecranon fossa
13. Most lateral intersection of the trochlea and olecranon fossa
14. Most superior point of the lateral supracondylar ridge

Radius

1. Most superior point on the anterior surface of the articular circumference of the head of the radius
2. Most superior point on the posterior surface of the articular circumference of the head of the radius
3. Most inferomedial point at the intersection of the articular circumference and neck
4. Most inferolateral point at the intersection of the articular circumference and neck
5. Point of maximum curvature of the medial intersection of the trochlea and body
6. Most medial point of the ulnar notch
7. Most inferior point of the styloid process
8. Most inferior point of the trochlea lateral to the styloid process
9. Most lateral point of the trochlea opposite the ulnar notch
10. Point of maximum curvature of the lateral intersection of the trochlea and body

Ulna

1. Most superolateral point of the proximal tuberocity of the olecranon
2. Most anterolateral point of the cranial process of the trochlear notch
3. Most superomedial point of the proximal tuberocity of the olecranon
4. Most anteromedial point of the cranial process of the trochlear notch
5. Most anterior point of the craniolateral process of the trochlear notch
6. Most anterior point of the craniomedial process of the trochlear notch
7. Most inferoposterior point of the proximal tuberocity of the olecranon
8. Most superior point of the articular surface that articulates with the ulnar notch of the radius
9. Most inferior point of the articular surface that articulates with the ulnar notch of the radius
10. Most posterior point of the styloid process just superior to the insertion point of the carpi ulnaris muscle

11. Most anterior point of the styloid process just superior to the insertion point of the carpi ulnaris muscle

Femur

1. Center of the fovea capitis
2. Point of maximum curvature of the neck of the femur along the coronal plane
3. Point of maximum curvature between the femoral head and greater trochanter along the coronal plane
4. Most superior point of the greater trochanter
5. Most inferoposterior point of the lesser trochanter
6. Most superomedial point of the medial condyle
7. Most superolateral point of the medial condyle
8. Most superior point of the intercondylar fossa along the sagittal plane
9. Most superomedial point of the lateral condyle
10. Most superolateral point of the lateral condyle
11. Most anterior point of the lateral sesamoid facet
12. Most anterior point of the medial sesamoid facet

Tibia

1. Most lateral point of the lateral condyle
2. Most inferoposterior point of the lateral condyle
3. Most inferoposterior point of the medial condyle
4. Most medial point of the medial condyle
5. Most anterior point along the sagittal plane of the tibial tuberocity
6. Most superolateral point of the lateral malleolus
7. Most inferior point of the lateral malleolus
8. Most inferoposterior point of the distal epiphysis that is not part of the medial or lateral malleolus
9. Most inferior point of the medial malleolus
10. Most superomedial point of the medial malleolus

Fibula

1. Most anterior point of the head
2. Most superior point of the head anterior to the coronal plane
3. Most superior point of the head posterior to the coronal plane
4. Most posterior point of the head
5. Most medial point of the head along the coronal plane
6. Most anterior point of the lateral malleolus
7. Most inferior point of the malleolar articular surface
8. Most posterior point of the distal epiphysis lateral to the malleolar articular surface

C Supplemental Tables

Table 1. PC scores for the Humerus, Radius, Ulna, Femur, Tibia, and Fibula

Humerus

Specimen	PC1	PC2	PC3	PC4	PC5	PC6	PC7	PC8	PC9
ETMNH 600	2.52E-02	7.66E-03	-5.92E-03	9.90E-03	-5.48E-03	9.10E-03	-2.65E-04	7.79E-04	-3.14E-03
ETMNH 603	2.18E-02	1.08E-02	-6.94E-03	5.52E-03	2.24E-03	-4.59E-03	5.59E-03	4.77E-03	4.84E-03
ETMNH 607	2.04E-03	7.05E-03	5.13E-03	7.99E-03	1.28E-02	1.50E-03	7.35E-03	-1.60E-03	4.57E-03
ETMNH 608	1.84E-02	1.94E-02	-9.75E-04	4.02E-03	6.61E-03	8.24E-04	-8.69E-03	-1.61E-03	-5.20E-04
ETMNH 609	1.81E-02	1.31E-02	-5.76E-03	1.56E-03	2.95E-03	-7.65E-04	-5.98E-03	3.18E-04	9.30E-04
MSB 196536	-2.64E-02	3.11E-03	4.81E-03	-1.13E-03	3.93E-03	-2.66E-03	1.44E-03	-1.02E-02	-3.78E-03
MSB 196578	-1.20E-02	-5.03E-03	-1.33E-02	-2.79E-03	-3.78E-03	-3.22E-03	2.81E-03	-7.22E-03	3.87E-03
MSB 196581	1.59E-03	6.46E-03	-1.31E-02	-8.51E-03	3.21E-03	-1.25E-02	-1.77E-03	2.27E-04	8.96E-03
MSB 196582	-9.62E-03	-1.17E-02	-3.58E-03	1.75E-03	-3.22E-03	2.06E-03	3.29E-03	2.66E-03	-9.45E-03
MSB 196583	-2.81E-03	-1.79E-02	1.24E-02	5.79E-04	1.90E-03	3.37E-03	6.77E-03	2.96E-03	8.78E-03
MSB 196981	-1.25E-02	-2.33E-03	-1.38E-02	1.13E-02	-2.99E-03	-9.57E-03	6.70E-03	5.45E-03	-1.19E-02
MSB 197115	-3.04E-03	2.28E-03	-7.54E-03	-7.43E-03	-1.23E-02	3.23E-03	-6.42E-03	1.52E-03	-3.02E-03
MSB 224027	-2.33E-02	4.68E-03	2.79E-03	1.09E-03	3.53E-03	-3.00E-03	2.32E-04	6.03E-03	4.42E-03
MZ 177697	1.62E-03	-1.07E-02	4.30E-03	-4.93E-03	-2.83E-03	-3.17E-03	8.05E-03	4.10E-04	6.02E-03
MZ 177826	9.73E-03	-1.23E-02	-7.56E-03	-6.14E-03	4.32E-03	-3.05E-03	1.79E-03	6.07E-04	-3.43E-03
MZ 177827	-1.69E-02	-3.22E-03	1.27E-03	3.53E-03	8.07E-03	-1.03E-02	-3.57E-03	-4.15E-03	-3.40E-03
NY 14241	8.70E-03	-1.06E-02	-4.31E-03	-3.65E-03	-4.31E-03	-3.70E-03	9.56E-05	3.57E-03	4.88E-03
NY 14242	1.51E-02	-8.04E-03	1.09E-02	-1.60E-02	6.99E-03	-1.82E-03	-5.78E-03	9.79E-04	-4.32E-03
NY 14387	2.13E-02	-9.69E-03	-5.85E-03	1.97E-03	6.29E-04	1.50E-03	-5.12E-05	-1.02E-02	2.71E-03
NY 14388	2.30E-02	-1.20E-02	6.19E-03	-6.76E-03	3.16E-03	-2.05E-03	-7.16E-03	5.28E-03	-2.89E-04
UAM 101819	-8.34E-03	6.82E-04	-3.57E-03	-1.22E-02	7.28E-03	8.43E-04	-6.04E-03	-7.49E-04	-7.53E-03
UAM 101828	-5.88E-03	-1.03E-02	9.45E-03	2.01E-02	1.93E-03	-1.02E-03	-1.22E-02	-1.25E-03	3.02E-03
UAM 101851	3.84E-03	-1.22E-02	-1.10E-03	1.20E-02	-1.12E-02	7.96E-04	-6.98E-03	3.90E-03	3.38E-03
UAM 24794	-3.73E-02	3.44E-06	3.53E-03	5.59E-03	3.00E-03	2.44E-03	-2.66E-03	5.25E-03	1.77E-05

Humerus continued

Specimen	PC1	PC2	PC3	PC4	PC5	PC6	PC7	PC8	PC9
UAM 59579	-4.45E-03	3.30E-03	-2.64E-03	4.75E-03	2.17E-03	2.17E-03	-5.73E-04	-9.33E-03	3.33E-03
UF 31142	4.85E-03	4.74E-03	3.33E-03	-2.71E-03	4.12E-03	1.10E-02	7.74E-03	-1.15E-03	-8.15E-04
UF 31328	-6.24E-03	-2.53E-03	1.10E-03	3.99E-04	-5.54E-04	1.66E-04	-4.35E-03	-4.71E-03	-2.55E-03
UF 31370	2.51E-03	-5.96E-03	-7.97E-03	-4.78E-03	5.08E-03	7.43E-03	6.68E-03	6.87E-03	-4.96E-04
UF 31427	-5.13E-04	2.49E-03	-8.38E-04	1.56E-04	6.08E-03	9.07E-03	1.03E-03	2.65E-03	-3.20E-03
USNM	-2.80E-02	-8.17E-04	3.43E-04	1.14E-03	-3.84E-03	7.20E-03	2.69E-04	1.07E-03	-2.05E-03
USNM	1.48E-02	-5.02E-03	-7.38E-03	2.05E-03	1.86E-03	4.93E-03	3.37E-03	-3.78E-03	-2.95E-04
USNM	2.22E-03	4.84E-03	1.17E-02	-5.91E-03	-1.60E-02	-4.90E-03	2.23E-03	-1.01E-02	-1.70E-03
USNM	-5.62E-03	5.54E-03	-2.72E-04	-8.56E-04	-5.75E-03	-3.51E-03	1.39E-03	2.87E-03	6.76E-03
USNM	-1.18E-02	1.57E-02	1.31E-02	-1.92E-04	-1.95E-03	-9.70E-03	6.48E-03	6.38E-03	-3.81E-03
USNM	3.82E-02	-3.57E-03	1.18E-02	4.06E-03	-1.34E-03	-4.38E-03	-7.82E-05	1.31E-03	-6.54E-03
USNM	2.13E-02	1.29E-02	9.42E-03	2.32E-05	-7.18E-03	6.65E-04	8.00E-03	-1.15E-03	-2.45E-03
USNM	-2.06E-02	1.94E-03	1.27E-03	-4.72E-03	-1.92E-03	7.79E-03	1.31E-03	-5.31E-03	1.68E-03
UWBM 81025	-7.14E-03	4.95E-03	-1.67E-03	-1.43E-03	-6.82E-04	1.38E-03	-1.37E-03	-6.52E-04	1.66E-03
UWBM 81688	-1.17E-02	1.22E-02	1.29E-03	-9.32E-03	-6.57E-03	6.36E-03	-8.70E-03	7.36E-03	4.88E-03

Humerus continued

Specimen	PC10	PC11	PC12	PC13	PC14	PC15	PC16	PC17	PC18
ETMNH 600	4.26E-04	-5.87E-03	1.10E-03	4.88E-03	-5.15E-03	5.48E-03	-2.77E-03	-1.92E-03	-3.15E-03
ETMNH 603	-6.26E-04	1.69E-03	4.31E-04	-1.76E-03	-1.67E-03	1.25E-03	-4.39E-03	1.24E-04	2.87E-03
ETMNH 607	-3.26E-04	1.40E-03	-7.85E-04	-1.67E-03	-6.86E-03	-3.14E-05	1.94E-03	-1.81E-03	2.05E-03
ETMNH 608	4.38E-03	-1.09E-04	5.36E-03	-5.78E-03	1.63E-03	6.55E-04	2.05E-03	1.03E-03	-1.07E-03
ETMNH 609	4.48E-04	-5.82E-03	-4.91E-03	1.07E-03	3.01E-03	-1.74E-03	-1.82E-03	2.04E-03	3.70E-03
MSB 196536	4.81E-03	4.15E-04	-7.35E-04	5.24E-03	2.00E-03	5.98E-03	3.03E-03	2.73E-03	3.40E-03
MSB 196578	4.81E-03	-1.33E-03	3.24E-04	-5.53E-03	-2.43E-03	-2.77E-03	7.69E-03	-6.11E-03	-2.48E-03
MSB 196581	2.52E-03	3.30E-03	-2.63E-03	5.27E-03	3.72E-03	3.83E-03	-2.26E-04	1.54E-03	-5.31E-03
MSB 196582	4.02E-03	3.86E-03	-3.08E-03	7.56E-03	2.01E-03	5.86E-04	-1.02E-03	2.86E-04	1.32E-03
MSB 196583	4.14E-03	-3.51E-03	-6.89E-03	-7.94E-03	6.29E-03	2.17E-03	-4.10E-03	1.52E-03	-3.27E-03
MSB 196981	2.52E-03	-2.26E-03	1.18E-03	-5.53E-03	2.08E-03	2.01E-04	-1.39E-03	3.24E-03	-1.38E-03
MSB 197115	1.16E-03	4.83E-03	-5.06E-03	-2.42E-03	4.40E-03	-4.59E-03	-8.41E-04	-3.74E-03	7.40E-04
MSB 224027	-2.76E-03	-7.44E-03	5.32E-03	7.66E-03	4.66E-03	-3.04E-03	-2.09E-03	-4.57E-03	1.36E-03
MZ 177697	-7.95E-03	-1.30E-03	6.83E-03	-1.59E-03	2.53E-03	5.19E-04	7.02E-04	4.83E-03	1.10E-03
MZ 177826	-4.19E-03	-1.93E-03	2.86E-03	3.33E-03	-1.14E-04	2.81E-03	4.03E-03	1.86E-03	1.63E-03
MZ 177827	-3.86E-03	-3.00E-03	2.26E-03	-2.58E-03	-1.89E-03	5.22E-04	-3.52E-03	-4.95E-03	-2.30E-03
NY 14241	1.10E-02	-4.80E-03	-7.35E-04	6.83E-04	-2.88E-03	2.03E-03	1.63E-03	5.17E-04	6.68E-03
NY 14242	-2.90E-04	2.76E-07	-7.57E-04	2.41E-03	-1.24E-03	7.31E-04	-9.77E-04	-4.44E-03	-2.88E-03
NY 14387	-8.91E-04	4.31E-03	6.85E-03	9.56E-04	3.11E-03	-6.10E-05	-5.17E-03	-1.24E-03	-2.37E-03
NY 14388	6.51E-03	7.02E-03	3.97E-03	2.28E-03	-5.17E-03	-3.09E-03	-2.00E-03	1.56E-03	8.17E-04
UAM 101819	-6.55E-03	-3.41E-03	-2.01E-03	-7.99E-03	1.14E-04	4.71E-04	-2.36E-03	5.14E-04	3.82E-03
UAM 101828	-1.06E-03	5.19E-04	-7.32E-03	7.51E-04	1.47E-03	1.09E-03	3.14E-03	-9.57E-04	8.83E-04
UAM 101851	-6.25E-03	2.70E-03	6.43E-03	-1.02E-03	-1.35E-03	-1.32E-03	8.54E-04	3.66E-04	1.27E-03
UAM 24794	7.59E-03	-1.36E-03	3.28E-03	1.54E-03	-4.24E-03	-4.07E-03	-2.01E-03	1.93E-03	-2.67E-03
UAM 59579	-5.19E-03	6.92E-03	-2.66E-03	2.03E-03	1.24E-03	-1.13E-03	3.26E-04	2.92E-03	3.36E-03

Humerus continued

Specimen	PC10	PC11	PC12	PC13	PC14	PC15	PC16	PC17	PC18
UF 31142	6.67E-03	2.23E-03	2.05E-03	-2.61E-03	2.79E-04	1.37E-03	-9.84E-04	-1.74E-03	1.14E-03
UF 31328	1.82E-03	1.54E-03	1.33E-03	-5.24E-03	-2.62E-04	-2.77E-03	-2.87E-03	2.05E-03	2.02E-03
UF 31370	-6.94E-03	3.22E-04	-4.61E-03	1.14E-04	-4.83E-03	-8.99E-04	1.43E-03	-2.07E-03	2.14E-03
UF 31427	-1.78E-03	-4.63E-03	-1.41E-05	2.37E-03	3.47E-03	-4.81E-03	4.26E-03	3.94E-03	-5.03E-03
USNM 592316	-3.04E-03	4.45E-03	1.58E-03	-7.06E-04	8.40E-04	1.00E-02	-1.07E-03	-4.24E-03	-4.66E-04
USNM 592896	-9.76E-04	3.04E-03	-4.50E-03	4.02E-04	-2.96E-03	-2.07E-03	8.06E-04	2.68E-03	-4.89E-03
USNM 592943	-1.38E-03	-7.43E-03	-2.59E-03	4.72E-04	-8.22E-03	2.03E-04	-2.67E-03	2.80E-03	-1.58E-03
USNM 600579	-2.73E-03	-7.20E-04	-3.02E-03	4.54E-04	-2.00E-03	-2.42E-03	1.64E-03	-3.80E-03	3.79E-04
USNM 600581	-2.12E-03	9.88E-03	-1.00E-03	-9.30E-04	-2.63E-03	-1.68E-03	1.78E-03	1.22E-03	-1.58E-03
USNM 600583	-1.76E-03	-2.80E-03	-3.99E-04	1.43E-04	3.30E-03	4.83E-04	6.63E-03	-8.22E-04	-9.75E-04
USNM 600584	1.85E-03	1.11E-03	1.20E-03	6.99E-04	7.68E-03	-1.83E-03	-5.23E-04	-4.00E-03	1.94E-03
USNM 600580	1.00E-03	-1.85E-03	5.21E-03	1.91E-03	1.10E-03	-5.61E-03	1.73E-03	1.20E-03	9.82E-04
UWBM 81025	-3.75E-03	-2.96E-04	-5.86E-03	4.22E-03	-7.12E-04	-2.95E-03	-4.05E-03	1.83E-03	-5.90E-04
UWBM 81688	-1.29E-03	3.39E-04	2.03E-03	-3.15E-03	-3.37E-04	6.48E-03	3.18E-03	3.68E-03	-1.61E-03

Radius

Specimen	PC1	PC2	PC3	PC4	PC5	PC6	PC7	PC8	PC9
ETMNH 600	-1.12E-02	-4.73E-03	-4.43E-03	6.03E-04	-6.14E-03	-2.25E-04	-4.92E-03	-1.08E-02	-6.52E-04
ETMNH 603	-1.07E-02	8.58E-04	-2.47E-03	-5.62E-03	7.65E-03	-3.83E-04	-2.54E-03	2.43E-03	-6.70E-03
ETMNH 607	-2.13E-03	-1.73E-03	-1.65E-02	-6.82E-03	-2.86E-04	-1.60E-03	7.32E-03	-3.73E-03	1.85E-03
ETMNH 608	-1.27E-02	8.97E-03	-1.58E-03	-9.74E-03	1.20E-03	-4.70E-03	-3.38E-04	2.50E-03	3.82E-03
ETMNH 609	-1.76E-02	6.20E-03	-9.52E-03	7.64E-03	8.73E-03	3.24E-03	-5.61E-03	1.56E-03	-3.21E-03
MSB 196536	-1.33E-02	9.48E-03	8.12E-03	1.03E-02	-5.62E-03	1.44E-03	4.59E-03	-2.97E-03	6.08E-03
MSB 196578	9.00E-04	9.99E-04	9.78E-03	-1.56E-02	-4.00E-03	5.05E-03	6.11E-03	3.83E-03	2.17E-03
MSB 196581	-1.09E-03	2.00E-03	4.76E-03	7.40E-04	1.77E-03	1.37E-03	4.97E-03	-3.21E-03	5.49E-03
MSB 196582	2.90E-03	1.13E-02	5.57E-03	-5.10E-03	-5.90E-04	7.86E-03	-1.07E-03	4.88E-03	5.31E-03
MSB 196981	1.37E-02	5.51E-03	9.81E-03	-2.37E-03	3.18E-03	-1.05E-03	-4.38E-03	-2.01E-03	4.26E-03
MSB 197115	1.24E-02	-8.96E-04	-3.20E-03	-2.57E-04	-3.70E-03	5.62E-03	8.13E-04	-1.57E-03	1.44E-03
MSB 224027	1.01E-02	3.88E-03	4.55E-04	-4.42E-03	-4.62E-03	4.54E-03	-1.44E-02	-4.92E-03	7.82E-04
MZ 177697	1.68E-02	-3.38E-03	-2.69E-03	2.08E-03	-5.47E-03	-5.57E-03	4.02E-03	-2.96E-03	-5.28E-03
MZ 177826	1.18E-02	-2.36E-03	-2.55E-03	-6.32E-03	6.69E-03	-6.96E-03	2.41E-03	5.94E-03	-2.31E-03
MZ 177827	1.66E-02	-1.22E-04	3.87E-03	5.14E-03	5.22E-03	-9.62E-03	-2.64E-03	-2.83E-03	3.97E-03
NY 14241	1.84E-02	-1.36E-02	-5.68E-03	-9.82E-05	1.13E-02	3.00E-03	2.61E-04	-2.82E-03	4.10E-03
NY 14242	2.57E-02	-2.67E-03	1.84E-03	-5.75E-04	-2.02E-03	-5.83E-03	-4.47E-03	6.44E-03	1.68E-03
NY 14387	2.09E-02	-1.55E-03	3.90E-03	2.69E-03	-6.26E-04	4.37E-03	1.05E-02	-4.42E-03	-4.87E-03
NY 14388	-1.43E-02	-4.27E-03	1.59E-02	2.53E-03	1.28E-02	6.93E-03	1.40E-03	-2.08E-03	-3.34E-03
UAM 101819	5.36E-03	1.38E-02	3.71E-03	1.71E-03	-2.01E-03	-8.06E-03	2.35E-03	1.93E-03	-7.06E-03
UAM 101828	2.82E-03	2.50E-03	-6.55E-03	1.43E-02	-4.21E-03	-4.11E-03	-1.32E-03	-1.43E-03	6.62E-03
UAM 101851	-8.36E-03	1.41E-02	-5.61E-03	4.35E-03	1.24E-04	-5.03E-03	4.07E-03	3.21E-03	-3.93E-04
UAM 24794	-1.38E-02	6.40E-03	1.79E-03	-3.93E-03	5.40E-04	-5.68E-03	-1.06E-03	2.18E-03	3.17E-03
UAM 59579	9.28E-03	-4.75E-04	-5.98E-03	1.65E-03	1.69E-03	5.93E-03	7.67E-03	5.06E-04	4.13E-03

Radius continued

Specimen	PC1	PC2	PC3	PC4	PC5	PC6	PC7	PC8	PC9
UF 31328	-1.01E-02	-3.51E-03	-3.04E-03	9.52E-04	4.26E-03	-1.36E-03	-4.28E-03	8.58E-04	5.60E-03
UF 31370	-2.54E-03	-1.19E-02	-2.43E-03	-8.16E-04	1.07E-02	-1.47E-03	-1.94E-03	-3.79E-03	-2.03E-03
UF 31427	8.01E-03	6.04E-03	-1.11E-02	-3.39E-03	-2.57E-03	-3.96E-04	-6.26E-03	3.32E-03	-5.51E-03
USNM	-5.82E-03	-4.71E-03	-2.13E-03	3.51E-03	1.00E-03	4.02E-03	1.53E-03	4.31E-03	7.46E-04
USNM	4.50E-03	2.66E-03	2.49E-04	8.59E-04	-3.62E-03	5.41E-03	-4.25E-03	1.30E-03	1.56E-03
USNM	-5.33E-03	1.34E-02	-4.88E-03	-4.77E-03	4.36E-04	5.23E-03	2.68E-03	-4.85E-03	-2.70E-03
USNM	-1.76E-02	6.02E-04	3.13E-03	1.32E-03	5.45E-04	-8.25E-03	4.11E-03	-3.54E-03	-1.61E-03
USNM	-8.04E-03	-1.49E-02	1.13E-02	-5.11E-03	-5.63E-03	-6.25E-03	9.23E-04	-3.01E-03	-2.02E-03
USNM	2.07E-04	3.69E-04	1.26E-02	2.17E-03	-3.94E-03	-1.90E-03	-7.01E-03	-2.53E-03	-6.31E-03
USNM	-5.60E-03	-3.81E-03	-7.00E-03	-3.04E-03	-8.15E-03	4.98E-03	3.40E-03	-2.97E-03	-5.55E-03
USNM	-4.85E-03	-1.16E-02	2.93E-03	1.02E-02	-3.76E-03	-5.05E-04	4.57E-03	1.06E-02	-2.08E-03
UWBM 81025	3.24E-03	-9.29E-04	1.05E-03	8.95E-03	-1.97E-03	1.03E-02	-3.66E-03	5.71E-03	-5.39E-03
UWBM 81688	-1.85E-02	-2.20E-02	-3.46E-03	-3.67E-03	-9.05E-03	-3.62E-04	-3.57E-03	4.87E-03	4.26E-03

Radius continued

Specimen	PC10	PC11	PC12	PC13	PC14
ETMNH 600	-4.14E-03	1.91E-04	4.08E-03	-8.64E-04	-2.18E-03
ETMNH 603	-7.79E-04	-3.29E-03	-1.60E-03	-1.69E-03	4.19E-03
ETMNH 607	2.36E-03	2.91E-03	3.05E-03	-3.96E-03	-3.08E-04
ETMNH 608	-4.03E-03	-4.87E-04	-3.59E-04	-3.81E-03	2.22E-03
ETMNH 609	-6.42E-04	3.68E-03	2.71E-03	-3.85E-03	-2.66E-03
MSB 196536	8.86E-04	-1.44E-03	7.98E-04	-3.61E-04	-1.09E-03
MSB 196578	-3.00E-03	3.92E-03	-5.23E-04	1.98E-03	7.12E-04
MSB 196581	-2.25E-05	1.28E-03	-4.58E-04	-3.65E-03	-5.11E-04
MSB 196582	-4.19E-03	1.48E-03	9.14E-04	-2.27E-03	-1.55E-03
MSB 196981	4.80E-03	-3.87E-03	9.27E-03	-1.29E-03	4.29E-04
MSB 197115	-3.56E-03	-3.10E-03	-1.87E-03	4.84E-03	1.46E-03
MSB 224027	5.34E-03	-2.39E-03	-5.41E-03	9.85E-05	1.52E-03
MZ 177697	-1.74E-03	2.66E-04	-1.62E-03	-1.36E-03	-4.45E-03
MZ 177826	-2.47E-04	-2.65E-03	3.43E-03	2.89E-03	-3.72E-03
MZ 177827	1.78E-03	6.34E-03	2.07E-03	-1.12E-03	-1.25E-03
NY 14241	-4.47E-03	4.06E-03	-6.76E-04	2.45E-03	6.92E-03
NY 14242	-2.46E-03	-4.36E-03	-3.90E-03	-3.01E-03	-3.19E-03
NY 14387	3.74E-03	4.04E-03	-1.10E-03	-6.11E-04	2.07E-03
NY 14388	2.53E-04	-6.40E-03	-1.18E-03	-1.57E-03	9.76E-05
UAM 101819	1.51E-03	-2.09E-03	4.16E-03	5.73E-03	9.88E-04
UAM 101828	-2.53E-03	-3.81E-03	1.04E-04	2.18E-03	5.14E-03
UAM 101851	-1.22E-03	-2.24E-03	-7.87E-03	4.95E-04	1.56E-03
UAM 24794	5.73E-04	1.76E-03	3.63E-03	5.13E-03	1.97E-03
UAM 59579	4.29E-03	-7.18E-03	-2.37E-03	-2.99E-03	-3.23E-03

Radius continued

Specimen	PC10	PC11	PC12	PC13	PC14
UF 31328	-1.40E-03	3.36E-03	-2.37E-03	-3.33E-04	-2.74E-03
UF 31370	-1.49E-03	-2.50E-03	-1.23E-03	4.40E-03	-2.95E-03
UF 31427	4.49E-03	8.64E-04	-4.57E-05	-4.46E-03	2.57E-03
USNM	1.57E-03	2.24E-03	-1.03E-03	4.27E-03	-4.90E-03
USNM	-2.79E-03	1.30E-03	5.14E-05	2.05E-03	-1.10E-03
USNM	6.35E-03	5.08E-03	-3.13E-03	4.08E-03	-1.23E-03
USNM	2.13E-03	-1.11E-03	-2.90E-03	8.08E-04	7.59E-04
USNM	4.34E-03	-2.09E-04	-1.01E-03	-4.18E-03	2.58E-03
USNM	-6.60E-03	5.44E-03	-3.51E-03	-1.64E-04	-1.80E-03
USNM	-8.88E-03	-5.26E-03	5.16E-03	-6.61E-04	2.23E-04
USNM	-1.35E-03	4.19E-03	6.69E-04	-3.02E-03	2.58E-03
UWBM 81025	4.35E-03	1.04E-03	4.21E-03	4.52E-04	1.49E-03
UWBM 81688	6.78E-03	-1.05E-03	-1.43E-04	3.35E-03	-6.07E-04

Ulna

Specimen	PC1	PC2	PC3	PC4	PC5	PC6	PC7	PC8	PC9
ETMNH 600	1.74E-03	-1.09E-02	-8.59E-03	-9.07E-04	1.18E-03	1.15E-03	2.75E-03	-2.44E-03	2.40E-03
ETMNH 603	7.30E-03	-7.55E-03	-1.36E-02	-9.68E-04	5.45E-03	4.96E-03	6.14E-03	3.25E-03	-6.23E-03
ETMNH 607	1.23E-03	-9.52E-03	-8.63E-03	-5.17E-04	3.43E-03	4.25E-03	7.07E-03	2.24E-03	1.53E-04
ETMNH 608	4.05E-03	-4.84E-03	-1.12E-02	-8.30E-04	-1.74E-03	5.00E-03	1.60E-03	-1.56E-03	2.41E-03
ETMNH 609	-2.65E-04	-1.86E-03	-1.04E-02	4.50E-03	-2.38E-03	2.42E-03	6.48E-03	-1.11E-02	-3.39E-03
MSB 196536	2.20E-03	-1.57E-02	-4.79E-04	5.02E-03	-6.69E-03	-4.00E-03	-3.10E-03	-2.22E-03	-1.59E-03
MSB 196578	5.07E-03	-6.36E-03	2.94E-03	-4.04E-04	-4.70E-03	-5.85E-03	1.84E-04	1.06E-03	7.23E-04
MSB 196581	1.05E-02	-4.85E-03	1.81E-03	-3.02E-03	-8.55E-03	-9.41E-03	-5.80E-04	-2.34E-03	4.04E-04
MSB 196582	4.76E-04	-9.06E-03	1.44E-03	6.51E-03	-1.52E-02	6.67E-03	-1.37E-03	9.89E-04	8.57E-04
MSB 196981	-1.90E-02	9.31E-03	1.13E-02	5.41E-03	3.77E-03	-1.88E-03	6.56E-03	-6.81E-03	-4.68E-03
MSB 197115	3.56E-03	-2.96E-02	2.52E-02	8.88E-03	1.35E-03	3.71E-03	-5.81E-03	1.06E-03	-1.59E-03
MSB 224027	7.92E-03	-3.93E-03	-2.55E-03	-1.53E-02	1.88E-03	-6.94E-03	-2.04E-03	-1.86E-03	7.05E-04
MZ 177697	-2.37E-03	-8.07E-03	-5.26E-03	-2.48E-03	3.40E-03	2.28E-03	6.44E-03	7.01E-03	9.44E-03
MZ 177826	-8.31E-03	1.80E-03	5.22E-03	1.22E-02	1.07E-02	-3.38E-03	2.78E-03	-3.89E-03	5.79E-03
MZ 177827	-1.77E-02	-1.32E-03	-4.28E-03	-1.03E-02	-7.02E-03	-7.66E-04	-5.42E-03	-4.52E-03	5.09E-03
NY 14241	-2.69E-02	3.35E-03	-3.76E-03	-6.33E-03	-5.24E-04	4.12E-04	-7.36E-03	-5.12E-03	-3.62E-03
NY 14242	-3.42E-03	-4.62E-03	1.15E-02	-1.76E-02	1.89E-02	-5.67E-03	-2.95E-04	9.54E-04	-4.66E-03
NY 14387	-1.93E-02	-3.97E-03	-1.64E-03	3.75E-03	2.42E-03	-8.18E-03	-3.80E-03	9.09E-03	3.38E-03
NY 14388	-2.23E-02	-1.28E-03	-1.27E-02	-8.93E-03	3.84E-03	5.97E-03	-1.96E-03	-3.39E-03	-3.18E-03
UAM 101819	-1.22E-02	-6.98E-03	-7.55E-03	7.50E-04	-5.78E-06	3.47E-05	-4.65E-03	-6.91E-04	1.08E-03
UAM 101828	-1.89E-02	7.00E-03	9.95E-03	5.61E-03	-4.39E-03	6.88E-03	-2.21E-03	3.30E-04	3.33E-03
UAM 101851	-9.45E-03	1.43E-02	1.78E-02	-7.50E-03	-3.18E-03	5.46E-03	6.59E-03	-5.32E-03	4.43E-03
UAM 24794	6.53E-03	4.91E-03	1.64E-03	-6.59E-03	-9.88E-03	-9.70E-04	-6.43E-03	6.19E-04	-9.23E-03
UAM 59579	-6.11E-04	1.54E-03	2.81E-03	-6.17E-03	-6.16E-03	-4.19E-03	2.58E-03	1.64E-03	4.18E-03

Ulna continued

Specimen	PC1	PC2	PC3	PC4	PC5	PC6	PC7	PC8	PC9
UF 31142	3.99E-03	8.36E-03	5.55E-03	2.22E-03	-2.43E-04	-5.30E-03	5.78E-03	4.76E-03	3.99E-04
UF 31328	1.34E-02	1.06E-02	2.68E-03	-1.16E-02	-7.97E-03	8.30E-04	5.30E-03	3.94E-03	2.06E-03
UF 31370	-1.10E-02	4.11E-03	1.56E-04	7.04E-04	3.43E-04	3.35E-03	4.93E-04	1.33E-02	-2.97E-03
UF 31427	1.56E-02	4.14E-03	-1.27E-03	-7.80E-03	2.86E-04	-2.85E-03	-1.31E-03	5.92E-03	2.99E-04
USNM	-3.04E-04	2.45E-03	4.24E-03	-1.59E-05	5.40E-04	3.58E-03	4.65E-03	1.31E-03	2.13E-04
USNM	7.54E-04	2.59E-03	1.47E-03	6.89E-03	4.73E-03	2.88E-03	6.73E-03	4.52E-03	-8.19E-03
USNM	2.14E-02	-2.95E-03	-2.18E-03	5.06E-03	1.14E-02	-3.68E-03	-3.68E-04	-9.73E-03	5.74E-03
USNM	6.91E-03	6.87E-04	1.94E-03	4.04E-03	-2.86E-03	5.24E-03	2.24E-03	4.10E-04	-2.72E-03
USNM	8.86E-03	8.24E-03	-7.16E-04	4.59E-03	4.35E-03	-1.03E-02	-8.04E-03	4.16E-04	-2.64E-03
USNM	1.24E-02	5.08E-03	-5.46E-04	7.21E-03	-1.22E-03	3.90E-03	-2.01E-03	5.25E-05	-2.75E-03
USNM	1.95E-02	8.41E-03	2.76E-03	-3.67E-03	-4.30E-03	-9.14E-05	6.41E-04	-3.39E-03	1.18E-03
USNM	-7.52E-03	1.47E-02	-1.14E-02	1.62E-02	6.53E-04	-7.35E-03	-4.43E-03	5.11E-03	2.95E-03
UWBM 81025	6.09E-03	9.25E-03	-3.88E-03	1.17E-02	-2.03E-03	-5.63E-03	5.56E-04	-4.27E-03	-3.34E-03
UWBM 81688	2.00E-02	1.25E-02	3.24E-04	-4.07E-04	1.04E-02	1.75E-02	-1.44E-02	5.93E-04	3.58E-03

Ulna continued

Specimen	PC10	PC11	PC12	PC13	PC14	PC15	PC16
ETMNH 600	-5.65E-04	5.06E-03	-1.55E-03	9.33E-04	-1.82E-03	-3.19E-03	3.62E-03
ETMNH 603	-2.78E-04	3.85E-03	3.04E-03	-3.02E-03	-1.47E-04	5.80E-04	9.01E-04
ETMNH 607	2.63E-03	-2.09E-03	-8.69E-04	-1.39E-03	4.28E-03	-9.24E-04	-1.71E-03
ETMNH 608	1.00E-03	1.87E-04	4.45E-03	2.77E-03	-6.74E-03	-3.56E-03	-5.89E-03
ETMNH 609	-7.00E-04	3.70E-05	-2.74E-03	-9.17E-04	4.77E-03	1.41E-03	1.90E-03
MSB 196536	3.66E-03	4.51E-03	-1.55E-03	1.79E-03	1.94E-03	1.77E-04	-4.53E-04
MSB 196578	-8.06E-05	-1.55E-04	-7.70E-03	2.71E-03	1.98E-03	-8.79E-04	-4.14E-03
MSB 196581	2.36E-03	-6.38E-04	-2.23E-03	1.86E-03	-7.13E-05	-1.27E-03	-9.08E-04
MSB 196582	-2.71E-03	-1.23E-03	4.72E-03	6.63E-03	-9.91E-04	4.27E-03	-6.69E-04
MSB 196981	7.13E-04	8.22E-04	-5.81E-04	-4.18E-03	2.29E-03	-3.28E-03	-2.34E-03
MSB 197115	-1.00E-03	-2.59E-03	1.30E-03	-4.40E-03	-1.45E-03	-3.13E-03	3.01E-03
MSB 224027	-3.86E-03	-3.63E-03	1.22E-03	-2.10E-03	9.18E-04	4.08E-03	-1.27E-03
MZ 177697	4.92E-03	-9.32E-03	1.51E-03	-5.06E-04	2.71E-03	-1.10E-03	1.73E-03
MZ 177826	-1.18E-02	-1.25E-03	-1.66E-03	3.38E-03	-4.14E-03	3.51E-03	-1.11E-03
MZ 177827	-4.65E-03	3.05E-03	5.75E-03	-3.40E-03	2.38E-03	-2.26E-03	-2.11E-03
NY 14241	3.03E-03	-6.15E-03	-3.03E-04	5.29E-04	-2.32E-03	3.78E-03	-8.02E-04
NY 14242	3.13E-04	1.54E-04	4.82E-03	3.09E-03	9.08E-04	6.11E-04	-3.92E-04
NY 14387	3.52E-03	3.12E-03	-4.91E-03	-3.54E-03	-1.24E-03	-1.47E-03	-4.17E-03
NY 14388	3.33E-04	2.38E-03	-3.71E-03	-1.76E-03	-3.76E-03	-1.04E-03	2.02E-03
UAM 101819	-3.59E-03	-3.64E-03	2.39E-03	2.24E-03	2.03E-03	4.83E-04	4.39E-03
UAM 101828	6.66E-03	5.32E-03	1.50E-03	-3.80E-03	-1.16E-03	2.73E-03	-3.89E-04
UAM 101851	3.44E-04	-2.66E-03	-5.29E-04	5.04E-03	1.95E-03	-3.21E-03	1.61E-03
UAM 24794	-2.97E-03	-4.50E-03	-6.84E-03	9.52E-04	4.75E-04	-1.04E-03	2.10E-03
UAM 59579	-1.38E-03	6.62E-03	-4.48E-03	-2.03E-03	-1.75E-03	7.00E-04	3.42E-03

Ulna continued

Specimen	PC10	PC11	PC12	PC13	PC14	PC15	PC16
UF 31142	-1.06E-03	1.66E-03	1.21E-03	-6.15E-03	-1.99E-03	5.05E-03	2.76E-03
UF 31328	-5.59E-03	4.92E-03	7.19E-04	5.99E-04	-7.60E-04	-3.51E-03	2.06E-04
UF 31370	-1.22E-03	7.60E-04	-1.91E-03	5.27E-03	-1.70E-03	3.83E-03	-1.82E-03
UF 31427	-7.87E-04	-2.11E-03	7.60E-04	-3.03E-03	-3.10E-03	-1.10E-05	3.10E-03
USNM	3.72E-03	1.20E-03	2.77E-03	4.39E-03	1.90E-03	-1.02E-03	1.53E-03
USNM	4.69E-05	-1.81E-03	-3.42E-03	3.23E-03	-1.29E-03	-2.68E-03	-1.48E-03
USNM	1.74E-03	1.95E-03	-4.74E-03	1.68E-03	-8.71E-04	2.96E-03	-8.04E-04
USNM	4.77E-04	3.91E-03	1.80E-03	-1.57E-03	5.33E-03	7.21E-03	-6.63E-04
USNM	3.90E-03	6.29E-03	7.62E-03	4.93E-03	4.39E-03	-1.84E-03	-3.22E-05
USNM	-9.42E-03	-2.87E-03	3.51E-03	-6.38E-03	1.46E-03	-2.70E-03	-4.89E-03
USNM	8.69E-03	-7.01E-03	5.77E-04	-3.75E-03	-1.71E-03	2.07E-03	-2.94E-03
USNM	-1.57E-03	-4.62E-03	-1.04E-04	-4.27E-04	5.17E-03	-2.65E-03	2.90E-03
UWBM 81025	4.12E-03	-1.76E-03	4.58E-03	2.15E-04	-8.95E-03	-1.64E-03	3.28E-03
UWBM 81688	1.01E-03	2.23E-03	-4.40E-03	1.01E-04	1.05E-03	-1.05E-03	4.99E-04

Femur

Specimen	PC1	PC2	PC3	PC4	PC5	PC6	PC7	PC8	PC9
ETMNH 600	-1.22E-02	-5.28E-03	-3.06E-04	3.83E-03	-8.25E-03	-3.45E-03	-2.58E-03	-9.86E-04	3.37E-03
ETMNH 603	-1.90E-03	5.69E-03	3.46E-03	3.90E-03	-4.40E-03	5.77E-03	3.90E-03	-2.34E-03	1.99E-03
ETMNH 607	-2.96E-03	5.19E-03	5.17E-03	3.68E-03	-2.16E-03	2.40E-04	1.04E-03	-3.55E-03	-1.85E-03
ETMNH 608	-5.39E-03	1.14E-03	2.74E-03	-6.24E-04	-9.50E-04	7.39E-04	3.25E-03	7.87E-03	-1.18E-03
ETMNH 609	-8.78E-03	-1.43E-03	2.70E-03	-1.92E-03	2.90E-03	4.66E-03	4.60E-03	-1.17E-03	-2.63E-03
MSB 196536	4.15E-03	-6.69E-03	-1.06E-02	-9.78E-04	4.79E-03	8.70E-03	7.90E-05	3.49E-03	-3.34E-03
MSB 196578	1.94E-02	3.79E-03	-1.75E-03	1.26E-03	-1.24E-05	-8.10E-03	1.31E-03	-3.24E-03	-3.97E-03
MSB 196581	6.59E-03	5.49E-03	-6.62E-03	5.04E-03	2.07E-03	1.26E-03	8.11E-03	-3.03E-03	3.69E-03
MSB 196582	9.04E-03	-6.15E-03	5.51E-03	-3.25E-03	1.65E-03	8.61E-04	2.75E-03	2.94E-03	5.38E-03
MSB 196583	9.77E-03	9.70E-03	4.68E-03	-6.06E-03	-1.13E-03	-8.32E-03	-2.51E-03	3.42E-03	-2.96E-04
MSB 196981	1.26E-02	-3.83E-03	4.64E-03	-1.31E-03	1.89E-03	4.86E-03	9.28E-04	3.47E-03	-1.75E-03
MSB 197115	3.56E-03	-6.36E-03	4.89E-05	-6.17E-03	-4.51E-03	5.00E-04	-2.56E-04	2.44E-04	-2.60E-03
MSB 224027	8.52E-03	1.65E-03	-6.24E-04	-7.97E-04	-6.80E-04	5.56E-03	-5.93E-03	1.04E-03	-3.34E-03
MZ 177697	-3.14E-03	-1.00E-02	-6.40E-03	5.47E-03	3.87E-03	-7.28E-03	-1.62E-03	1.35E-03	-1.64E-03
MZ 177826	-5.08E-03	3.01E-03	7.50E-04	2.83E-03	5.67E-03	-4.48E-03	-3.26E-03	1.43E-03	-1.72E-03
MZ 177827	-8.90E-03	-1.49E-02	2.07E-03	-2.49E-03	1.80E-04	-4.79E-03	-6.35E-04	4.63E-04	2.50E-03
NY 14241	-2.14E-03	-9.06E-03	2.22E-03	-9.09E-05	-4.64E-03	-1.94E-03	1.02E-02	8.26E-04	-4.80E-03
NY 14242	-3.27E-03	-8.62E-03	-5.87E-03	-4.17E-03	-4.77E-04	-3.55E-03	3.42E-03	-2.66E-03	5.36E-04
NY 14387	7.52E-04	-5.82E-04	-4.03E-04	-2.33E-03	2.59E-03	-1.36E-03	-5.40E-03	1.08E-04	-1.83E-03
NY 14388	-9.60E-03	-4.83E-03	1.33E-03	1.71E-04	2.78E-03	1.20E-03	-1.13E-03	-2.04E-03	-2.14E-03
UAM 101819	1.79E-03	5.83E-03	-9.58E-03	6.31E-03	-1.01E-03	-6.17E-04	1.04E-03	3.40E-03	2.01E-03
UAM 101828	-2.80E-03	-2.46E-03	8.00E-04	8.48E-04	-5.72E-03	2.21E-03	-1.15E-03	-7.85E-04	-1.04E-03
UAM 101851	-1.91E-03	4.25E-03	-1.39E-03	4.90E-03	-4.54E-03	9.63E-04	-1.23E-03	-4.78E-03	6.22E-04
UAM 24794	1.34E-03	3.22E-04	2.37E-03	4.07E-03	-1.73E-03	1.36E-04	-5.36E-03	4.15E-04	3.29E-03

Femur continued

Specimen	PC1	PC2	PC3	PC4	PC5	PC6	PC7	PC8	PC9
UF 31142	2.64E-03	8.45E-03	-2.82E-03	1.79E-03	1.23E-02	4.81E-03	-4.95E-04	1.15E-03	-4.41E-03
UF 31328	-1.22E-02	4.81E-03	7.26E-03	-1.76E-03	-1.01E-03	5.33E-04	2.96E-03	5.51E-03	-2.25E-03
UF 31370	-1.12E-02	1.07E-02	-7.07E-03	-2.00E-03	5.12E-03	-6.62E-03	-3.80E-03	5.40E-03	1.35E-03
UF 31427	-5.09E-03	-2.34E-03	4.44E-03	-4.03E-04	-8.01E-04	-6.10E-04	5.38E-03	-9.87E-04	-2.66E-03
USNM 592316	-9.97E-04	-1.50E-03	-3.96E-04	1.06E-04	-3.16E-03	3.94E-03	-8.20E-04	2.75E-03	6.20E-03
USNM 592896	-7.53E-03	3.27E-03	-1.41E-04	-4.81E-03	1.50E-03	6.64E-04	1.46E-03	1.58E-03	-3.76E-03
USNM 592943	6.54E-03	-1.43E-02	1.11E-03	5.35E-03	-2.77E-03	2.48E-04	2.91E-03	2.85E-03	4.35E-03
USNM 600579	5.72E-03	-1.32E-03	3.27E-03	-2.06E-05	-1.98E-03	8.00E-03	1.94E-03	-1.47E-03	3.01E-03
USNM 600581	1.23E-02	-4.97E-03	-3.12E-03	-7.67E-03	-4.70E-03	-5.53E-03	-7.44E-04	-1.43E-03	-3.45E-03
USNM 600583	5.12E-03	-4.59E-03	-1.71E-03	3.80E-03	-4.15E-03	2.49E-03	-7.18E-03	-3.54E-03	3.21E-03
USNM 600584	-3.42E-03	-1.46E-02	-3.66E-03	-2.53E-03	2.75E-03	-3.64E-03	1.51E-03	2.37E-03	2.08E-03
USNM 600580	-4.68E-03	-1.96E-03	-9.99E-04	1.18E-03	4.16E-03	3.95E-03	1.38E-03	3.81E-03	1.79E-03
UWBM 81025	-8.08E-03	-5.05E-03	1.68E-03	2.78E-03	6.40E-03	-4.42E-03	9.79E-04	-2.98E-03	2.73E-03
UWBM 81688	-3.23E-04	-7.87E-03	1.64E-03	1.26E-04	5.07E-03	-4.77E-03	3.16E-03	-5.82E-03	-4.70E-03

Femur continued

Specimen	PC10	PC11	PC12	PC13	PC14	PC15	PC16	PC17	PC18
ETMNH 600	9.35E-04	-2.84E-03	-1.75E-03	-1.55E-03	3.42E-03	-1.72E-03	8.96E-04	3.00E-03	1.26E-03
ETMNH 603	-2.69E-04	3.46E-03	-2.89E-04	1.12E-03	3.86E-03	-1.43E-03	-1.45E-05	-1.03E-03	-4.73E-04
ETMNH 607	2.35E-04	1.20E-03	3.87E-03	3.02E-03	2.96E-04	-5.66E-04	1.94E-03	-1.62E-04	-1.21E-03
ETMNH 608	4.81E-04	-3.06E-03	2.96E-03	-2.95E-03	-3.02E-03	6.33E-04	1.91E-03	-1.10E-03	1.82E-03
ETMNH 609	1.52E-03	3.66E-04	2.70E-03	-8.52E-04	3.38E-03	-1.99E-04	-3.87E-03	-9.29E-04	-4.35E-04
MSB 196536	3.35E-03	-8.69E-04	-4.81E-03	-1.66E-03	-2.42E-03	-2.51E-03	2.10E-03	1.84E-03	3.40E-04
MSB 196578	7.14E-04	1.35E-04	-5.86E-03	1.64E-03	-3.27E-03	4.20E-04	-2.15E-03	4.37E-03	-1.11E-04
MSB 196581	-2.34E-03	4.23E-03	-1.21E-03	-1.24E-04	-1.60E-03	2.88E-03	1.20E-03	-3.08E-03	5.11E-04
MSB 196582	6.62E-03	-4.54E-03	-1.06E-03	-9.68E-04	3.42E-03	-8.08E-04	2.85E-03	-1.73E-03	7.03E-05
MSB 196583	2.99E-03	2.82E-03	-4.81E-03	9.72E-04	-1.03E-03	9.81E-04	-2.78E-03	-1.61E-03	-1.23E-03
MSB 196981	2.61E-03	1.69E-03	2.01E-03	-1.26E-03	-2.35E-03	-4.41E-03	-2.19E-05	-3.16E-04	-2.17E-03
MSB 197115	3.23E-03	3.78E-03	3.29E-04	-5.39E-03	4.98E-03	7.52E-04	2.80E-03	-8.52E-04	-1.69E-03
MSB 224027	1.27E-03	-3.46E-03	8.09E-04	1.54E-03	-2.01E-03	7.09E-04	4.43E-03	2.03E-04	6.05E-04
MZ 177697	6.90E-03	-4.22E-03	2.40E-03	3.38E-03	-2.79E-04	2.40E-04	-4.50E-03	-2.40E-03	4.02E-04
MZ 177826	9.92E-04	-1.68E-03	-3.43E-03	-5.77E-03	2.33E-03	2.68E-04	-2.04E-03	1.72E-03	5.73E-04
MZ 177827	1.39E-04	-6.00E-03	4.33E-03	-2.16E-05	-8.13E-04	3.58E-03	1.19E-03	-3.41E-04	1.00E-03
NY 14241	-1.83E-03	2.59E-04	7.69E-04	1.88E-03	-3.17E-04	-1.36E-03	-5.85E-04	1.94E-03	-1.40E-03
NY 14242	-3.06E-03	2.50E-03	-1.94E-03	-1.45E-03	-1.39E-03	6.73E-04	2.73E-03	1.31E-03	8.65E-04
NY 14387	2.72E-03	-7.74E-04	-2.89E-03	7.01E-03	7.50E-04	1.72E-03	4.77E-04	-1.24E-03	1.89E-03
NY 14388	-1.24E-03	-1.47E-03	2.37E-04	6.97E-04	-7.03E-05	-9.05E-04	-1.73E-03	-3.46E-03	1.52E-03
UAM 101819	-3.05E-03	1.94E-03	5.99E-04	-3.99E-03	2.55E-03	9.06E-04	-2.23E-03	-3.39E-03	-1.77E-04
UAM 101828	1.39E-03	5.56E-03	9.48E-04	-3.36E-04	-3.94E-04	1.56E-03	1.02E-03	1.62E-03	-1.21E-03
UAM 101851	4.31E-03	2.62E-03	9.93E-04	-1.70E-03	-1.88E-03	1.03E-03	1.62E-03	-7.14E-04	1.39E-03
UAM 24794	2.90E-03	1.71E-03	2.19E-03	6.27E-04	1.61E-03	6.17E-04	-2.48E-03	3.48E-03	3.49E-03

Femur continued

Specimen	PC10	PC11	PC12	PC13	PC14	PC15	PC16	PC17	PC18
UF 31142	-2.90E-03	-2.40E-03	2.46E-03	-2.53E-03	1.00E-03	9.78E-04	-1.42E-04	1.38E-03	-2.30E-03
UF 31328	1.75E-03	-2.79E-03	-2.61E-03	9.66E-04	-4.21E-03	4.39E-04	7.23E-04	-8.76E-04	-4.76E-03
UF 31370	-2.85E-03	2.01E-03	4.90E-03	2.33E-03	-7.08E-04	-1.24E-03	-1.59E-03	1.49E-03	2.60E-03
UF 31427	-2.17E-03	-1.49E-03	4.04E-03	1.86E-03	-6.36E-04	1.21E-03	5.95E-05	2.95E-03	-1.82E-03
USNM 592316	-1.15E-03	-2.10E-03	-6.31E-04	-2.33E-03	-2.61E-03	-1.89E-03	-1.29E-03	-1.22E-03	5.96E-04
USNM 592896	-3.02E-03	1.55E-03	1.45E-03	1.54E-03	-8.54E-04	-5.51E-03	1.10E-03	-3.73E-03	-1.37E-03
USNM 592943	-4.20E-03	1.53E-03	9.15E-04	-6.23E-04	-4.53E-03	-2.60E-03	-3.34E-04	-4.19E-04	3.69E-04
USNM 600579	-5.12E-04	1.35E-03	-1.76E-04	2.87E-03	3.52E-03	-5.74E-03	1.62E-03	2.70E-03	1.04E-03
USNM 600581	-4.13E-03	-1.93E-03	6.09E-04	4.19E-03	4.36E-03	8.43E-04	3.53E-04	3.91E-04	-1.12E-03
USNM 600583	-4.46E-03	-1.07E-03	1.70E-03	-1.28E-03	3.04E-04	4.89E-03	-1.47E-04	1.53E-03	-1.52E-03
USNM 600584	2.38E-03	2.07E-03	1.28E-03	-1.68E-03	-2.30E-03	7.12E-04	-5.17E-03	1.52E-03	-2.50E-03
USNM 600580	-1.91E-03	3.91E-03	-4.89E-03	3.84E-03	1.00E-03	3.56E-03	1.27E-05	-1.59E-03	2.08E-03
UWBM 81025	-5.54E-03	-4.56E-03	-5.39E-03	7.37E-04	2.47E-03	1.00E-04	9.00E-05	-6.47E-04	-3.36E-03
UWBM 81688	-5.03E-03	-2.95E-03	-2.46E-03	-3.43E-03	-1.17E-03	-1.30E-03	-1.26E-03	-9.13E-04	5.49E-03

Tibia

Specimen	PC1	PC2	PC3	PC4	PC5	PC6	PC7	PC8	PC9
ETMNH 600	1.29E-03	1.09E-02	1.25E-03	5.45E-04	4.26E-03	1.91E-04	7.43E-04	-8.39E-04	-7.59E-04
ETMNH 603	6.29E-03	-1.02E-03	-3.79E-03	5.44E-03	-7.09E-05	4.96E-03	6.80E-03	-1.85E-03	2.59E-03
ETMNH 607	5.90E-03	2.16E-03	1.27E-03	4.53E-03	1.20E-03	9.44E-03	2.20E-03	-7.18E-04	-4.31E-03
ETMNH 608	8.67E-03	3.23E-03	2.20E-03	3.42E-03	-2.77E-03	5.39E-03	-5.53E-03	-7.14E-05	2.14E-03
ETMNH 609	5.36E-03	6.97E-03	-3.59E-03	-1.31E-03	-6.28E-04	3.01E-03	-2.89E-03	6.27E-03	-3.54E-03
MSB 196536	-1.05E-02	9.41E-03	-5.40E-03	-9.43E-04	-5.03E-03	-2.79E-03	2.32E-03	-5.90E-03	1.13E-03
MSB 196578	-9.13E-03	7.89E-03	8.19E-03	2.80E-03	-4.34E-03	-2.31E-03	-2.21E-03	3.46E-03	1.69E-03
MSB 196581	-3.86E-03	1.08E-03	4.95E-03	6.04E-03	-1.28E-02	-1.57E-03	1.01E-03	-3.51E-03	-3.68E-03
MSB 196582	-1.24E-03	1.00E-03	-3.03E-03	2.22E-03	-6.70E-03	-7.27E-03	4.25E-04	7.75E-03	2.42E-03
MSB 196583	-9.30E-03	-1.23E-02	2.91E-03	7.87E-03	5.40E-03	-3.85E-03	-7.76E-03	-1.00E-03	-3.64E-03
MSB 196981	-7.48E-03	-2.10E-03	-1.44E-02	-1.00E-03	-1.10E-03	-1.26E-04	-1.53E-03	-4.70E-03	6.89E-04
MSB 197115	-3.36E-03	-3.27E-03	-5.96E-03	2.89E-03	-8.35E-03	-1.00E-03	7.53E-03	8.45E-04	1.81E-03
MSB 224027	-7.37E-03	1.03E-03	-2.74E-03	1.27E-03	-1.10E-03	6.02E-04	-2.62E-03	1.53E-03	4.82E-04
MZ 177697	-8.48E-03	-4.09E-03	3.58E-03	2.96E-03	1.84E-03	7.58E-04	-9.53E-04	6.48E-03	-1.95E-03
MZ 177826	-7.13E-03	-3.60E-03	-6.78E-03	-6.08E-03	1.95E-03	-3.28E-03	-1.79E-03	-2.92E-03	4.19E-03
MZ 177827	-1.33E-02	4.54E-03	2.86E-03	-6.03E-03	1.88E-03	1.25E-02	-5.80E-03	1.88E-03	2.96E-03
NY 14241	-1.35E-02	-9.26E-03	4.43E-03	1.67E-03	-1.02E-03	3.84E-03	3.75E-04	-1.33E-03	-2.60E-03
NY 14242	-5.59E-03	-8.19E-03	4.94E-03	-1.81E-05	1.07E-03	-5.74E-03	1.56E-03	-1.75E-04	2.59E-04
NY 14387	-3.27E-03	-6.77E-03	-1.59E-03	-3.03E-03	9.27E-05	-8.43E-04	2.21E-03	3.50E-03	-5.85E-03
NY 14388	-9.12E-03	-3.37E-03	-9.42E-03	4.04E-03	2.82E-03	5.43E-03	-1.57E-04	3.92E-04	1.38E-03
UAM 101819	-1.64E-03	4.70E-03	1.57E-04	-3.79E-03	-4.33E-03	2.89E-03	5.02E-03	1.92E-03	-3.54E-03
UAM 101828	2.32E-03	-6.43E-03	8.09E-03	4.25E-04	9.86E-04	1.31E-03	7.10E-03	-3.95E-03	4.37E-03
UAM 101851	4.60E-05	-7.00E-03	-2.12E-03	-3.76E-03	6.48E-03	-2.26E-03	1.73E-03	-1.13E-03	2.48E-03
UAM 24794	-1.63E-03	2.88E-03	1.25E-03	-7.86E-03	7.90E-03	-6.05E-03	4.67E-03	1.98E-03	-3.14E-03
UAM 59579	8.71E-03	3.55E-03	1.88E-03	8.64E-03	7.55E-03	9.08E-04	6.34E-03	1.62E-05	-2.17E-04

Tibia continued

Specimen	PC1	PC2	PC3	PC4	PC5	PC6	PC7	PC8	PC9
UF 31142	6.37E-03	-2.18E-03	4.02E-03	6.33E-03	3.38E-03	-2.54E-03	7.98E-04	1.03E-03	4.77E-03
UF 31328	3.26E-03	8.61E-03	2.67E-03	-3.66E-03	-1.84E-03	-3.76E-03	-7.36E-03	-1.69E-03	1.23E-03
UF 31370	5.39E-03	-1.51E-03	8.48E-03	-5.28E-03	-2.21E-03	4.39E-04	3.83E-04	3.05E-03	8.33E-03
UF 31427	5.15E-03	4.84E-03	2.54E-03	2.85E-03	3.85E-03	-9.04E-05	-2.75E-03	8.59E-04	1.66E-03
USNM 592316	-4.46E-03	1.12E-02	2.96E-03	-5.23E-03	3.66E-03	-4.55E-03	5.23E-03	2.73E-03	-2.22E-03
USNM 592896	-8.45E-04	8.86E-04	5.81E-03	-6.79E-03	6.86E-04	3.32E-03	2.97E-03	-3.60E-03	-3.35E-03
USNM 592943	8.16E-03	4.13E-03	-3.19E-03	-3.33E-04	-6.65E-04	-4.91E-04	-1.40E-03	-7.44E-03	-1.38E-03
USNM 600579	1.84E-03	6.28E-03	-3.93E-03	1.74E-03	5.89E-03	-2.89E-03	-2.57E-03	-4.78E-03	-1.70E-03
USNM 600581	1.02E-02	-1.23E-02	5.06E-03	-8.39E-03	-2.01E-03	3.08E-03	-8.13E-04	7.31E-05	-1.22E-03
USNM 600583	5.92E-03	1.48E-03	-3.08E-03	9.20E-03	2.18E-03	-2.80E-03	-2.69E-03	2.63E-03	-3.68E-05
USNM 600584	1.61E-02	-5.84E-03	-1.61E-02	-4.52E-03	-1.77E-03	8.40E-04	-8.72E-04	5.74E-03	-8.31E-04
USNM 600580	7.30E-04	-1.12E-03	-9.71E-04	-2.45E-03	-1.62E-03	9.22E-04	-6.04E-04	-7.86E-04	3.00E-03
UWBM 81025	3.37E-03	-1.43E-03	8.87E-04	-2.40E-03	1.30E-03	-2.21E-03	-4.86E-03	-2.50E-03	2.35E-04
UWBM 81688	1.62E-02	-4.88E-03	5.72E-03	-2.02E-03	-6.05E-03	-3.37E-03	-4.26E-03	-3.27E-03	-3.84E-03

Tibia continued

Specimen	PC10	PC11	PC12	PC13	PC14	PC15
ETMNH 600	2.38E-05	3.83E-04	-3.19E-03	1.98E-03	1.50E-03	4.91E-04
ETMNH 603	-2.77E-03	-1.78E-03	-9.77E-04	-2.11E-03	3.56E-04	3.17E-03
ETMNH 607	1.16E-03	-1.09E-03	6.53E-04	-1.07E-03	-3.11E-03	-9.44E-04
ETMNH 608	2.57E-04	8.38E-05	2.09E-03	-6.25E-04	2.19E-03	-6.18E-04
ETMNH 609	8.91E-04	1.17E-03	8.66E-04	-3.16E-03	3.45E-04	1.73E-03
MSB 196536	6.37E-03	9.25E-05	1.53E-03	3.61E-03	-5.39E-03	1.08E-03
MSB 196578	5.58E-03	2.63E-03	-3.39E-03	-8.11E-04	1.64E-03	-1.25E-03
MSB 196581	-9.60E-04	-3.83E-03	-9.52E-04	-3.48E-03	4.77E-04	1.59E-03
MSB 196582	3.94E-03	-1.38E-03	-1.36E-03	-1.14E-03	-1.14E-03	-2.52E-03
MSB 196583	8.52E-04	2.20E-03	1.37E-03	-5.52E-04	-2.09E-05	1.50E-04
MSB 196981	1.16E-03	-8.98E-04	-3.93E-03	6.11E-04	4.49E-03	-1.42E-03
MSB 197115	-5.13E-03	8.02E-03	3.68E-04	-7.49E-07	-1.21E-03	2.77E-03
MSB 224027	-1.44E-03	2.08E-03	-6.78E-04	2.28E-03	3.73E-03	2.16E-03
MZ 177697	-2.75E-03	1.01E-03	-1.28E-04	1.63E-03	1.11E-03	3.49E-05
MZ 177826	-3.01E-03	-3.49E-03	3.24E-04	9.72E-04	2.57E-03	-8.44E-04
MZ 177827	-7.79E-04	6.82E-04	-1.61E-03	2.70E-03	-2.32E-03	2.90E-03
NY 14241	1.51E-03	-2.20E-03	6.14E-03	1.01E-04	-1.12E-03	-1.63E-03
NY 14242	-4.15E-05	-5.11E-04	1.50E-03	-2.86E-04	9.28E-04	1.56E-03
NY 14387	3.55E-04	-4.51E-03	-2.95E-03	-5.04E-04	7.79E-05	1.01E-03
NY 14388	1.33E-03	-1.07E-03	-1.70E-03	-1.33E-03	-1.03E-03	-1.29E-03
UAM 101819	-3.99E-03	-4.39E-03	2.57E-03	2.77E-03	2.37E-03	-2.34E-03
UAM 101828	-1.20E-04	3.78E-04	-2.21E-03	1.93E-03	-1.42E-03	-3.41E-03
UAM 101851	2.73E-03	-5.99E-04	-3.64E-03	-4.22E-03	-4.06E-03	1.85E-03
UAM 24794	-2.93E-03	-2.61E-05	-1.37E-04	-1.95E-03	-4.36E-04	1.98E-03
UAM 59579	4.68E-03	1.33E-03	-2.96E-04	9.41E-04	3.14E-03	4.29E-04

Tibia continued

Specimen	PC10	PC11	PC12	PC13	PC14	PC15
UF 31142	-9.91E-05	-1.14E-03	2.23E-03	2.51E-03	-3.22E-04	1.88E-04
UF 31328	-3.45E-03	-1.66E-03	3.45E-04	-3.61E-03	-3.66E-03	-4.87E-04
UF 31370	1.75E-03	-2.86E-03	4.78E-03	-1.27E-03	1.63E-03	1.94E-03
UF 31427	-1.18E-03	-2.48E-03	-5.41E-03	-9.23E-04	4.93E-04	-1.37E-03
USNM 592316	-6.56E-04	2.33E-04	1.70E-03	2.63E-03	-9.46E-05	-1.01E-03
USNM 592896	7.89E-04	6.14E-03	-2.14E-04	-3.51E-03	1.18E-04	-3.52E-03
USNM 592943	-1.74E-03	-2.26E-03	5.64E-04	-7.54E-06	6.16E-04	-1.74E-04
USNM 600579	3.32E-03	6.40E-04	6.09E-03	-1.49E-03	2.00E-03	1.78E-03
USNM 600581	2.56E-03	-9.35E-04	-2.11E-03	1.81E-03	-1.98E-04	5.43E-04
USNM 600583	-6.55E-03	-1.09E-03	6.53E-05	2.13E-03	-4.78E-03	-1.58E-03
USNM 600584	3.78E-03	1.55E-03	3.01E-03	1.20E-03	-1.14E-03	-1.38E-03
USNM 600580	-3.39E-03	3.82E-03	1.23E-03	-4.41E-03	2.39E-03	-2.44E-03
UWBM 81025	-3.08E-03	3.91E-03	5.84E-04	2.59E-03	-1.43E-03	-1.23E-03
UWBM 81688	1.04E-03	1.86E-03	-3.15E-03	4.07E-03	7.19E-04	2.12E-03

Fibula

Specimen	PC1	PC2	PC3	PC4	PC5	PC6	PC7	PC8	PC9
ETMNH 600	-1.22E-02	-5.28E-03	-3.06E-04	3.83E-03	-8.25E-03	-3.45E-03	-2.58E-03	-9.86E-04	3.37E-03
ETMNH 603	-1.90E-03	5.69E-03	3.46E-03	3.90E-03	-4.40E-03	5.77E-03	3.90E-03	-2.34E-03	1.99E-03
ETMNH 607	-2.96E-03	5.19E-03	5.17E-03	3.68E-03	-2.16E-03	2.40E-04	1.04E-03	-3.55E-03	-1.85E-03
ETMNH 608	-5.39E-03	1.14E-03	2.74E-03	-6.24E-04	-9.50E-04	7.39E-04	3.25E-03	7.87E-03	-1.18E-03
ETMNH 609	-8.78E-03	-1.43E-03	2.70E-03	-1.92E-03	2.90E-03	4.66E-03	4.60E-03	-1.17E-03	-2.63E-03
MSB 196536	4.15E-03	-6.69E-03	-1.06E-02	-9.78E-04	4.79E-03	8.70E-03	7.90E-05	3.49E-03	-3.34E-03
MSB 196578	1.94E-02	3.79E-03	-1.75E-03	1.26E-03	-1.24E-05	-8.10E-03	1.31E-03	-3.24E-03	-3.97E-03
MSB 196581	6.59E-03	5.49E-03	-6.62E-03	5.04E-03	2.07E-03	1.26E-03	8.11E-03	-3.03E-03	3.69E-03
MSB 196582	9.04E-03	-6.15E-03	5.51E-03	-3.25E-03	1.65E-03	8.61E-04	2.75E-03	2.94E-03	5.38E-03
MSB 196583	9.77E-03	9.70E-03	4.68E-03	-6.06E-03	-1.13E-03	-8.32E-03	-2.51E-03	3.42E-03	-2.96E-04
MSB 196981	1.26E-02	-3.83E-03	4.64E-03	-1.31E-03	1.89E-03	4.86E-03	9.28E-04	3.47E-03	-1.75E-03
MSB 197115	3.56E-03	-6.36E-03	4.89E-05	-6.17E-03	-4.51E-03	5.00E-04	-2.56E-04	2.44E-04	-2.60E-03
MSB 224027	8.52E-03	1.65E-03	-6.24E-04	-7.97E-04	-6.80E-04	5.56E-03	-5.93E-03	1.04E-03	-3.34E-03
MZ 177697	-3.14E-03	-1.00E-02	-6.40E-03	5.47E-03	3.87E-03	-7.28E-03	-1.62E-03	1.35E-03	-1.64E-03
MZ 177826	-5.08E-03	3.01E-03	7.50E-04	2.83E-03	5.67E-03	-4.48E-03	-3.26E-03	1.43E-03	-1.72E-03
MZ 177827	-8.90E-03	-1.49E-02	2.07E-03	-2.49E-03	1.80E-04	-4.79E-03	-6.35E-04	4.63E-04	2.50E-03
NY 14241	-2.14E-03	-9.06E-03	2.22E-03	-9.09E-05	-4.64E-03	-1.94E-03	1.02E-02	8.26E-04	-4.80E-03
NY 14242	-3.27E-03	-8.62E-03	-5.87E-03	-4.17E-03	-4.77E-04	-3.55E-03	3.42E-03	-2.66E-03	5.36E-04
NY 14387	7.52E-04	-5.82E-04	-4.03E-04	-2.33E-03	2.59E-03	-1.36E-03	-5.40E-03	1.08E-04	-1.83E-03
NY 14388	-9.60E-03	-4.83E-03	1.33E-03	1.71E-04	2.78E-03	1.20E-03	-1.13E-03	-2.04E-03	-2.14E-03
UAM 101819	1.79E-03	5.83E-03	-9.58E-03	6.31E-03	-1.01E-03	-6.17E-04	1.04E-03	3.40E-03	2.01E-03
UAM 101828	-2.80E-03	-2.46E-03	8.00E-04	8.48E-04	-5.72E-03	2.21E-03	-1.15E-03	-7.85E-04	-1.04E-03
UAM 101851	-1.91E-03	4.25E-03	-1.39E-03	4.90E-03	-4.54E-03	9.63E-04	-1.23E-03	-4.78E-03	6.22E-04
UAM 24794	1.34E-03	3.22E-04	2.37E-03	4.07E-03	-1.73E-03	1.36E-04	-5.36E-03	4.15E-04	3.29E-03
UAM 59579	8.12E-04	3.49E-04	-1.05E-02	-2.76E-03	-4.94E-03	1.26E-03	-3.30E-03	-2.17E-03	-9.81E-04

Fibula continued

Specimen	PC1	PC2	PC3	PC4	PC5	PC6	PC7	PC8	PC9
UF 31328	-1.26E-03	-4.86E-03	2.32E-03	2.06E-03	7.18E-03	-1.68E-03	6.83E-06	-2.78E-03	-2.47E-03
UF 31370	8.23E-03	2.41E-03	4.41E-03	-5.27E-03	4.85E-03	-2.36E-03	5.46E-03	-3.67E-03	1.82E-03
UF 31427	8.32E-03	-3.20E-03	-5.19E-03	-2.66E-03	-4.98E-03	-1.79E-03	-3.83E-03	1.88E-04	4.17E-03
UWBM 81025	9.30E-03	-3.06E-03	3.91E-03	-5.98E-04	-3.16E-03	7.01E-04	-3.97E-05	1.28E-03	5.39E-03
UWBM 81688	5.77E-03	5.32E-04	-5.04E-04	5.74E-03	5.11E-04	3.99E-03	3.53E-04	-4.94E-03	-9.43E-06
USNM 600579	-8.81E-03	1.47E-02	-3.08E-03	-5.98E-03	4.47E-03	-2.19E-03	1.14E-04	-1.78E-03	-1.90E-03
USNM 600583	-2.65E-03	5.70E-03	6.95E-03	-1.10E-04	-9.92E-03	1.86E-03	-9.00E-04	3.17E-03	-4.92E-03
USNM 600584	-1.08E-02	7.51E-03	-6.65E-03	-1.41E-02	-4.98E-04	2.77E-03	5.95E-04	-1.45E-03	3.85E-03
USNM 600581	-3.83E-03	1.51E-03	3.74E-03	-2.39E-03	5.70E-03	3.71E-03	-2.59E-03	2.16E-03	3.00E-03
USNM 600580	-5.54E-03	9.02E-03	-2.28E-03	3.22E-03	1.96E-04	-2.62E-03	5.50E-04	3.97E-03	-3.42E-03
USNM 592943	-7.02E-03	2.92E-03	9.43E-03	8.86E-04	3.08E-03	-1.62E-03	-1.33E-03	-3.41E-03	1.98E-03
USNM 592316	-4.66E-03	4.81E-03	-1.25E-03	7.38E-03	4.19E-03	-2.98E-04	2.10E-03	7.05E-03	4.56E-03
USNM 592896	2.65E-03	-4.19E-03	3.75E-03	2.45E-03	5.13E-03	4.50E-03	-6.73E-03	-3.49E-03	-3.38E-04

Fibula continued

Specimen	PC10	PC11
ETMNH 600	1.38E-03	-2.64E-03
ETMNH 603	2.39E-03	8.77E-04
ETMNH 607	-3.02E-03	-3.99E-06
ETMNH 608	3.50E-03	1.61E-03
ETMNH 609	-1.22E-03	-1.99E-03
MSB 196536	-4.91E-03	1.19E-03
MSB 196578	2.13E-03	3.50E-03
MSB 196581	6.45E-04	-3.01E-03
MSB 196582	-2.24E-03	1.79E-03
MSB 196583	-6.07E-04	-6.44E-04
MSB 196981	7.74E-04	-1.65E-03
MSB 197115	-2.65E-04	-9.26E-04
MSB 224027	3.77E-04	-1.26E-03
MZ 177697	-1.10E-03	4.01E-03
MZ 177826	-3.51E-03	-2.42E-03
MZ 177827	6.50E-04	-3.52E-03
NY 14241	2.92E-03	4.23E-03
NY 14242	-2.34E-03	-3.93E-04
NY 14387	2.18E-03	-6.38E-04
NY 14388	-1.42E-03	-1.58E-03
UAM 101819	4.64E-03	2.19E-04
UAM 101828	3.18E-03	-4.37E-04
UAM 101851	-3.87E-03	3.40E-04
UAM 24794	1.52E-03	1.32E-03
UAM 59579	1.01E-03	1.48E-03

Fibula continued

Specimen	PC10	PC11
UF 31328	3.47E-03	-3.16E-03
UF 31370	3.19E-04	-4.40E-03
UF 31427	-1.58E-03	-3.43E-03
UWBM 81025	-3.59E-03	2.32E-03
UWBM 81688	-2.77E-03	-6.96E-04
USNM 600579	2.68E-03	-1.55E-03
USNM 600583	-1.03E-03	-2.69E-03
USNM 600584	1.01E-03	4.16E-03
USNM 600581	-2.80E-04	4.38E-04
USNM 600580	-5.93E-03	8.05E-04
USNM 592943	-2.88E-03	6.91E-03
USNM 592316	1.52E-03	-1.05E-03
USNM 592896	6.26E-03	2.90E-03

Table 2. Proportion of Variance Explained by Each PC

Element	PC1	PC2	PC3	PC4	PC5	PC6	PC7	PC8	PC9	PC10	PC11	PC12	PC13	PC14	PC15
Humerus	*36.9%*	*10.8%*	*7.1%*	*6.5%*	*4.7%*	*4.1%*	*3.9%*	*3.2%*	*3.1%*	*2.5%*	*2.1%*	*1.9%*	*1.9%*	*1.7%*	*1.4%*
Radius	*29%*	*13%*	*10%*	*7.2%*	*6.1%*	*5.5%*	*5.1%*	*3.8%*	*3.6%*	*2.9%*	*2.5%*	*2.2%*	*1.8%*	*1.5%*	1.1%
Ulna	*25.0%*	*13.6%*	*11.1%*	*9.6%*	*7.0%*	*5.5%*	*4.3%*	*4.0%*	*2.7%*	*2.6%*	*2.4%*	*2.1%*	*1.9%*	*1.6%*	*1.3%*
Femur	*16.6%*	*15.0%*	*10.0%*	*8.5%*	*6.4%*	*5.9%*	*5.5%*	*4.7%*	*3.9%*	*3.1%*	*2.7%*	*2.6%*	*2.3%*	*2.0%*	*1.7%*
Tibia	*21.4%*	*13.9%*	*11.9%*	*8.1%*	*7.1%*	*6.2%*	*5.7%*	*4.5%*	*3.4%*	*3.2%*	*2.6%*	*2.5%*	*1.9%*	*1.9%*	*1.2%*
Fibula	*23.2%*	*17.0%*	*10.4%*	*9.3%*	*7.6%*	*6.5%*	*5.7%*	*4.3%*	*3.8%*	*3.3%*	*2.8%*	*2.4%*	1.7%	1.1%	0.8%

Table 2 continued

Element	PC16	PC17	PC18	PC19	PC20	PC21	PC22	PC23	PC24	PC25	PC26	PC27	PC28	PC29	PC30
Humerus	*1.2%*	*1.1%*	*1.0%*	0.7%	0.7%	0.7%	0.6%	0.4%	0.4%	0.3%	0.2%	0.2%	0.2%	0.1%	0.1%
Radius	1.0%	0.8%	0.6%	0.6%	0.2%	0.2%	0.2%	0.1%							
Ulna	*1.1%*	1.1%	0.8%	0.8%	0.4%	0.4%	0.2%	0.2%	0.2%	0.1%	0.07%				
Femur	*1.5%*	*1.3%*	*1.2%*	1.1%	0.8%	0.7%	0.7%	0.5%	0.4%	0.3%	0.2%	0.2%	0.03%		
Tibia	1.1%	1.0%	0.7%	0.6%	0.4%	0.3%	0.3%	0.2%							
Fibula	0.7%	0.4%													

Table 2 continued

Element	PC31	PC32	PC33	PC34	PC35	PC21	PC22	PC23	PC24	PC25	PC26	PC27	PC28	PC29	PC30
Humerus	0.07%	0.02%	0.01%	0.007%	0.003%										
Radius															
Ulna															
Femur															
Tibia															
Fibula															

*Italicized values indicate the PCs whose cumulative variation equals 95% and, therefore, are the PCs included in the PERMANOVA.

D Thin plate spline warps figure captions

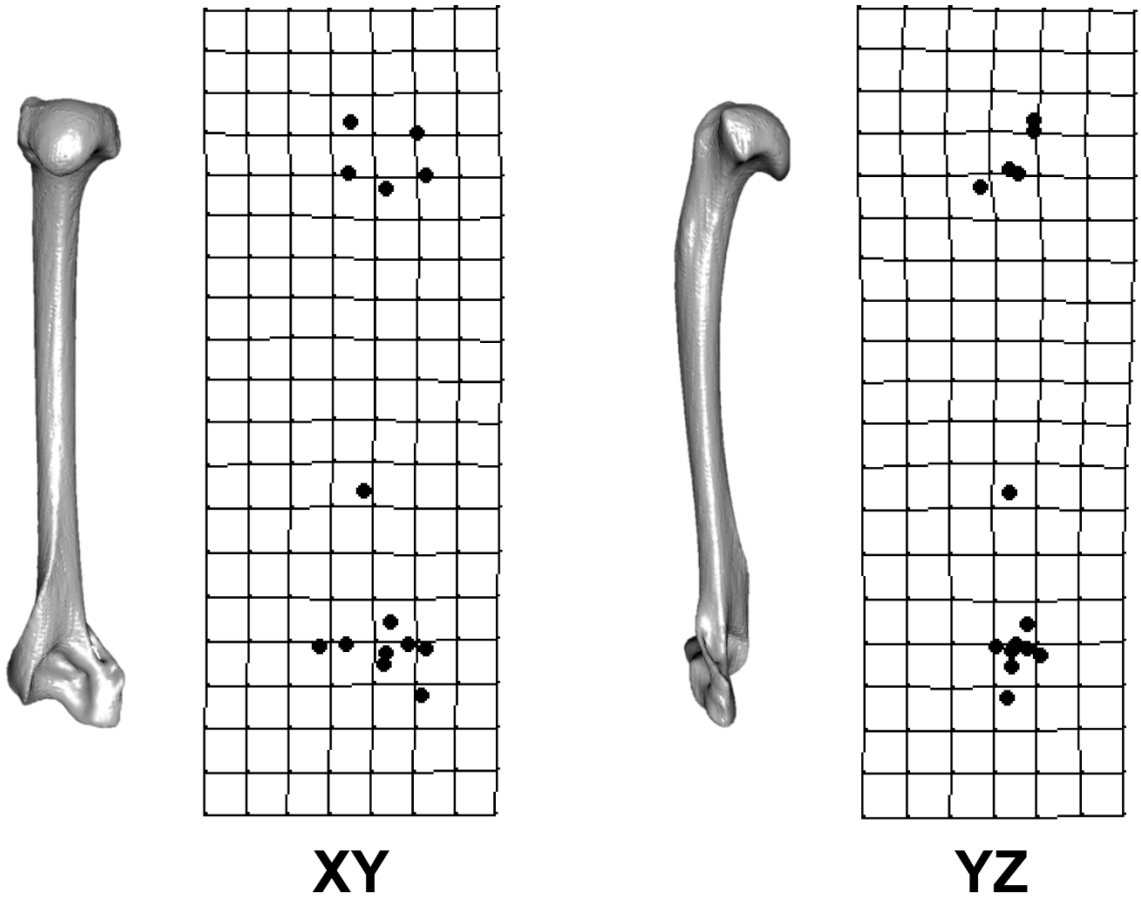

Figure S1. Thin plate spline of the humerus of Broadleaf warped into Boreal in XY and YZ views. Surface model of the humerus depicts the orientation of bone in each spline.

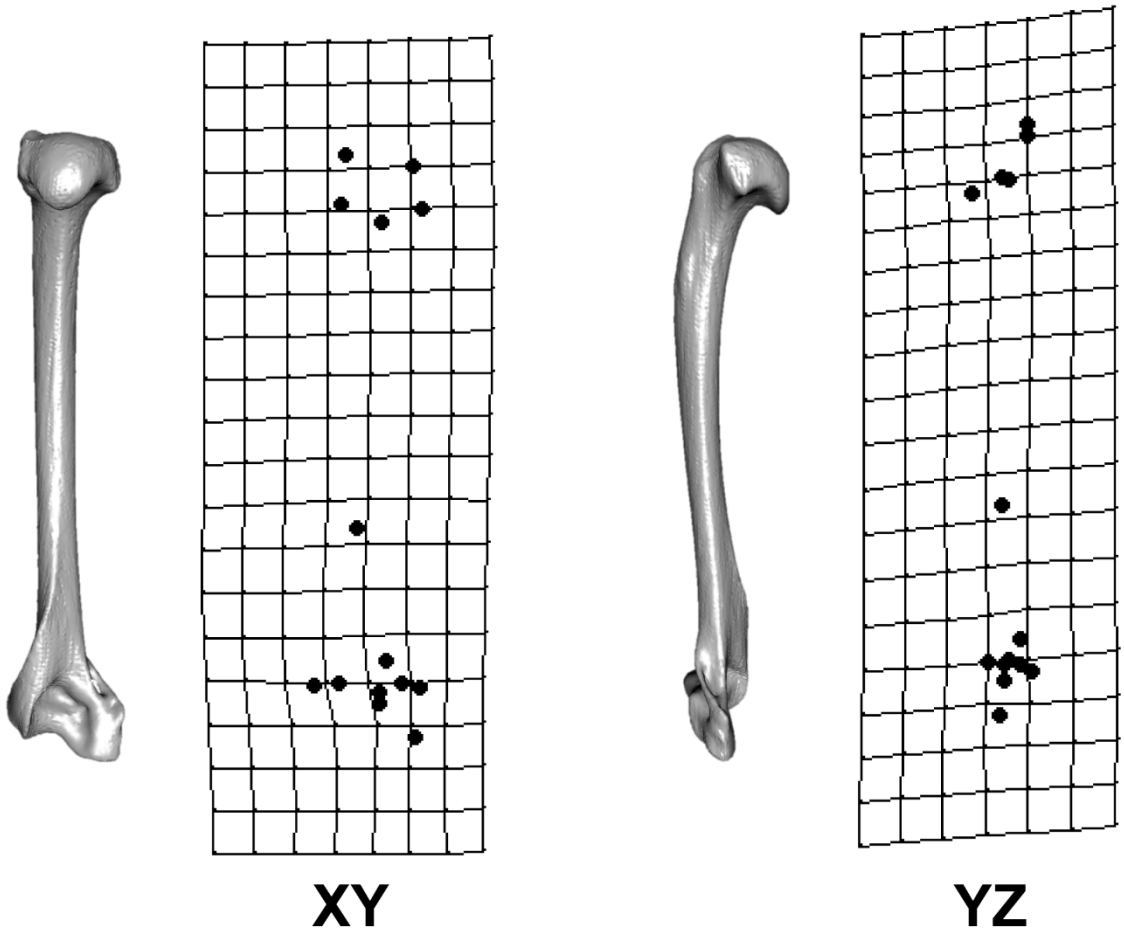

Figure S2. Thin plate spline of the humerus of Coniferous warped into Boreal in XY and YZ views. Surface model of the humerus depicts the orientation of bone in each spline.

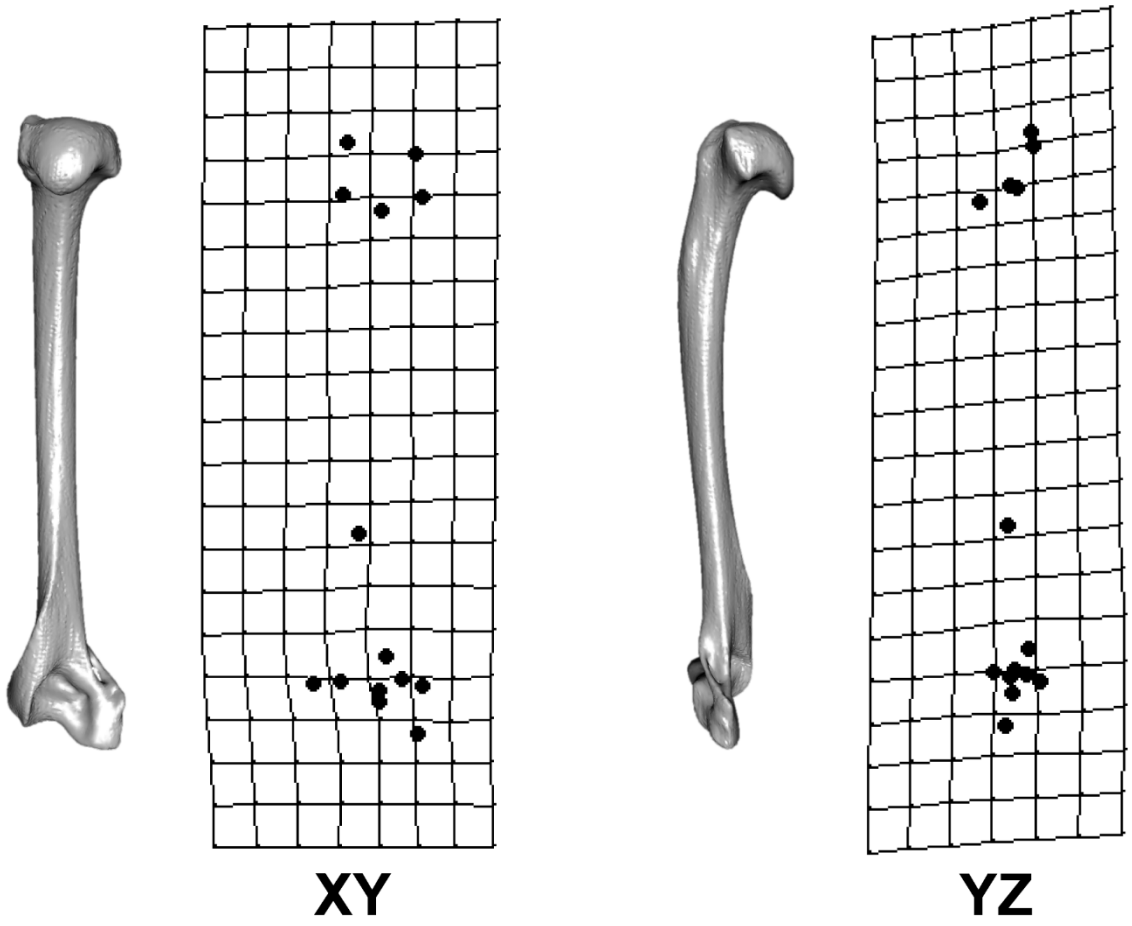

Figure S3. Thin plate spline of the humerus of Coniferous warped into Broadleaf in XY and YZ views. Surface model of the humerus depicts the orientation of bone in each spline.

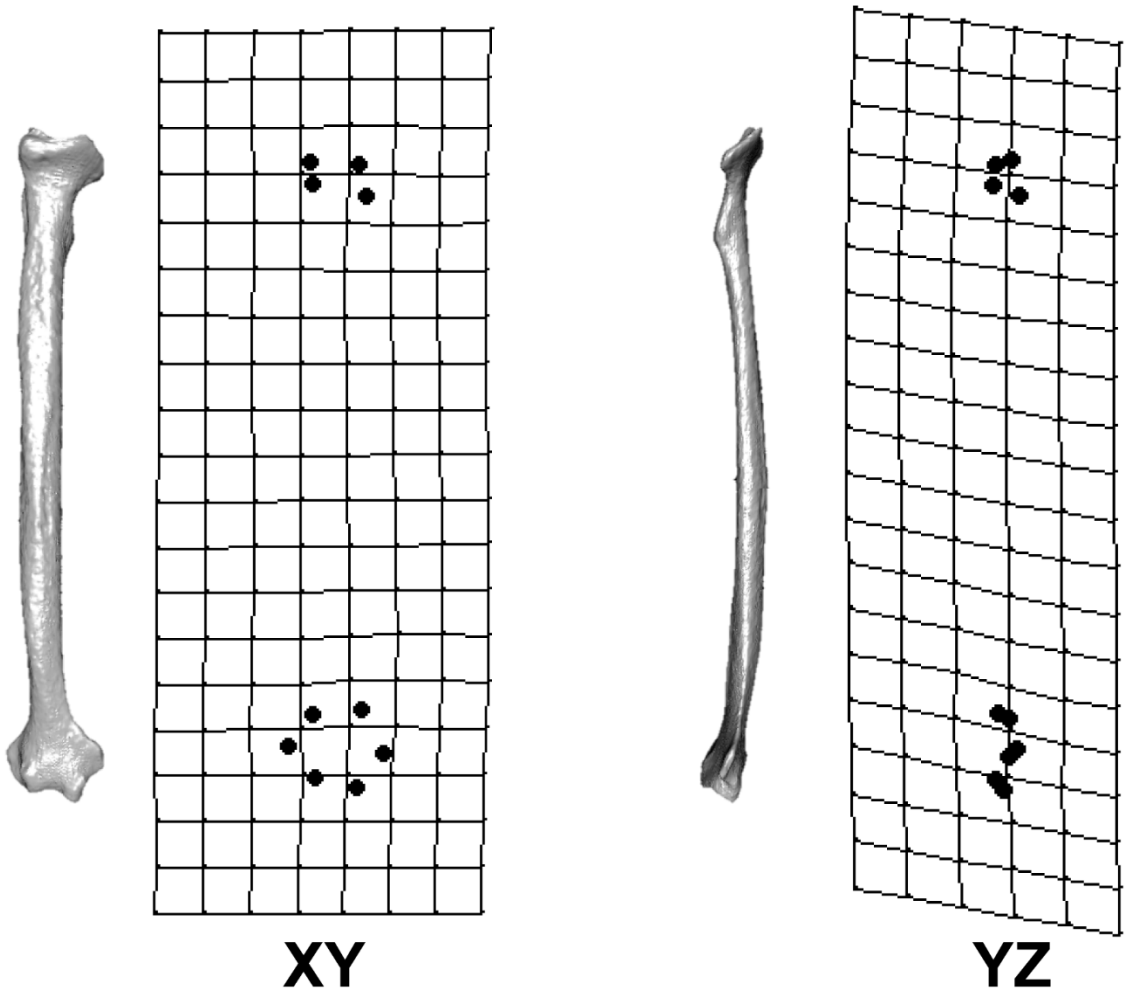

Figure S4. Thin plate spline of the radius of Broadleaf warped into Boreal in XY and YZ views. Surface model of the radius depicts the orientation of bone in each spline.

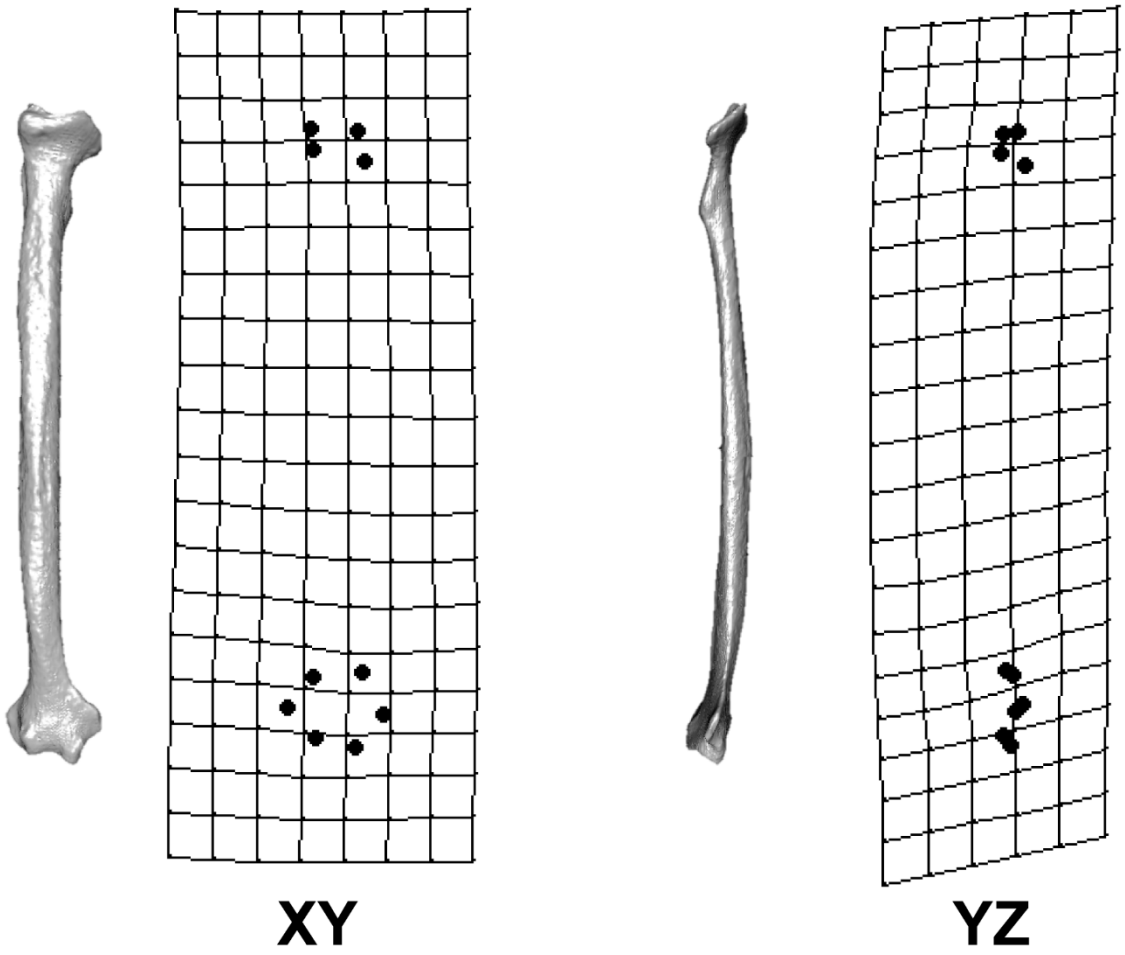

Figure S5. Thin plate spline of the radius of Coniferous warped into Boreal in XY and YZ views. Surface model of the radius depicts the orientation of bone in each spline.

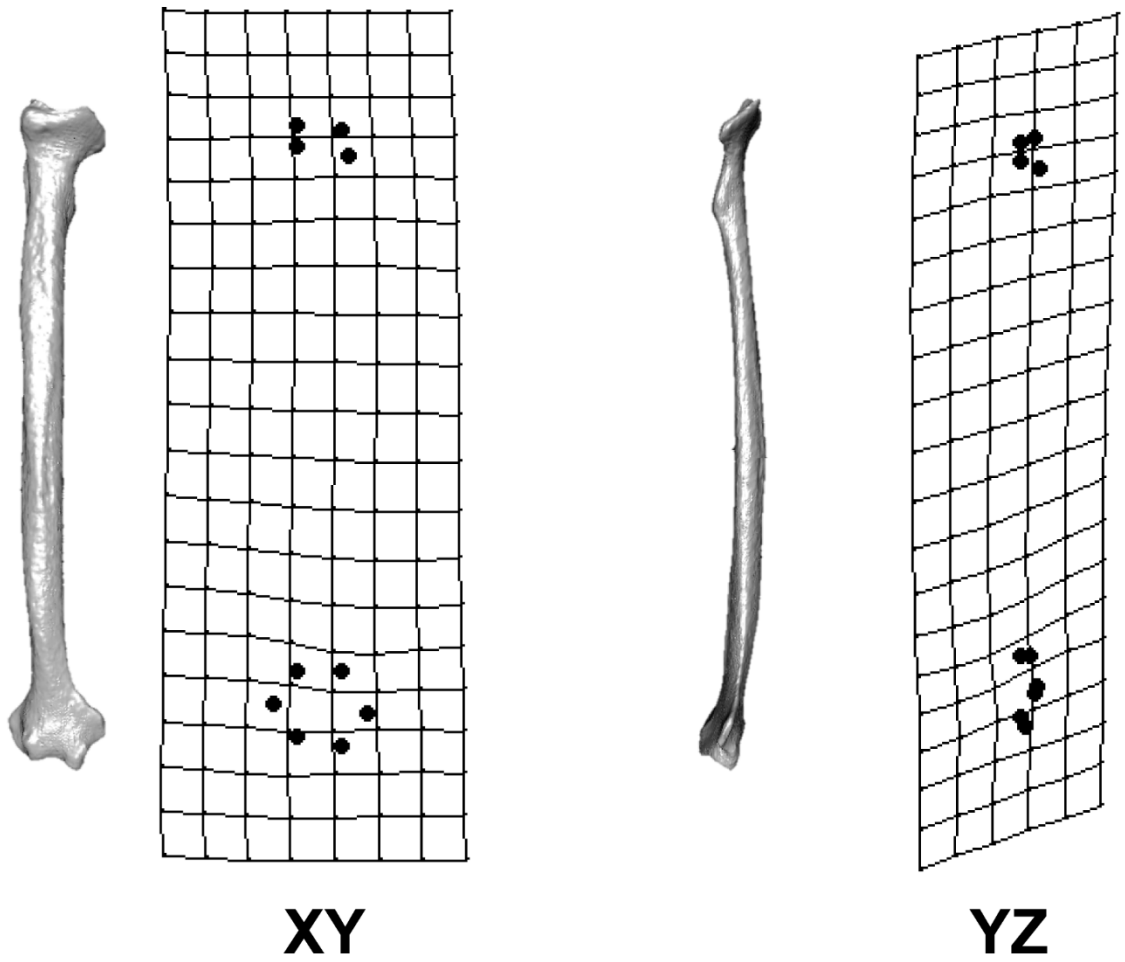

Figure S6. Thin plate spline of the radius of Coniferous warped into Broadleaf in XY and YZ views. Surface model of the radius depicts the orientation of bone in each spline.

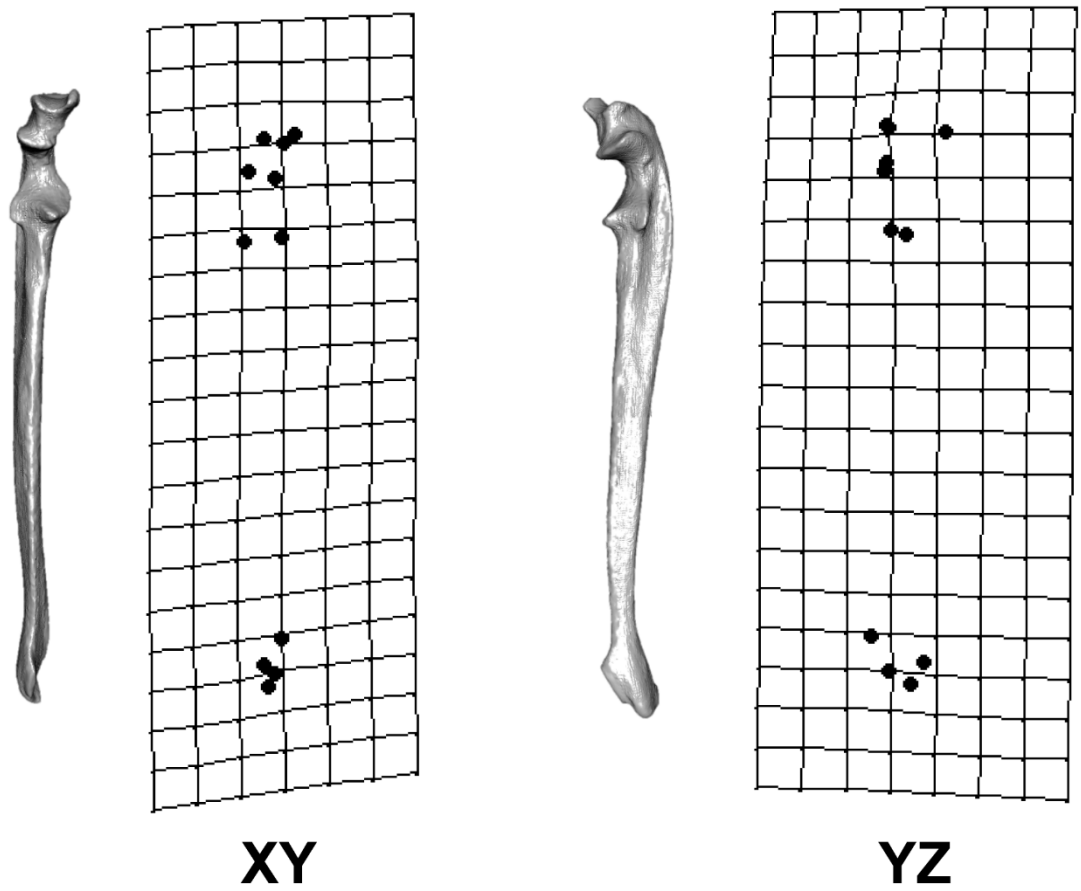

Figure S7. Thin plate spline of the ulna of Broadleaf warped into Boreal in XY and YZ views. Surface model of the ulna depicts the orientation of bone in each spline.

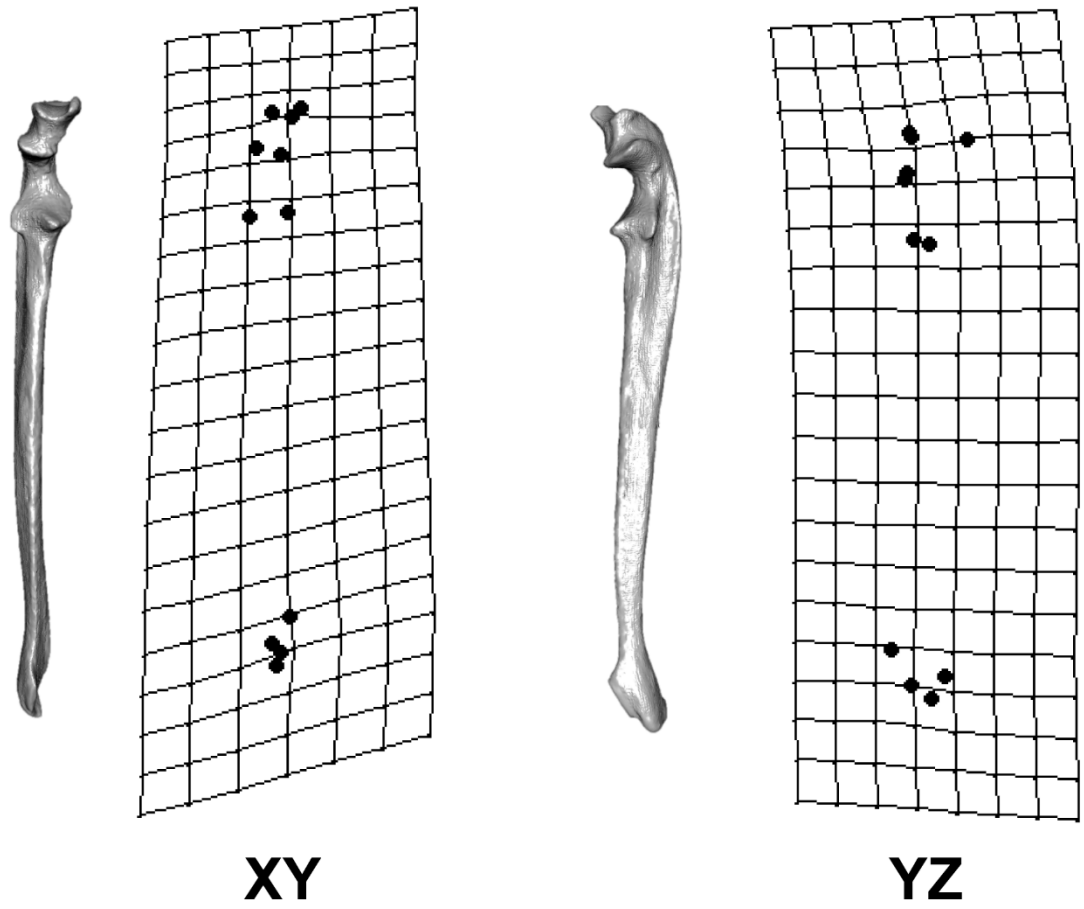

Figure S8. Thin plate spline of the ulna of Coniferous warped into Boreal in XY and YZ views. Surface model of the ulna depicts the orientation of bone in each spline.

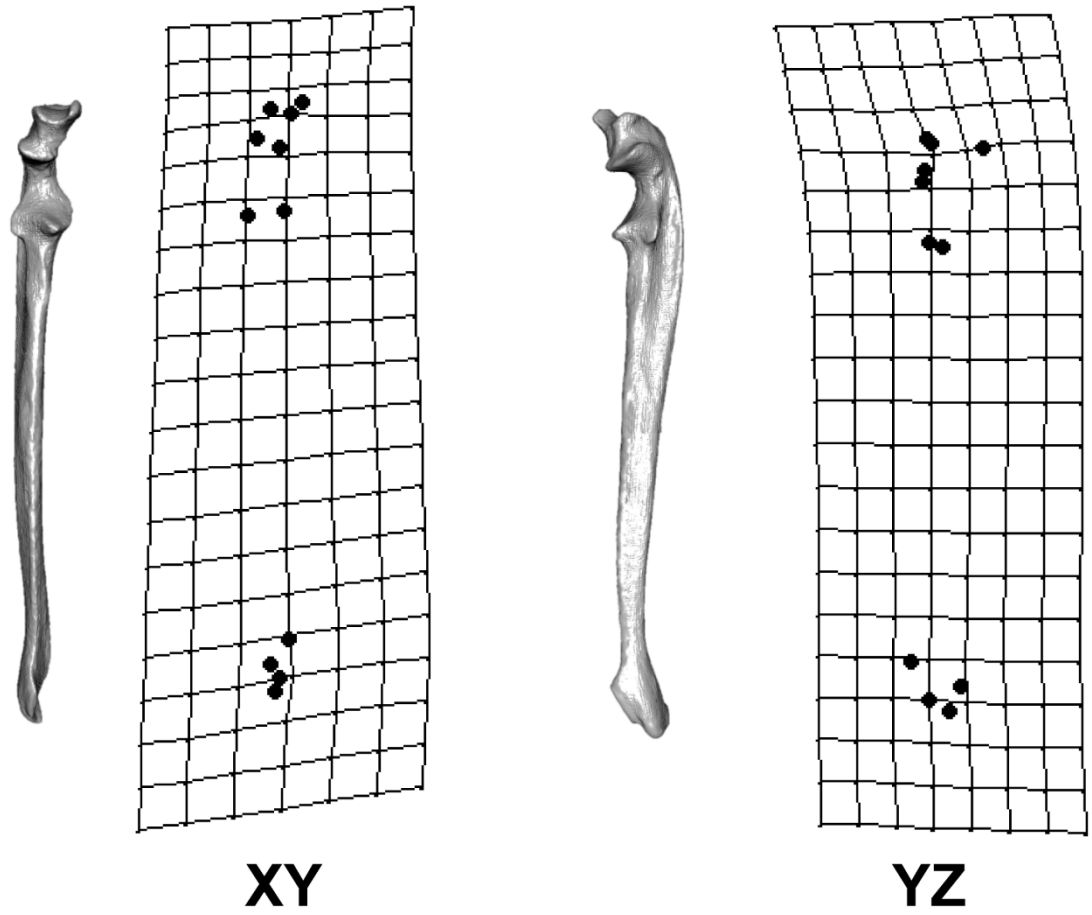

Figure S9. Thin plate spline of the ulna of Coniferous warped into Broadleaf in XY and YZ views. Surface model of the ulna depicts the orientation of bone in each spline.

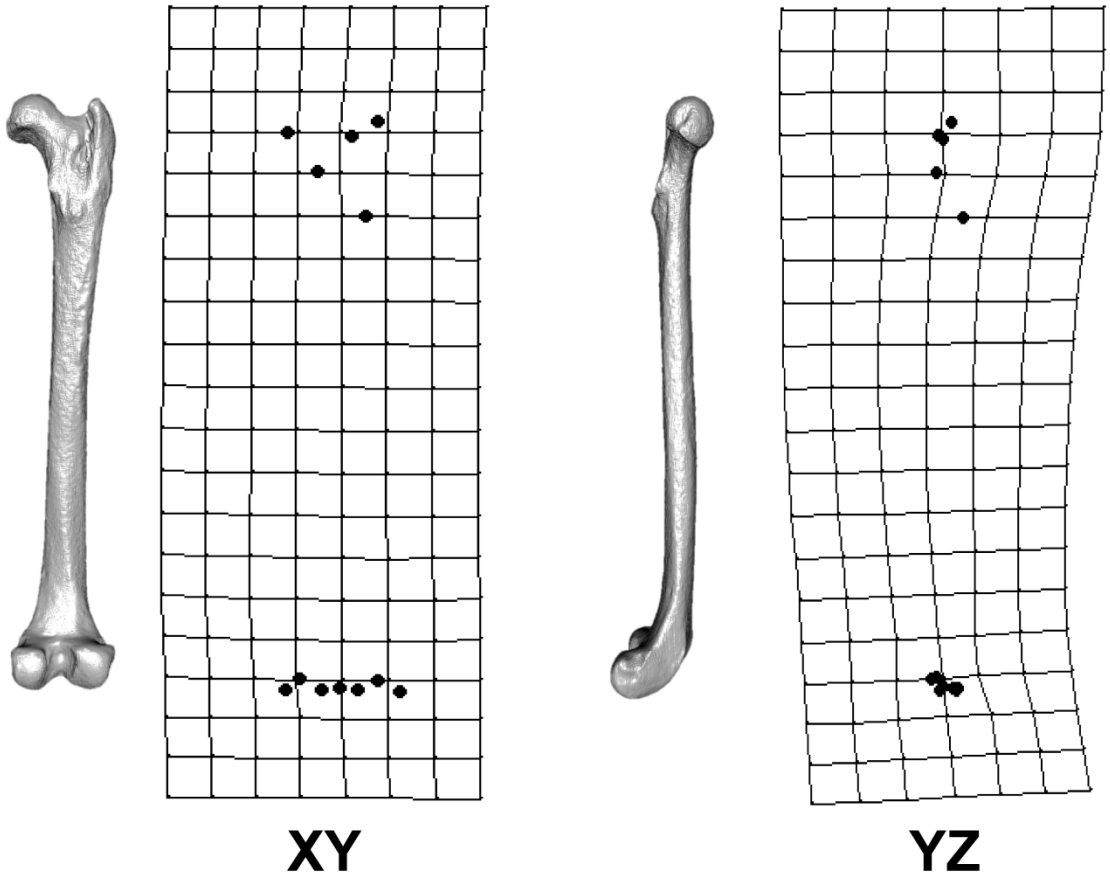

Figure S10. Thin plate spline of the femur of Broadleaf warped into Boreal in XY and YZ views. Surface model of the femur depicts the orientation of bone in each spline.

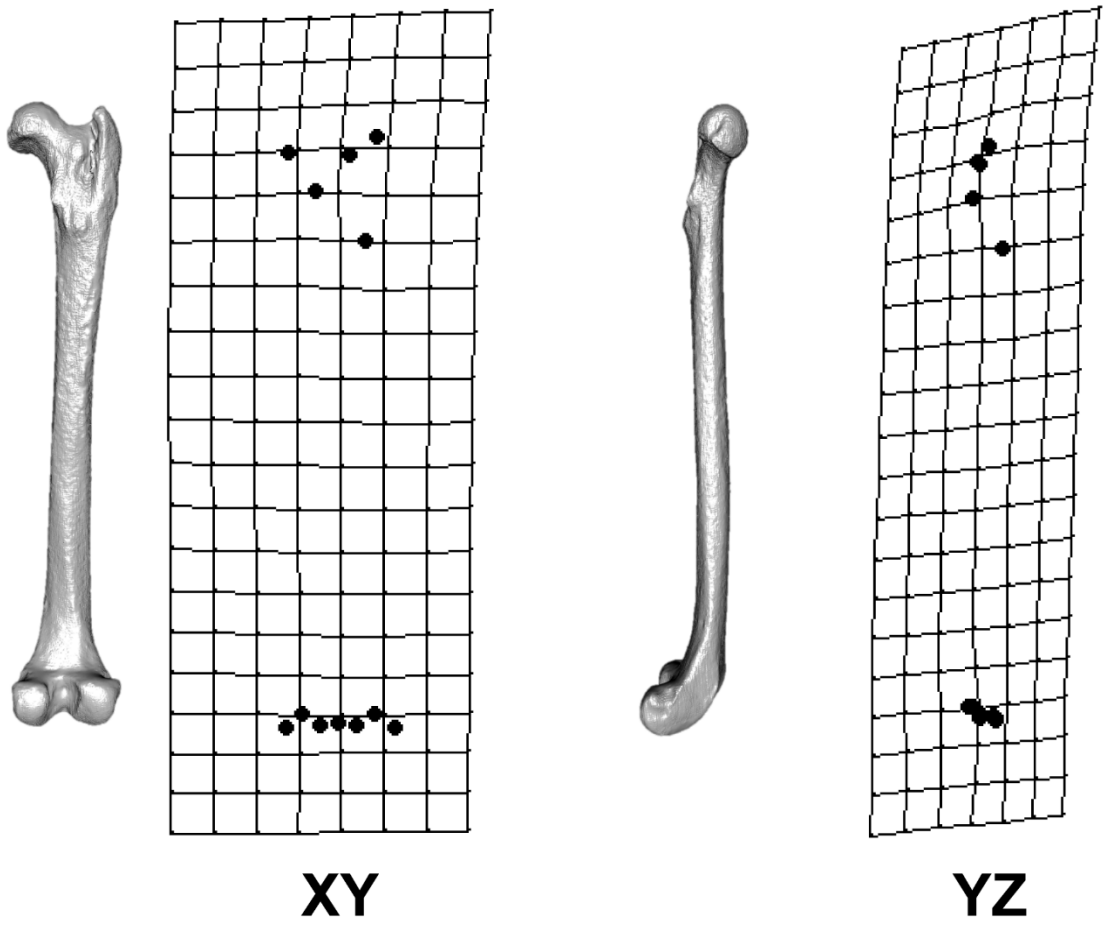

Figure S11. Thin plate spline of the femur of Coniferous warped into Boreal in XY and YZ views. Surface model of the femur depicts the orientation of bone in each spline.

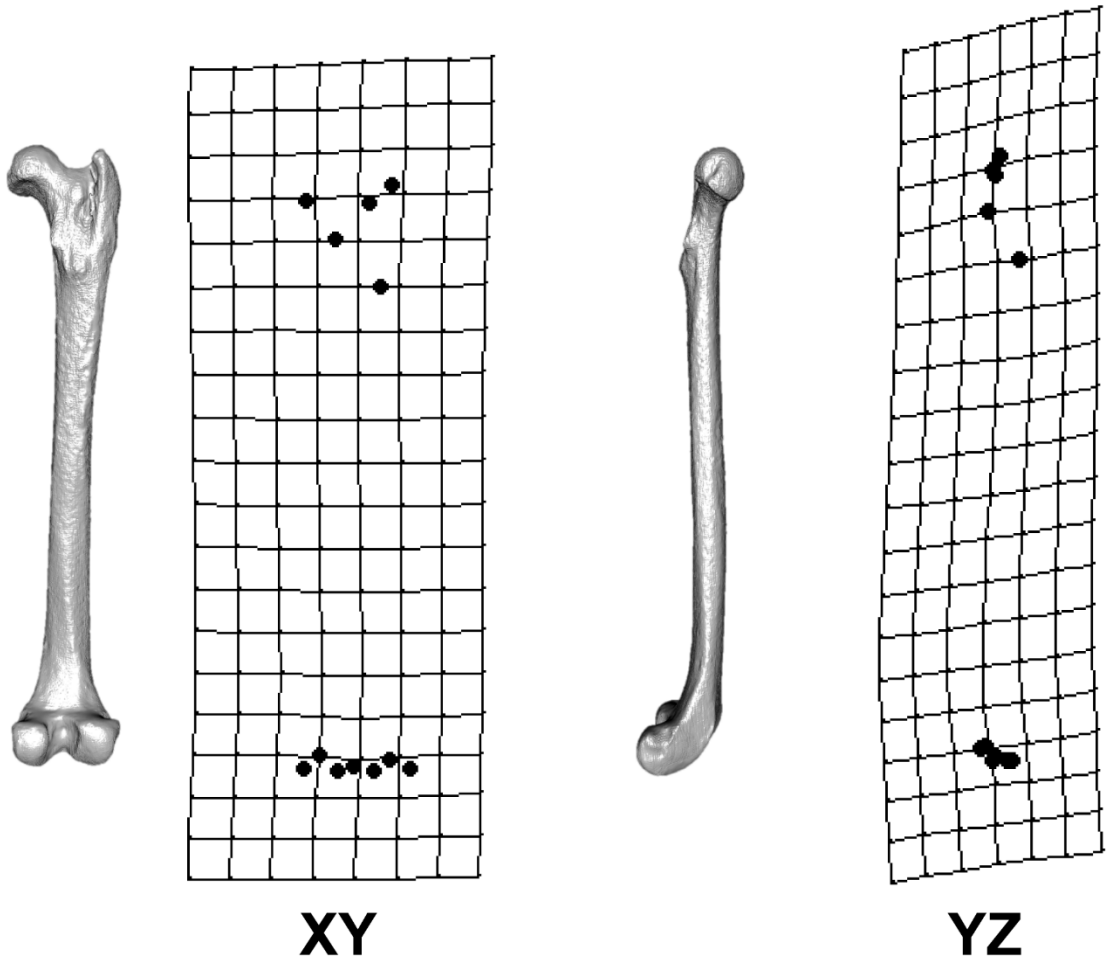

Figure S12. Thin plate spline of the femur of Coniferous warped into Broadleaf in XY and YZ views. Surface model of the femur depicts the orientation of bone in each spline.

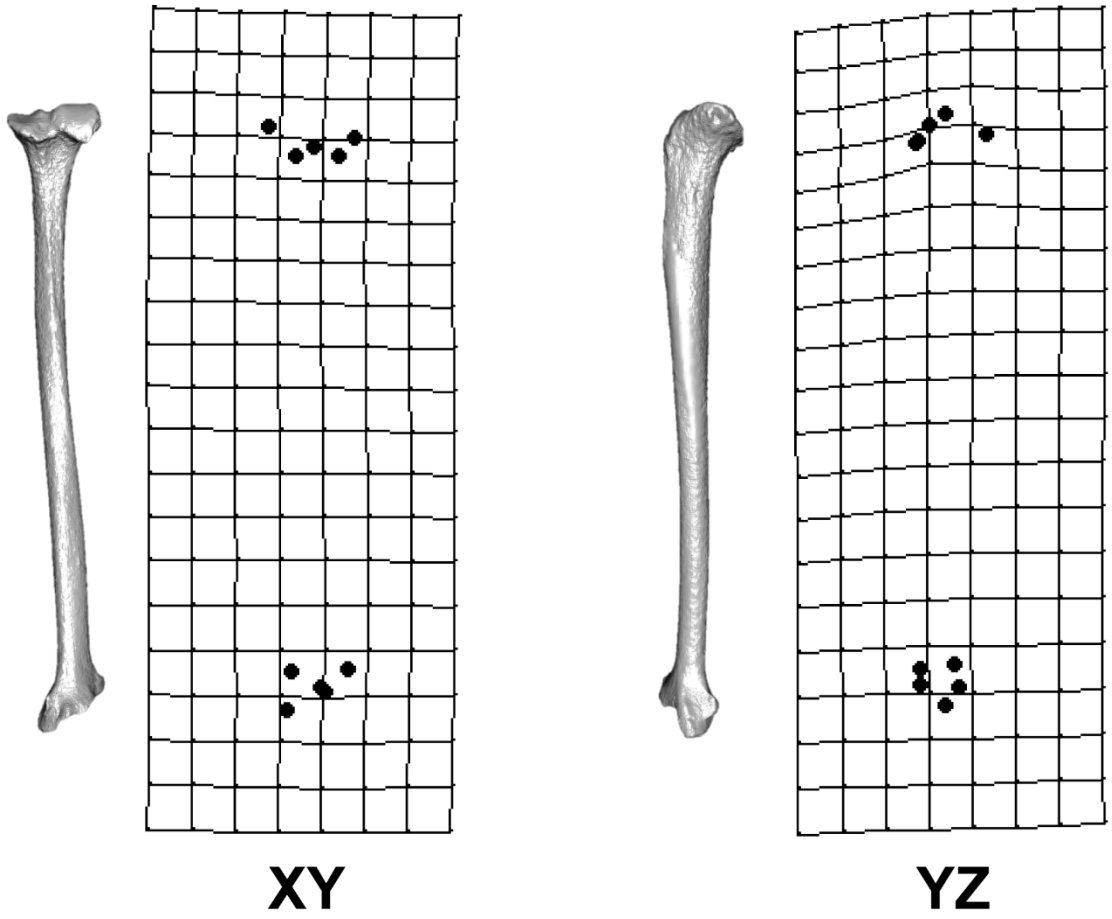

Figure S13. Thin plate spline of the tibia of Broadleaf warped into Boreal in XY and YZ views. Surface model of the tibia depicts the orientation of bone in each spline.

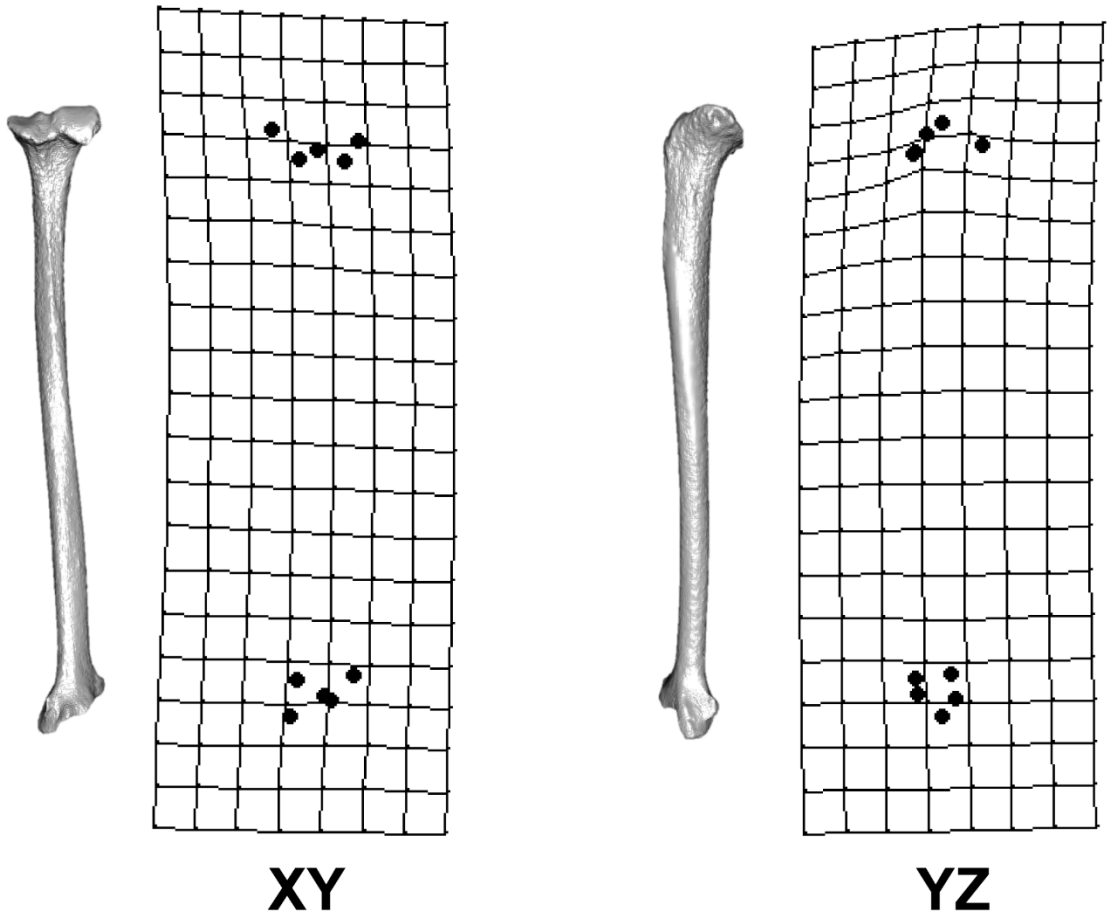

Figure S14. Thin plate spline of the tibia of Coniferous warped into Boreal in XY and YZ views. Surface model of the tibia depicts the orientation of bone in each spline.

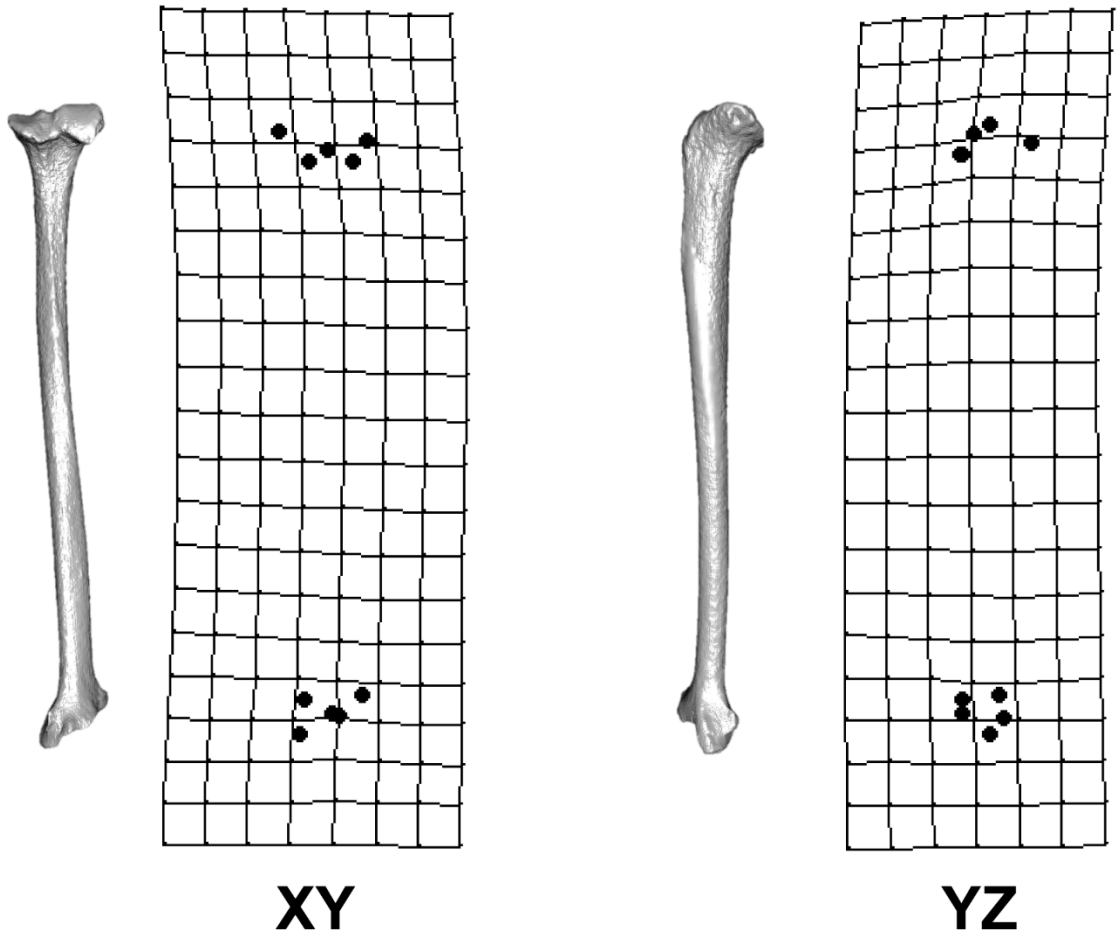

Figure S15. Thin plate spline of the tibia of Coniferous warped into Broadleaf in XY and YZ views. Surface model of the tibia depicts the orientation of bone in each spline.

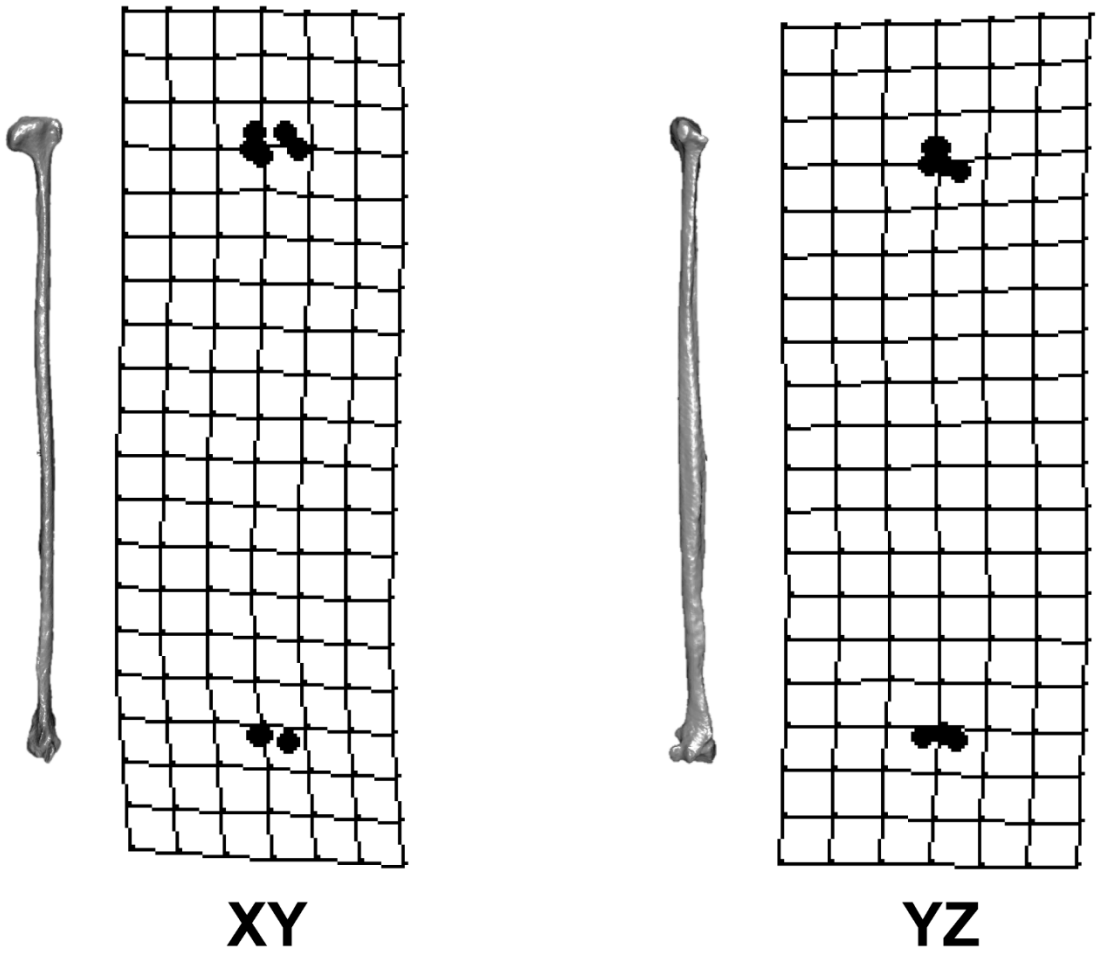

Figure S16. Thin plate spline of the fibula of Broadleaf warped into Boreal in XY and YZ views. Surface model of the fibula depicts the orientation of bone in each spline.

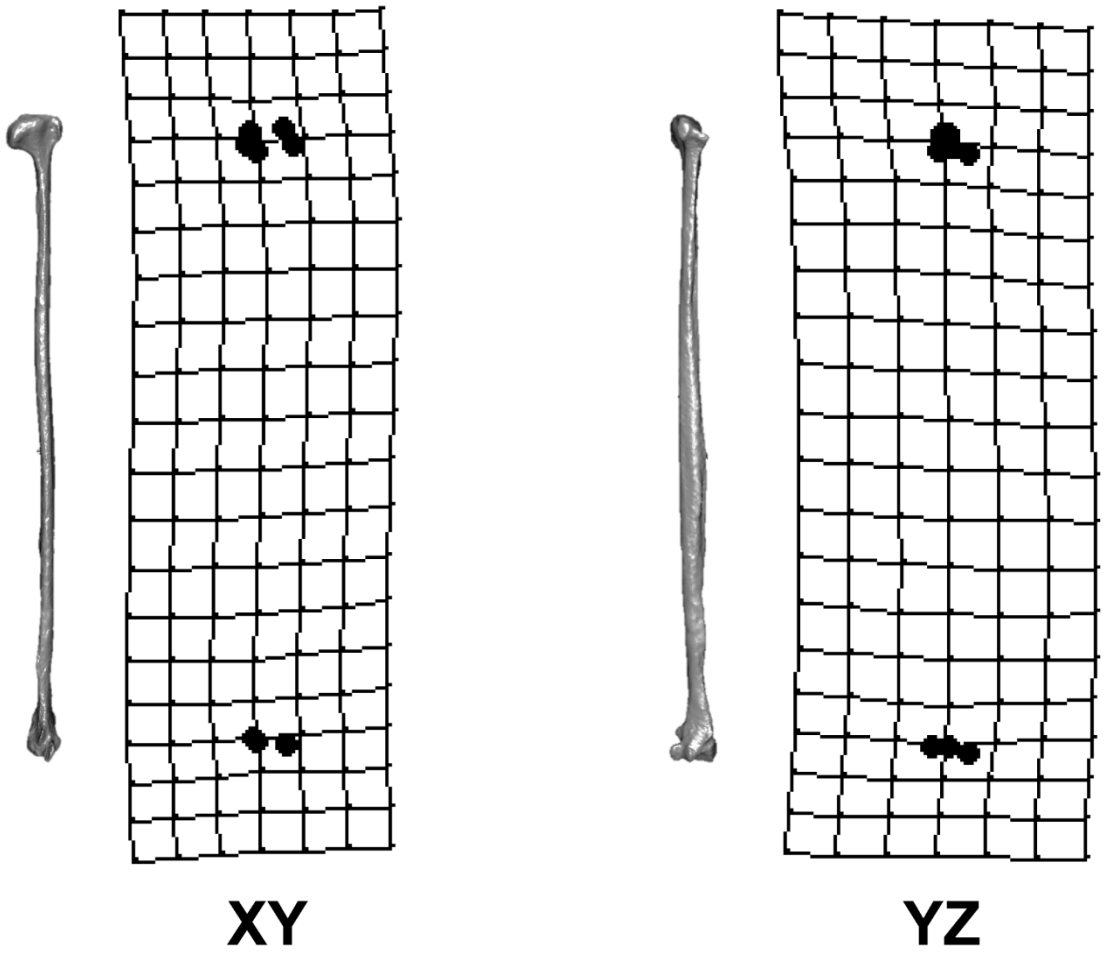

Figure S17. Thin plate spline of the fibula of Coniferous warped into Boreal in XY and YZ views. Surface model of the fibula depicts the orientation of bone in each spline.

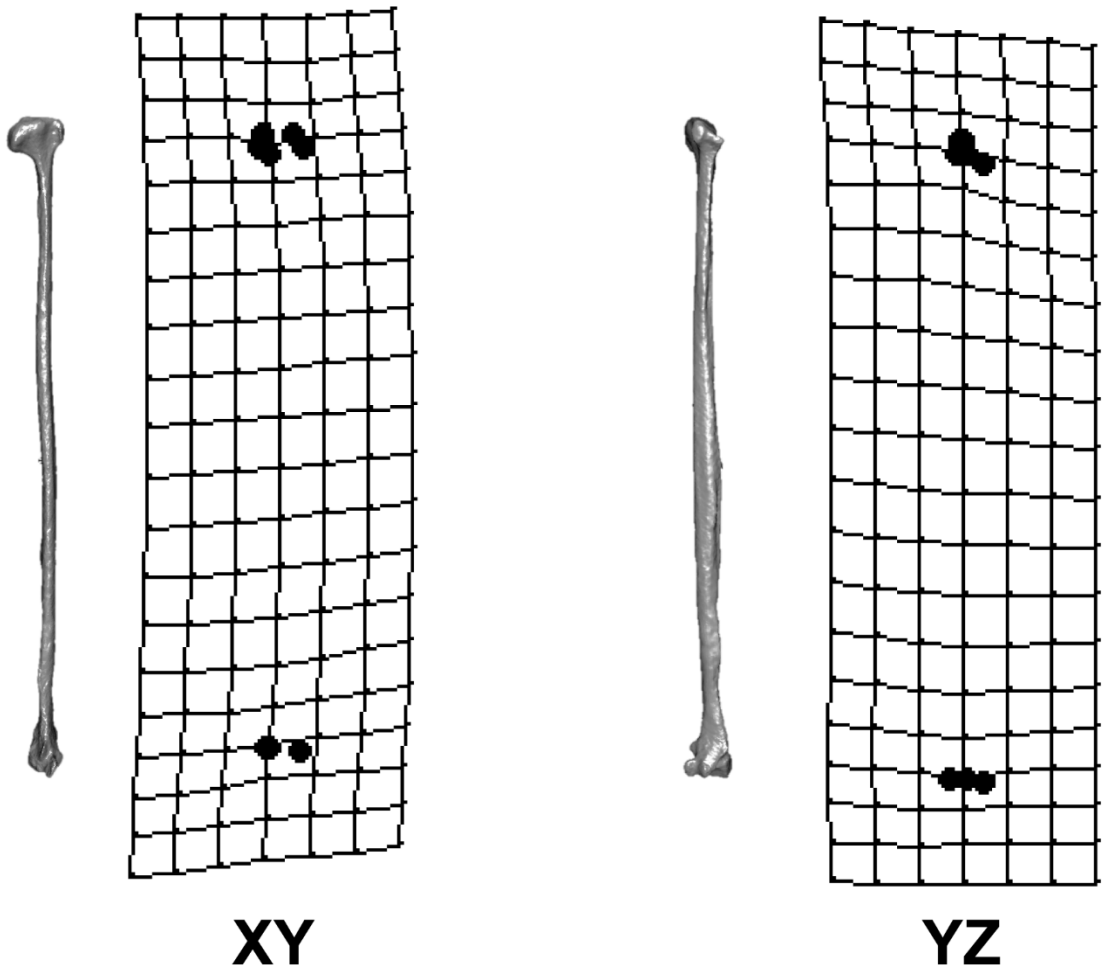

Figure S18. Thin plate spline of the fibula of Coniferous warped into Broadleaf in XY and YZ views. Surface model of the fibula depicts the orientation of bone in each spline.

E R Code for Landmark Alignment and PCA

```
install.packages("geomorph", dependecies=TRUE)

library(geomorph)

setwd("F:/research/Dissertation/Morpho/digitizer/geographic variation")


#read in data

mydata<-read.csv("ulna geographic.csv", header=TRUE, stringsAsFactors =
FALSE)#new file for each limb bone

mydata

specimen<- as.matrix(mydata[,1])

locality<- as.factor(mydata[,2])

biome<- as.factor(mydata[,3])

SKL<-as.matrix(mydata[,4])

coords<- as.matrix(mydata[, -c(1,2,3,4)])

p<- ncol(coords)/3

n<- length(specimen)

k<- 3

land<- arrayspecs(coords, p, k)

dim(land)

dimnames(land)[[3]]

dimnames(land)[[3]]<- rownames(mydata)

plotAllSpecimens(land, mean=FALSE) #plots raw landmarks


Y.gpa<- gpagen(land) #GPA alignment


#plot PCA

gp<- as.factor(paste(biome))
```

```
PCA<-plotTangentSpace(Y.gpa$coords, groups=gp, label = TRUE)

PCscore<-PCA$pc.scores

#must change file name each time

write.table(PCscore, file="ulna geographic PC")#writes as a space deliminated file for PAST



#warp 3D mesh

ply<-read.ply("ulna ETMNH 609.ply")#3D surface scan of bone

meshland<-digit.fixed(ply,11)#right click to place landmark, then confirm, number indicates how many landmarks

nmeshland

refmesh<-warpRefMesh(ply, meshland, ref, centered=TRUE)

plotspec(refmesh, ref, fixed=5, ptsize=1, centered=FALSE, shininess=128.0, specular=49)#plots the specimen with landmarks



#warp mean shape of each group into another

#Broadleaf indicated as TBM

#COniferous indicated as TCF

#Boreal indicated as BFT

coordinates<-Y.gpa$coords

TCF<-as.array(coordinates[,,c(6:13,28,29,38,39)])#will have to change for each specimen femur-6:13,28,29,38,39 radius-6:12,26,27,36,37 ulna-6:12,27,28,37,38 tibia-6:13,28,29,38,39, fibula-6:13,27:30

TBM<-as.array(coordinates[,,c(1:5,14:20,30:37)])#will have to change for each specimen femur-1:5,14:20,30:37 radius- 1:5,13:19,28:35 ulna- 1:5,13:19,29:36 tibia-1:5,14:20,30:37, fibula-1:5, 14:20, 31:38

BFT<-as.array(coordinates[,,c(21:27)])#will have to change for each specimen femur-21:27 radius-20:25 ulna-20:26 tibia-21:27, fibula- 21:26
```

```
TCFshape<-mshape(TCF)

TBMshape<-mshape(TBM)

BFTshape<-mshape(BFT)

#TCF to TBM

plotRefToTarget(TCFshape, TBMshape, method="TPS")#R plot window

warpRefMesh(ply, meshland, TCFshape, centered=TRUE)

warpRefMesh(ply, meshland, TBMshape, centered=TRUE)

#TCF to BFT

plotRefToTarget(TCFshape, BFTshape, method="TPS")#R plot window

warpRefMesh(ply, meshland, BFTshape, centered=TRUE)

#TBM to BFT

plotRefToTarget(TBMshape, BFTshape, method="TPS")#R plot window



################################################################################
######

########################## Calculate centroid
size#################################

#centroid size

Y.gpa$Csize #a vector of centroid size

centroid<- Y.gpa$Csize #a vector of centroid size

hist(centroid)

#must change file name each time

write.csv(centroid, file="fibula centroid.csv")
```

```
##########################################################################
######

############################## Is morphological variation due to
allometry?############

#allometry to centroid

gpadata<- Y.gpa$coords

geographyallom<- procD.allometry(gpadata~ log(centroid), iter=999) #multivariate
regression

geographyallom

plot(geographyallom, method="CAC")

plot(geographyallom, method="RegScore")

#allometry to Skull Length

SKLspec<-as.matrix(mydata[-c(12,14,26,29,38),4])#must change for each bone humerus-
12,14,27,31,38 femur-  fibula- 12,14,26,29,38, tibia- 12,14,27,31,38 radius-
11,13,25,29,36 ulna- 11,13,26,30,37

SKLcoords<- as.matrix(coords[-c(12,14,26,29,38),]) #must change for each bone, same
values as previous line

p<- ncol(SKLcoords)/3

n<- length(SKLspec)

k<- 3

SKLland<- arrayspecs(SKLcoords, p, k)

dim(SKLland)

dimnames(SKLland)[[3]]

dimnames(SKLland)[[3]]<- rownames(mydata)

plotAllSpecimens(SKLland, mean=FALSE)

SKL.gpa<- gpagen(SKLland)
```

```
SKLgpdata<-SKL.gpa$coords

geographyallomSKL<- procD.allometry(SKLgpdata~ SKLspec, iter=999) #multivariate regression

geographyallomSKL

plot(geographyallomSKL, method="CAC")

plot(geographyallomSKL, method="RegScore")
```

Appendix II- Chapter 3 Supplemental Files

A Sequences from GenBank

M. americana AF 154969.1, 154970.1, 154968.1, 057130.1, 448238.1, 268274.1, 154971.1, 154972.1, 154973.1, 154974.1, 448237.1, 154967.1, 268272.1, 268273.1, 154964.1, 154965.1, 154966.1; NC 020642; HM 106324.1; AY 121352.1, 121344.1, 121341.1, 121321.1, 121318.1, 448237.1, 121273.1, 121187.1, 121193.1, 121249.1, 121250.1, 121275.1, 121277.1, 121279.1, 121280.1; EU 873311.1, 873311.1, 873309.1, 87330831, 873307.1, 873304.1, 873303.1, 873302.1, 873301.1, 873300.1, 873299.1, 873298.1, 87329731, 873296.1, 873295.1, 873294.1, 873293.1, 873292.1, 873291.1, 873290.1, 873289.1, 873288.1, 873287.1; AB 051234.1

M. foina HM 106325.1

B Specimens sampled for DNA

UAMN (UAM) 24805, 101819, 22680, 22736, 101828, 47308, 24794, 24808, 22678, 59579, 101851; BMUW (UWBM) 81064, 81688, 81025, 81059; FMNH (UF) 31427, 31328; NYSM (NY) 14388, 14242, 14387, 14241, USNM 600580, 600583, 592896, 592895, 592316, 600581, 600579, 600584

C Specimens from which sequences were provided

MSB 197115, 196581

University of Alaska Museum of the North (UAMN)
Burke Museum of Natural History and Culture (BMUW)
Florida Museum of Natural History (FMNH)
New York State Museum (NYSM)
Smithsonian Institution National Museum of Natural History (USNM)
Museum of Southwestern Biology (MSB)

D Supplemental Tables

Table 1. Sample Weight and DNA Concentration After Elution

Specimen #	Tissue Weight (g)	DNA Concentration (ng/µL)
USNM 600581	0.025	9.2
USNM 600579	0.025	13.7
USNM 592896	0.025	4.6
USNM 600580	0.025	25.5
USNM 592895	0.025	25.6
USNM 600584	0.025	8.6
USNM 592316	0.025	12.5
USNM 600583	0.025	14.8
UAMN 101819	0.025	23.4
UAMN 101828	0.025	10.5
UAMN 101851	0.025	21.3
UAMN 24805	0.025	28.9
UAMN 22680	0.025	45.8
UAMN 22736	0.025	29.3
UAMN 47308	0.025	35.8
UAMN 24794	0.025	15.2
UAMN 24808	0.025	29.7
UAMN 22678	0.025	52.7
UAMN 59579	0.025	17.2
FMNH 31427	0.025	26.0
FMNH 31328	0.025	27.0
NYSM 14242	0.025	23.9
NYSM 14387	0.025	22.7
NYSM 14241	0.025	44.7
NYSM 14388	0.025	26.1
BMUW 81688	0.025	25.1
BMUW 81025	0.025	21.0
BMUW 81064	0.025	27.2
BMUW 81059	0.025	55.3

Appendix III- Chapter 4 Supplemental Files

A Specimens sampled for DNA

FMNH (UF) 31427, 31328; BMUW (UWBM) 81025, 81688, 81064, 81059; ETMNH 600,603, 607,608,609; NYSM (NY)14388, 14242, 14241, 14387; USNM 600580, 600583, 592896, 600579, 592316, 600581, 600584, 592895; UAMN (UAM) 59579, 101828, 101819, 101851; UMMZ (MZ) 177697, 177826, 177827

B Specimens from which sequences were provided

MSB 196581

C Sequences from GenBank

M. foina HM 106325.1

Museum of Southwestern Biology (MSB)
Florida Museum of Natural History (FMNH)
Burke Museum of Natural History and Culture (BMUW)
East Tennessee State Museum of Natural History (ETMNH)
New York State Museum (NYSM)
Smithsonian Institution National Museum of Natural History (USNM)
University of Alaska Museum of the North (UAMN)
University of Michigan Museum of Zoology (UMMZ)

D Supplemental Tables

Table 1. Sample Weight and DNA Quantity After Elution

Specimen #	Tissue Weight (g)	DNA Quantity (ng/µL)
USNM 600581	0.025	9.2
USNM 600583	0.025	14.8
USNM 600579	0.025	13.7
USNM 592896	0.025	4.6
USNM 600580	0.025	25.5
USNM 592895	0.025	25.6
USNM 600584	0.025	8.6
USNM 592316	0.025	12.5
UAMN 101819	0.025	23.4
UAMN 101828	0.025	10.5
UAMN 101851	0.025	21.3
UAMN 59579	0.025	17.2
FMNH 31427	0.025	26.0
FMNH 31328	0.025	27.0
NYSM 14242	0.025	23.9
NYSM 14387	0.025	22.7
NYSM 14241	0.025	44.7
NYSM 14388	0.025	26.1
BMUW 81688	0.025	25.1
BMUW 81025	0.025	21.0
BMUW 81064	0.025	27.2
BMUW 81059	0.025	55.3
ETMNH 603	0.045	4.3
ETMNH 608	0.037	8.3
ETMNH 607	0.116	6.9
ETMNH 609	0.033	8.0
ETMNH 600	0.032	4.8
UMMZ 177697	0.052	20.3
UMMZ 177826	0.052	6.6
UMMZ 177827	0.086	18.1

Table 2. Polymorphic Sites in the Concatenated Sequence

Specimen	**9**	**10**	**11**	**12**	**14**	**16**	**17**	**36**	**37**	**38**	**42**	**48**	**50**	**69**	**115**
M. foina	T	A	C	A	C	A	C	A	A	C	C	C	G	T	G
MSB 196581	C	·	·	G	·	T	·	·	·	·	A	·	·	·	A
BMUW 81025	–	–	–	–	–	–	–	–	–	–	–	·	·	K	A
NMNH 600581	–	–	–	–	–	–	–	–	–	–	–	–	–	–	–
NMNH 592895	C	·	Y	G	·	T	·	·	·	·	G	A	·	·	A
UAMN 59579	C	·	·	G	·	T	·	·	·	·	G	A	·	·	A
NYSM 14241	C	·	·	G	·	T	·	·	·	·	G	A	·	·	A
BMUW 81688	C	·	·	G	·	T	·	·	·	·	A	·	·	·	A
USNM 592316	C	·	·	G	·	T	·	·	·	·	G	A	S	·	A
FMNH 31427	–	–	–	–	–	–	–	·	·	·	A	·	·	·	A
UAMN 101819	C	·	·	G	·	T	·	·	·	·	G	A	·	·	A
NYSM 14242	C	·	·	·	·	C	·	T	T	T	G	A	·	·	A
FMNH 31328	C	W	Y	G	Y	T	Y	·	·	·	G	A	·	·	A
NYSM 14388	C	·	·	·	·	C	·	·	·	·	G	A	·	·	–
NMNH 600580	–	–	–	–	–	–	–	–	–	–	–	–	–	–	–
NMNH 600579	–	–	–	–	–	–	–	–	–	–	–	–	–	–	–
NMNH 600583	–	–	–	–	–	–	–	–	–	–	–	–	–	–	–
NMNH 592896	–	–	–	–	–	–	–	–	–	–	–	–	–	–	–
UAMN 101851	–	–	–	–	–	–	–	–	–	–	–	–	–	–	–

*– indicates no nucleotide at that position, · indicates no difference from *M. foina*

* some nucleotides are ambiguous and are represented by M (A or C), K (G or T), W (A or T), Y (C or T), R (A or G), or D (A, G, or T) based on IUPAC designations

Table 2 continued

Specimen	118	134	138	148	151	156	177	187	197	198	204	206	215	217	218
M. foina	T	A	C	G	C	T	C	A	G	A	A	C	C	A	G
MSB 196581	C	·	T	A	·	·	T	·	A	·	C	·	·	·	·
BMUW 81025	C	·	T	A	·	·	T	·	A	·	C	·	·	·	·
NMNH 600581	–	–	–	–	–	–	–	–	–	–	–	–	–	–	–
NMNH 592895	C	R	A	A	·	K	T	–	–	–	–	–	–	–	–
UAMN 59579	C	·	A	A	·	·	T	·	A	·	C	T	·	·	·
NYSM 14241	C	·	A	A	·	·	T	·	A	·	C	T	·	·	·
BMUW 81688	C	·	T	A	·	·	T	·	A	·	C	·	·	·	·
USNM 592316	C	·	A	A	·	·	T	T	A	·	C	T	·	·	·
FMNH 31427	C	·	T	A	·	·	T	·	A	·	C	·	·	·	–
UAMN 101819	C	·	A	A	·	·	T	·	A	·	C	T	·	·	·
NYSM 14242	C	·	A	A	G	·	T	·	A	·	C	T	T	–	A
FMNH 31328	C	·	A	A	·	·	T	·	A	R	C	K	·	R	·
NYSM 14388	–	–	–	–	–	–	–	–	–	–	–	–	–	–	–
NMNH 600580	–	–	–	–	–	–	–	–	–	–	–	–	–	–	–
NMNH 600579	–	–	–	–	–	–	–	–	–	–	–	–	–	–	–
NMNH 600583	–	–	–	–	–	–	–	–	–	–	–	–	–	–	–
NMNH 592896	–	–	–	–	–	–	–	–	–	–	–	–	–	–	–
UAMN 101851	–	–	–	–	–	–	–	–	–	–	–	–	–	–	–

*– indicates no nucleotide at that position, · indicates no difference from *M. foina*

* some nucleotides are ambiguous and are represented by M (A or C), K (G or T), W (A or T), Y (C or T), R (A or G), or D (A, G, or T) based on IUPAC designations

Table 2 continued

Specimen	**219**	**220**	**221**	**222**	**232**	**234**	**235**	**236**	**275**	**284**	**285**	**286**	**290**	**294**	**295**
M. foina	A	C	G	A	G	G	C	A	A	G	C	A	A	G	T
MSB 196581	·	·	·	·	·	·	·	·	·	·	·	·	·	·	·
BMUW 81025	·	·	·	·	·	·	·	·	·	·	·	·	·	·	·
NMNH 600581	–	–	–	–	·	·	·	·	·	·	·	·	·	·	·
NMNH 592895	–	–	–	–	·	K	·	·	·	·	·	·	·	·	·
UAMN 59579	·	·	·	G	·	·	·	·	·	·	·	·	·	·	·
NYSM 14241	·	·	·	·	·	T	·	·	·	·	·	·	·	·	·
BMUW 81688	·	·	·	G	·	·	·	·	·	·	·	·	·	·	·
USNM 592316	R	S	·	·	·	·	·	·	·	·	·	·	·	·	·
FMNH 31427	–	–	–	–	–	–	–	–	W	K	Y	R	R	R	K
UAMN 101819	·	·	A	·	K	·	·	·	·	·	·	·	·	·	·
NYSM 14242	T	T	T	T	T	T	T	·	·	·	·	·	·	·	·
FMNH 31328	·	·	·	·	·	T	T	·	·	·	·	·	·	·	·
NYSM 14388	–	–	–	–	–	–	–	–	–	–	–	–	–	–	–
NMNH 600580	–	–	–	–	·	·	·	·	·	·	·	·	·	·	·
NMNH 600579	–	–	–	–	·	·	·	W	·	·	·	·	·	·	·
NMNH 600583	–	–	–	–	–	–	–	–	·	·	·	·	·	·	·
NMNH 592896	–	–	–	–	–	–	–	–	·	·	·	·	·	·	·
UAMN 101851	–	–	–	–	–	–	–	–	–	–	–	–	–	–	–

*– indicates no nucleotide at that position, · indicates no difference from *M. foina*

* some nucleotides are ambiguous and are represented by M (A or C), K (G or T), W (A or T), Y (C or T), R (A or G), or D (A, G, or T) based on IUPAC designations

Table 2 continued

Specimen	297	300	301	302	304	318	342	344	350	367	379	380	389	404	431
M. foina	A	A	G	C	T	A	C	C	G	G	A	A	T	G	G
MSB 196581	·	·	·	·	·	·	T	T	A	A	–	–	·	·	A
BMUW 81025	·	·	·	·	·	·	T	T	A	A	·	–	·	·	A
NMNH 600581	·	·	·	·	·	·	T	T	A	A	–	–	·	·	A
NMNH 592895	·	·	·	·	·	·	T	T	A	A	–	–	·	·	A
UAMN 59579	·	·	·	·	·	·	T	T	A	A	–	–	·	A	A
NYSM 14241	·	·	·	·	·	·	T	T	A	A	–	–	·	·	A
BMUW 81688	·	·	·	·	·	·	T	T	A	A	·	–	·	·	A
USNM 592316	·	·	·	·	·	·	T	T	A	A	–	–	·	·	A
FMNH 31427	W	·	·	M	Y	R	T	T	A	A	–	–	K	·	A
UAMN 101819	·	·	·	·	·	·	T	T	A	A	–	–	·	–	–
NYSM 14242	·	·	·	·	·	·	T	T	A	A	–	–	·	·	A
FMNH 31328	·	·	·	·	·	·	T	T	A	A	–	–	·	·	A
NYSM 14388	–	–	–	–	–	–	–	–	–	–	–	–	–	–	–
NMNH 600580	·	·	·	·	·	·	T	T	A	A	–	–	·	·	A
NMNH 600579	·	G	C	·	·	·	T	T	A	A	–	–	·	·	A
NMNH 600583	·	·	·	·	·	·	T	T	A	A	–	–	·	·	A
NMNH 592896	·	·	·	·	·	·	T	T	A	A	–	–	·	·	A
UAMN 101851	–	–	–	–	–	–	–	–	–	–	–	–	–	–	–

*– indicates no nucleotide at that position, · indicates no difference from *M. foina*

* some nucleotides are ambiguous and are represented by M (A or C), K (G or T), W (A or T), Y (C or T), R (A or G), or D (A, G, or T) based on IUPAC designations

Table 2 continued

Specimen	**433**	**434**	**435**	**437**	**439**	**446**	**448**	**459**	**468**	**475**	**476**	**477**	**479**	**480**	**483**
M. foina	G	G	A	A	A	C	T	T	C	A	T	A	C	C	T
MSB 196581	·	·	·	·	·	·	·	·	·	·	·	G	·	·	·
BMUW 81025	·	·	·	·	·	·	·	·	·	·	·	G	·	·	·
NMNH 600581	·	·	·	·	·	–	–	–	–	–	–	–	–	–	–
NMNH 592895	·	·	·	·	·	·	·	–	–	–	–	–	–	–	–
UAMN 59579	·	·	·	·	·	·	·	·	·	·	·	G	·	·	·
NYSM 14241	·	·	·	·	·	·	·	C	·	·	·	G	·	·	·
BMUW 81688	·	·	·	·	·	·	·	·	·	·	Y	G	·	·	·
USNM 592316	·	·	·	·	·	G	A	·	·	·	·	Y	·	·	·
FMNH 31427	·	·	·	T	–	–	–	·	·	·	·	G	·	·	·
UAMN 101819	–	–	–	–	–	–	–	·	·	·	–	G	·	·	·
NYSM 14242	C	C	T	·	G	–	–	·	·	·	·	G	·	·	·
FMNH 31328	·	·	·	·	–	–	–	–	–	T	·	G	T	T	–
NYSM 14388	–	–	–	–	–	–	–	–	–	–	–	–	–	–	–
NMNH 600580	·	·	·	·	·	·	·	·	·	·	·	G	·	·	·
NMNH 600579	·	·	·	·	·	–	–	·	·	·	·	G	·	·	·
NMNH 600583	·	·	·	·	·	·	·	·	·	M	C	R	·	·	M
NMNH 592896	·	·	·	·	·	–	–	–	–	·	·	G	·	·	·
UAMN 101851	–	–	–	–	–	–	–	·	·	·	·	G	·	·	·

*– indicates no nucleotide at that position, · indicates no difference from *M. foina*

* some nucleotides are ambiguous and are represented by M (A or C), K (G or T), W (A or T), Y (C or T), R (A or G), or D (A, G, or T) based on IUPAC designations

Table 2 continued

Specimen	484	486	492	494	495	496	497	510	511	513	515	518	525	534	556
M. foina	G	T	A	A	A	T	A	–	T	A	C	T	C	T	T
MSB 196581	·	·	·	·	·	C	·	A	C	·	T	·	T	C	C
BMUW 81025	·	·	·	·	·	C	·	A	C	·	T	·	T	C	C
NMNH 600581	–	–	–	–	–	–	–	–	–	–	–	–	–	–	–
NMNH 592895	–	–	–	–	–	–	–	–	–	–	–	–	–	–	–
UAMN 59579	·	·	·	·	·	C	·	A	C	·	T	·	T	C	C
NYSM 14241	·	·	·	·	·	C	·	A	C	·	T	·	T	C	C
BMUW 81688	·	·	·	·	·	C	·	A	C	·	T	·	T	C	C
USNM 592316	·	·	·	·	·	C	·	A	C	·	T	·	T	C	C
FMNH 31427	·	·	·	·	·	C	·	A	C	·	T	·	T	C	C
UAMN 101819	·	·	·	·	·	C	·	A	C	·	T	·	T	C	C
NYSM 14242	·	·	·	·	·	C	·	A	C	·	T	·	T	C	C
FMNH 31328	·	·	M	·	M	C	M	A	C	M	T	·	T	C	C
NYSM 14388	–	–	·	C	·	A	C	A	C	·	T	·	T	C	C
NMNH 600580	·	·	·	·	·	C	·	A	C	·	T	·	T	C	C
NMNH 600579	·	·	·	·	·	C	·	A	C	·	T	·	T	C	C
NMNH 600583	M	K	·	·	·	C	·	A	C	·	M	M	T	C	C
NMNH 592896	·	·	·	·	·	C	·	A	C	·	T	·	T	C	C
UAMN 101851	·	·	·	·	·	C	·	A	C	·	T	·	T	C	C

*– indicates no nucleotide at that position, · indicates no difference from *M. foina*

* some nucleotides are ambiguous and are represented by M (A or C), K (G or T), W (A or T), Y (C or T), R (A or G), or D (A, G, or T) based on IUPAC designations

Table 2 continued

Specimen	563	644	676	743	754	757	805	806	807	808	809	810	824	827	829
M. foina	C	C	C	–	C	C	T	C	C	C	C	G	G	T	C
MSB 196581	T	T	T	–	T	·	C	·	·	·	·	·	A	A	T
BMUW 81025	T	T	–	A	T	·	C	·	·	·	·	·	A	A	T
NMNH 600581	–	–	–	–	–	–	–	–	–	–	–	–	–	–	–
NMNH 592895	–	–	–	–	–	–	–	–	–	–	–	–	–	–	–
UAMN 59579	T	T	T	–	T	·	C	·	·	·	·	·	A	G	T
NYSM 14241	T	T	T	–	T	·	C	·	·	·	·	·	A	G	T
BMUW 81688	T	T	T	–	T	·	C	·	·	·	·	·	A	A	T
USNM 592316	T	T	T	–	T	·	C	·	·	·	·	·	A	G	T
FMNH 31427	T	T	T	–	T	·	C	·	·	·	·	·	A	A	T
UAMN 101819	T	T	T	–	T	·	C	·	·	·	·	·	A	G	T
NYSM 14242	T	T	T	–	T	·	C	·	·	·	·	·	A	G	T
FMNH 31328	T	T	T	–	T	·	Y	Y	Y	Y	Y	K	A	G	T
NYSM 14388	T	T	T	–	T	G	C	·	·	·	·	·	A	G	T
NMNH 600580	T	T	T	–	T	·	C	·	·	·	·	·	A	G	T
NMNH 600579	T	T	T	–	T	·	C	·	·	·	·	·	A	G	T
NMNH 600583	T	T	T	–	T	·	C	·	·	·	·	·	A	G	T
NMNH 592896	T	T	T	–	T	·	C	·	·	·	·	·	A	G	T
UAMN 101851	T	T	T	–	T	·	C	·	·	·	·	·	A	G	T

*– indicates no nucleotide at that position, · indicates no difference from *M. foina*

* some nucleotides are ambiguous and are represented by M (A or C), K (G or T), W (A or T), Y (C or T), R (A or G), or D (A, G, or T) based on IUPAC designations

Table 2 continued

Specimen	**833**	**859**	**880**	**881**	**898**	**899**	**903**	**909**	**910**	**923**	**924**	**961**	**984**	**990**	**1014**
M. foina	T	C	A	T	C	A	T	G	A	A	G	A	T	A	C
MSB 196581	·	T	G	A	·	·	C	A	G	G	·	·	C	T	T
BMUW 81025	·	T	G	A	·	·	C	A	G	G	·	T	C	T	T
NMNH 600581	–	T	G	A	·	·	C	A	G	G	A	·	C	·	T
NMNH 592895	–	–	–	–	–	–	–	–	–	–	–	–	–	–	–
UAMN 59579	·	T	G	A	·	·	C	A	G	G	A	·	C	·	T
NYSM 14241	·	T	G	A	·	·	C	A	G	G	A	·	C	·	T
BMUW 81688	·	T	G	A	·	·	C	A	G	G	·	·	C	T	T
USNM 592316	·	T	G	A	·	·	C	A	G	G	A	·	C	·	T
FMNH 31427	·	T	G	A	A	G	C	A	G	G	G	·	C	T	T
UAMN 101819	·	T	G	A	·	·	C	A	G	G	A	·	C	·	T
NYSM 14242	·	T	G	A	·	G	C	A	–	–	–	–	–	–	–
FMNH 31328	K	T	G	A	·	·	C	–	–	–	–	–	–	–	–
NYSM 14388	·	T	G	A	·	·	C	A	G	G	A	·	C	·	T
NMNH 600580	·	T	G	A	·	·	C	A	G	G	A	·	C	·	T
NMNH 600579	·	T	G	A	·	·	C	A	G	G	R	·	C	·	T
NMNH 600583	·	T	G	A	·	·	C	A	G	G	·	·	C	·	T
NMNH 592896	·	T	G	A	·	·	C	A	G	G	A	·	C	·	T
UAMN 101851	·	T	G	A	·	·	C	A	G	G	A	·	C	·	T

*– indicates no nucleotide at that position, · indicates no difference from *M. foina*

* some nucleotides are ambiguous and are represented by M (A or C), K (G or T), W (A or T), Y (C or T), R (A or G), or D (A, G, or T) based on IUPAC designations

Table 2 continued

Specimen	1104	1106	1131	1179	1180	1205	1233	1234	1249	1263	1264	1269	1271	1278	1279
M. foina	C	A	C	C	T	C	A	C	C	A	A	G	C	T	A
MSB 196581	·	·	·	·	·	T	G	T	·	·	·	·	·	·	·
BMUW 81025	S	T	–	–	–	–	–	–	–	–	–	–	–	–	–
NMNH 600581	·	·	T	·	·	T	·	·	·	·	·	·	·	·	·
NMNH 592895	–	–	–	–	–	–	–	–	–	–	–	–	–	–	–
UAMN 59579	·	·	T	·	·	T	·	·	·	M	M	·	·	Y	M
NYSM 14241	·	·	T	·	·	T	·	·	·	·	·	·	·	·	·
BMUW 81688	·	·	·	·	·	T	G	T	·	·	·	·	·	·	·
USNM 592316	·	·	T	·	·	T	·	·	·	·	·	·	·	·	·
FMNH 31427	·	·	·	·	·	T	G	T	·	·	·	·	·	·	·
UAMN 101819	·	·	T	·	·	T	·	·	·	·	·	·	·	·	·
NYSM 14242	–	–	–	–	–	–	–	–	–	–	–	–	–	–	–
FMNH 31328	–	–	–	–	–	–	–	–	–	–	–	–	–	–	–
NYSM 14388	·	·	T	·	·	T	–	·	·	·	·	A	G	–	–
NMNH 600580	·	·	T	·	·	T	·	·	·	·	·	·	·	·	·
NMNH 600579	·	·	T	·	·	T	·	·	·	·	·	·	·	·	·
NMNH 600583	·	·	T	M	W	T	·	·	M	·	·	·	·	·	·
NMNH 592896	·	·	T	·	·	T	·	·	·	·	·	·	·	·	·
UAMN 101851	·	·	T	·	·	T	·	·	·	·	·	·	·	·	·

*– indicates no nucleotide at that position, · indicates no difference from *M. foina*

* some nucleotides are ambiguous and are represented by M (A or C), K (G or T), W (A or T), Y (C or T), R (A or G), or D (A, G, or T) based on IUPAC designations

Table 2 continued

Specimen	1284	1285	1286	1287	1288	1289	1290	1296	1329	1342	1343	1344	1345	1368	1369
M. foina	A	A	T	G	C	C	T	C	C	–	T	A	C	C	C
MSB 196581	·	·	·	·	·	·	·	·	T	C	–	·	·	·	·
BMUW 81025	–	–	–	–	–	–	–	–	–	C	–	·	·	·	·
NMNH 600581	·	·	·	·	·	·	·	·	·	C	–	·	·	·	·
NMNH 592895	–	–	–	–	–	–	–	–	–	C	C	·	·	·	·
UAMN 59579	C	T	·	·	·	·	S	·	·	C	–	·	·	·	·
NYSM 14241	·	·	·	·	·	·	·	·	·	–	–	–	–	–	–
BMUW 81688	·	·	W	·	·	·	·	·	T	C	C	·	M	Y	·
USNM 592316	·	·	·	·	·	·	·	·	·	C	C	·	·	·	·
FMNH 31427	·	·	W	·	·	·	·	·	T	–	–	–	–	–	–
UAMN 101819	·	·	·	·	·	·	·	·	·	C	–	·	T	·	·
NYSM 14242	–	–	–	–	–	–	–	–	–	C	–	·	·	·	·
FMNH 31328	–	–	–	–	–	–	–	–	–	C	–	·	·	·	·
NYSM 14388	–	–	–	–	–	–	–	–	–	–	–	–	–	–	–
NMNH 600580	·	·	W	R	·	·	·	Y	·	–	–	–	–	–	–
NMNH 600579	·	·	·	·	·	·	·	·	·	C	–	M	M	T	·
NMNH 600583	·	·	·	R	M	S	·	·	·	C	–	·	·	·	·
NMNH 592896	·	·	·	·	·	·	·	·	·	–	–	–	–	T	K
UAMN 101851	·	·	·	·	·	·	·	·	·	–	–	–	–	–	–

*– indicates no nucleotide at that position, · indicates no difference from *M. foina*

* some nucleotides are ambiguous and are represented by M (A or C), K (G or T), W (A or T), Y (C or T), R (A or G), or D (A, G, or T) based on IUPAC designations

Table 2 continued

Specimen	1370	1414	1434	1520	1525	1554	1573	1600	1603	1673	1680	1692	1736	1749	1815
M. foina	A	C	C	T	A	T	C	T	T	T	T	A	T	C	T
MSB 196581	·	T	T	·	G	·	T	C	C	·	C	G	·	·	C
BMUW 81025	·	T	T	·	G	·	T	C	C	·	C	G	·	·	C
NMNH [redacted]	·	T	T	C	G	·	T	C	C	·	C	G	·	T	C
NMNH [redacted]	·	T	T	C	G	·	T	C	C	·	C	G	·	T	C
UAMN 59579	·	T	T	·	G	·	T	C	C	·	C	G	·	·	C
NYSM 14241	–	–	–	–	–	–	–	–	–	–	–	–	–	–	–
BMUW 81688	·	T	T	·	G	·	T	C	C	·	C	G	·	·	C
USNM 592316	·	T	T	C	G	·	T	C	C	·	C	G	·	T	C
FMNH 31427	–	–	–	–	–	–	–	–	–	–	–	–	–	–	–
UAMN [redacted]	·	T	T	C	G	·	T	C	C	·	C	G	·	T	C
NYSM 14242	·	T	T	C	G	D	T	C	C	·	C	G	·	T	C
FMNH 31328	·	T	T	C	G	·	T	C	C	·	C	G	·	T	C
NYSM 14388	–	–	–	–	–	–	–	–	–	–	–	–	–	–	–
NMNH [redacted]	–	T	T	C	G	·	T	C	C	·	C	G	Y	T	C
NMNH [redacted]	·	T	T	C	G	·	T	C	C	·	C	G	·	T	C
NMNH [redacted]	·	T	T	C	G	·	T	C	C	C	C	G	·	T	C
NMNH [redacted]	K	T	T	C	G	·	T	C	C	·	C	G	·	T	C
UAMN [redacted]	–	T	T	C	G	·	T	C	C	·	C	G	·	T	C

*– indicates no nucleotide at that position, · indicates no difference from *M. foina*

* some nucleotides are ambiguous and are represented by M (A or C), K (G or T), W (A or T), Y (C or T), R (A or G), or D (A, G, or T) based on IUPAC designations

Table 2 continued

Specimen	1817	1834	1877	1938	1940	1943	1963	1974	1989	2023	2029	2041	2044	2045	2047
M. foina	A	C	T	C	A	T	C	G	C	A	T	T	A	G	C
MSB 196581	·	·	·	·	T	C	T	A	T	G	C	·	·	·	T
BMUW 81025	·	·	·	·	T	C	T	A	T	G	–	–	–	–	T
NMNH 600581	·	·	C	·	T	C	T	A	T	G	C	·	·	·	T
NMNH 592895	·	·	C	·	T	C	T	A	T	G	–	–	–	–	–
UAMN 59579	·	·	·	·	T	C	T	A	T	G	C	·	·	R	T
NYSM 14241	–	–	–	–	–	–	–	–	–	–	–	–	–	–	–
BMUW 81688	·	·	·	·	T	C	T	A	T	G	C	·	·	·	T
USNM 592316	·	·	C	·	T	C	T	A	T	G	C	·	·	·	T
FMNH 31427	–	–	–	–	–	–	–	–	–	–	C	·	·	·	T
UAMN 101819	·	·	C	·	T	C	T	A	T	G	C	·	·	·	T
NYSM 14242	·	·	C	·	T	C	T	A	T	–	C	·	·	·	T
FMNH 31328	·	·	C	·	T	C	T	A	T	G	–	Y	M	·	–
NYSM 14388	–	–	–	–	–	–	–	–	–	–	C	·	·	·	T
NMNH 600580	M	Y	C	–	–	–	–	–	–	–	–	·	·	·	T
NMNH 600579	·	·	C	·	T	C	T	A	T	G	C	·	·	·	T
NMNH 600583	·	·	C	M	T	C	T	A	–	–	–	–	–	–	–
NMNH 592896	·	·	C	·	T	C	T	A	T	G	–	·	·	·	T
UAMN 101851	·	M	C	·	T	C	T	A	–	–	C	·	·	·	T

*– indicates no nucleotide at that position, · indicates no difference from *M. foina*

* some nucleotides are ambiguous and are represented by M (A or C), K (G or T), W (A or T), Y (C or T), R (A or G), or D (A, G, or T) based on IUPAC designations

Table 2 continued

Specimen	2054	2060	2064	2069	2074	2075	2080	2081	2101	2129	2131	2142	2146	2147	2155
M. foina	T	A	A	A	G	G	G	A	C	G	T	G	T	A	T
MSB 196581	C	·	·	·	A	·	A	G	T	·	C	·	C	·	C
BMUW 81025	C	·	·	W	R	M	A	G	T	·	C	·	C	·	C
NMNH 600581	C	·	·	·	A	·	A	G	T	·	C	·	C	·	C
NMNH 592895	–	–	–	–	–	–	–	–	T	·	C	·	C	G	C
UAMN 59579	C	·	W	R	A	A	A	G	T	·	C	·	C	·	C
NYSM 14241	–	–	–	–	–	–	–	G	T	·	C	·	C	·	C
BMUW 81688	C	·	·	·	A	·	A	G	T	·	C	·	C	·	C
USNM 592316	C	·	·	·	A	R	A	G	T	·	C	·	C	·	C
FMNH 31427	C	·	·	·	A	R	A	G	T	·	C	·	C	·	C
UAMN 101819	C	·	·	·	A	·	A	G	T	·	C	·	C	·	C
NYSM 14242	C	·	·	·	A	·	A	G	T	·	C	·	C	·	C
FMNH 31328	C	·	·	·	A	·	–	G	T	S	C	R	C	·	C
NYSM 14388	C	·	·	·	A	·	A	G	T	·	C	·	C	·	C
NMNH 600580	C	·	·	·	A	·	A	G	T	·	C	·	C	·	C
NMNH 600579	C	·	·	·	A	·	A	G	T	·	C	·	C	·	C
NMNH 600583	–	–	–	–	–	–	–	–	–	–	–	–	–	–	–
NMNH 592896	C	R	·	·	A	·	R	G	T	·	C	·	C	G	C
UAMN 101851	C	·	·	·	A	·	A	G	T	·	C	S	C	·	C

*– indicates no nucleotide at that position, · indicates no difference from *M. foina*

* some nucleotides are ambiguous and are represented by M (A or C), K (G or T), W (A or T), Y (C or T), R (A or G), or D (A, G, or T) based on IUPAC designations

Table 2 continued

Specimen	2157	2158	2163	2169	2174	2197	2203	2213	2229	2231	2233	2242	2245	2248	2258
M. foina	A	C	C	T	T	C	G	T	T	T	C	A	C	C	T
MSB 196581	·	T	·	·	·	T	·	·	A	C	T	G	T	T	C
BMUW 81025	·	T	·	·	·	T	·	·	A	C	T	G	T	T	C
NMNH 600581	·	T	·	·	·	·	A	·	A	C	·	G	T	T	C
NMNH 592895	·	T	·	·	·	·	A	·	A	C	·	G	T	T	C
UAMN 59579	·	T	·	·	·	·	A	·	A	C	·	G	T	T	C
NYSM 14241	·	T	·	·	·	·	A	·	A	C	·	G	T	T	C
BMUW 81688	·	T	·	·	·	T	·	·	A	C	T	G	T	T	C
USNM 592316	·	T	·	·	·	·	A	·	A	C	·	G	T	T	C
FMNH 31427	·	T	·	·	·	T	·	·	A	C	T	G	T	T	C
UAMN 101819	·	T	·	·	·	·	A	·	A	C	·	G	T	T	C
NYSM 14242	·	T	·	·	·	·	A	·	A	C	·	G	T	T	C
FMNH 31328	R	T	S	K	K	·	A	G	A	C	·	G	K	T	C
NYSM 14388	·	T	·	·	·	·	A	·	A	C	·	G	T	T	C
NMNH 600580	·	T	·	·	·	·	A	·	A	C	·	G	T	T	C
NMNH 600579	·	T	·	·	·	·	A	·	A	C	·	G	T	T	C
NMNH 600583	–	–	–	–	–	–	–	–	A	C	·	G	T	T	C
NMNH 592896	·	T	·	·	·	·	A	·	A	C	·	G	T	T	C
UAMN 101851	·	T	·	·	·	·	A	·	A	C	·	G	T	T	C

*– indicates no nucleotide at that position, · indicates no difference from *M. foina*

* some nucleotides are ambiguous and are represented by M (A or C), K (G or T), W (A or T), Y (C or T), R (A or G), or D (A, G, or T) based on IUPAC designations

Table 2 continued

Specimen	2269	2275	2294	2300	2313	2332	2341	2347	2348	2350	2353	2368	2379	2380	2383
M. foina	T	G	·	C	A	A	T	T	C	A	A	T	G	C	C
MSB 196581	A	A	·	·	·	G	·	C	·	·	G	C	·	T	·
BMUW 81025	A	A	·	·	·	G	·	C	·	·	G	C	·	T	·
NMNH 600581	A	A	·	·	·	G	·	C	T	G	G	C	·	T	T
NMNH 592895	A	A	·	·	R	G	·	C	T	G	G	C	·	T	T
UAMN 59579	A	A	·	·	·	G	·	C	T	G	G	C	·	T	T
NYSM 14241	A	A	·	·	·	G	·	C	T	G	G	C	·	T	T
BMUW 81688	A	A	·	·	·	G	·	C	·	·	G	C	·	T	·
USNM 592316	A	A	·	·	·	G	·	C	T	G	G	C	·	T	T
FMNH 31427	A	A	·	·	·	G	C	C	·	·	G	C	·	T	·
UAMN 101819	A	A	·	·	R	G	·	C	T	G	G	C	·	T	T
NYSM 14242	A	A	·	·	·	G	·	C	T	G	G	C	·	T	T
FMNH 31328	A	A	Y	·	·	G	·	C	T	G	G	C	·	T	T
NYSM 14388	A	A	·	·	·	G	·	C	T	G	G	C	A	T	T
NMNH 600580	A	A	·	·	·	G	·	C	T	G	G	C	·	T	T
NMNH 600579	A	A	·	·	·	G	·	C	T	G	G	C	·	T	T
NMNH 600583	A	A	·	Y	·	G	·	C	T	G	G	C	·	T	T
NMNH 592896	A	A	·	·	·	G	·	C	T	G	G	C	·	T	T
UAMN 101851	A	A	·	·	R	G	·	C	T	G	G	C	·	T	T

*– indicates no nucleotide at that position, · indicates no difference from *M. foina*

* some nucleotides are ambiguous and are represented by M (A or C), K (G or T), W (A or T), Y (C or T), R (A or G), or D (A, G, or T) based on IUPAC designations

Table 2 continued

Specimen	2401	2404	2406	2409	2413	2419	2422	2431	2439	2452	2461	2464	2466	2468	2472
M. foina	G	G	T	C	A	A	C	A	T	T	A	T	T	A	C
MSB 196581	A	A	·	·	·	G	T	·	·	·	·	C	·	G	T
BMUW 81025	A	A	·	·	·	G	T	G	·	·	·	C	·	·	T
NMNH 600581	A	A	·	·	·	G	T	G	·	·	·	C	·	·	·
NMNH 592895	A	A	·	·	·	G	T	G	·	·	·	C	·	·	·
UAMN 59579	A	A	·	·	·	G	T	G	·	·	·	C	·	·	·
NYSM 14241	A	A	·	·	·	G	T	G	·	C	·	C	·	·	·
BMUW 81688	A	A	·	·	·	G	T	G	·	·	·	C	·	·	T
USNM 592316	A	A	·	·	·	G	T	G	·	·	·	C	·	·	·
FMNH 31427	A	A	·	·	·	G	T	·	·	·	·	C	·	G	T
UAMN 101819	A	A	·	·	·	G	T	G	·	·	·	C	·	·	·
NYSM 14242	A	A	·	·	·	G	T	G	·	·	·	C	·	·	·
FMNH 31328	A	A	·	S	R	G	T	G	Y	·	R	C	K	·	·
NYSM 14388	A	A	·	·	·	G	T	G	·	·	·	C	·	·	·
NMNH 600580	A	A	·	·	·	G	T	G	·	C	·	C	·	·	·
NMNH 600579	A	A	·	·	·	G	T	G	·	·	·	C	·	·	·
NMNH 600583	A	A	W	·	·	G	T	G	·	·	·	C	·	·	·
NMNH 592896	A	A	·	·	·	G	T	G	·	·	·	C	·	·	·
UAMN 101851	A	A	·	·	·	G	T	G	·	·	·	C	·	·	·

*– indicates no nucleotide at that position, · indicates no difference from *M. foina*

* some nucleotides are ambiguous and are represented by M (A or C), K (G or T), W (A or T), Y (C or T), R (A or G), or D (A, G, or T) based on IUPAC designations

Table 2 continued

Specimen	2473	2474	2476	2477	2479	2488	2492	2506	2512	2518	2521	2530	2531	2533	2543
M. foina	G	G	C	T	A	A	C	C	G	C	C	C	G	G	G
MSB 196581	A	·	A	·	G	·	·	T	A	·	T	A	·	A	·
BMUW 81025	A	·	A	C	G	·	·	T	A	·	T	A	·	A	·
NMNH 600581	A	·	A	·	·	T	·	·	A	·	T	A	·	A	·
NMNH 592895	A	·	A	·	·	T	·	·	A	·	T	A	·	A	·
UAMN 59579	A	·	A	·	·	T	·	·	A	·	T	A	·	A	·
NYSM 14241	A	·	A	·	·	T	·	·	A	·	T	A	·	A	·
BMUW 81688	A	·	A	·	G	·	·	T	A	·	T	A	·	A	·
USNM 592316	A	·	A	·	·	T	·	·	A	·	T	A	·	A	·
FMNH 31427	A	·	A	·	G	·	Y	T	A	·	T	A	·	A	·
UAMN 101819	A	·	A	·	·	T	·	·	A	·	T	A	·	A	R
NYSM 14242	A	·	A	·	·	T	·	·	A	·	T	A	·	A	·
FMNH 31328	A	R	A	·	·	T	·	·	A	S	T	A	·	A	·
NYSM 14388	A	·	A	·	·	T	·	·	A	·	T	A	·	A	·
NMNH 600580	A	·	A	·	·	T	·	·	A	·	T	A	·	A	·
NMNH 600579	A	·	A	·	·	T	·	·	A	·	T	A	·	A	·
NMNH 600583	A	·	A	·	·	T	·	·	G	·	T	A	·	A	·
NMNH 592896	A	·	A	·	·	T	·	·	A	·	T	A	·	A	·
UAMN 101851	A	·	A	·	·	T	·	·	A	·	T	A	T	A	·

*– indicates no nucleotide at that position, · indicates no difference from *M. foina*

* some nucleotides are ambiguous and are represented by M (A or C), K (G or T), W (A or T), Y (C or T), R (A or G), or D (A, G, or T) based on IUPAC designations

Table 2 continued

Specimen	**2545**	**2546**	**2548**	**2573**	**2578**	**2591**	**2596**	**2603**	**2616**	**2623**	**2625**	**2650**	**2653**	**2668**	**2673**
M. foina	C	T	C	T	T	T	T	C	C	G	C	G	A	T	C
MSB 196581	T	·	T	·	C	C	C	T	·	A	T	T	G	C	T
BMUW 81025	T	·	T	·	C	C	C	T	·	A	T	T	G	C	T
NMNH 600581	T	·	T	·	C	C	C	T	T	A	T	T	G	C	T
NMNH 592895	T	·	T	·	C	C	C	T	T	A	T	T	G	C	T
UAMN 59579	T	·	T	·	C	C	C	T	T	A	T	T	G	C	·
NYSM 14241	T	·	T	·	C	C	C	T	T	A	·	T	G	C	T
BMUW 81688	T	·	T	·	C	C	C	T	·	A	T	T	G	C	T
USNM 592316	T	·	T	·	C	C	C	T	T	A	T	T	G	C	T
FMNH 31427	T	·	T	·	C	C	C	T	·	A	T	T	G	C	T
UAMN 101819	T	W	T	K	C	C	C	T	T	A	T	T	G	C	·
NYSM 14242	T	·	T	·	C	C	C	T	T	A	T	T	G	C	T
FMNH 31328	T	·	T	·	C	C	C	T	T	A	T	T	G	C	T
NYSM 14388	T	·	T	·	C	C	C	T	T	A	T	T	G	C	T
NMNH 600580	T	·	T	·	C	C	C	T	T	A	·	T	G	C	T
NMNH 600579	T	·	T	·	C	C	C	T	T	A	T	T	G	C	T
NMNH 600583	T	·	T	·	C	C	C	T	T	A	T	T	G	C	Y
NMNH 592896	T	·	T	·	C	C	C	T	T	A	T	T	G	C	T
UAMN 101851	T	·	T	K	C	C	C	T	T	A	T	T	G	C	C

*– indicates no nucleotide at that position, · indicates no difference from *M. foina*

* some nucleotides are ambiguous and are represented by M (A or C), K (G or T), W (A or T), Y (C or T), R (A or G), or D (A, G, or T) based on IUPAC designations

Table 2 continued

Specimen	2686	2689	2695	2701	2713	2716	2722	2737	2744	2746	2752	2761	2789	2790	2792
M. foina	A	T	G	T	C	G	T	C	C	A	T	T	–	C	T
MSB	G	C	A	C	T	·	C	T	·	G	C	C	–	T	C
BMUW	G	C	A	C	T	·	C	T	·	G	C	C	–	T	C
NMNH	·	C	·	C	·	A	C	T	T	·	C	C	–	T	C
NMNH	·	C	·	C	·	A	C	T	T	·	C	C	–	T	C
UAMN	·	C	·	C	·	A	C	T	T	·	C	C	–	–	C
NYSM	·	C	·	C	·	A	C	T	T	·	C	C	–	T	C
BMUW	G	C	A	C	T	·	C	T	·	G	C	C	–	T	C
USNM	·	C	·	C	·	A	C	T	T	·	C	C	–	T	C
FMNH	G	C	A	C	T	·	C	T	C	G	C	C	–	T	C
UAMN	·	C	·	C	·	A	C	T	T	·	C	C	–	T	C
NYSM	·	C	·	C	·	A	C	T	T	·	C	C	–	T	C
FMNH	·	C	A	C	·	A	C	T	T	·	C	C	A	T	C
NYSM	·	C	·	C	·	A	C	T	T	·	C	C	–	T	C
NMNH	·	C	·	C	·	A	C	T	T	·	C	C	–	–	C
NMNH	·	C	·	C	·	A	C	T	T	·	C	C	–	T	C
NMNH	·	C	·	C	·	A	C	T	T	·	C	C	–	T	C
NMNH	·	C	·	C	·	A	C	T	T	·	C	C	–	T	C
UAMN	·	C	·	C	·	A	C	T	T	·	C	C	–	T	C

*– indicates no nucleotide at that position, · indicates no difference from *M. foina*

* some nucleotides are ambiguous and are represented by M (A or C), K (G or T), W (A or T), Y (C or T), R (A or G), or D (A, G, or T) based on IUPAC designations

Table 2 continued

Specimen	2801	2803	2805	2808	2811	2815	2817	2821	2823	2826	2829	2835	2845	2848	2872
M. foina	A	–	T	A	C	A	T	C	A	T	C	G	A	A	T
MSB 196581	·	–	C	G	A	G	C	T	G	C	T	A	G	·	·
BMUW	·	–	C	G	A	G	C	T	G	C	T	A	G	·	·
NMNH	G	–	C	G	A	·	C	T	G	·	T	A	G	·	·
NMNH	G	–	C	G	A	·	C	T	G	·	T	A	G	·	·
UAMN	G	–	C	G	A	·	C	T	G	·	T	A	G	·	–
NYSM	G	–	C	G	A	·	C	T	G	·	T	A	G	·	·
BMUW	·	–	C	G	A	G	C	T	G	C	T	A	G	·	–
USNM	G	–	C	G	A	·	C	T	G	·	T	A	G	·	·
FMNH	·	–	C	G	A	G	C	T	G	C	T	A	G	·	·
UAMN	G	–	C	G	A	·	C	T	G	·	T	A	G	·	·
NYSM	G	–	C	G	A	·	C	T	G	·	T	A	G	·	·
FMNH	G	G	C	G	A	·	C	T	G	·	T	A	G	M	W
NYSM	G	A	C	G	A	·	C	T	G	·	T	A	G	·	·
NMNH	G	–	C	G	A	·	C	T	G	·	T	A	G	·	·
NMNH	G	–	C	G	A	·	C	T	G	·	T	A	G	M	·
NMNH	G	–	C	G	A	·	C	T	G	·	T	A	G	·	·
NMNH	G	–	C	G	A	·	C	T	G	·	T	A	G	·	·
UAMN	G	–	C	G	A	·	C	T	G	·	T	A	G	·	·

*– indicates no nucleotide at that position, · indicates no difference from *M. foina*

* some nucleotides are ambiguous and are represented by M (A or C), K (G or T), W (A or T), Y (C or T), R (A or G), or D (A, G, or T) based on IUPAC designations

Table 2 continued

Specimen	2877	2880	2889	2892	2895	2904	2906	2908	2910	2916	2931	2937	2940	2942	2943
M. foina	G	C	A	A	C	C	C	T	G	A	–	G	C	C	A
MSB 196581	A	·	·	·	T	T	·	·	A	G	C	A	·	·	·
BMUW [illegible]	A	·	·	G	T	T	·	·	A	G	C	A	·	·	·
NMNH [illegible]	A	·	·	·	T	T	·	·	A	G	C	A	·	·	·
NMNH [illegible]	A	·	·	·	T	C	·	·	A	G	C	A	·	·	·
UAMN [illegible]	–	–	–	–	–	–	–	–	–	–	–	–	–	–	–
NYSM [illegible]	A	·	·	·	T	C	·	·	A	G	C	A	·	·	·
BMUW [illegible]	–	·	·	G	T	T	·	·	A	G	C	A	·	T	C
USNM [illegible]	A	·	·	·	T	C	·	·	A	G	C	A	·	·	·
FMNH [illegible]	A	·	·	·	T	T	·	·	A	G	C	A	·	·	·
UAMN [illegible]	A	·	·	·	T	C	·	·	A	G	C	A	·	·	·
NYSM [illegible]	A	·	·	·	T	C	·	K	A	G	C	A	·	·	·
FMNH [illegible]	–	·	R	·	T	C	·	·	A	G	C	A	·	G	·
NYSM [illegible]	A	T	·	·	T	C	·	·	A	G	C	A	·	·	·
NMNH [illegible]	A	·	·	·	T	C	T	·	A	G	C	A	·	·	·
NMNH [illegible]	A	·	·	·	T	T	·	·	A	G	C	A	·	·	·
NMNH [illegible]	A	·	·	·	T	C	·	·	A	G	C	A	Y	·	·
NMNH [illegible]	A	·	·	·	T	C	·	·	A	G	C	A	·	·	·
UAMN [illegible]	A	·	·	·	T	C	·	·	A	G	C	A	·	·	·

*– indicates no nucleotide at that position, · indicates no difference from *M. foina*

* some nucleotides are ambiguous and are represented by M (A or C), K (G or T), W (A or T), Y (C or T), R (A or G), or D (A, G, or T) based on IUPAC designations

Table 2 continued

Specimen	2944	2945	2946	2952	2957	2958	2961	2962	2964	2968	2974	2990	2992	2993	2995
M. foina	T	T	T	C	G	C	A	C	T	C	T	G	C	C	C
MSB 196581	·	·	C	T	·	T	·	·	·	·	C	A	T	T	T
BMUW	·	–	C	T	–	T	G	·	·	T	C	A	T	T	T
NMNH	·	–	C	T	–	T	C	·	·	T	C	A	T	T	T
NMNH	·	–	C	T	–	T	C	–	–	–	–	–	–	–	–
UAMN	–	–	–	–	–	–	–	·	·	T	C	A	T	T	T
NYSM	·	–	C	T	–	T	C	·	·	T	C	A	T	T	T
BMUW	A	·	C	T	–	–	–	·	·	·	C	A	T	T	T
USNM	·	–	C	T	–	T	C	·	·	T	C	A	T	T	T
FMNH	·	–	C	T	–	T	G	–	·	C	C	A	T	T	T
UAMN	·	–	C	T	–	T	C	·	·	T	C	A	T	T	T
NYSM	·	–	C	T	–	T	G	–	–	–	–	–	–	–	–
FMNH	·	–	C	–	–	T	–	–	–	–	–	–	–	–	–
NYSM	·	–	C	T	–	T	C	T	·	T	C	A	T	T	T
NMNH	·	–	C	T	–	T	G	–	–	–	–	–	–	–	–
NMNH	·	–	C	T	–	T	C	–	–	–	–	–	–	–	–
NMNH	·	–	C	T	–	T	C	·	Y	T	C	A	T	T	T
NMNH	·	–	C	T	–	T	C	·	·	T	C	A	T	T	T
UAMN	·	–	C	T	–	T	C	·	·	T	C	A	T	T	T

*– indicates no nucleotide at that position, · indicates no difference from *M. foina*

* some nucleotides are ambiguous and are represented by M (A or C), K (G or T), W (A or T), Y (C or T), R (A or G), or D (A, G, or T) based on IUPAC designations

Table 2 continued

Specimen	3002	3003	3014	3022	3023	3027	3092	3093	3120	3132	3163	3178	3180	3181	3182
M. foina	T	A	A	A	T	T	G	A	T	A	G	A	G	C	T
MSB 196581	C	C	G	·	·	·	A	G	·	·	T	·	·	T	·
BMUW	C	C	G	·	·	·	A	G	C	·	T	·	·	T	·
NMNH	C	C	G	·	·	·	A	G	·	G	T	G	A	T	C
NMNH	–	–	–	–	–	–	–	–	–	–	–	–	–	–	–
UAMN	C	C	G	·	·	·	A	G	·	G	T	·	A	T	C
NYSM	C	C	G	·	·	·	A	G	·	G	T	·	A	T	C
BMUW	C	C	G	·	·	·	A	G	C	·	T	·	·	T	·
USNM	C	C	G	·	·	·	A	G	·	G	T	·	A	T	C
FMNH	C	C	R	W	K	·	A	G	·	·	T	·	·	T	·
UAMN	C	C	G	·	·	·	A	G	·	G	T	·	A	T	C
NYSM	–	–	–	–	–	·	A	G	·	G	T	·	A	T	C
FMNH	–	–	–	–	–	–	–	–	–	–	–	–	–	–	–
NYSM	C	C	G	·	·	W	A	G	·	G	T	·	A	T	C
NMNH	–	–	–	–	–	–	–	–	–	–	–	–	–	–	–
NMNH	–	–	–	–	–	–	–	–	–	–	–	–	–	–	–
NMNH	C	C	G	·	·	·	A	G	·	G	T	G	A	T	C
NMNH	C	C	G	·	·	·	A	G	·	G	T	·	A	T	C
UAMN	C	C	G	·	·	T	A	G	·	G	T	·	A	T	C

*– indicates no nucleotide at that position, · indicates no difference from *M. foina*

* some nucleotides are ambiguous and are represented by M (A or C), K (G or T), W (A or T), Y (C or T), R (A or G), or D (A, G, or T) based on IUPAC designations

Table 2 continued

Specimen	3184	3207	3210	3213	3214	3221	3236	3256	3258	3261	3269	3274	3275	3276	3280
M. foina	T	C	G	T	A	G	A	T	A	T	A	T	G	G	T
MSB 196581	·	·	·	G	G	·	·	·	·	C	G	C	·	·	C
BMUW	·	T	·	G	G	·	·	C	·	C	G	C	·	·	C
NMNH	·	·	·	G	G	·	·	·	G	C	G	C	T	A	C
NMNH	–	–	–	–	–	–	–	–	–	–	–	–	–	–	–
UAMN	·	·	A	G	G	·	·	·	G	C	G	C	T	A	C
NYSM	·	·	·	G	G	·	·	·	G	Y	·	C	T	A	C
BMUW	·	·	·	G	G	·	·	C	·	C	G	C	·	·	C
USNM	·	·	·	G	G	·	·	·	G	C	·	C	T	A	C
FMNH	·	·	·	G	G	·	·	·	·	C	G	C	·	·	C
UAMN	·	·	A	G	G	·	·	·	G	C	·	C	T	A	C
NYSM	K	·	·	G	G	·	·	·	G	C	·	C	T	A	C
FMNH	–	–	–	–	–	–	–	–	–	–	–	–	–	–	–
NYSM	·	·	·	G	G	·	G	·	G	C	·	C	T	A	C
NMNH	–	–	–	–	–	–	–	–	–	–	–	–	–	–	–
NMNH	–	–	–	–	–	–	–	–	–	–	–	–	–	–	–
NMNH	·	·	·	G	G	A	·	·	G	C	G	C	T	A	C
NMNH	·	·	·	A	G	·	·	·	G	C	·	C	T	A	C
UAMN	·	·	A	G	G	·	·	·	G	C	·	C	T	A	C

*– indicates no nucleotide at that position, · indicates no difference from *M. foina*

* some nucleotides are ambiguous and are represented by M (A or C), K (G or T), W (A or T), Y (C or T), R (A or G), or D (A, G, or T) based on IUPAC designations

Table 2 continued

Specimen	3283	3294	3295	3233	3327	3339	3360	3374	3376	3381	3384	3388	3404	3408	3410
M. foina	A	G	T	A	T	G	–	A	C	T	G	T	T	A	T
MSB 196581	G	A	·	·	·	A	–	·	G	G	A	·	·	G	·
BMUW	G	A	·	G	·	A	–	·	G	G	A	C	·	G	·
NMNH	G	·	·	G	·	A	–	·	G	G	A	·	·	G	C
NMNH	–	–	–	–	–	–	–	–	–	–	–	–	–	–	–
UAMN	G	A	C	G	·	A	–	G	G	G	A	·	·	G	C
NYSM	G	A	·	G	·	A	–	·	G	G	A	·	·	G	C
BMUW	G	A	·	G	·	A	–	·	G	G	A	·	·	G	·
USNM	G	·	·	G	·	A	–	·	G	G	A	·	·	G	C
FMNH	G	A	·	·	·	A	–	·	G	G	A	·	·	G	·
UAMN	G	A	·	G	·	A	–	·	G	G	A	·	·	G	C
NYSM	G	A	·	G	·	A	–	·	G	G	A	·	·	G	C
FMNH	–	–	–	–	–	–	–	–	–	–	–	–	–	–	–
NYSM	G	A	·	G	·	A	A	·	G	G	A	·	B	G	C
NMNH	–	–	–	–	–	–	–	–	–	–	–	–	–	–	–
NMNH	–	–	–	–	–	–	–	–	–	–	–	–	–	–	–
NMNH	G	A	·	G	·	A	–	·	G	G	A	·	·	G	C
NMNH	G	A	·	G	·	A	–	·	G	G	A	·	·	G	C
UAMN	G	A	·	G	C	A	A	·	G	G	A	·	·	G	C

*– indicates no nucleotide at that position, · indicates no difference from *M. foina*

* some nucleotides are ambiguous and are represented by M (A or C), K (G or T), W (A or T), Y (C or T), R (A or G), or D (A, G, or T) based on IUPAC designations

Table 2 continued

Specimen	3411	3416	3419	3424
M. foina	G	G	–	G
MSB 196581	A	·	G	A
BMUW 81025	A	·	G	A
NMNH	A	A	–	A
NMNH	–	–	–	–
UAMN 59579	A	A	–	A
NYSM 14241	A	A	–	A
BMUW 81688	A	·	G	A
USNM 592316	A	A	–	A
FMNH 31427	A	G	G	A
UAMN	A	A	–	·
NYSM 14242	A	A	–	A
FMNH 31328	–	–	–	–
NYSM 14388	A	A	–	A
NMNH	–	–	–	–
NMNH	–	–	–	–
NMNH	A	A	–	A
NMNH	A	A	–	A
UAMN	A	A	–	A

*– indicates no nucleotide at that position, · indicates no difference from *M. foina*

* some nucleotides are ambiguous and are represented by M (A or C), K (G or T), W (A or T), Y (C or T), R (A or G), or D (A, G, or T) based on IUPAC designation

Table 3. Figure 2 and 3 Phylogeny Specimen Labels

Specimen Number	**Phylogeny Label**
UAMN 101851	Alaska 1
UAMN 101819	Alaska 2
USNM 592316	Minnesota 1
FMNH 31328	Alaska 3
NYSM 14388	New York1
NYSM 14242	New York 2
NYSM 14241	New York 3
USNM 592896	Minnesota 2
USNM 592895	Minnesota 3
USNM 600583	New Hampshire 1
USNM 600579	New Hampshire 2
USNM 600581	New Hampshire 3
UAMN 101828	Alaska 4
USNM 600580	New Hampshire 4
BMUW 81688	Washington 1
BMUW 81025	Washington 2
FMNH 31427	Idaho 1
MSB 196581	Wyoming 1

E Supplemental Figures

Figure S1. Primer design overlap in 12S, 16S, Dloop, and cytb. Arrows indicate the region of each gene targeted by a primer set. Arrows pointing right represent forward primers and those pointing left are reverse primers. The length of the arrow represents the primer sequence length. Matching arrow colors within a gene represent primer pairs.

F R script

```
setwd("F:/research/Dissertation/morpho genetics test/modern/node calibrate/centroid")#User enters working directory


install.packages("ape",dependencies=TRUE )

install.packages("phytools",dependencies=TRUE )


library(ape)

library(phytools)



#Load Phylogeny

tree<-read.tree("3 calibrate tree.phy")

plot(tree, cex=0.6)



#Lineage Through Time Plot with Test of Gamma Statistic Pybus and Harvey 2000

Lineage<-ltt(tree, plot=TRUE, log.lineages=TRUE, gamma=TRUE)

Lineage$gamma

Lineage$p
```

Appendix IV- Chapter 5 Supplemental Files

A Specimens

MSB 196581; FMNH (UF) 31427, 31328; BMUW (UWBM) 81025, 81688; NYSM (NY)14388, 14242, 14241; USNM 600580, 600583, 592896, 600579, 592316, 600581; UAMN (UAM) 101828, 101819, 101851

Museum of Southwestern Biology (MSB)
New York State Museum (NYSM)
University of Alaska Museum of the North (UAMN)
Florida Museum of Natural History (FMNH)
Smithsonian Institution National Museum of Natural History (USNM)
Burke Museum of Natural History and Culture (BMUW)

B Geometric Morphometric Landmark Definitions:

Humerus

15. Most superior point of the lesser tubercle
16. Most inferomedial point of the lesser tubercle
17. Most inferior point of the head
18. Most superior point of the greater tubercle
19. Most inferior and medial point on the greater tubercle
20. Most superior point within the entepicondylar foramen
21. Most inferior point within the entepicondylar foramen
22. Most superior point of the medial epicondyle
23. Most inferior point of the medial epicondyle
24. Most medial intersection of the trochlea and coronoid fossa
25. Most lateral intersection of the trochlea and coronoid fossa
26. Most medial intersection of the trochlea and olecranon fossa
27. Most lateral intersection of the trochlea and olecranon fossa
28. Most superior point of the lateral supracondylar ridge

Radius

11. Most superior point on the anterior surface of the articular circumference of the head of the radius
12. Most superior point on the posterior surface of the articular circumference of the head of the radius
13. Most inferomedial point at the intersection of the articular circumference and neck
14. Most inferolateral point at the intersection of the articular circumference and neck
15. Point of maximum curvature of the medial intersection of the trochlea and body
16. Most medial point of the ulnar notch
17. Most inferior point of the styloid process
18. Most inferior point of the trochlea lateral to the styloid process
19. Most lateral point of the trochlea opposite the ulnar notch
20. Point of maximum curvature of the lateral intersection of the trochlea and body

Ulna

12. Most superolateral point of the proximal tuberocity of the olecranon
13. Most anterolateral point of the cranial process of the trochlear notch
14. Most superomedial point of the proximal tuberocity of the olecranon
15. Most anteromedial point of the cranial process of the trochlear notch
16. Most anterior point of the craniolateral process of the trochlear notch
17. Most anterior point of the craniomedial process of the trochlear notch
18. Most inferoposterior point of the proximal tuberocity of the olecranon
19. Most superior point of the articular surface that articulates with the ulnar notch of the radius
20. Most inferior point of the articular surface that articulates with the ulnar notch of the radius
21. Most posterior point of the styloid process just superior to the insertion point of the carpi ulnaris muscle

22. Most anterior point of the styloid process just superior to the insertion point of the carpi ulnaris muscle

Femur

13. Center of the fovea capitis
14. Point of maximum curvature of the neck of the femur along the coronal plane
15. Point of maximum curvature between the femoral head and greater trochanter along the coronal plane
16. Most superior point of the greater trochanter
17. Most inferoposterior point of the lesser trochanter
18. Most superomedial point of the medial condyle
19. Most superolateral point of the medial condyle
20. Most superior point of the intercondylar fossa along the sagittal plane
21. Most superomedial point of the lateral condyle
22. Most superolateral point of the lateral condyle
23. Most anterior point of the lateral sesamoid facet
24. Most anterior point of the medial sesamoid facet

Tibia

11. Most lateral point of the lateral condyle
12. Most inferoposterior point of the lateral condyle
13. Most inferoposterior point of the medial condyle
14. Most medial point of the medial condyle
15. Most anterior point along the sagittal plane of the tibial tuberocity
16. Most superolateral point of the lateral malleolus
17. Most inferior point of the lateral malleolus
18. Most inferoposterior point of the distal epiphysis that is not part of the medial or lateral malleolus
19. Most inferior point of the medial malleolus
20. Most superomedial point of the medial malleolus

Fibula

9. Most anterior point of the head
10. Most superior point of the head anterior to the coronal plane
11. Most superior point of the head posterior to the coronal plane
12. Most posterior point of the head
13. Most medial point of the head along the coronal plane
14. Most anterior point of the lateral malleolus
15. Most inferior point of the malleolar articular surface
16. Most posterior point of the distal epiphysis lateral to the malleolar articular surface

C Supplemental Tables

Table 1. Figure 2 Phylogeny Specimen Labels

Specimen Number	**Phylogeny Label**
UAMN 101851	Alaska 1
UAMN 101819	Alaska 2
USNM 592316	Minnesota 1
FMNH 31328	Alaska 3
NYSM 14388	New York1
NYSM 14242	New York 2
NYSM 14241	New York 3
USNM 592896	Minnesota 2
USNM 592895	Minnesota 3
USNM 600583	New Hampshire 1
USNM 600579	New Hampshire 2
USNM 600581	New Hampshire 3
UAMN 101828	Alaska 4
USNM 600580	New Hampshire 4
BMUW 81688	Washington 1
BMUW 81025	Washington 2
FMNH 31427	Idaho 1
MSB 196581	Wyoming 1

Table 2. Bone Centroid Size

Specimen	Humerus	Radius	Ulna	Femur	Tibia	Fibula
MSB196581	96.8395	67.44557	82.13473	103.3983	109.4516	92.24231
NY14241	91.66826	68.83815	82.23941	99.61098	109.6948	92.33572
NY14242	91.97825	68.2315	82.33631	97.45535	107.2522	90.1031
NY14387	89.61338	68.12289	81.09728	96.2457	106.2323	89.59357
UAM101819	103.8495	78.17896	93.56572	112.1575	119.3155	100.3932
UAM101828	103.7372	76.27671	91.61918	110.5859	121.4114	101.6584
UAM101851	89.10758	67.12427	81.69687	99.62422	105.561	89.85633
UF31427	105.5108	77.73883	93.82431	110.8945	121.9176	81.57621
UF31328	100.7167	70.74709	84.89048	106.5076	113.4249	94.13255
USNM592316	97.07095	72.83099	86.4179	104.3223	112.6123	94.97868
USNM592896	85.19975	64.82772	77.94916	91.42793	99.66878	84.1345
USNM600579	80.85333	60.50016	71.49111	87.08442	95.6588	81.7244
USNM600581	87.61561	67.51092	80.63243	95.09902	106.2658	90.35481
USNM600583	90.65173	69.1211	82.67027	97.94284	107.997	91.91396
USNM600580	78.31227	56.70782	67.46908	84.8128	91.95106	77.48209
UWBM81025	95.46184	66.93507	81.6357	100.7735	106.9657	90.42166
UWBM81688	100.4836	70.19279	83.8706	106.231	111.2066	93.76539

D R code for Multivariate Phylogenetic Signal and Evolutionary Tempo Analyses

```
setwd("")#user inputs working directory


#Load required packages

install.packages("geomorph", dependecies=TRUE)

install.packages("geiger", dependencies=TRUE)

library(geomorph)

library(geiger)



#Load phylogeny

tree<-read.tree("3 calibrate tree.phy")

plot(tree, cex=0.6)



################################################################################
######

########################## Humerus Analysis
#####################################

Humerusdata<-read.csv("humerus_landmark.csv", header=TRUE, stringsAsFactors =
FALSE, row.names=1)

Humerusdata

Hlandmarks<-as.matrix(Humerusdata[,-c(1,2)])

Hspecies<-Humerusdata[,1, drop=FALSE]

Hbiome<-Humerusdata[,2, drop=FALSE]


#Match tip labels to data

tdH<-treedata(tree,Hlandmarks, sort=TRUE)
```

```
Hdata<-tdH$data

Htree<-tdH$phy


#Match tip labels of biome to data

tdHB<-treedata(Htree,Hbiome, sort=TRUE)

Hbiodata<-tdHB$data

Hbiotree<-tdHB$phy

Hbiomef<-as.factor(Hbiodata)



#match tip labels of species to data

tdHS<- treedata(Htree, Hspecies, sort=TRUE)

Hspdata<-tdHS$data

Hsptree<-tdHS$phy

Hspf<-as.factor(Hspdata)


#align landmarks

Hcoords<- as.matrix(Hdata, drop=FALSE)

Hp<- ncol(Hcoords)/3

Hn<- length(Hdata)

Hk<- 3

Hland<- arrayspecs(Hcoords, Hp, Hk)

Hgpa<-gpagen(Hland)

HGPAcoords<-Hgpa$coords


Hcentroid<-Hgpa$Csize
```

```
####Phylogenetic Signal

#multivariate K test

HPS.shape <- physignal(A=Hgpa$coords,phy=Htree,iter=999)

summary(HPS.shape)

plot(HPS.shape)



####Evolutionary Rates Between the 2 species

names(Hspf)<-dimnames(HGPAcoords)[[3]]

Hspfa<-as.factor(Hspf)

Hrates<-compare.evol.rates(phy=Htree, A=HGPAcoords, gp=Hspfa, iter=999,
method="permutation")

summary(Hrates)



####Evolutionary Rates Between the 3 Biomes

names(Hbiomef)<-dimnames(HGPAcoords)[[3]]

Hbiomefa<-as.factor(Hbiomef)

Hrates<-compare.evol.rates(phy=Htree, A=HGPAcoords, gp=Hbiomefa, iter=999,
method="permutation")

summary(Hrates)



##########################################################################
######

########################## Radius Analysis
#########################################
```

```
Radiusdata<-read.csv("radius_landmark.csv", header=TRUE, stringsAsFactors =
FALSE, row.names=1)

Radiusdata

Rlandmarks<-as.matrix(Radiusdata[,-c(1,2)])

Rspecies<-Radiusdata[,1, drop=FALSE]

Rbiome<-Radiusdata[,2, drop=FALSE]


#Match tip labels to data

tdR<-treedata(tree,Rlandmarks, sort=TRUE)

Rdata<-tdR$data

Rtree<-tdR$phy


#match tip labels of species to data

tdRS<- treedata(Rtree, Rspecies, sort=TRUE)

Rspdata<-tdRS$data

Rsptree<-tdRS$phy

Rspf<-as.factor(Rspdata)


#Match tip labels of biome to data

tdRB<-treedata(Rtree,Rbiome, sort=TRUE)

Rbiodata<-tdRB$data

Rbiotree<-tdRB$phy

Rbiomef<-as.factor(Rbiodata)



#align landmarks

Rcoords<- as.matrix(Rdata, drop=FALSE)
```

```
Rp<- ncol(Rcoords)/3

Rn<- length(Rdata)

Rk<- 3

Rland<- arrayspecs(Rcoords, Rp, Rk)

Rgpa<-gpagen(Rland)

RGPAcoords<-Rgpa$coords


Rcentroid<-Rgpa$Csize


####Phylogenetic Signal

#multivariate K test

RPS.shape <- physignal(A=Rgpa$coords,phy=Rtree,iter=999)

summary(RPS.shape)

plot(RPS.shape)


####Evolutionary Rates Between the 2 species

names(Rspf)<-dimnames(RGPAcoords)[[3]]

Rspfa<-as.factor(Rspf)

Rrates<-compare.evol.rates(phy=Rtree, A=RGPAcoords, gp=Rspfa, iter=999,
method="permutation")

summary(Rrates)


####Evolutionary Rates Between the 3 Biomes

names(Rbiomef)<-dimnames(RGPAcoords)[[3]]

Rbiomefa<-as.factor(Rbiomef)

Rrates<-compare.evol.rates(phy=Rtree, A=RGPAcoords, gp=Rbiomefa, iter=999,
method="permutation")
```

```
summary(Rrates)



################################################################################
######

########################## Ulna Analysis
#######################################

Ulnadata<-read.csv("ulna_landmark.csv", header=TRUE, stringsAsFactors = FALSE,
row.names=1)

Ulnadata

Ulandmarks<-as.matrix(Ulnadata[,-c(1,2)])

Uspecies<-Ulnadata[,1, drop=FALSE]

Ubiome<-Ulnadata[,2, drop=FALSE]


#Match tip labels to data

tdU<-treedata(tree,Ulandmarks, sort=TRUE)

Udata<-tdU$data

Utree<-tdU$phy


#match tip labels of species to data

tdUS<- treedata(Utree, Uspecies, sort=TRUE)

Uspdata<-tdUS$data

Usptree<-tdUS$phy

Uspf<-as.factor(Uspdata)


#Match tip labels of biome to data

tdUB<-treedata(Utree,Ubiome, sort=TRUE)

Ubiodata<-tdUB$data
```

```
Ubiotree<-tdUB$phy

Ubiomef<-as.factor(Ubiodata)



#align landmarks

Ucoords<- as.matrix(Udata, drop=FALSE)

Up<- ncol(Ucoords)/3

Un<- length(Udata)

Uk<- 3

Uland<- arrayspecs(Ucoords, Up, Uk)

Ugpa<-gpagen(Uland)

UGPAcoords<-Ugpa$coords


Ucentroid<-Ugpa$Csize


####Phylogenetic Signal

#multivariate K test

UPS.shape <- physignal(A=Ugpa$coords,phy=Utree,iter=999)

summary(UPS.shape)

plot(UPS.shape)


####Evolutionary Rates Between the 2 species

names(Uspf)<-dimnames(UGPAcoords)[[3]]

Uspfa<-as.factor(Uspf)

Urates<-compare.evol.rates(phy=Utree, A=UGPAcoords, gp=Uspfa, iter=999,
method="permutation")

summary(Urates)
```

```
####Evolutionary Rates Between the 3 Biomes

names(Ubiomef)<-dimnames(UGPAcoords)[[3]]

Ubiomefa<-as.factor(Ubiomef)

Urates<-compare.evol.rates(phy=Utree, A=UGPAcoords, gp=Ubiomefa, iter=999,
method="permutation")

summary(Urates)



################################################################################
######

########################## Femur Analysis
########################################

Femurdata<-read.csv("femur_landmark.csv", header=TRUE, stringsAsFactors = FALSE,
row.names=1)

Femurdata

FElandmarks<-as.matrix(Femurdata[,-c(1,2)])

FEspecies<-Femurdata[,1, drop=FALSE]

FEbiome<-Femurdata[,2, drop=FALSE]


#Match tip labels to data

tdFE<-treedata(tree,FElandmarks, sort=TRUE)

FEdata<-tdFE$data

FEtree<-tdFE$phy


#match tip labels of species to data

tdFES<- treedata(FEtree, FEspecies, sort=TRUE)

FEspdata<-tdFES$data
```

```
FEsptree<-tdFES$phy

FEspf<-as.factor(FEspdata)


#Match tip labels of biome to data

tdFEB<-treedata(FEtree,FEbiome, sort=TRUE)

FEbiodata<-tdFEB$data

FEbiotree<-tdFEB$phy

FEbiomef<-as.factor(FEbiodata)



#align landmarks

FEcoords<- as.matrix(FEdata, drop=FALSE)

FEp<- ncol(FEcoords)/3

FEn<- length(FEdata)

FEk<- 3

FEland<- arrayspecs(FEcoords, FEp, FEk)

FEgpa<-gpagen(FEland)

FEGPAcoords<-FEgpa$coords


FEcentroid<-FEgpa$Csize


####Phylogenetic Signal

#multivariate K test

FEPS.shape <- physignal(A=FEgpa$coords,phy=FEtree,iter=999)

summary(FEPS.shape)

plot(FEPS.shape)
```

```
####Evolutionary Rates Between the 2 species

names(FEspf)<-dimnames(FEGPAcoords)[[3]]

FEspfa<-as.factor(FEspf)

FErates<-compare.evol.rates(phy=FEtree, A=FEGPAcoords, gp=FEspfa, iter=999,
method="permutation")

summary(FErates)



####Evolutionary Rates Between the 3 Biomes

names(FEbiomef)<-dimnames(FEGPAcoords)[[3]]

FEbiomefa<-as.factor(FEbiomef)

FErates<-compare.evol.rates(phy=FEtree, A=FEGPAcoords, gp=FEbiomefa, iter=999,
method="permutation")

summary(FErates)



##########################################################################
######

########################## Tibia Analysis
#########################################

Tibiadata<-read.csv("tibia_landmark.csv", header=TRUE, stringsAsFactors = FALSE,
row.names=1)

Tibiadata

Tlandmarks<-as.matrix(Tibiadata[,-c(1,2)])

Tspecies<-Tibiadata[,1, drop=FALSE]

Tbiome<-Tibiadata[,2, drop=FALSE]
```

```
#Match tip labels to data
tdT<-treedata(tree,Tlandmarks, sort=TRUE)
Tdata<-tdT$data
Ttree<-tdU$phy

#match tip labels of species to data
tdTS<- treedata(Ttree, Tspecies, sort=TRUE)
Tspdata<-tdTS$data
Tsptree<-tdTS$phy
Tspf<-as.factor(Tspdata)

#Match tip labels of biome to data
tdTB<-treedata(Ttree,Tbiome, sort=TRUE)
Tbiodata<-tdTB$data
Tbiotree<-tdTB$phy
Tbiomef<-as.factor(Tbiodata)


#align landmarks
Tcoords<- as.matrix(Tdata, drop=FALSE)
Tp<- ncol(Tcoords)/3
Tn<- length(Tdata)
Tk<- 3
Tland<- arrayspecs(Tcoords, Tp, Tk)
Tgpa<-gpagen(Tland)
```

```
TGPAcoords<-Tgpa$coords


Tcentroid<-Tgpa$Csize


####Phylogenetic Signal

#multivariate K test

TPS.shape <- physignal(A=Tgpa$coords,phy=Ttree,iter=999)

summary(TPS.shape)

plot(TPS.shape)


####Evolutionary Rates Between the 2 species

names(Tspf)<-dimnames(TGPAcoords)[[3]]

Tspfa<-as.factor(Tspf)

Trates<-compare.evol.rates(phy=Ttree, A=TGPAcoords, gp=Tspfa, iter=999,
method="permutation")

summary(Trates)


####Evolutionary Rates Between the 3 Biomes

names(Tbiomef)<-dimnames(TGPAcoords)[[3]]

Tbiomefa<-as.factor(Tbiomef)

Trates<-compare.evol.rates(phy=Ttree, A=TGPAcoords, gp=Tbiomefa, iter=999,
method="permutation")

summary(Trates)




##########################################################################
######
```

```
######################### Fibula Analysis
#####################################

Fibuladata<-read.csv("fibula_landmark.csv", header=TRUE, stringsAsFactors = FALSE,
row.names=1)

Fibuladata

FIlandmarks<-as.matrix(Fibuladata[,-c(1,2)])

FIspecies<-Fibuladata[,1, drop=FALSE]

FIbiome<-Fibuladata[,2, drop=FALSE]


#Match tip labels to data

tdFI<-treedata(tree,FIlandmarks, sort=TRUE)

FIdata<-tdFI$data

FItree<-tdFI$phy


#match tip labels of species to data

tdFIS<- treedata(FItree, FIspecies, sort=TRUE)

FIspdata<-tdFIS$data

FIsptree<-tdFIS$phy

FIspf<-as.factor(FIspdata)



#Match tip labels of biome to data

tdFIB<-treedata(FItree,FIbiome, sort=TRUE)

FIbiodata<-tdFIB$data

FIbiotree<-tdFIB$phy

FIbiomef<-as.factor(FIbiodata)
```

```
#align landmarks

FIcoords<- as.matrix(FIdata, drop=FALSE)

FIp<- ncol(FIcoords)/3

FIn<- length(FIdata)

FIk<- 3

FIland<- arrayspecs(FIcoords, FIp, FIk)

FIgpa<-gpagen(FIland)

FIGPAcoords<-FIgpa$coords


FIcentroid<-FIgpa$Csize


####Phylogenetic Signal

#multivariate K test

FIPS.shape <- physignal(A=FIgpa$coords,phy=FItree,iter=999)

summary(FIPS.shape)

plot(FIPS.shape)


####Evolutionary Rates Between the 2 species

names(FIspf)<-dimnames(FIGPAcoords)[[3]]

FIspfa<-as.factor(FIspf)

FIrates<-compare.evol.rates(phy=FItree, A=FIGPAcoords, gp=FIspfa, iter=999,
method="permutation")

summary(FIrates)


####Evolutionary Rates Between the 3 Biomes

names(FIbiomef)<-dimnames(FIGPAcoords)[[3]]
```

```
FIbiomefa<-as.factor(FIbiomef)

FIrates<-compare.evol.rates(phy=FItree, A=FIGPAcoords, gp=FIbiomefa, iter=999,
method="permutation")

summary(FIrates)
```

E R Code for Evolutionary Mode Analysis

```
setwd("")#User enters working directory


install.packages("geiger",dependencies=TRUE )

install.packages("phytools",dependencies=TRUE )


library(geiger)

library(phytools)


#Load Phylogeny

tree<-read.tree("3 calibrate tree.phy")

plot(tree, cex=0.6)


#Load Data


#input limb proportions data

mydata<-read.csv("all bones centroid cal.csv", header=TRUE, row.names= 1)

mydata

femur<-as.matrix(mydata[,1, drop=FALSE])

tibia<-as.matrix(mydata[,2, drop=FALSE])

fibula<-as.matrix(mydata[,3, drop=FALSE])
```

```
humerus<-as.matrix(mydata[,4, drop=FALSE])

radius<-as.matrix(mydata[,5, drop=FALSE])

ulna<-as.matrix(mydata[,6, drop=FALSE])



#Convert to data frame

femurdata<-as.data.frame(femur)

tibiadata<-as.data.frame(tibia)

fibuladata<-as.data.frame(fibula)

humerusdata<-as.data.frame(humerus)

radiusdata<-as.data.frame(radius)

ulnadata<-as.data.frame(ulna)



################################################################################
######

##########################Phylogenetic
Signal####################################

####Humerus####

#Match tip labels to data

tdHU<-treedata(tree,humerusdata, sort=FALSE)

dataHU<-tdHU$data

treeHU<-tdHU$phy


phylosig(treeHU, dataHU, method="K", test=TRUE, nsim=999)

phylosig(treeHU, dataHU, method="lambda", test=FALSE)
```

```
####Radius####
#Match tip labels to data
tdRA<-treedata(tree,radiusdata, sort=FALSE)
dataRA<-tdRA$data
treeRA<-tdRA$phy

phylosig(treeRA, dataRA, method="K", test=TRUE, nsim=999)
phylosig(treeRA, dataRA, method="lambda", test=FALSE)

####Ulna####
#Match tip labels to data
tdUL<-treedata(tree,ulnadata, sort=FALSE)
dataUL<-tdUL$data
treeUL<-tdUL$phy

phylosig(treeUL, dataUL, method="K", test=TRUE, nsim=999)
phylosig(treeUL, dataUL, method="lambda", test=FALSE)

####Femur####
#Match tip labels to data
tdFE<-treedata(tree,femurdata, sort=FALSE)
dataFE<-tdFE$data
treeFE<-tdFE$phy

phylosig(treeFE, dataFE, method="K", test=TRUE, nsim=999)
phylosig(treeFE, dataFE, method="lambda", test=FALSE)
```

```
####Tibia####

#Match tip labels to data

tdTI<-treedata(tree,tibiadata, sort=FALSE)

dataTI<-tdTI$data

treeTI<-tdTI$phy


phylosig(treeTI, dataTI, method="K", test=TRUE, nsim=999)

phylosig(treeTI, dataTI, method="lambda", test=FALSE)


####Fibula####

#Match tip labels to data

tdFI<-treedata(tree,fibuladata, sort=FALSE)

dataFI<-tdFI$data

treeFI<-tdFI$phy


phylosig(treeFI, dataFI, method="K", test=TRUE, nsim=999)

phylosig(treeFI, dataFI, method="lambda", test=FALSE)



##########################################################################
######

########################## Disparity Through Time
##################################

#Humerus

dipsHU<-dtt(treeHU, dataHU, index=c("avg.sq"), mdi.range=c(0,1), nsim=1000,
CI=0.95, plot=TRUE)

dipsHU
```

```
#Radius

dipsRA<-dtt(treeRA, dataRA, index=c("avg.sq"), mdi.range=c(0,1), nsim=1000,
CI=0.95, plot=TRUE)

dipsRA


#Ulna

dipsUL<-dtt(treeUL, dataUL, index=c("avg.sq"), mdi.range=c(0,1), nsim=1000, CI=0.95,
plot=TRUE)

dipsUL


#Femur

dipsFE<-dtt(treeFE, dataFE, index=c("avg.sq"), mdi.range=c(0,1), nsim=1000, CI=0.95,
plot=TRUE)

dipsFE


#Tibia

dipsTI<-dtt(treeTI, dataTI, index=c("avg.sq"), mdi.range=c(0,1), nsim=1000, CI=0.95,
plot=TRUE)

dipsTI


#Fibula

dipsFI<-dtt(treeFI, dataFI, index=c("avg.sq"), mdi.range=c(0,1), nsim=1000, CI=0.95,
plot=TRUE)

dipsFI
```

Appendix V- Chapter 6 Supplemental Files

A Specimens whose morphology was measured

USNM 265584, 265585, 266142, 546139, 546140, 546141; UAMN 509, 511, 11236, 11237, 13542, 22678, 24794, 24805, 24808, 22680, 22736, 47308, 59579, 101819, 101828, 101851; SNOMNH 11542, 11543, 11544, 11545, 11546, 11547, 11548, 11549, 11550, 11551, FMNH 31142, 31328

B Specimens sampled for DNA

USNM 265584, 265585, 266142, 546139, 546140, 546141; UAMN 509, 511, 11236, 11237, 13542, 22678, 24794, 24805, 24808, 22680, 22736, 47308, 59579, 101819, 101828, 101851; SNOMNH 11542, 11543, 11544, 11545, 11546, 11547, 11548, 11549, 11550, 11551, FMNH 31328

C Sequences from GenBank

M. foina HM 106325.1

Smithsonian Institution National Museum of Natural History (USNM)
University of Alaska Museum of the North (UAMN)
Sam Noble Oklahoma Museum of Natural History (SNOMNH)
Florida Museum of Natural History (FMNH)

D Geometric Morphometric Landmark Definitions:

Humerus

29. Most superior point of the lesser tubercle
30. Most inferomedial point of the lesser tubercle
31. Most inferior point of the head
32. Most superior point of the greater tubercle
33. Most inferior and medial point on the greater tubercle
34. Most superior point within the entepicondylar foramen
35. Most inferior point within the entepicondylar foramen
36. Most superior point of the medial epicondyle
37. Most inferior point of the medial epicondyle
38. Most medial intersection of the trochlea and coronoid fossa
39. Most lateral intersection of the trochlea and coronoid fossa
40. Most medial intersection of the trochlea and olecranon fossa
41. Most lateral intersection of the trochlea and olecranon fossa
42. Most superior point of the lateral supracondylar ridge

Radius

21. Most superior point on the anterior surface of the articular circumference of the head of the radius
22. Most superior point on the posterior surface of the articular circumference of the head of the radius
23. Most inferomedial point at the intersection of the articular circumference and neck
24. Most inferolateral point at the intersection of the articular circumference and neck
25. Point of maximum curvature of the medial intersection of the trochlea and body
26. Most medial point of the ulnar notch
27. Most inferior point of the styloid process
28. Most inferior point of the trochlea lateral to the styloid process
29. Most lateral point of the trochlea opposite the ulnar notch
30. Point of maximum curvature of the lateral intersection of the trochlea and body

Ulna

23. Most superolateral point of the proximal tuberocity of the olecranon
24. Most anterolateral point of the cranial process of the trochlear notch
25. Most superomedial point of the proximal tuberocity of the olecranon
26. Most anteromedial point of the cranial process of the trochlear notch
27. Most anterior point of the craniolateral process of the trochlear notch
28. Most anterior point of the craniomedial process of the trochlear notch
29. Most inferoposterior point of the proximal tuberocity of the olecranon
30. Most superior point of the articular surface that articulates with the ulnar notch of the radius
31. Most inferior point of the articular surface that articulates with the ulnar notch of the radius
32. Most posterior point of the styloid process just superior to the insertion point of the carpi ulnaris muscle

33. Most anterior point of the styloid process just superior to the insertion point of the carpi ulnaris muscle

Femur

25. Center of the fovea capitis
26. Point of maximum curvature of the neck of the femur along the coronal plane
27. Point of maximum curvature between the femoral head and greater trochanter along the coronal plane
28. Most superior point of the greater trochanter
29. Most inferoposterior point of the lesser trochanter
30. Most superomedial point of the medial condyle
31. Most superolateral point of the medial condyle
32. Most superior point of the intercondylar fossa along the sagittal plane
33. Most superomedial point of the lateral condyle
34. Most superolateral point of the lateral condyle
35. Most anterior point of the lateral sesamoid facet
36. Most anterior point of the medial sesamoid facet

Tibia

21. Most lateral point of the lateral condyle
22. Most inferoposterior point of the lateral condyle
23. Most inferoposterior point of the medial condyle
24. Most medial point of the medial condyle
25. Most anterior point along the sagittal plane of the tibial tuberocity
26. Most superolateral point of the lateral malleolus
27. Most inferior point of the lateral malleolus
28. Most inferoposterior point of the distal epiphysis that is not part of the medial or lateral malleolus
29. Most inferior point of the medial malleolus
30. Most superomedial point of the medial malleolus

Fibula

17. Most anterior point of the head
18. Most superior point of the head anterior to the coronal plane
19. Most superior point of the head posterior to the coronal plane
20. Most posterior point of the head
21. Most medial point of the head along the coronal plane
22. Most anterior point of the lateral malleolus
23. Most inferior point of the malleolar articular surface
24. Most posterior point of the distal epiphysis lateral to the malleolar articular surface

E Supplemental Tables

Table 1. Bone Centroid Size

Specimen	Humerus	Radius	Ulna	Femur	Tibia	Fibula
USNM 265584	90.31	68.64	NA	117.75	106.18	107.45
USNM 265585	91.81	68.27	81.70	117.43	NA	NA
USNM 266142	104.18	80.24	95.42	103.17	NA	NA
USNM 546139	89.56	65.12	78.50	98.18	107.41	89.65
USNM 546140	90.71	65.79	91.62	100.07	124.80	92.07
USNM 546141	95.72	73.14	95.96	112.05	102.72	104.54
UAMNH 509	93.33	81.90	79.39	97.29	108.40	88.07
UAMN 511	109.17	71.07	84.05	110.96	127.78	103.61
UAMN 11236	106.82	67.12	81.94	100.46	123.07	91.61
UAMN 11237	89.11	66.15	94.70	113.19	105.56	103.94
UAMN 13542	89.85	78.58	77.42	110.32	105.14	105.08
UAMN 22678	104.07	78.17	79.45	99.91	121.60	91.78
UAMN 24794	92.28	65.63	95.30	114.66	107.83	105.11
UAMN 24805	89.73	81.03	92.32	117.19	105.32	107.61
UAMN 24808	109.84	77.96	81.65	99.05	127.53	91.30
UAMN 22680	104.38	64.08	87.89	116.30	123.90	108.11
UAMN 47308	102.75	70.40	95.12	92.93	121.31	83.65
UAMN 59579	95.18	76.28	93.57	96.65	108.83	88.85
UAMN 22736	87.27	68.97	98.30	113.50	99.27	103.17
UAMN 101819	90.23	77.74	80.06	112.16	103.82	100.39
UAMN 101828	105.51	80.71	93.82	110.59	121.92	101.66
FMNH 31142	103.73	NA	97.73	95.90	121.41	NA
FMNH 31328	103.85	78.18	83.82	110.89	119.32	102.61
SNOMNH 11542	103.89	76.48	91.44	109.51	119.63	101.47
SNOMNH 11543	104.20	NA	NA	111.98	122.38	103.46
SNOMNH 11544	105.45	77.36	93.84	111.81	123.62	102.28
SNOMNH 11545	88.11	62.86	76.86	93.76	98.62	83.81
SNOMNH 11546	108.21	79.93	95.86	116.07	126.79	107.16
SNOMNH 11547	91.96	67.52	81.14	100.24	106.78	NA
SNOMNH 11548	104.65	NA	NA	111.80	122.00	104.01
SNOMNH 11549	107.07	80.74	95.79	115.04	127.60	106.28
SNOMNH 11550	100.54	NA	NA	106.38	115.33	97.75
SNOMNH 11551	106.57	80.04	95.43	113.14	127.11	106.46

Table 2. PC scores for the Humerus, Radius, Ulna, Femur, Tibia, and Fibula

Humerus

Specimen	PC1	PC2	PC3	PC4	PC5	PC6	PC7	PC8	PC9
USNM 265584	7.40E-03	-1.56E-03	1.09E-02	-1.07E-03	8.40E-04	-8.75E-04	5.53E-03	-2.60E-03	5.40E-03
USNM 265585	1.24E-02	8.50E-04	-2.11E-04	-1.59E-03	-9.96E-03	3.63E-03	6.33E-04	1.46E-03	3.57E-03
USNM 266142	1.04E-02	6.67E-03	8.37E-03	5.70E-03	-4.05E-03	-9.89E-03	-1.99E-03	-4.28E-04	1.24E-05
UAMN 509	-1.40E-02	-9.85E-03	4.54E-03	5.20E-03	-2.86E-03	8.53E-04	-4.06E-03	-7.61E-04	-1.60E-03
UAMN 511	5.62E-03	-7.79E-04	-1.93E-02	8.47E-03	1.97E-03	-9.84E-03	-9.94E-04	-1.61E-03	4.52E-03
SNOMNH 11542	-7.05E-03	-4.50E-03	-7.21E-03	5.81E-03	5.99E-06	9.18E-04	5.23E-03	2.83E-04	9.60E-04
SNOMNH 11543	1.31E-02	-5.30E-03	-2.28E-03	-1.67E-03	5.24E-03	5.30E-03	-4.75E-03	6.96E-04	-6.45E-03
SNOMNH 11544	5.82E-03	-8.19E-03	-1.29E-03	-3.34E-03	1.50E-03	-2.93E-03	5.74E-03	5.27E-03	-1.94E-03
SNOMNH 11545	-8.62E-03	-5.91E-03	-5.26E-03	-9.68E-03	4.54E-03	7.94E-03	2.77E-03	-1.12E-03	5.86E-03
SNOMNH 11546	-4.17E-03	5.26E-04	-4.27E-03	6.01E-04	4.44E-03	4.78E-03	-8.55E-03	-1.38E-04	-1.89E-03
SNOMNH 11547	-8.49E-03	-5.85E-03	-2.07E-03	-1.65E-03	-1.78E-03	-3.45E-04	2.95E-03	1.82E-04	2.70E-03
SNOMNH 11548	4.87E-03	-3.50E-03	1.20E-03	5.87E-03	7.72E-03	3.85E-03	-2.87E-03	1.57E-03	4.68E-03
SNOMNH 11549	2.69E-03	1.07E-03	3.87E-05	-9.38E-04	5.23E-03	9.20E-04	4.19E-03	-4.07E-03	3.78E-03
SNOMNH 11550	-7.04E-04	1.28E-02	-3.24E-03	-5.81E-03	6.65E-03	-5.19E-03	-1.31E-03	-9.20E-03	5.78E-04
SNOMNH 11551	9.80E-04	1.16E-03	8.66E-04	-3.58E-04	1.04E-02	-4.16E-04	3.83E-03	2.69E-03	-8.39E-03
UAMN 11236	-4.48E-04	2.85E-03	4.02E-03	7.71E-03	-5.61E-04	7.16E-04	1.38E-03	-5.07E-04	2.96E-03
UAMN 11237	1.16E-02	1.41E-03	-2.02E-04	1.20E-03	-1.22E-03	9.30E-04	6.21E-03	-3.25E-03	-2.10E-03

Humerus continued

Specimen	PC1	PC2	PC3	PC4	PC5	PC6	PC7	PC8	PC9
UAMN 13542	5.81E-03	-4.21E-03	-2.40E-03	1.83E-03	-1.08E-03	2.62E-03	-6.81E-03	-2.25E-03	7.25E-04
USNM 546139	-8.07E-03	3.16E-03	3.38E-03	-3.87E-03	-4.12E-03	1.15E-03	-1.39E-03	-6.38E-03	1.96E-03
USNM 546140	-8.14E-03	5.55E-03	3.82E-03	-2.84E-03	-7.84E-04	-2.37E-03	3.08E-03	-3.43E-05	-2.35E-03
USNM 546141	-1.59E-03	1.01E-02	-2.47E-03	-1.22E-04	-6.10E-03	6.34E-03	7.60E-04	-3.32E-03	-3.27E-03
UAMN 22678	-3.60E-03	-1.33E-02	7.82E-03	-5.67E-04	3.26E-03	-4.56E-03	-5.59E-03	-1.94E-03	1.66E-03
UAMN 22680	-5.04E-03	1.06E-03	3.41E-03	-2.10E-03	-2.50E-03	2.90E-03	-2.86E-03	1.00E-03	4.57E-04
UAMN 22736	8.66E-04	3.62E-04	3.90E-03	9.45E-03	-4.02E-03	4.31E-03	-5.23E-04	-2.56E-03	-1.50E-03
UAMN 24794	-3.19E-03	1.76E-03	2.36E-03	-1.73E-04	-1.80E-03	-5.50E-04	-4.06E-04	7.89E-03	4.57E-03
UAMN 24805	-7.97E-03	1.27E-02	-1.76E-03	-2.11E-03	3.34E-04	1.15E-03	8.07E-04	-1.98E-03	-1.19E-03
UAMN 24808	-4.51E-04	-5.80E-03	-1.47E-03	-4.70E-03	-2.58E-03	-5.22E-03	5.23E-03	2.62E-03	-4.54E-03
UAMN 47308	6.03E-03	-3.78E-03	4.02E-03	-1.00E-02	7.88E-04	-8.03E-03	-6.26E-03	-2.21E-03	-1.65E-03
UAMN 101819	-4.21E-04	-6.83E-04	-8.43E-03	-3.29E-03	-1.27E-02	-8.85E-04	-2.09E-03	-4.27E-04	-4.34E-03
UAMN 101828	-4.46E-03	7.84E-03	-2.10E-03	-3.73E-03	-8.14E-04	-2.97E-03	-5.19E-03	1.20E-02	2.59E-03
UAMN 101851	1.24E-02	-4.83E-03	-5.28E-04	-5.67E-03	-2.23E-03	4.36E-03	2.21E-03	2.70E-03	1.89E-03
UAMN 59579	-1.07E-03	-8.90E-03	9.72E-04	6.34E-03	7.67E-05	2.92E-03	1.90E-03	-1.55E-03	-5.05E-03
FMNH 31142	-1.61E-02	-5.58E-04	1.85E-03	3.58E-03	1.12E-03	-5.57E-03	3.49E-03	2.09E-03	-1.88E-03
FMNH 31328	3.57E-03	1.77E-02	3.00E-03	3.55E-03	5.03E-03	4.09E-03	-2.92E-04	5.89E-03	-7.16E-04

Humerus continued

Specimen	PC10	PC11	PC12	PC13	PC14	PC15	PC16	PC17
USNM 265584	-2.14E-03	4.62E-04	-6.07E-03	2.94E-03	1.72E-04	1.25E-04	1.31E-03	-1.79E-03
USNM 265585	9.17E-04	6.40E-03	-7.62E-04	-2.63E-03	4.40E-03	2.80E-03	-1.79E-03	4.88E-04
USNM 266142	-5.69E-03	-1.54E-03	2.76E-03	-5.22E-04	1.61E-03	6.82E-04	3.01E-03	-1.86E-03
UAMN 509	1.67E-03	1.09E-03	-5.90E-03	-2.48E-03	3.11E-03	-3.37E-03	2.79E-03	3.17E-03
UAMN 511	-1.42E-04	5.37E-04	5.95E-04	1.17E-03	3.79E-04	-2.04E-03	6.88E-04	-6.05E-04
SNOMNH 11542	-6.37E-04	4.10E-03	5.56E-04	1.33E-03	-1.43E-03	2.01E-03	5.44E-04	2.75E-03
SNOMNH 11543	-3.39E-03	-3.80E-03	-8.62E-04	-8.17E-04	2.86E-04	1.19E-03	-1.83E-03	2.81E-03
SNOMNH 11544	2.55E-04	-3.77E-03	-5.92E-04	-5.42E-04	8.35E-04	2.36E-03	5.70E-06	-4.20E-04
SNOMNH 11545	-4.44E-03	6.95E-05	1.13E-03	3.64E-04	-6.39E-04	-6.85E-05	-1.35E-03	-1.53E-03
SNOMNH 11546	6.54E-04	3.51E-03	-2.33E-03	1.65E-04	2.42E-04	1.98E-03	1.69E-03	-4.90E-03
SNOMNH 11547	7.85E-04	-5.17E-03	-8.40E-04	-8.25E-04	5.11E-03	4.39E-03	1.02E-04	-7.24E-04
SNOMNH 11548	3.48E-03	-6.29E-03	9.39E-04	1.21E-03	1.41E-03	-1.90E-03	-1.19E-03	-4.04E-04
SNOMNH 11549	4.35E-03	-6.65E-04	3.49E-04	-4.84E-04	-4.64E-04	-1.31E-03	2.76E-03	4.23E-03
SNOMNH 11550	-1.80E-04	1.99E-03	3.11E-04	-4.15E-03	-3.07E-04	2.39E-03	-2.70E-04	1.95E-03
SNOMNH 11551	1.50E-03	2.54E-03	-9.18E-04	-1.15E-03	1.16E-03	-3.92E-04	1.59E-03	-2.17E-03
UAMN 11236	4.34E-03	3.07E-04	-2.20E-03	-2.54E-03	-1.56E-03	-3.28E-03	-4.68E-03	-3.11E-03
UAMN 11237	1.00E-03	-4.46E-04	-3.14E-03	1.00E-03	-2.56E-03	1.19E-03	-7.62E-04	8.59E-04

Humerus continued

Specimen	PC10	PC11	PC12	PC13	PC14	PC15	PC16	PC17
UAMN 13542	-7.17E-03	1.07E-04	-8.33E-04	9.00E-04	-6.13E-04	-2.41E-04	-2.08E-03	-5.29E-04
USNM 546139	-4.10E-03	-2.00E-03	1.35E-03	2.42E-03	-3.72E-04	-2.76E-03	-2.90E-04	8.86E-04
USNM 546140	3.68E-03	-7.03E-04	6.13E-03	2.08E-03	2.58E-03	-1.57E-04	-2.86E-03	-5.94E-04
USNM 546141	-5.45E-04	-3.52E-03	7.64E-04	2.91E-03	1.93E-03	-2.99E-03	1.21E-03	-8.11E-05
UAMN 22678	2.47E-03	3.75E-04	4.37E-03	-4.02E-03	-2.21E-03	2.85E-05	-8.31E-04	-3.43E-04
UAMN 22680	-1.18E-03	1.52E-03	1.47E-03	-1.81E-03	-3.97E-03	1.21E-03	2.95E-03	8.17E-04
UAMN 22736	3.03E-03	-1.93E-03	1.35E-03	1.88E-03	-6.15E-03	5.07E-03	-3.29E-04	4.43E-04
UAMN 24794	-1.09E-03	3.96E-03	1.24E-03	-9.98E-04	2.02E-04	1.46E-04	-1.86E-03	1.24E-03
UAMN 24805	2.80E-03	1.22E-03	-2.05E-03	7.61E-04	-8.00E-04	5.18E-04	5.49E-04	-2.94E-03
UAMN 24808	-3.11E-03	1.64E-03	-1.51E-03	-8.82E-04	-4.73E-03	-4.41E-03	-2.28E-03	-1.98E-04
UAMN 47308	4.13E-03	1.79E-03	-1.73E-03	5.16E-03	1.34E-03	1.01E-04	-1.58E-03	1.16E-03
UAMN 101819	3.58E-03	-3.68E-03	-6.70E-04	-3.72E-03	-1.17E-04	-5.05E-04	-4.16E-04	-4.51E-04
UAMN 101828	1.91E-03	-1.11E-03	-1.56E-03	5.00E-03	-2.64E-03	5.61E-04	1.31E-03	1.58E-03
UAMN 101851	1.69E-03	-4.31E-05	4.27E-03	-2.21E-03	-1.16E-03	-2.80E-03	5.02E-03	-2.11E-03
UAMN 59579	-6.21E-04	5.86E-03	4.55E-03	4.91E-03	2.96E-03	-7.11E-04	7.48E-05	3.63E-04
FMNH 31142	-5.29E-03	-3.00E-03	-6.91E-04	-1.39E-03	2.26E-04	1.86E-03	4.92E-05	-5.02E-04
FMNH 31328	-2.50E-03	1.87E-04	5.30E-04	-3.05E-03	1.77E-03	-1.68E-03	-1.24E-03	2.51E-03

Radius

Specimen	PC1	PC2	PC3	PC4	PC5	PC6	PC7	PC8	PC9
USNM 265584	-5.21E-03	-2.28E-03	5.39E-03	-6.85E-03	-3.57E-04	-4.67E-03	3.14E-04	3.68E-03	-5.40E-03
USNM 265585	2.18E-03	1.20E-02	-3.76E-03	-5.35E-03	-1.76E-03	9.38E-04	6.82E-03	4.05E-03	-7.40E-03
USNM 266142	4.90E-03	-2.31E-03	9.49E-03	6.45E-03	-8.95E-03	-2.72E-03	-1.81E-03	5.60E-03	-1.44E-03
UAMN 509	4.29E-03	-6.84E-03	2.33E-04	3.36E-03	-6.25E-03	-2.37E-03	5.25E-03	-3.81E-03	-3.91E-03
UAMN 511	1.48E-03	-1.60E-02	-6.84E-04	9.26E-03	-5.65E-04	-5.19E-05	-7.40E-03	-5.56E-03	3.55E-03
SNOMNH 11542	-4.91E-03	9.34E-03	2.92E-03	-3.30E-03	-4.29E-03	-2.14E-03	-2.69E-03	9.18E-03	2.67E-03
SNOMNH 11544	6.09E-03	1.16E-02	4.80E-04	6.51E-03	3.65E-03	-8.25E-03	4.77E-03	-3.44E-03	2.29E-03
SNOMNH 11545	3.74E-03	-5.59E-03	6.30E-03	-1.75E-03	1.17E-02	1.40E-03	-3.18E-04	-2.02E-03	-6.72E-03
SNOMNH 11546	-4.68E-03	-6.21E-03	-1.02E-02	-2.28E-03	8.80E-03	4.05E-03	3.02E-03	1.10E-03	-2.30E-03
SNOMNH 11547	-1.12E-02	-5.10E-04	7.69E-03	-2.54E-04	6.48E-03	4.71E-03	-1.45E-03	2.26E-03	-2.39E-03
SNOMNH 11549	-3.77E-03	4.83E-03	-6.65E-03	1.57E-03	2.59E-03	-1.20E-04	-3.46E-03	3.13E-03	-1.60E-03
SNOMNH 11551	-4.76E-04	7.24E-03	-8.03E-03	5.62E-03	6.15E-03	-6.32E-03	-1.82E-04	3.50E-03	2.58E-04
UAMN 11236	-1.22E-03	-1.32E-02	6.33E-03	-9.16E-04	-5.19E-04	2.04E-03	-3.31E-03	6.50E-03	2.60E-03
UAMN 11237	-2.00E-03	4.46E-03	7.62E-04	-9.59E-03	-5.54E-04	1.94E-03	-1.61E-04	8.39E-04	9.49E-03

Radius continued

Specimen	PC1	PC2	PC3	PC4	PC5	PC6	PC7	PC8	PC9
UAMN 13542	3.43E-02	-6.19E-03	-1.00E-02	-1.09E-02	-1.23E-03	-4.92E-03	5.96E-04	3.78E-04	3.17E-03
USNM 546139	-2.25E-03	-7.12E-03	6.75E-03	4.86E-03	5.72E-03	-5.31E-04	6.46E-03	2.35E-03	4.66E-03
USNM 546140	-3.94E-03	-8.91E-03	-8.84E-03	-1.08E-03	-7.27E-03	9.66E-04	1.26E-03	-1.92E-03	-3.11E-03
USNM 546141	6.28E-03	6.10E-03	5.01E-03	-1.75E-03	-4.67E-03	4.62E-03	-4.95E-03	2.77E-03	7.13E-04
UAMN 22678	-9.74E-03	-1.43E-03	-1.97E-02	4.20E-03	-5.35E-03	4.22E-03	5.43E-03	5.27E-04	6.07E-04
UAMN 22680	-1.39E-03	2.15E-03	-2.77E-03	-5.18E-03	5.04E-03	8.12E-03	6.78E-03	-1.75E-03	5.00E-03
UAMN 22736	-6.35E-04	-1.03E-03	6.21E-03	1.88E-03	-1.34E-02	5.62E-03	4.60E-03	-3.61E-04	-7.05E-04
UAMN 24794	-4.89E-04	1.35E-02	-5.06E-05	1.16E-02	-2.53E-03	-3.50E-04	-2.56E-03	-7.69E-03	-1.13E-04
UAMN 24805	-7.84E-03	9.31E-03	6.01E-04	3.08E-03	-4.68E-04	-2.04E-04	-1.68E-03	-2.93E-03	6.38E-03
UAMN 24808	-6.69E-03	-4.19E-03	1.20E-02	-4.98E-03	-2.71E-03	-1.08E-03	6.31E-03	-7.56E-03	-3.02E-04
UAMN 47308	-1.51E-02	-8.62E-04	-9.70E-03	-1.21E-02	-2.88E-03	-5.15E-03	-1.10E-02	-4.20E-03	-2.14E-03
UAMN 101819	1.63E-02	6.13E-03	-9.55E-04	6.90E-03	2.74E-03	1.40E-02	-7.11E-03	-9.09E-04	-3.47E-03
UAMN 101828	-3.20E-03	-9.08E-03	-6.33E-03	9.74E-03	2.34E-03	-5.23E-03	-7.72E-04	2.96E-03	7.02E-04
UAMN 101851	3.33E-03	1.63E-03	5.95E-03	7.34E-03	3.24E-03	-6.34E-03	1.85E-04	1.43E-03	-2.28E-03
UAMN 59579	-9.68E-04	-2.23E-03	5.96E-03	-5.58E-03	4.35E-03	2.66E-04	-3.92E-04	-1.39E-03	3.80E-03
FMNH 31328	2.74E-03	5.64E-03	5.77E-03	-1.06E-02	9.72E-04	-2.47E-03	-2.56E-03	-6.69E-03	-2.61E-03

Radius continued

Specimen	PC10	PC11	PC12
USNM 265584	1.55E-03	-1.76E-03	6.50E-04
USNM 265585	1.23E-03	-6.40E-03	-4.01E-03
USNM 266142	-3.22E-03	-1.24E-03	-1.57E-03
UAMN 509	-5.01E-04	-1.25E-03	-1.81E-03
UAMN 511	3.69E-04	-4.18E-03	-1.82E-03
SNOMNH 11542	2.60E-03	3.13E-03	-3.10E-04
SNOMNH 11544	1.13E-03	5.43E-04	3.18E-03
SNOMNH 11545	9.28E-04	3.83E-03	3.11E-03
SNOMNH 11546	-2.80E-03	-1.86E-04	-4.13E-04
SNOMNH 11547	-2.68E-03	3.43E-03	-4.24E-03
SNOMNH 11549	-9.12E-04	-1.62E-03	1.08E-03
SNOMNH 11551	-2.67E-03	1.16E-03	5.24E-04
UAMN 11236	3.34E-04	9.29E-04	-1.20E-03
UAMN 11237	1.88E-04	3.10E-03	1.55E-03

Radius continued

Specimen	PC10	PC11	PC12
UAMN 13542	-8.00E-04	2.06E-03	-2.46E-03
USNM 546139	-3.48E-03	-2.36E-03	6.84E-03
USNM 546140	-4.15E-03	4.48E-03	3.45E-03
USNM 546141	-8.53E-03	-2.08E-03	1.54E-03
UAMN 22678	7.25E-04	4.06E-03	-1.56E-03
UAMN 22680	1.02E-03	-3.99E-03	5.12E-04
UAMN 22736	6.67E-03	2.13E-04	5.65E-03
UAMN 24794	-1.01E-03	3.20E-03	-9.48E-04
UAMN 24805	-1.56E-03	-3.23E-03	-3.51E-03
UAMN 24808	-3.06E-03	1.81E-03	-5.52E-03
UAMN 47308	1.82E-03	-7.95E-04	2.20E-03
UAMN 101819	3.30E-03	8.33E-05	2.02E-04
UAMN 101828	4.03E-03	-5.45E-03	-4.67E-04
UAMN 101851	3.04E-03	4.91E-03	-7.25E-04
UAMN 59579	7.23E-03	1.08E-03	-3.58E-03
FMNH 31328	-7.90E-04	-3.48E-03	3.66E-03

Ulna

Specimen	PC1	PC2	PC3	PC4	PC5	PC6	PC7	PC8	PC9
USNM 265585	3.65E-03	-3.71E-03	1.37E-03	-6.12E-03	4.12E-03	-5.90E-04	4.08E-03	-2.11E-03	2.93E-03
USNM 266142	-5.95E-03	-6.31E-03	-6.45E-03	8.97E-03	1.13E-03	-1.88E-03	-1.03E-03	-2.74E-03	-2.92E-03
UAMN 509	3.72E-03	-1.02E-02	-5.15E-03	-4.74E-03	-4.44E-03	5.89E-03	-7.43E-03	-1.65E-03	2.18E-03
UAMN 511	1.72E-03	1.86E-02	-4.05E-03	1.88E-03	6.42E-04	5.03E-03	-5.13E-03	-6.81E-03	4.11E-03
SNOMNH 11542	-5.47E-03	9.93E-03	6.45E-03	2.74E-03	-3.29E-03	-2.70E-03	-1.11E-03	-3.92E-03	-1.05E-03
SNOMNH 11544	-5.66E-03	-2.19E-03	-5.51E-04	-1.10E-03	-9.39E-05	8.21E-04	-3.24E-03	6.72E-04	6.70E-03
SNOMNH 11545	-3.70E-03	-8.60E-03	1.00E-02	-6.94E-03	1.02E-03	2.00E-03	1.25E-03	3.65E-03	2.85E-04
SNOMNH 11546	-7.43E-03	-3.33E-04	5.30E-03	8.88E-03	4.52E-03	1.72E-03	8.06E-04	7.14E-03	5.64E-03
SNOMNH 11547	-7.32E-03	2.05E-03	4.69E-03	-2.05E-03	1.10E-03	2.55E-03	-2.13E-04	-2.38E-03	4.75E-03
SNOMNH 11549	-9.95E-03	-1.95E-03	1.73E-04	9.04E-03	2.53E-03	-8.64E-03	-2.03E-03	2.21E-03	5.23E-03
SNOMNH 11551	-1.13E-02	-2.81E-03	-6.31E-04	-6.99E-04	3.94E-03	1.09E-03	4.14E-03	5.35E-03	3.95E-03
UAMN 11236	-5.68E-03	6.93E-03	2.43E-03	-8.38E-03	-4.92E-04	-7.43E-03	-4.18E-03	8.03E-03	-5.79E-03
UAMN 11237	-2.46E-03	1.85E-04	-1.11E-03	-1.03E-03	2.67E-04	1.15E-03	2.24E-03	1.54E-03	3.58E-03

Ulna continued

Specimen	PC1	PC2	PC3	PC4	PC5	PC6	PC7	PC8	PC9
UAMN 13542	2.94E-02	-1.15E-03	6.66E-03	7.62E-04	-1.04E-02	-4.56E-03	-6.44E-03	4.22E-04	4.93E-03
USNM 546139	5.75E-03	-8.44E-04	-3.73E-03	3.90E-04	-1.02E-04	-3.02E-03	1.46E-02	-3.04E-03	-1.37E-03
USNM 546140	2.04E-02	-1.56E-03	1.33E-03	-4.30E-03	5.20E-03	-3.36E-03	3.14E-03	2.46E-03	-5.76E-04
USNM 546141	9.26E-03	-5.70E-03	-1.04E-02	4.61E-03	9.54E-03	1.69E-03	-7.20E-03	2.62E-04	-3.44E-03
UAMN 22678	-3.34E-05	-7.52E-03	5.01E-03	5.94E-04	-6.46E-03	3.77E-03	-3.05E-03	6.14E-03	-5.39E-03
UAMN 22680	4.15E-03	8.48E-03	-1.46E-02	9.91E-03	-1.23E-02	4.38E-03	5.15E-03	7.00E-03	-7.45E-04
UAMN 22736	-5.95E-03	1.03E-02	-7.67E-04	6.45E-04	6.12E-03	-4.34E-03	-4.27E-03	2.62E-03	-6.51E-03
UAMN 24794	-1.11E-02	6.39E-04	-4.03E-03	-1.28E-02	-5.83E-03	6.53E-03	2.84E-03	-2.56E-03	-2.81E-04
UAMN 24805	-1.33E-02	-3.90E-03	-2.04E-03	5.23E-04	-4.11E-03	-5.50E-03	-3.11E-03	-5.85E-03	-3.98E-03
UAMN 24808	1.30E-02	2.41E-03	8.90E-04	-1.89E-03	2.08E-03	-1.95E-03	3.37E-03	3.93E-04	-4.83E-03
UAMN 47308	-6.86E-04	-4.87E-03	-1.20E-02	-7.77E-03	2.96E-03	-7.64E-04	-9.25E-04	-2.08E-03	-2.50E-03
UAMN 101819	9.25E-03	4.18E-03	6.89E-03	3.69E-03	1.23E-02	9.18E-03	-1.67E-04	-3.12E-03	-1.86E-03
UAMN 101828	-4.37E-03	3.50E-04	1.24E-02	5.21E-03	-5.04E-03	1.10E-02	1.16E-03	-1.21E-03	-6.69E-03
UAMN 101851	-1.91E-03	1.06E-02	4.67E-03	-6.52E-03	-3.05E-03	-7.10E-03	9.81E-04	-2.79E-03	1.44E-03
UAMN 59579	-2.88E-03	-1.32E-02	4.34E-03	7.98E-03	-3.60E-03	-5.73E-03	1.46E-03	-7.83E-03	-1.34E-03
FMNH 31142	-3.69E-04	-1.15E-03	-7.16E-03	-5.16E-03	8.04E-04	1.86E-03	-8.95E-04	1.18E-03	3.06E-03
FMNH 31328	5.31E-03	1.42E-03	6.01E-06	3.69E-03	9.96E-04	-1.10E-03	5.21E-03	-9.82E-04	4.94E-04

Ulna continued

Specimen	PC10	PC11	PC12	PC13	PC14	PC15
USNM 265585	-9.67E-04	-7.60E-04	8.90E-04	2.55E-03	-1.55E-03	4.00E-03
USNM 266142	2.99E-03	2.59E-03	1.04E-03	3.38E-03	-1.78E-03	2.42E-03
UAMN 509	-2.13E-03	-2.14E-04	-4.43E-03	3.39E-04	-2.50E-03	-6.36E-03
UAMN 511	-9.69E-04	2.03E-03	5.57E-03	-1.87E-03	-2.70E-03	-5.27E-04
SNOMNH 11542	4.23E-03	-9.90E-04	-2.18E-03	-2.72E-03	9.43E-04	-5.90E-04
SNOMNH 11544	4.61E-03	-1.88E-03	1.53E-03	2.69E-03	6.48E-03	2.54E-03
SNOMNH 11545	9.26E-04	-4.62E-03	2.22E-03	-2.37E-03	-1.92E-03	1.42E-03
SNOMNH 11546	-8.57E-04	3.47E-03	9.29E-04	4.67E-03	-3.82E-03	-5.91E-04
SNOMNH 11547	1.95E-04	-6.78E-03	-2.94E-03	2.26E-03	-2.18E-03	7.96E-04
SNOMNH 11549	-2.74E-03	-1.00E-03	3.82E-04	-2.77E-04	4.11E-03	-4.20E-03
SNOMNH 11551	-2.80E-03	3.40E-03	-2.57E-03	-3.95E-03	-6.43E-04	1.52E-03
UAMN 11236	-2.81E-03	1.42E-03	7.01E-03	-2.43E-03	-1.98E-03	-5.94E-04
UAMN 11237	3.31E-03	6.54E-03	-1.45E-03	-5.58E-03	3.35E-03	3.95E-05

Ulna continued

Specimen	PC10	PC11	PC12	PC13	PC14	PC15
UAMN 13542	-9.31E-04	4.07E-03	-1.75E-03	-9.27E-04	2.66E-04	2.69E-03
USNM 546139	4.14E-04	-6.37E-04	-6.41E-04	-2.53E-03	1.82E-03	-1.59E-03
USNM 546140	3.38E-03	-1.64E-03	2.13E-03	4.47E-03	1.42E-03	-4.62E-03
USNM 546141	7.91E-04	-2.57E-03	4.17E-03	-4.59E-04	3.40E-03	1.55E-03
UAMN 22678	-1.13E-03	-2.87E-03	-1.01E-03	-2.54E-03	1.24E-03	6.40E-05
UAMN 22680	-3.26E-04	-6.40E-03	9.30E-05	-1.45E-04	-7.21E-04	9.03E-04
UAMN 22736	5.92E-03	2.36E-04	-7.12E-03	1.60E-03	-1.61E-03	-9.80E-04
UAMN 24794	-1.04E-03	1.41E-03	3.75E-03	3.11E-03	1.97E-03	-2.17E-03
UAMN 24805	-1.14E-02	-2.26E-04	-2.25E-03	1.90E-03	2.20E-03	1.98E-03
UAMN 24808	-3.50E-03	1.19E-03	-1.98E-03	3.22E-03	-6.90E-04	2.07E-03
UAMN 47308	3.78E-03	4.08E-03	-2.13E-03	-2.04E-03	-4.33E-04	8.78E-04
UAMN 101819	-5.59E-03	-3.93E-03	-1.45E-03	-4.06E-03	1.14E-03	-2.43E-04
UAMN 101828	3.86E-03	5.41E-03	6.69E-04	2.98E-03	2.45E-03	8.98E-05
UAMN 101851	1.51E-03	-3.67E-03	-1.22E-03	1.14E-03	1.23E-03	3.01E-04
UAMN 59579	4.93E-03	-2.24E-03	4.10E-03	-3.09E-03	-4.55E-03	-1.04E-03
FMNH 31142	2.15E-03	-4.14E-04	-1.86E-03	-4.73E-04	-3.58E-03	1.84E-03
FMNH 31328	-5.85E-03	5.01E-03	4.82E-04	1.17E-03	-1.35E-03	-1.59E-03

Femur

Specimen	PC1	PC2	PC3	PC4	PC5	PC6	PC7	PC8	PC9
USNM 265584	7.40E-03	-1.56E-03	1.09E-02	-1.07E-03	8.40E-04	-8.75E-04	5.53E-03	-2.60E-03	5.40E-03
USNM 265585	1.24E-02	8.50E-04	-2.11E-04	-1.59E-03	-9.96E-03	3.63E-03	6.33E-04	1.46E-03	3.57E-03
USNM 266142	1.04E-02	6.67E-03	8.37E-03	5.70E-03	-4.05E-03	-9.89E-03	-1.99E-03	-4.28E-04	1.24E-05
UAMN 509	-1.40E-02	-9.85E-03	4.54E-03	5.20E-03	-2.86E-03	8.53E-04	-4.06E-03	-7.61E-04	-1.60E-03
UAMN 511	5.62E-03	-7.79E-04	-1.93E-02	8.47E-03	1.97E-03	-9.84E-03	-9.94E-04	-1.61E-03	4.52E-03
SNOMNH 11542	-7.05E-03	-4.50E-03	-7.21E-03	5.81E-03	5.99E-06	9.18E-04	5.23E-03	2.83E-04	9.60E-04
SNOMNH 11543	1.31E-02	-5.30E-03	-2.28E-03	-1.67E-03	5.24E-03	5.30E-03	-4.75E-03	6.96E-04	-6.45E-03
SNOMNH 11544	5.82E-03	-8.19E-03	-1.29E-03	-3.34E-03	1.50E-03	-2.93E-03	5.74E-03	5.27E-03	-1.94E-03
SNOMNH 11545	-8.62E-03	-5.91E-03	-5.26E-03	-9.68E-03	4.54E-03	7.94E-03	2.77E-03	-1.12E-03	5.86E-03
SNOMNH 11546	-4.17E-03	5.26E-04	-4.27E-03	6.01E-04	4.44E-03	4.78E-03	-8.55E-03	-1.38E-04	-1.89E-03
SNOMNH 11547	-8.49E-03	-5.85E-03	-2.07E-03	-1.65E-03	-1.78E-03	-3.45E-04	2.95E-03	1.82E-04	2.70E-03
SNOMNH 11548	4.87E-03	-3.50E-03	1.20E-03	5.87E-03	7.72E-03	3.85E-03	-2.87E-03	1.57E-03	4.68E-03
SNOMNH 11549	2.69E-03	1.07E-03	3.87E-05	-9.38E-04	5.23E-03	9.20E-04	4.19E-03	-4.07E-03	3.78E-03
SNOMNH 11550	-7.04E-04	1.28E-02	-3.24E-03	-5.81E-03	6.65E-03	-5.19E-03	-1.31E-03	-9.20E-03	5.78E-04
SNOMNH 11551	9.80E-04	1.16E-03	8.66E-04	-3.58E-04	1.04E-02	-4.16E-04	3.83E-03	2.69E-03	-8.39E-03
UAMN 11236	-4.48E-04	2.85E-03	4.02E-03	7.71E-03	-5.61E-04	7.16E-04	1.38E-03	-5.07E-04	2.96E-03
UAMN 11237	1.16E-02	1.41E-03	-2.02E-04	1.20E-03	-1.22E-03	9.30E-04	6.21E-03	-3.25E-03	-2.10E-03

Femur continued

Specimen	PC1	PC2	PC3	PC4	PC5	PC6	PC7	PC8	PC9
UAMN 13542	5.81E-03	-4.21E-03	-2.40E-03	1.83E-03	-1.08E-03	2.62E-03	-6.81E-03	-2.25E-03	7.25E-04
USNM 546139	-8.07E-03	3.16E-03	3.38E-03	-3.87E-03	-4.12E-03	1.15E-03	-1.39E-03	-6.38E-03	1.96E-03
USNM 546140	-8.14E-03	5.55E-03	3.82E-03	-2.84E-03	-7.84E-04	-2.37E-03	3.08E-03	-3.43E-05	-2.35E-03
USNM 546141	-1.59E-03	1.01E-02	-2.47E-03	-1.22E-04	-6.10E-03	6.34E-03	7.60E-04	-3.32E-03	-3.27E-03
UAMN 22678	-3.60E-03	-1.33E-02	7.82E-03	-5.67E-04	3.26E-03	-4.56E-03	-5.59E-03	-1.94E-03	1.66E-03
UAMN 24794	-5.04E-03	1.06E-03	3.41E-03	-2.10E-03	-2.50E-03	2.90E-03	-2.86E-03	1.00E-03	4.57E-04
UAMN 24805	8.66E-04	3.62E-04	3.90E-03	9.45E-03	-4.02E-03	4.31E-03	-5.23E-04	-2.56E-03	-1.50E-03
UAMN 24808	-3.19E-03	1.76E-03	2.36E-03	-1.73E-04	-1.80E-03	-5.50E-04	-4.06E-04	7.89E-03	4.57E-03
UAMN 22680	-7.97E-03	1.27E-02	-1.76E-03	-2.11E-03	3.34E-04	1.15E-03	8.07E-04	-1.98E-03	-1.19E-03
UAMN 22736	-4.51E-04	-5.80E-03	-1.47E-03	-4.70E-03	-2.58E-03	-5.22E-03	5.23E-03	2.62E-03	-4.54E-03
UAMN 47308	6.03E-03	-3.78E-03	4.02E-03	-1.00E-02	7.88E-04	-8.03E-03	-6.26E-03	-2.21E-03	-1.65E-03
UAMN 101819	1.24E-02	-4.83E-03	-5.28E-04	-5.67E-03	-2.23E-03	4.36E-03	2.21E-03	2.70E-03	1.89E-03
UAMN 101828	-1.07E-03	-8.90E-03	9.72E-04	6.34E-03	7.67E-05	2.92E-03	1.90E-03	-1.55E-03	-5.05E-03
UAMN 101851	-1.61E-02	-5.58E-04	1.85E-03	3.58E-03	1.12E-03	-5.57E-03	3.49E-03	2.09E-03	-1.88E-03
UAMN 59579	-4.21E-04	-6.83E-04	-8.43E-03	-3.29E-03	-1.27E-02	-8.85E-04	-2.09E-03	-4.27E-04	-4.34E-03
FMNH 31142	-4.46E-03	7.84E-03	-2.10E-03	-3.73E-03	-8.14E-04	-2.97E-03	-5.19E-03	1.20E-02	2.59E-03
FMNH 31328	3.57E-03	1.77E-02	3.00E-03	3.55E-03	5.03E-03	4.09E-03	-2.92E-04	5.89E-03	-7.16E-04

Femur continued

Specimen	PC10	PC11	PC12	PC13	PC14	PC15	PC16	PC17
USNM 265584	-2.14E-03	4.62E-04	-6.07E-03	2.94E-03	1.72E-04	1.25E-04	1.31E-03	-1.79E-03
USNM 265585	9.17E-04	6.40E-03	-7.62E-04	-2.63E-03	4.40E-03	2.80E-03	-1.79E-03	4.88E-04
USNM 266142	-5.69E-03	-1.54E-03	2.76E-03	-5.22E-04	1.61E-03	6.82E-04	3.01E-03	-1.86E-03
UAMN 509	1.67E-03	1.09E-03	-5.90E-03	-2.48E-03	3.11E-03	-3.37E-03	2.79E-03	3.17E-03
UAMN 511	-1.42E-04	5.37E-04	5.95E-04	1.17E-03	3.79E-04	-2.04E-03	6.88E-04	-6.05E-04
SNOMNH 11542	-6.37E-04	4.10E-03	5.56E-04	1.33E-03	-1.43E-03	2.01E-03	5.44E-04	2.75E-03
SNOMNH 11543	-3.39E-03	-3.80E-03	-8.62E-04	-8.17E-04	2.86E-04	1.19E-03	-1.83E-03	2.81E-03
SNOMNH 11544	2.55E-04	-3.77E-03	-5.92E-04	-5.42E-04	8.35E-04	2.36E-03	5.70E-06	-4.20E-04
SNOMNH 11545	-4.44E-03	6.95E-05	1.13E-03	3.64E-04	-6.39E-04	-6.85E-05	-1.35E-03	-1.53E-03
SNOMNH 11546	6.54E-04	3.51E-03	-2.33E-03	1.65E-04	2.42E-04	1.98E-03	1.69E-03	-4.90E-03
SNOMNH 11547	7.85E-04	-5.17E-03	-8.40E-04	-8.25E-04	5.11E-03	4.39E-03	1.02E-04	-7.24E-04
SNOMNH 11548	3.48E-03	-6.29E-03	9.39E-04	1.21E-03	1.41E-03	-1.90E-03	-1.19E-03	-4.04E-04
SNOMNH 11549	4.35E-03	-6.65E-04	3.49E-04	-4.84E-04	-4.64E-04	-1.31E-03	2.76E-03	4.23E-03
SNOMNH 11550	-1.80E-04	1.99E-03	3.11E-04	-4.15E-03	-3.07E-04	2.39E-03	-2.70E-04	1.95E-03
SNOMNH 11551	1.50E-03	2.54E-03	-9.18E-04	-1.15E-03	1.16E-03	-3.92E-04	1.59E-03	-2.17E-03
UAMN 11236	4.34E-03	3.07E-04	-2.20E-03	-2.54E-03	-1.56E-03	-3.28E-03	-4.68E-03	-3.11E-03
UAMN 11237	1.00E-03	-4.46E-04	-3.14E-03	1.00E-03	-2.56E-03	1.19E-03	-7.62E-04	8.59E-04

Femur continued

Specimen	PC10	PC11	PC12	PC13	PC14	PC15	PC16	PC17
UAMN 13542	-7.17E-03	1.07E-04	-8.33E-04	9.00E-04	-6.13E-04	-2.41E-04	-2.08E-03	-5.29E-04
USNM 546139	-4.10E-03	-2.00E-03	1.35E-03	2.42E-03	-3.72E-04	-2.76E-03	-2.90E-04	8.86E-04
USNM 546140	3.68E-03	-7.03E-04	6.13E-03	2.08E-03	2.58E-03	-1.57E-04	-2.86E-03	-5.94E-04
USNM 546141	-5.45E-04	-3.52E-03	7.64E-04	2.91E-03	1.93E-03	-2.99E-03	1.21E-03	-8.11E-05
UAMN 22678	2.47E-03	3.75E-04	4.37E-03	-4.02E-03	-2.21E-03	2.85E-05	-8.31E-04	-3.43E-04
UAMN 24794	-1.18E-03	1.52E-03	1.47E-03	-1.81E-03	-3.97E-03	1.21E-03	2.95E-03	8.17E-04
UAMN 24805	3.03E-03	-1.93E-03	1.35E-03	1.88E-03	-6.15E-03	5.07E-03	-3.29E-04	4.43E-04
UAMN 24808	-1.09E-03	3.96E-03	1.24E-03	-9.98E-04	2.02E-04	1.46E-04	-1.86E-03	1.24E-03
UAMN 22680	2.80E-03	1.22E-03	-2.05E-03	7.61E-04	-8.00E-04	5.18E-04	5.49E-04	-2.94E-03
UAMN 22736	-3.11E-03	1.64E-03	-1.51E-03	-8.82E-04	-4.73E-03	-4.41E-03	-2.28E-03	-1.98E-04
UAMN 47308	4.13E-03	1.79E-03	-1.73E-03	5.16E-03	1.34E-03	1.01E-04	-1.58E-03	1.16E-03
UAMN 101819	1.69E-03	-4.31E-05	4.27E-03	-2.21E-03	-1.16E-03	-2.80E-03	5.02E-03	-2.11E-03
UAMN 101828	-6.21E-04	5.86E-03	4.55E-03	4.91E-03	2.96E-03	-7.11E-04	7.48E-05	3.63E-04
UAMN 101851	-5.29E-03	-3.00E-03	-6.91E-04	-1.39E-03	2.26E-04	1.86E-03	4.92E-05	-5.02E-04
UAMN 59579	3.58E-03	-3.68E-03	-6.70E-04	-3.72E-03	-1.17E-04	-5.05E-04	-4.16E-04	-4.51E-04
FMNH 31142	1.91E-03	-1.11E-03	-1.56E-03	5.00E-03	-2.64E-03	5.61E-04	1.31E-03	1.58E-03
FMNH 31328	-2.50E-03	1.87E-04	5.30E-04	-3.05E-03	1.77E-03	-1.68E-03	-1.24E-03	2.51E-03

Tibia

Specimen	PC1	PC2	PC3	PC4	PC5	PC6	PC7	PC8	PC9
USNM 265584	1.29E-02	1.54E-03	-2.85E-03	-7.60E-03	-7.14E-03	-1.48E-03	4.76E-03	2.27E-03	-1.16E-03
UAMN 509	-1.11E-02	-4.87E-03	8.78E-03	2.26E-03	7.93E-04	-3.69E-03	4.60E-03	7.33E-06	-1.77E-03
UAMN 511	9.36E-03	-3.10E-03	-5.15E-04	1.41E-03	-2.04E-03	-2.14E-03	-6.77E-04	-2.80E-03	-4.21E-03
SNOMNH 11542	-7.83E-03	-8.87E-05	-7.24E-04	-3.23E-03	-7.97E-03	3.51E-04	-3.12E-03	1.84E-03	3.68E-03
SNOMNH 11543	2.59E-03	3.92E-03	-3.20E-03	-4.14E-03	2.67E-03	3.50E-03	-3.42E-03	-4.52E-03	5.65E-03
SNOMNH 11544	-6.54E-03	5.14E-03	-9.82E-03	1.89E-03	3.08E-03	-1.54E-03	1.03E-03	6.47E-05	-1.33E-03
SNOMNH 11545	2.91E-03	6.49E-03	8.01E-04	2.88E-03	6.98E-03	6.70E-03	-1.27E-03	-6.63E-03	-3.36E-03
SNOMNH 11546	-8.44E-03	4.12E-03	1.57E-03	2.02E-03	-5.14E-03	4.49E-03	2.21E-03	4.30E-04	-2.21E-03
SNOMNH 11547	-6.67E-03	8.30E-03	-9.14E-04	-5.72E-04	-8.25E-04	2.17E-03	-1.21E-03	-1.28E-04	-1.03E-03
SNOMNH 11548	-7.86E-04	-6.54E-04	6.40E-05	-2.03E-03	-1.99E-03	6.45E-03	-3.12E-03	1.44E-03	-5.78E-03
SNOMNH 11549	1.93E-03	1.10E-02	6.13E-04	-2.48E-03	2.38E-03	-1.35E-02	4.86E-04	-4.28E-03	2.40E-03
SNOMNH 11550	4.85E-03	-4.73E-03	-1.36E-02	2.56E-03	8.04E-04	3.55E-03	-4.16E-03	5.19E-03	2.67E-04
SNOMNH 11551	-8.65E-03	1.31E-03	-4.16E-03	-2.74E-03	-2.18E-03	-3.91E-04	-1.98E-03	-1.65E-03	-2.53E-03
UAMN 11236	-1.54E-03	-8.92E-03	7.50E-04	-4.56E-03	5.53E-03	-1.05E-03	-4.20E-03	-1.91E-04	1.54E-03
UAMN 11237	-2.46E-04	8.20E-03	6.56E-03	-5.91E-03	-5.25E-03	4.99E-03	2.25E-03	1.10E-03	1.41E-03

Tibia continued

Specimen	PC1	PC2	PC3	PC4	PC5	PC6	PC7	PC8	PC9
UAMN 13542	6.48E-03	1.15E-02	4.52E-03	4.93E-03	-1.47E-03	1.52E-03	4.05E-04	7.30E-03	3.37E-03
USNM 546139	1.00E-02	-2.49E-03	6.95E-03	-5.82E-03	1.12E-02	5.48E-04	3.24E-03	7.29E-03	1.35E-03
USNM 546140	-5.27E-03	4.41E-03	5.57E-03	1.14E-03	2.53E-03	-3.90E-03	-1.49E-03	9.95E-05	-4.45E-03
USNM 546141	9.37E-03	-3.60E-03	-6.55E-03	9.58E-03	-5.66E-03	-2.80E-03	3.55E-03	-3.02E-03	6.38E-04
UAMN 22678	2.44E-03	-1.43E-03	1.78E-03	-2.95E-03	-1.59E-03	2.38E-03	1.00E-03	-6.12E-03	4.24E-03
UAMN 22680	3.25E-03	-5.08E-03	3.80E-04	-1.04E-02	-2.84E-03	-1.36E-03	-4.93E-03	2.65E-03	-1.87E-03
UAMN 22736	1.31E-03	-6.88E-03	-6.05E-03	-4.03E-03	4.97E-03	2.87E-03	1.16E-02	-2.78E-03	-4.99E-03
UAMN 24794	-1.09E-03	-5.82E-03	6.25E-03	3.16E-03	-1.90E-03	4.15E-03	-3.12E-03	-2.44E-03	-1.94E-04
UAMN 24805	2.44E-03	7.20E-03	2.52E-03	-3.43E-03	-7.78E-04	-6.98E-04	4.06E-04	-2.64E-03	-4.12E-04
UAMN 24808	-2.94E-03	-1.40E-02	4.37E-03	2.63E-03	-2.59E-04	-2.67E-03	-3.98E-03	5.38E-04	1.29E-03
UAMN 47308	3.07E-03	1.65E-03	-1.63E-03	8.07E-03	3.09E-03	-2.19E-03	-3.42E-04	5.29E-05	4.13E-03
UAMN 101819	-1.24E-02	-3.04E-04	-5.97E-03	-3.53E-03	7.62E-03	-3.08E-03	1.39E-03	3.12E-03	2.08E-03
UAMN 101828	-5.77E-03	-1.88E-03	-8.48E-03	5.84E-04	-3.74E-03	-9.39E-04	1.76E-03	1.93E-03	3.71E-03
UAMN 101851	-1.93E-03	-7.89E-03	5.52E-03	4.28E-03	1.03E-04	5.64E-03	5.55E-03	-2.17E-03	7.04E-03
UAMN 59579	-7.62E-04	3.19E-03	2.46E-03	1.08E-02	4.95E-04	-3.55E-04	1.95E-03	5.89E-03	-3.26E-03
FMNH 31142	2.53E-03	-7.31E-03	4.01E-03	7.12E-04	-5.82E-03	-7.76E-03	-3.12E-04	-3.20E-04	-2.50E-03
FMNH 31328	6.50E-03	1.05E-03	9.84E-04	4.57E-03	4.36E-03	2.57E-04	-8.81E-03	-1.53E-03	-1.74E-03

Tibia continued

Specimen	PC10	PC11	PC12	PC13	PC14	PC15	PC16	PC17
USNM 265584	-1.57E-03	4.30E-03	3.59E-04	1.98E-03	-1.12E-03	3.53E-03	1.82E-03	5.20E-04
UAMN 509	1.29E-03	-1.61E-03	2.10E-03	4.91E-04	-3.60E-03	-1.11E-03	3.80E-03	1.18E-03
UAMN 511	-4.18E-03	-7.32E-04	-2.00E-03	-1.68E-03	1.74E-03	2.35E-03	8.79E-05	1.41E-03
SNOMNH 11542	-1.32E-03	-2.19E-03	-1.50E-03	-2.87E-03	3.10E-03	1.93E-03	-1.39E-04	2.20E-03
SNOMNH 11543	9.40E-04	3.75E-03	2.95E-03	-1.60E-03	3.62E-04	-5.24E-04	2.99E-03	-1.80E-04
SNOMNH 11544	-8.63E-04	-2.04E-03	2.71E-03	-1.18E-03	4.41E-04	2.89E-04	1.49E-03	1.73E-04
SNOMNH 11545	-2.02E-03	1.49E-03	2.01E-03	-1.01E-03	-1.18E-03	1.65E-03	2.01E-03	-5.12E-04
SNOMNH 11546	1.76E-03	3.60E-03	3.94E-03	-2.45E-03	1.55E-03	7.91E-04	-2.67E-03	1.13E-03
SNOMNH 11547	9.05E-04	2.82E-03	1.01E-03	4.48E-03	-1.76E-04	2.02E-03	-2.51E-03	-2.65E-04
SNOMNH 11548	3.22E-03	-1.96E-03	1.01E-03	-9.10E-04	-4.25E-03	1.64E-03	-1.60E-03	-7.41E-04
SNOMNH 11549	6.35E-03	-1.10E-03	-3.04E-04	-3.12E-03	-2.42E-03	1.05E-04	-2.06E-03	-8.04E-05
SNOMNH 11550	4.28E-03	2.52E-04	-1.71E-03	-1.98E-04	-1.81E-03	-1.71E-03	1.15E-03	1.21E-03
SNOMNH 11551	7.44E-04	8.27E-04	-3.85E-04	1.71E-03	3.01E-03	-2.74E-03	-6.31E-04	-9.30E-04
UAMN 11236	-1.04E-03	-2.37E-03	-1.03E-03	-9.19E-04	3.91E-04	5.48E-04	-6.67E-04	9.36E-04
UAMN 11237	8.76E-04	-5.78E-03	-3.85E-03	3.37E-03	-1.89E-03	2.31E-04	1.02E-03	-9.92E-04

Tibia continued

Specimen	PC10	PC11	PC12	PC13	PC14	PC15	PC16	PC17
UAMN 13542	-5.38E-03	9.47E-04	-4.59E-04	-3.99E-03	-1.01E-03	-3.38E-03	1.95E-04	-2.82E-04
USNM 546139	1.92E-03	-2.98E-04	3.01E-03	3.95E-04	1.33E-03	1.16E-03	-1.46E-03	1.82E-04
USNM 546140	-2.94E-03	9.55E-04	-8.82E-06	2.77E-03	1.84E-03	-2.41E-03	1.31E-03	2.38E-03
USNM 546141	-1.61E-03	-7.05E-03	4.98E-03	1.35E-03	6.33E-04	4.23E-04	-9.98E-04	-5.15E-04
UAMN 22678	-5.96E-04	-1.46E-03	-4.23E-04	1.39E-03	6.73E-04	-1.69E-03	1.06E-03	-1.70E-03
UAMN 22680	1.95E-03	-1.92E-03	4.03E-03	5.36E-04	2.90E-03	-3.15E-03	7.33E-04	-1.02E-03
UAMN 22736	5.88E-04	7.13E-04	-4.16E-03	-1.66E-03	7.15E-04	-2.72E-03	-1.06E-03	6.65E-04
UAMN 24794	3.33E-03	-4.02E-04	-3.52E-03	-3.74E-03	1.25E-03	1.67E-03	9.31E-04	-1.91E-03
UAMN 24805	-1.37E-03	-1.02E-03	-2.12E-03	-4.50E-04	2.01E-04	-4.55E-04	-1.18E-03	2.74E-03
UAMN 24808	-1.17E-03	1.33E-03	7.05E-04	5.59E-04	-2.67E-03	1.78E-03	2.62E-05	2.22E-03
UAMN 47308	4.72E-03	2.29E-03	-3.20E-03	3.87E-03	3.08E-03	1.81E-03	1.09E-03	9.18E-04
UAMN 101819	-5.91E-03	-1.43E-03	-1.16E-03	-1.44E-04	2.33E-04	3.40E-03	-2.70E-04	-3.17E-03
UAMN 101828	-1.25E-03	2.33E-03	-1.14E-03	6.64E-04	-3.92E-03	-1.72E-03	-3.52E-04	1.43E-04
UAMN 101851	-4.13E-04	1.35E-03	1.45E-03	9.01E-04	3.16E-04	-1.25E-03	-2.56E-03	8.05E-05
UAMN 59579	3.08E-03	-1.04E-03	-9.83E-04	-3.53E-04	2.42E-03	3.91E-04	1.31E-03	-1.62E-03
FMNH 31142	-1.11E-03	5.73E-03	-6.54E-04	-4.53E-04	-2.26E-04	-7.65E-04	-2.17E-04	-3.65E-03
FMNH 31328	-3.20E-03	-2.49E-04	-1.66E-03	2.26E-03	-1.91E-03	-2.09E-03	-2.66E-03	-5.01E-04

Fibula

Specimen	PC1	PC2	PC3	PC4	PC5	PC6	PC7	PC8	PC9
USNM 265584	-1.35E-02	1.08E-02	-8.66E-04	-6.18E-03	-6.12E-03	-4.90E-03	6.98E-04	1.05E-03	3.26E-03
UAMN 509	1.06E-03	-5.30E-03	-6.39E-03	-1.20E-03	-9.63E-04	1.18E-03	3.95E-04	2.10E-03	-2.95E-03
UAMN 511	1.22E-02	7.26E-03	-2.20E-03	-5.19E-03	6.36E-03	-3.55E-03	-9.24E-04	7.41E-04	-1.33E-03
SNOMNH 11542	-7.94E-03	2.37E-03	4.41E-03	1.77E-04	1.35E-03	5.81E-03	-1.76E-03	3.03E-03	2.00E-03
SNOMNH 11543	-6.53E-03	-6.92E-03	-4.24E-03	-1.92E-03	4.54E-03	1.12E-03	-1.33E-04	1.58E-04	-2.32E-03
SNOMNH 11544	6.56E-05	-3.49E-03	8.69E-03	-8.42E-03	-2.57E-03	2.34E-03	3.94E-03	-2.17E-03	-1.16E-03
SNOMNH 11545	-2.88E-03	-3.14E-03	2.65E-03	2.66E-03	8.15E-04	-6.24E-04	5.24E-04	-1.30E-03	-8.86E-04
SNOMNH 11546	-6.24E-03	-8.49E-04	-1.75E-03	-5.17E-04	9.94E-04	3.37E-04	-2.80E-03	9.36E-04	3.85E-03
SNOMNH 11548	1.10E-03	6.09E-03	2.11E-03	1.62E-03	-1.34E-03	-4.35E-03	-2.54E-03	-2.44E-03	-5.52E-03
SNOMNH 11549	3.79E-04	-2.50E-03	-5.12E-04	1.50E-03	1.26E-03	5.80E-03	-5.56E-03	1.42E-03	5.13E-04
SNOMNH 11550	1.36E-03	-7.77E-03	5.69E-03	-1.80E-03	-1.95E-03	-1.41E-03	4.48E-03	-3.41E-03	-3.31E-03
SNOMNH 11551	-8.44E-03	-3.03E-03	-6.12E-03	4.29E-05	7.38E-04	-1.56E-03	-9.60E-04	-3.64E-03	1.49E-03
UAMN 11236	5.99E-03	-2.22E-03	-6.94E-03	5.14E-03	-1.00E-02	1.78E-03	-2.98E-03	-1.72E-03	-2.77E-03
UAMN 11237	9.30E-06	-4.61E-03	4.02E-03	-2.33E-03	2.58E-03	7.31E-06	-1.55E-03	6.16E-03	-3.24E-04

Fibula continued

Specimen	PC1	PC2	PC3	PC4	PC5	PC6	PC7	PC8	PC9
UAMN 13542	5.24E-03	4.69E-03	-3.35E-03	-3.43E-03	4.21E-03	4.71E-03	-9.62E-04	-1.42E-03	-1.50E-03
USNM 546139	8.16E-03	1.48E-03	-1.10E-03	-7.87E-03	-5.72E-03	4.70E-03	6.75E-04	1.05E-03	2.49E-03
USNM 546140	5.56E-03	-4.87E-04	-2.46E-03	-6.83E-04	-6.25E-03	2.60E-03	2.79E-03	1.37E-03	2.73E-03
USNM 546141	1.77E-03	-1.07E-03	-7.28E-03	4.77E-03	1.71E-03	-1.75E-03	6.74E-03	3.40E-03	3.38E-03
UAMN 22678	3.69E-03	1.26E-02	4.83E-03	3.32E-03	1.00E-03	-1.08E-03	-1.83E-03	3.82E-03	-2.23E-03
UAMN 22680	5.06E-03	-2.59E-03	-3.82E-03	1.16E-03	2.06E-03	-2.49E-03	2.27E-03	2.77E-03	1.20E-03
UAMN 22736	3.35E-03	2.68E-03	-6.97E-04	2.18E-03	4.57E-03	-4.84E-03	2.07E-03	-3.49E-03	3.99E-03
UAMN 24794	1.75E-03	1.89E-03	1.16E-03	-1.03E-03	4.39E-03	2.87E-03	6.50E-04	-2.34E-03	-9.58E-04
UAMN 24805	-8.54E-03	-8.46E-04	-3.59E-03	4.30E-04	3.86E-04	-7.38E-04	-9.21E-04	2.53E-03	-6.61E-03
UAMN 24808	-4.01E-03	5.81E-03	-1.09E-03	1.99E-03	3.97E-03	4.71E-03	4.12E-03	-5.29E-03	3.32E-04
UAMN 47308	-2.90E-04	-5.19E-03	6.47E-03	6.16E-03	2.52E-03	3.71E-03	-7.33E-04	-4.23E-04	2.87E-03
UAMN 101819	5.93E-03	-7.13E-03	5.73E-03	1.66E-03	-1.12E-03	-6.01E-03	-3.94E-03	1.70E-03	3.45E-03
UAMN 101828	-5.01E-03	1.66E-03	5.83E-04	-1.05E-03	-1.26E-03	-2.52E-03	-3.45E-04	1.91E-03	-2.11E-04
UAMN 101851	1.62E-03	2.76E-04	-5.62E-04	2.03E-06	-1.64E-03	-1.51E-03	-6.60E-03	-6.69E-03	3.12E-03
UAMN 59579	-5.59E-04	-6.96E-03	1.88E-03	-7.79E-04	6.62E-05	-6.00E-03	1.22E-03	-4.08E-04	-1.44E-03
FMNH 31328	-3.70E-04	6.51E-03	4.73E-03	9.56E-03	-4.57E-03	1.68E-03	3.96E-03	5.91E-04	-1.14E-03

Fibula continued

Specimen	PC10	PC11	PC12
USNM 265584	9.22E-04	-7.42E-04	-1.23E-03
UAMN 509	-1.70E-03	3.20E-03	1.36E-03
UAMN 511	1.63E-03	-8.63E-04	-1.11E-03
SNOMNH 11542	-3.25E-03	-3.02E-03	6.23E-04
SNOMNH 11543	-2.14E-03	-2.26E-03	-1.50E-03
SNOMNH 11544	3.06E-03	1.14E-03	2.70E-03
SNOMNH 11545	4.91E-04	-6.92E-03	2.65E-04
SNOMNH 11546	-3.06E-03	1.09E-03	-3.75E-03
SNOMNH 11548	-2.33E-03	-3.75E-04	-2.47E-03
SNOMNH 11549	4.36E-03	-6.67E-04	5.64E-04
SNOMNH 11550	-1.36E-04	1.33E-03	-3.61E-03
SNOMNH 11551	2.69E-03	1.87E-03	1.10E-03
UAMN 11236	1.19E-03	-1.51E-03	5.76E-04
UAMN 11237	3.00E-03	1.88E-03	-6.71E-04

Fibula continued

Specimen	PC10	PC11	PC12
UAMN 13542	-1.20E-03	8.21E-04	-3.45E-03
USNM 546139	-3.59E-03	-2.15E-03	2.18E-03
USNM 546140	1.07E-03	2.41E-03	-3.27E-03
USNM 546141	1.12E-03	8.87E-05	1.75E-03
UAMN 22678	-1.22E-03	2.87E-03	2.61E-03
UAMN 22680	-2.25E-03	-2.41E-03	-5.77E-05
UAMN 22736	7.06E-04	8.91E-04	1.10E-03
UAMN 24794	1.32E-03	-2.23E-03	2.34E-03
UAMN 24805	2.16E-03	1.22E-03	1.21E-03
UAMN 24808	1.98E-03	1.27E-04	-5.78E-04
UAMN 47308	-2.72E-03	4.23E-03	-1.86E-04
UAMN 101819	3.75E-03	-2.25E-03	-1.69E-03
UAMN 101828	1.04E-03	1.28E-03	1.05E-03
UAMN 101851	-1.37E-03	1.69E-03	2.32E-03
UAMN 59579	-5.63E-03	2.61E-04	2.70E-03
FMNH 31328	1.09E-04	-1.02E-03	-8.95E-04

Table 3. Proportion of Variance Explained by Each PC

Element	PC1	PC2	PC3	PC4	PC5	PC6	PC7	PC8	PC9	PC10	PC11	PC12	PC13	PC14	PC15
Humerus	*35.5%*	*9.9%*	*7.8%*	*7.0%*	*6.0%*	*4.2%*	*4.1%*	*3.7%*	*2.9%*	*2.6%*	*2.4%*	*2.2%*	*1.9%*	*1.6%*	*1.4%*
Radius	*19.2%*	*16.9%*	*11.0%*	*9.1%*	*8.5%*	*7.3%*	*5.4%*	*4.9%*	*4.7%*	*3.6%*	*3.1%*	*2.3%*	1.6%	1.1%	0.7%
Ulna	*23.0%*	*12.2%*	*10.3%*	*8.8%*	*7.3%*	*6.1%*	*5.3%*	*4.3%*	*4.0%*	*3.6%*	*3.0%*	*2.3%*	*2.0%*	*1.7%*	*1.3%*
Femur	*18.8%*	*15.3%*	*9.5%*	*7.7%*	*7.3%*	*6.5%*	*5.2%*	*5.0%*	*4.0%*	*3.1%*	*2.8%*	*2.2%*	*2.0%*	*1.9%*	*1.6%*
Tibia	*16.5%*	*15.1%*	*11.1%*	*9.6%*	*8.2%*	*7.1%*	*6.0%*	*4.8%*	*4.2%*	*3.2%*	*2.9%*	*2.2%*	*1.8%*	*1.7%*	*1.5%*
Fibula	*19.2%*	*16.9%*	*11.0%*	*9.1%*	*8.5%*	*7.3%*	*5.4%*	*4.9%*	*4.7%*	*3.6%*	*3.1%*	*2.3%*	1.6%	1.1%	0.7%

Table 3 continued

Element	PC16	PC17	PC18	PC19	PC20	PC21	PC22	PC23	PC24	PC25	PC26	PC27	PC28	PC29	PC30
Humerus	*1.2%*	*1.0%*	0.8%	0.8%	0.7%	0.6%	0.4%	0.3%	0.3%	0.2%	0.2%	0.1%	0.08%	0.06%	0.05%
Radius	0.5%	0.2%													
Ulna	1.1%	0.9%	0.7%	0.6%	0.4%	0.3%	0.3%	0.2%	0.2%	0.05%	0.02%				
Femur	*1.3%*	*1.2%*	1.1%	0.8%	0.6%	0.6%	0.4%	0.3%	0.3%	0.1%	0.08%	0.06%	0.04%	0.02%	
Tibia	1.1%	0.9%	0.8%	0.5%	0.3%	0.2%	0.2%	0.1%							
Fibula	0.5%	0.2%													

Table 3 continued

Element	PC31	PC32	PC33	PC19	PC20	PC21	PC22	PC23	PC24	PC25	PC26	PC27	PC28	PC29	PC30
Humerus	0.02%	0.006%	0.004%												
Radius															
Ulna															
Femur															
Tibia															
Fibula															

*Italicized values indicate the PCs whose cumulative variation equals 95% and, therefore, are the PCs included in the PERMANOVA.

Table 4. Sample Weight and DNA Quantity After Elution

Specimen #	Tissue Weight (g)	DNA Quantity (ng/µL)
USNM 265584	0.072	4.7
USNM 265585	0.125	2.9
USNM 266142	0.066	2.3
USNM 546139	0.058	11.1
USNM 546140	0.054	6.3
USNM 546141	0.061	8.0
UAMNH 509	0.110	10.5
UAMN 511	0.160	3.4
UAMN 11236	0.130	4.6
UAMN 11237	0.170	11.2
UAMN 13542	0.200	11.7
UAMN 22678	0.025	52.7
UAMN 24794	0.025	14.9
UAMN 24805	0.025	28.9
UAMN 24808	0.025	29.0
UAMN 22680	0.025	45.8
UAMN 47308	0.025	35.8
UAMN 59579	0.025	17.2
UAMN 22736	0.025	29.3
UAMN 101819	0.025	23.4
UAMN 101828	0.025	10.5
FMNH 31328	0.025	27.0
SNOMNH 11542	0.114	5.6
SNOMNH 11543	0.092	3.0
SNOMNH 11544	0.170	3.8
SNOMNH 11545	0.077	8.2
SNOMNH 11546	0.086	3.6
SNOMNH 11547	0.076	2.5
SNOMNH 11548	0.145	4.4
SNOMNH 11549	0.112	12.8
SNOMNH 11550	0.150	3.1
SNOMNH 11551	0.102	9.9

Table 5. Sites of Polymorphisms in the Concatenated Sequence

Specimen	**31**	**32**	**33**	**34**	**35**	**132**	**139**	**152**	**154**	**177**	**189**	**190**	**195**	**214**	**238**
M. foina	A	C	T	A	C	C	C	C	C	G	A	A	A	G	T
UAMN 22736	–	–	–	–	–	–	–	–	–	–	–	–	–	–	·
UAMN 24794	·	·	·	·	·	·	·	T	T	A	–	–	·	A	K
UAMN 11236	–	–	–	–	–	–	–	–	–	–	–	–	–	–	·
UAMN 11236	–	–	–	–	–	T	S	T	T	A	–	–	R	A	·
UAMN 11236	–	–	–	–	–	·	·	T	T	A	–	–	·	A	·
NMNH 546139	–	–	–	–	–	·	·	T	T	A	–	–	·	·	·
USNM 546141	–	–	–	–	–	·	·	T	T	A	–	–	·	·	·
USMN 266142	·	·	·	·	·	–	–	–	–	–	–	–	–	–	–
USNM 546140	–	–	–	–	–	·	·	T	T	A	–	–	·	A	–
SNOMNH 11550	R	S	K	R	S	·	·	T	T	A	–	–	·	A	·
SNOMNH 11549	·	·	·	·	·	·	·	T	T	A	–	–	·	A	·
SNOMNH 11544	–	–	–	–	–	·	·	T	T	A	–	–	·	·	·
SNOMNH 11542	–	–	–	–	–	·	·	T	T	A	–	–	·	·	–
UAMN 101828	·	·	·	·	·	·	·	T	T	A	–	–	·	A	·
UAMN 101819	·	·	·	·	·	·	·	T	T	A	–	–	·	–	·
UAMN 101851	–	–	–	–	–	–	–	–	–	–	–	–	–	–	·

*– indicates no nucleotide at that position, · indicates no difference from *M. foina*

* some nucleotides are ambiguous and are represented by M (A or C), K (G or T), W (A or T), Y (C or T), R (A or G), or D (A, G, or T) based on IUPAC designations

Table 5 Continued

Specimen	**252**	**256**	**258**	**260**	**261**	**266**	**267**	**278**	**284**	**298**	**299**	**303**	**306**	**307**	**308**
M. foina	A	C	G	C	G	C	C	T	T	–	T	C	T	A	A
UAMN 22736	·	T	A	·	·	S	S	K	C	A	C	·	K	R	R
UAMN 24794	R	T	A	·	·	·	·	·	C	A	C	T	·	·	·
UAMN 11236	W	T	A	·	·	·	·	·	C	A	C	T	·	·	·
UAMN 11236	·	T	A	·	·	·	·	·	C	A	C	T	·	·	·
UAMN 11236	·	T	A	·	·	·	·	·	C	A	C	T	·	·	·
NMNH 546139	·	T	A	·	·	·	·	·	C	A	C	T	·	·	·
USNM 546141	·	T	A	·	·	·	·	·	C	A	C	T	·	·	·
USMN 266142	–	–	–	–	–	–	–	–	–	–	–	–	–	–	–
USNM 546140	–	–	–	–	·	·	·	·	C	A	C	T	·	·	·
SNOMNH 11550	·	T	A	G	R	·	·	·	C	W	C	T	·	·	·
SNOMNH 11549	·	T	W	T	·	·	·	·	C	A	C	T	·	·	·
SNOMNH 11544	·	T	A	·	·	·	·	·	C	A	C	T	·	·	·
SNOMNH 11542	·	T	A	·	·	·	·	·	C	A	C	T	·	·	·
UAMN 101828	·	T	A	·	·	·	·	·	C	A	C	T	·	·	·
UAMN 101819	·	T	A	·	·	·	·	·	C	A	C	T	·	·	·
UAMN 101851	·	T	A	·	·	·	·	·	C	A	C	T	·	·	·

*– indicates no nucleotide at that position, · indicates no difference from *M. foina*

* some nucleotides are ambiguous and are represented by M (A or C), K (G or T), W (A or T), Y (C or T), R (A or G), or D (A, G, or T) based on IUPAC designations

Table 5 Continued

Specimen	311	313	322	344	345	351	425	430	432	444	450	460	464	465	480
M. foina	C	C	T	T	G	C	A	A	C	G	–	T	A	C	A
UAMN 22736	S	T	C	C	·	T	·	·	T	·	–	·	·	T	G
UAMN 24794	·	T	C	C	·	T	·	·	T	·	–	·	·	T	G
UAMN 11236	·	T	C	C	·	T	·	R	Y	·	–	K	·	T	–
UAMN 11236	·	T	C	C	·	T	·	·	T	·	–	·	·	T	G
UAMN 11236	·	T	C	C	·	T	·	·	T	S	–	·	C	T	G
NMNH 546139	·	T	C	C	·	T	·	·	T	·	–	·	·	T	G
USNM 546141	·	T	C	C	·	T	R	·	T	·	–	·	·	T	·
USMN 266142	–	–	–	–	–	–	–	–	–	–	–	–	–	–	G
USNM 546140	·	T	C	C	·	T	·	·	T	·	–	·	·	T	–
SNOMNH 11550	·	T	C	C	·	T	·	·	T	·	A	·	M	T	G
SNOMNH 11549	·	T	C	C	·	T	R	·	T	·	–	·	C	T	G
SNOMNH 11544	·	T	C	C	S	T	·	·	T	·	–	·	·	T	–
SNOMNH 11542	·	T	C	C	·	T	·	·	T	·	–	·	·	T	G
UAMN 101828	·	T	C	C	·	T	·	·	T	·	–	·	·	T	G
UAMN 101819	·	T	C	C	·	T	·	·	T	·	–	·	·	T	G
UAMN 101851	·	T	C	C	·	T	·	·	T	·	–	·	·	T	G

*– indicates no nucleotide at that position, · indicates no difference from *M. foina*

* some nucleotides are ambiguous and are represented by M (A or C), K (G or T), W (A or T), Y (C or T), R (A or G), or D (A, G, or T) based on IUPAC designations

Table 5 Continued

Specimen	481	503	509	510	523	524	584	614	640	645	679	692	722	731	751
M. foina	T	T	G	A	A	G	T	C	A	G	G	C	A	C	A
UAMN 22736	A	C	A	G	G	A	C	T	·	·	·	·	·	T	·
UAMN 24794	A	C	A	G	G	A	C	T	·	·	·	·	·	T	·
UAMN 11236	–	C	A	G	G	A	C	T	·	·	·	·	–	–	·
UAMN 11236	A	C	A	G	G	A	C	T	·	·	·	·	·	T	·
UAMN 11236	A	C	A	G	G	A	C	T	·	·	R	·	·	T	·
NMNH 546139	A	C	A	G	G	·	C	T	·	·	·	·	·	T	C
USNM 546141	G	C	A	G	G	·	C	T	·	·	·	·	·	T	·
USMN 266142	A	C	A	G	G	·	C	T	Y	R	·	Y	–	–	–
USNM 546140	A	–	–	–	–	–	–	–	–	–	–	–	–	T	·
SNOMNH 11550	A	C	A	G	G	A	C	T	·	·	·	·	·	M	·
SNOMNH 11549	A	C	A	G	G	A	C	T	·	·	·	·	R	T	–
SNOMNH 11544	–	–	–	–	–	–	–	–	–	–	–	–	–	–	–
SNOMNH 11542	A	C	A	G	G	·	C	T	·	·	·	·	·	T	·
UAMN 101828	A	C	A	G	G	A	C	T	·	·	·	·	·	T	·
UAMN 101819	A	C	A	G	G	A	C	T	·	·	·	·	·	T	·
UAMN 101851	A	C	A	G	G	A	C	T	·	·	·	·	·	T	·

*– indicates no nucleotide at that position, · indicates no difference from *M. foina*

* some nucleotides are ambiguous and are represented by M (A or C), K (G or T), W (A or T), Y (C or T), R (A or G), or D (A, G, or T) based on IUPAC designations

Table 5 Continued

Specimen	**752**	**759**	**760**	**761**	**776**	**779**	**782**	**783**	**784**	**789**	**800**	**805**	**822**	**825**	**827**
M. foina	G	T	T	T	G	C	C	G	T	T	C	C	T	C	A
UAMN 22736	·	·	·	·	·	·	·	·	·	·	·	T	W	Y	M
UAMN 24794	·	·	·	·	·	·	·	·	·	·	·	T	·	·	·
UAMN 11236	·	W	·	·	·	·	·	·	·	Y	·	T	·	·	·
UAMN 11236	·	·	·	·	·	·	·	·	·	·	·	T	·	·	·
UAMN 11236	·	·	·	K	·	·	·	·	·	·	·	T	·	·	·
NMNH 546139	A	–	–	–	–	–	–	–	–	–	–	–	–	–	–
USNM 546141	·	·	·	K	·	·	·	·	·	·	·	T	·	·	·
USMN 266142	–	–	–	–	–	–	–	–	–	–	–	–	–	–	–
USNM 546140	·	·	·	·	·	Y	·	·	·	·	·	T	·	·	·
SNOMNH 11550	·	·	·	K	R	M	·	·	·	·	·	T	·	·	·
SNOMNH 11549	·	·	·	K	·	·	·	·	·	·	·	T	·	·	·
SNOMNH 11544	–	–	–	–	·	·	·	·	W	·	Y	T	·	·	–
SNOMNH 11542	·	·	K	K	·	·	M	R	W	·	·	T	·	·	·
UAMN 101828	·	·	·	·	·	·	·	·	·	·	·	T	·	·	·
UAMN 101819	·	·	·	·	·	·	·	·	·	·	·	T	·	·	·
UAMN 101851	·	·	·	·	·	·	·	·	·	·	·	T	·	·	·

*– indicates no nucleotide at that position, · indicates no difference from *M. foina*

* some nucleotides are ambiguous and are represented by M (A or C), K (G or T), W (A or T), Y (C or T), R (A or G), or D (A, G, or T) based on IUPAC designations

Table 5 Continued

Specimen	**828**	**836**	**844**	**849**	**852**	**863**	**864**	**868**	**873**	**875**	**878**	**879**	**880**	**881**	**883**
M. foina	T	A	C	C	A	A	A	A	C	C	T	A	C	T	G
UAMN 22736	Y	·	·	S	·	M	·	·	·	–	–	–	–	–	–
UAMN 24794	·	·	·	·	·	·	·	·	·	·	·	·	·	·	·
UAMN 11236	·	·	·	·	·	·	·	·	·	·	·	·	Y	·	·
UAMN 11236	·	·	·	·	·	·	·	·	·	·	·	·	·	·	·
UAMN 11236	·	·	·	·	·	·	·	·	·	·	·	·	·	·	·
NMNH 546139	–	–	–	–	–	–	–	–	–	–	–	–	–	–	–
USNM 546141	·	·	·	·	·	·	·	·	·	·	·	·	·	·	·
USMN 266142	–	–	–	–	–	–	–	–	–	–	–	–	–	–	–
USNM 546140	·	·	·	·	·	·	·	·	·	·	·	·	·	·	·
SNOMNH 11550	·	·	·	·	·	·	·	·	·	·	·	·	·	·	·
SNOMNH 11549	·	·	·	·	·	·	·	·	·	·	·	·	·	·	·
SNOMNH 11544	·	W	S	·	R	·	·	R	Y	Y	·	·	Y	W	R
SNOMNH 11542	·	·	·	·	·	·	·	·	·	·	·	·	·	·	·
UAMN 101828	·	·	·	·	·	M	M	·	·	·	Y	M	·	·	·
UAMN 101819	·	·	·	·	·	·	·	·	·	·	·	·	·	·	·
UAMN 101851	·	·	·	·	·	·	·	·	·	·	·	·	·	·	·

*– indicates no nucleotide at that position, · indicates no difference from *M. foina*

* some nucleotides are ambiguous and are represented by M (A or C), K (G or T), W (A or T), Y (C or T), R (A or G), or D (A, G, or T) based on IUPAC designations

Table 5 Continued

Specimen	887	890	900	905	914	915	923	925	933	934	936	938	941	961	965
M. foina	G	T	T	G	T	T	C	A	T	A	T	T	T	G	T
UAMN 22736	–	–	–	–	–	–	–	–	–	–	–	–	–	·	C
UAMN 24794	·	·	·	·	·	·	·	·	·	·	·	–	–	A	C
UAMN 11236	Y	W	·	·	Y	Y	–	–	–	–	–	–	–	–	–
UAMN 11236	·	·	·	·	·	·	·	M	·	·	·	C	·	–	–
UAMN 11236	·	·	·	·	·	·	·	M	·	R	·	C	·	–	–
NMNH 546139	–	–	–	–	–	–	–	–	–	–	–	–	–	–	–
USNM 546141	·	·	·	·	·	·	·	·	·	·	·	·	·	–	–
USMN 266142	–	–	–	–	–	–	–	–	–	–	–	–	–	–	–
USNM 546140	·	·	·	·	·	·	·	·	·	·	·	C	·	–	–
SNOMNH 11550	·	·	·	·	·	·	·	·	·	·	·	C	·	–	–
SNOMNH 11549	·	·	·	·	·	·	·	·	·	·	·	C	·	–	–
SNOMNH 11544	·	·	K	R	·	·	M	–	Y	C	W	Y	W	–	–
SNOMNH 11542	·	·	·	·	·	·	·	·	·	·	·	C	·	–	–
UAMN 101828	·	S	·	·	·	·	·	·	·	·	–	–	–	–	C
UAMN 101819	·	·	·	·	·	·	·	·	·	·	–	–	–	·	C
UAMN 101851	·	·	·	·	·	·	·	·	·	·	–	–	–	–	C

*– indicates no nucleotide at that position, · indicates no difference from *M. foina*

* some nucleotides are ambiguous and are represented by M (A or C), K (G or T), W (A or T), Y (C or T), R (A or G), or D (A, G, or T) based on IUPAC designations

Table 5 Continued

Specimen	971	974	989	992	999	1009	1014	1019	1020	1046	1076	1087	1091	1100	1103
M. foina	G	T	A	C	T	A	A	G	G	C	T	G	T	T	C
UAMN 22736	–	C	·	T	C	·	·	A	·	T	C	·	C	C	T
UAMN 24794	–	C	W	T	C	·	·	A	R	T	C	·	C	C	T
UAMN 11236	–	–	–	–	–	–	–	–	–	–	–	–	–	–	–
UAMN 11236	–	–	–	–	–	–	–	–	–	–	–	–	–	–	–
UAMN 11236	–	–	–	–	–	–	–	–	–	–	–	–	–	–	–
NMNH 546139	–	–	–	–	–	–	–	–	–	–	–	–	–	–	–
USNM 546141	–	–	–	–	–	–	–	–	–	–	–	–	–	–	–
USMN 266142	–	–	–	–	–	–	–	–	–	–	–	–	–	–	–
USNM 546140	–	–	–	–	–	–	–	–	–	–	–	–	–	–	–
SNOMNH 11550	–	–	–	–	–	–	–	–	–	–	–	–	–	–	–
SNOMNH 11549	–	–	–	–	–	–	–	–	–	–	–	–	–	–	–
SNOMNH 11544	–	–	–	–	–	–	–	–	–	–	–	–	–	–	–
SNOMNH 11542	–	–	–	–	–	–	–	–	–	–	–	–	–	–	–
UAMN 101828	A	C	·	T	C	W	R	A	A	T	C	·	C	C	T
UAMN 101819	–	C	·	T	C	·	·	A	·	T	C	S	C	C	T
UAMN 101851	–	C	·	T	C	·	·	A	·	T	C	S	C	C	T

*– indicates no nucleotide at that position, · indicates no difference from *M. foina*

* some nucleotides are ambiguous and are represented by M (A or C), K (G or T), W (A or T), Y (C or T), R (A or G), or D (A, G, or T) based on IUPAC designations

Table 5 Continued

Specimen	1106	1116	1135	1148	1154	1169	1176	1187	1190	1193	1203	1214	1218	1219	1220
M. foina	A	T	T	G	A	T	T	A	C	C	T	T	A	T	G
UAMN 22736	G	·	·	A	·	·	C	G	T	T	C	A	·	·	A
UAMN 24794	G	·	·	A	·	·	C	G	T	T	C	A	·	·	A
UAMN 11236	–	–	–	–	–	–	–	–	–	–	–	–	–	–	–
UAMN 11236	–	–	–	–	–	–	–	–	–	–	–	–	–	–	–
UAMN 11236	–	–	–	–	–	–	–	–	–	–	–	–	–	–	–
NMNH 546139	–	–	–	–	–	K	C	G	T	T	C	A	·	·	A
USNM 546141	–	–	–	–	–	–	–	G	T	T	C	A	·	·	A
USMN 266142	–	–	–	–	–	–	–	–	–	–	–	–	–	–	–
USNM 546140	–	–	·	A	·	·	C	G	T	T	C	A	·	·	A
SNOMNH 11550	–	–	C	A	T	·	C	G	T	T	C	A	·	A	·
SNOMNH 11549	–	–	–	–	–	–	–	–	–	–	C	A	G	A	·
SNOMNH 11544	–	C	·	A	·	·	C	G	T	T	C	A	·	·	A
SNOMNH 11542	–	–	–	–	–	–	–	–	–	–	–	–	–	–	–
UAMN 101828	G	·	·	A	·	·	C	G	T	T	C	A	·	·	A
UAMN 101819	G	·	·	A	·	·	C	G	T	T	C	A	·	·	A
UAMN 101851	G	·	·	A	·	·	C	G	T	T	C	A	·	·	A

*– indicates no nucleotide at that position, · indicates no difference from *M. foina*

* some nucleotides are ambiguous and are represented by M (A or C), K (G or T), W (A or T), Y (C or T), R (A or G), or D (A, G, or T) based on IUPAC designations

Table 5 Continued

Specimen	**1222**	**1224**	**1225**	**1226**	**1227**	**1228**	**1229**	**1230**	**1236**	**1240**	**1244**	**1248**	**1258**	**1277**	**1285**
M. foina	C	A	C	A	G	C	A	T	G	A	T	C	A	A	T
UAMN 22736	·	·	·	·	·	·	·	·	·	·	·	·	·	G	·
UAMN 24794	·	·	·	·	·	·	·	·	·	·	C	·	·	G	·
UAMN 11236	–	–	–	–	–	–	–	–	–	–	–	–	–	–	–
UAMN 11236	–	–	–	–	–	–	–	–	–	–	–	–	–	–	–
UAMN 11236	–	–	–	–	–	–	–	–	–	–	–	–	–	–	–
NMNH 546139	·	·	·	·	Y	·	·	–	K	W	·	S	·	G	W
USNM 546141	·	·	·	·	·	·	·	·	·	·	·	S	W	G	·
USMN 266142	–	–	–	–	–	–	–	–	–	–	–	–	–	–	–
USNM 546140	·	·	·	·	·	·	·	·	·	·	·	·	·	G	·
SNOMNH 11550	·	·	·	·	·	·	·	·	·	·	·	·	·	G	·
SNOMNH 11549	G	K	K	R	·	S	R	K	·	·	·	·	·	G	·
SNOMNH 11544	·	·	·	·	·	·	·	·	·	·	·	·	·	G	·
SNOMNH 11542	–	–	–	–	–	–	–	–	–	–	–	–	–	–	–
UAMN 101828	·	·	·	·	·	·	·	·	·	·	·	·	·	G	·
UAMN 101819	·	·	·	·	·	·	·	·	·	·	·	·	R	G	·
UAMN 101851	·	·	·	·	·	·	·	·	·	·	·	·	R	G	·

*– indicates no nucleotide at that position, · indicates no difference from *M. foina*

* some nucleotides are ambiguous and are represented by M (A or C), K (G or T), W (A or T), Y (C or T), R (A or G), or D (A, G, or T) based on IUPAC designations

Table 5 Continued

Specimen	1292	1293	1295	1298	1312	1313	1323	1325	1326	1329	1333	1336	1347	1350	1351
M. foina	T	C	A	A	A	T	–	G	C	C	G	T	G	G	T
UAMN 22736	C	T	G	G	·	C	–	·	T	T	·	·	A	A	·
UAMN 24794	C	T	G	G	·	C	C	·	T	T	·	·	A	A	·
UAMN 11236	–	–	–	–	–	–	–	–	–	–	–	–	A	A	·
UAMN 11236	–	–	–	–	–	–	–	–	–	–	–	–	A	A	·
UAMN 11236	–	–	–	–	–	–	–	–	–	–	–	–	A	W	Y
NMNH 546139	C	T	G	G	R	C	–	T	C	–	–	–	–	–	–
USNM 546141	C	T	G	G	·	C	–	·	T	T	·	·	A	A	·
USMN 266142	–	–	–	–	–	–	–	–	–	–	–	–	–	–	–
USNM 546140	C	T	G	G	·	C	–	·	T	T	·	R	A	A	K
SNOMNH 11550	C	T	G	G	·	C	–	·	T	T	·	·	A	A	·
SNOMNH 11549	C	T	G	G	·	C	–	·	T	T	S	·	A	A	·
SNOMNH 11544	C	T	G	G	·	C	–	·	T	T	·	·	A	A	·
SNOMNH 11542	–	–	–	–	–	–	–	–	–	–	–	–	A	A	·
UAMN 101828	C	T	G	G	·	C	–	·	T	T	·	·	A	A	·
UAMN 101819	C	T	G	G	·	C	–	·	T	T	·	·	A	A	·
UAMN 101851	C	T	G	G	·	C	–	·	T	T	·	·	A	A	·

*– indicates no nucleotide at that position, · indicates no difference from *M. foina*

* some nucleotides are ambiguous and are represented by M (A or C), K (G or T), W (A or T), Y (C or T), R (A or G), or D (A, G, or T) based on IUPAC designations

Table 5 Continued

Specimen	1352	1353	1354	1355	1357	1360	1365	1367	1368	1371	1376	1377	1383	1388	1396
M. foina	T	C	T	C	G	G	A	C	C	C	C	A	C	C	T
UAMN 22736	·	·	·	·	·	·	G	·	T	·	·	G	·	·	·
UAMN 24794	·	·	·	·	·	·	G	·	T	·	·	G	·	·	·
UAMN 11236	·	Y	K	W	K	·	G	·	T	·	·	G	·	·	Y
UAMN 11236	·	·	·	·	·	·	G	S	T	·	·	G	·	·	·
UAMN 11236	·	·	·	K	·	·	G	S	T	·	·	G	·	·	·
NMNH 546139	–	–	–	–	–	–	–	–	–	–	–	–	·	A	·
USNM 546141	K	·	·	·	C	W	·	K	T	A	·	·	–	–	–
USMN 266142	–	–	–	–	–	–	–	–	–	–	–	–	–	·	·
USNM 546140	·	·	·	·	R	·	–	–	–	–	–	–	Y	·	·
SNOMNH 11550	·	·	·	·	·	·	G	·	T	·	M	R	·	–	–
SNOMNH 11549	·	·	·	·	·	·	G	·	T	·	·	·	·	·	·
SNOMNH 11544	·	·	·	·	·	·	G	·	T	·	·	R	·	–	·
SNOMNH 11542	·	Y	·	·	·	·	G	·	T	·	·	G	·	·	·
UAMN 101828	·	·	·	·	·	·	G	·	T	·	·	G	·	·	·
UAMN 101819	·	·	·	·	·	·	G	·	T	·	·	G	·	·	·
UAMN 101851	·	·	·	·	·	·	G	·	T	·	·	G	·	·	·

*– indicates no nucleotide at that position, · indicates no difference from *M. foina*

* some nucleotides are ambiguous and are represented by M (A or C), K (G or T), W (A or T), Y (C or T), R (A or G), or D (A, G, or T) based on IUPAC designations

Table 5 Continued

Specimen	1404	1410	1418	1419	1422	1423	1426	1432	1434	1441	1448	1452	1455	1459	1468
M. foina	G	T	C	G	C	T	G	G	A	C	T	C	–	G	C
UAMN 22736	·	C	·	A	A	·	A	·	T	·	·	·	–	A	T
UAMN 24794	·	C	·	A	A	·	·	·	T	·	·	·	–	A	T
UAMN 11236	·	C	·	A	A	·	·	·	T	·	·	·	–	A	T
UAMN 11236	·	C	·	A	A	·	·	·	T	·	·	·	–	A	T
UAMN 11236	·	C	·	A	A	·	·	·	T	·	·	·	–	A	T
NMNH 546139	A	C	·	A	A	·	·	·	T	·	·	·	C	A	T
USNM 546141	–	–	–	–	–	–	–	–	–	–	Y	·	–	A	T
USMN 266142	·	C	·	A	A	·	·	·	T	·	·	·	–	A	T
USNM 546140	·	C	·	A	A	·	·	·	T	·	·	·	–	A	T
SNOMNH 11550	–	–	·	A	A	·	·	·	T	A	·	·	–	A	T
SNOMNH 11549	·	C	·	A	A	G	·	T	T	·	·	Y	–	A	T
SNOMNH 11544	·	C	Y	R	A	·	·	·	T	·	·	Y	–	A	T
SNOMNH 11542	·	C	·	A	A	·	·	·	T	·	·	·	–	A	T
UAMN 101828	·	C	·	A	A	·	·	·	T	·	·	·	–	A	T
UAMN 101819	·	C	·	A	A	·	·	·	T	·	·	·	–	A	T
UAMN 101851	·	C	·	A	A	·	·	·	T	·	·	·	–	A	T

*– indicates no nucleotide at that position, · indicates no difference from *M. foina*

* some nucleotides are ambiguous and are represented by M (A or C), K (G or T), W (A or T), Y (C or T), R (A or G), or D (A, G, or T) based on IUPAC designations

Table 5 Continued

Specimen	1471	1477	1478	1480	1489	1490	1492	1493	1495	1519	1520	1525	1530	1538	1539
M. foina	C	C	G	G	C	G	C	T	C	C	T	T	A	T	T
UAMN 22736	·	A	·	A	·	·	T	·	T	·	·	C	·	C	·
UAMN 24794	·	A	·	A	·	·	T	·	T	·	·	C	·	C	·
UAMN 11236	·	A	·	A	·	·	T	·	T	–	–	–	–	–	–
UAMN 11236	·	A	·	A	·	·	T	·	T	·	·	C	–	–	–
UAMN 11236	·	A	·	A	·	·	T	·	T	·	·	C	–	–	–
NMNH 546139	·	A	·	A	·	·	T	·	T	·	·	C	·	–	–
USNM 546141	·	A	·	A	·	·	T	·	T	·	·	C	R	C	Y
USMN 266142	·	A	·	A	·	·	T	·	T	·	·	C	·	C	·
USNM 546140	·	A	·	A	·	·	T	·	T	·	–	–	–	–	–
SNOMNH 11550	·	A	·	A	·	·	T	·	T	T	·	–	–	C	·
SNOMNH 11549	·	T	·	A	T	·	T	·	T	·	W	C	–	–	–
SNOMNH 11544	Y	A	·	A	·	·	T	·	T	·	·	C	·	C	·
SNOMNH 11542	·	A	·	A	·	·	T	·	T	·	–	–	–	–	–
UAMN 101828	·	A	·	A	·	·	T	·	T	·	·	C	·	C	·
UAMN 101819	·	A	·	A	·	R	T	W	T	·	K	C	·	C	·
UAMN 101851	·	A	T	A	·	·	T	·	T	·	K	C	·	C	·

*– indicates no nucleotide at that position, · indicates no difference from *M. foina*

* some nucleotides are ambiguous and are represented by M (A or C), K (G or T), W (A or T), Y (C or T), R (A or G), or D (A, G, or T) based on IUPAC designations

Table 5 Continued

Specimen	1546	1548	1554	1563	1591	1593	1594	1601	1602	1604	1605	1608	1611	1615	1617
M. foina	C	A	T	T	C	T	T	T	A	T	T	A	C	A	T
UAMN 22736	T	·	C	C	T	C	·	·	G	·	C	G	A	·	C
UAMN 24794	Y	·	C	C	T	C	·	·	G	·	C	G	A	·	C
UAMN 11236	T	·	C	C	T	C	·	·	G	·	C	G	A	·	C
UAMN 11236	T	·	C	C	T	C	·	·	G	·	C	G	A	·	C
UAMN 11236	–	–	–	–	–	–	–	–	–	–	–	–	–	–	–
NMNH 546139	T	·	C	C	T	C	·	·	G	·	C	G	A	·	C
USNM 546141	T	·	C	C	T	C	·	·	G	·	C	G	A	·	C
USMN 266142	T	W	C	C	T	C	·	·	G	·	C	G	A	·	C
USNM 546140	T	·	C	C	T	C	·	·	G	·	C	G	A	·	C
SNOMNH 11550	T	·	C	C	T	C	K	K	G	K	C	G	A	·	C
SNOMNH 11549	–	–	–	–	–	–	–	–	–	–	–	–	A	R	C
SNOMNH 11544	T	·	C	C	T	C	·	·	G	·	C	G	A	·	C
SNOMNH 11542	–	–	C	C	T	C	·	·	G	·	C	G	A	·	C
UAMN 101828	T	·	C	C	T	C	·	·	G	·	C	G	A	·	C
UAMN 101819	T	·	C	C	T	C	·	·	G	·	C	G	A	·	C
UAMN 101851	T	·	C	C	T	C	·	·	G	·	C	G	A	·	C

*– indicates no nucleotide at that position, · indicates no difference from *M. foina*

* some nucleotides are ambiguous and are represented by M (A or C), K (G or T), W (A or T), Y (C or T), R (A or G), or D (A, G, or T) based on IUPAC designations

Table 5 Continued

Specimen	1621	1623	1626	1629	1635	1636	1640	1645	1650	1651	1665	1677	1695	1710	1716
M. foina	C	A	T	C	G	A	A	A	G	A	T	G	C	G	A
UAMN 22736	T	G	·	T	A	·	·	G	·	·	C	–	T	A	G
UAMN 24794	T	G	·	T	A	·	·	G	·	·	C	–	T	A	G
UAMN 11236	T	G	·	T	A	·	·	G	·	·	C	A	T	A	G
UAMN 11236	T	G	·	T	A	·	·	G	A	G	C	A	T	A	G
UAMN 11236	–	–	·	T	A	·	·	R	·	·	C	A	T	A	G
NMNH 546139	T	G	·	T	A	·	·	G	·	·	C	–	T	A	G
USNM 546141	T	G	·	T	A	·	·	G	·	·	C	A	T	A	G
USMN 266142	T	G	·	T	A	·	·	G	·	·	C	A	T	A	G
USNM 546140	T	G	·	T	A	R	W	G	·	·	C	–	–	–	–
SNOMNH 11550	T	G	·	T	A	·	·	G	·	·	C	A	T	A	G
SNOMNH 11549	T	G	Y	T	A	·	·	G	·	·	C	A	T	A	G
SNOMNH 11544	T	G	·	T	A	·	·	G	·	·	C	A	T	–	G
SNOMNH 11542	T	G	·	T	A	·	·	G	·	·	C	–	–	–	–
UAMN 101828	T	G	·	T	A	·	·	G	·	–	–	–	–	–	–
UAMN 101819	T	G	·	T	A	·	·	G	·	·	C	A	T	A	G
UAMN 101851	T	G	·	T	A	·	·	G	·	·	C	A	T	A	G

*– indicates no nucleotide at that position, · indicates no difference from *M. foina*

* some nucleotides are ambiguous and are represented by M (A or C), K (G or T), W (A or T), Y (C or T), R (A or G), or D (A, G, or T) based on IUPAC designations

Table 5 Continued

Specimen	1737	1746	1752	1758	1759	1760	1761	1770	1773	1776	1778	1786	1837	1844	1849
M. foina	G	T	C	C	C	A	A	A	C	C	A	A	C	C	C
UAMN 22736	A	C	T	·	–	–	–	–	–	–	–	–	T	T	T
UAMN 24794	A	C	T	·	–	–	–	–	–	–	–	–	T	T	T
UAMN 11236	A	C	T	T	S	R	S	G	·	·	·	–	T	T	T
UAMN 11236	A	C	T	T	·	·	·	G	·	·	·	A	·	T	K
UAMN 11236	A	C	T	T	·	·	·	G	S	·	C	–	–	–	–
NMNH 546139	A	C	T	T	·	·	·	G	·	·	·	R	–	–	–
USNM 546141	A	C	T	T	·	·	·	G	·	S	·	R	–	–	–
USMN 266142	A	C	T	T	·	·	·	G	·	·	·	A	–	–	–
USNM 546140	–	–	–	–	–	–	–	–	–	–	–	–	–	–	–
SNOMNH 11550	A	C	T	T	·	·	·	G	·	·	·	A	–	–	–
SNOMNH 11549	A	C	T	T	·	·	·	G	·	·	·	A	–	–	–
SNOMNH 11544	A	C	T	T	·	·	·	R	·	·	·	A	–	–	–
SNOMNH 11542	–	–	–	–	–	–	–	–	–	–	–	–	–	–	–
UAMN 101828	–	–	–	–	–	–	–	–	–	–	–	–	T	T	T
UAMN 101819	A	C	T	T	·	·	–	–	–	–	–	–	·	T	T
UAMN 101851	A	C	T	T	·	·	–	–	–	–	–	–	T	T	T

*– indicates no nucleotide at that position, · indicates no difference from *M. foina*

* some nucleotides are ambiguous and are represented by M (A or C), K (G or T), W (A or T), Y (C or T), R (A or G), or D (A, G, or T) based on IUPAC designations

Table 5 Continued

Specimen	1850	1852	1876	1879	1884	1886	1889	1900	1921	1933	1937	1965	1966	1977	1980
M. foina	A	T	C	A	G	T	C	–	C	A	T	A	C	T	A
UAMN 22736	G	C	T	C	C	·	·	–	T	R	C	·	T	C	G
UAMN 24794	G	C	T	C	C	·	·	–	T	·	C	·	T	C	G
UAMN 11236	G	C	T	C	C	·	–	–	–	–	–	–	–	–	–
UAMN 11236	G	C	T	C	C	·	M	–	T	·	C	·	·	C	G
UAMN 11236	–	–	–	–	–	–	–	–	–	·	C	·	T	C	G
NMNH 546139	–	–	–	–	–	–	–	–	–	·	C	·	T	C	G
USNM 546141	–	–	–	–	–	–	–	–	–	·	C	·	T	C	G
USMN 266142	–	–	–	–	–	–	–	–	–	–	–	·	Y	C	G
USNM 546140	–	–	–	–	–	–	–	–	–	–	–	–	–	C	G
SNOMNH 11550	–	–	–	–	–	–	–	–	–	·	C	·	Y	C	G
SNOMNH 11549	–	–	–	–	–	–	–	–	–	·	C	·	Y	C	G
SNOMNH 11544	–	–	–	–	–	–	–	–	–	–	–	–	–	–	–
SNOMNH 11542	–	–	–	–	–	–	–	–	–	–	–	–	–	–	–
UAMN 101828	G	C	T	C	C	C	·	–	T	·	C	G	T	C	G
UAMN 101819	G	C	T	C	C	·	·	–	T	·	C	·	T	C	G
UAMN 101851	G	C	T	C	C	·	·	T	T	G	C	·	T	C	G

*– indicates no nucleotide at that position, · indicates no difference from *M. foina*

* some nucleotides are ambiguous and are represented by M (A or C), K (G or T), W (A or T), Y (C or T), R (A or G), or D (A, G, or T) based on IUPAC designations

Table 5 Continued

Specimen	1984	1985	1986	1991	1992	1995	1999	2002	2004	2009	2029	2030	2036	2039	2045
M. foina	C	C	A	T	C	A	A	T	A	C	A	A	C	C	C
UAMN 22736	T	A	G	·	·	·	G	C	·	·	·	·	·	·	·
UAMN 24794	T	A	G	C	·	·	G	C	·	·	·	·	·	·	·
UAMN 11236	–	–	–	–	–	–	–	–	–	–	–	–	–	–	–
UAMN 11236	T	A	G	·	·	·	G	C	·	·	·	·	·	·	·
UAMN 11236	T	A	G	C	·	·	G	C	·	·	·	·	·	·	·
NMNH 546139	T	A	G	·	·	·	G	C	·	·	·	·	·	·	·
USNM 546141	T	A	G	·	·	·	G	C	·	·	·	·	·	·	·
USMN 266142	T	M	G	Y	Y	·	G	T	G	R	·	·	·	·	·
USNM 546140	T	A	G	·	·	·	G	C	·	·	·	·	·	·	·
SNOMNH 11550	T	M	G	Y	T	M	G	T	G	·	·	·	·	·	Y
SNOMNH 11549	T	M	G	C	·	·	G	Y	R	·	·	·	·	·	·
SNOMNH 11544	T	·	G	C	T	·	G	T	R	·	W	Y	S	S	·
SNOMNH 11542	–	–	–	–	–	–	–	–	–	–	–	–	–	–	–
UAMN 101828	T	A	G	C	·	·	G	C	·	·	·	·	·	·	·
UAMN 101819	T	A	G	·	·	·	G	C	·	·	·	·	·	·	·
UAMN 101851	T	A	G	·	·	·	G	C	·	·	·	·	·	·	·

*– indicates no nucleotide at that position, · indicates no difference from *M. foina*

* some nucleotides are ambiguous and are represented by M (A or C), K (G or T), W (A or T), Y (C or T), R (A or G), or D (A, G, or T) based on IUPAC designations

Table 5 Continued

Specimen	2046	2047	2048	2049	2050	2051	2052	2076	2078	2079	2080	2097	2128	2140	2143
M. foina	T	A	G	A	C	G	T	A	A	G	C	C	T	A	G
UAMN 22736	C	C	·	·	T	·	·	·	G	A	T	A	C	·	·
UAMN 24794	C	C	·	·	T	·	·	·	G	A	T	A	C	·	·
UAMN 11236	–	–	–	–	–	–	–	–	–	–	–	–	C	·	·
UAMN 11236	C	S	·	·	T	·	·	·	G	A	T	A	C	·	·
UAMN 11236	C	C	·	·	T	·	·	·	G	A	T	A	C	G	·
NMNH 546139	C	C	·	·	C	·	·	·	G	A	·	A	·	G	·
USNM 546141	C	C	·	·	C	·	·	·	G	A	·	A	·	G	R
USMN 266142	C	C	·	·	C	A	·	·	·	A	·	A	·	G	·
USNM 546140	C	C	·	·	T	·	·	·	G	A	T	A	C	G	·
SNOMNH 11550	Y	C	R	R	S	·	K	·	·	A	·	A	·	G	·
SNOMNH 11549	C	C	·	·	H	·	·	·	G	A	Y	A	Y	G	·
SNOMNH 11544	C	C	·	·	·	·	·	·	R	A	Y	A	Y	G	·
SNOMNH 11542	–	–	–	–	–	·	·	M	G	A	T	A	·	·	·
UAMN 101828	C	C	·	·	T	·	·	·	G	A	T	A	C	·	·
UAMN 101819	C	C	·	·	T	·	·	·	G	A	T	A	C	·	·
UAMN 101851	C	C	·	·	T	·	·	·	G	A	T	A	C	·	·

*– indicates no nucleotide at that position, · indicates no difference from *M. foina*

* some nucleotides are ambiguous and are represented by M (A or C), K (G or T), W (A or T), Y (C or T), R (A or G), or D (A, G, or T) based on IUPAC designations

Table 5 Continued

Specimen	2144	2150	2152	2155	2167	2168	2177	2178	2195	2205	2234	2246	2257	2258	2267
M. foina	T	A	C	A	T	C	G	A	T	G	T	T	T	A	G
UAMN 22736	·	·	·	·	C	T	·	·	·	·	·	C	–	–	A
UAMN 24794	·	·	·	·	C	T	·	·	·	·	·	C	–	–	A
UAMN 11236	·	W	T	W	C	T	·	·	·	S	·	C	–	–	–
UAMN 11236	·	·	·	·	C	T	·	·	·	·	·	C	–	–	A
UAMN 11236	·	·	·	·	C	T	·	T	K	·	–	C	–	–	A
NMNH 546139	·	·	·	·	C	T	·	·	·	·	·	C	–	–	A
USNM 546141	·	·	·	·	C	T	·	·	·	·	·	C	–	–	A
USMN 266142	·	·	·	·	C	T	·	·	·	·	·	C	–	–	A
USNM 546140	W	·	·	·	C	T	·	·	·	·	·	C	–	–	A
SNOMNH 11550	·	·	·	·	C	T	·	·	·	·	K	C	–	–	A
SNOMNH 11549	·	·	·	·	C	T	·	·	·	·	·	C	–	–	A
SNOMNH 11544	·	·	·	·	C	T	R	·	·	S	·	C	–	–	–
SNOMNH 11542	·	W	·	·	C	T	·	·	·	·	·	C	–	–	A
UAMN 101828	·	·	·	·	C	T	·	·	·	·	·	C	–	–	A
UAMN 101819	·	·	·	·	C	T	·	·	·	·	·	C	–	–	A
UAMN 101851	·	·	·	·	C	T	·	·	·	·	·	C	–	–	A

*– indicates no nucleotide at that position, · indicates no difference from *M. foina*

* some nucleotides are ambiguous and are represented by M (A or C), K (G or T), W (A or T), Y (C or T), R (A or G), or D (A, G, or T) based on IUPAC designations

Table 5 Continued

Specimen	2272	2288	2294	2308	2311	2315	2317	2320	2324	2326
M. foina	C	A	G	G	G	G	T	C	T	G
UAMN 22736	T	G	A	·	·	A	W	·	·	·
UAMN 24794	T	G	A	·	·	–	–	–	–	–
UAMN 11236	–	–	–	–	–	–	–	–	–	–
UAMN 11236	T	G	A	·	·	A	·	·	W	S
UAMN 11236	T	–	–	–	–	–	–	–	–	–
NMNH 546139	T	G	A	S	·	A	·	·	–	–
USNM 546141	T	G	A	·	·	A	·	–	–	–
USMN 266142	T	–	–	–	–	–	–	–	–	–
USNM 546140	T	G	A	R	·	A	·	·	·	·
SNOMNH 11550	T	G	A	–	–	–	–	–	–	–
SNOMNH 11549	T	G	A	·	·	A	·	Y	·	·
SNOMNH 11544	–	–	–	–	–	–	–	–	–	–
SNOMNH 11542	T	G	A	·	·	A	·	·	·	–
UAMN 101828	T	G	A	·	·	A	·	·	·	·
UAMN 101819	T	G	A	·	R	A	·	·	·	·
UAMN 101851	T	G	A	·	·	A	·	·	·	·

*– indicates no nucleotide at that position, · indicates no difference from *M. foina*

* some nucleotides are ambiguous and are represented by M (A or C), K (G or T), W (A or T), Y (C or T), R (A or G), or D (A, G, or T) based on IUPAC designations

Table 6. Figure 4 Phylogeny Specimen Labels

Specimen Number	**Phylogeny Label**
UAMN 22736	1991A
UAMN 24794	1990A
UAMN 11237	1976A
UAMN 101851	2006A
UAMN 13542	1981A
UAMN 101819	2006B
UAMN 101828	2006C
UAMN 11236	1976B
SNOMNH 11549	1968A
USNM 546140	1983A
SNOMNH 11542	1968B
USNM 546139	1983B
USNM 546141	1983C
SNOMNH 11550	1968C
SNOMNH 11544	1968D
USNM 266142	1940A

F Supplemental Figures

Figure S1. Primer design overlap in 16S, Dloop, and cytb. Arrows indicate the region of each gene targeted by a primer set. Arrows pointing right represent forward primers and those pointing left are reverse primers. The length of the arrow represents the primer sequence length. Matching arrow colors within a gene represent primer pairs.

G R Code for Landmark Alignment and PCA

```
install.packages('geomorph', dependencies = TRUE)

library(geomorph)

setwd(" ")#User sets working directory

#########################################################################
######

Hmydata<-read.csv("Historic humerus.csv", header=TRUE, stringsAsFactors = FALSE)

Hmydata

Hspecimen<- as.matrix(Hmydata[,1])

Htimebin<- as.factor(Hmydata[,2])

Hcoords<- as.matrix(Hmydata[, -c(1:2)])


#Convert coordinates to array

Hp<- ncol(Hcoords)/3

Hn<- length(Hspecimen)

Hk<- 3

Hland<- arrayspecs(Hcoords, Hp, Hk)

dim(Hland)

dimnames(Hland)[[3]]

dimnames(Hland)[[3]]<- rownames(Hmydata)

plotAllSpecimens(Hland, mean=FALSE) #plots raw landmarks


#plot PCA

Humerus.gpa<- gpagen(Hland) #GPA alignment

HumerusPCA<-plotTangentSpace(Humerus.gpa$coords, groups=Htimebin, label =
TRUE)

summary(HumerusPCA)
```

```
HumerusPCA23<- plotTangentSpace(Humerus.gpa$coords, groups=Htimebin, axis1=2,
axis2=3, label=TRUE)

HumerusPCA34<- plotTangentSpace(Humerus.gpa$coords, groups=Htimebin, axis1=3,
axis2=4, label=TRUE)

HumerusPCA45<- plotTangentSpace(Humerus.gpa$coords, groups=Htimebin, axis1=4,
axis2=5, label=TRUE)

HumerusPCscore<-HumerusPCA$pc.scores

HumerusPCscore



#writes PC scores as a space deliminated file for PAST

write.table(HumerusPCscore, file="Humerus time PC")



##########################################################################
######

#Radius

Rmydata<-read.csv("Historic radius.csv", header=TRUE, stringsAsFactors = FALSE)

Rmydata

Rspecimen<- as.matrix(Rmydata[,1])

Rtimebin<- as.factor(Rmydata[,2])

Rcoords<- as.matrix(Rmydata[, -c(1:2)])


#Convert coordinates to array

Rp<- ncol(Rcoords)/3

Rn<- length(Rspecimen)

Rk<- 3
```

```
Rland<- arrayspecs(Rcoords, Rp, Rk)

dim(Rland)

dimnames(Rland)[[3]]

dimnames(Rland)[[3]]<- rownames(Rmydata)

plotAllSpecimens(Rland, mean=FALSE) #plots raw landmarks


#plot PCA

Radius.gpa<- gpagen(Rland) #GPA alignment

RadiusPCA<-plotTangentSpace(Radius.gpa$coords, groups=Rtimebin, label = TRUE)

summary(RadiusPCA)

RadiusPCA23<- plotTangentSpace(Radius.gpa$coords, groups=Rtimebin, axis1=2,
axis2=3, label=TRUE)

RadiusPCA34<- plotTangentSpace(Radius.gpa$coords, groups=Rtimebin, axis1=3,
axis2=4, label=TRUE)

RadiusPCA45<- plotTangentSpace(Radius.gpa$coords, groups=Rtimebin, axis1=4,
axis2=5, label=TRUE)

RadiusPCscore<-RadiusPCA$pc.scores

RadiusPCscore


#writes as a space deliminated file for PAST

write.table(RadiusPCscore, file="Radius time PC")



##########################################################################
######

#Ulna

Umydata<-read.csv("Historic ulna.csv", header=TRUE, stringsAsFactors = FALSE)

Umydata
```

```
Uspecimen<- as.matrix(Umydata[,1])

Utimebin<- as.factor(Umydata[,2])

Ucoords<- as.matrix(Umydata[, -c(1:2)])


#Convert coordinates to array

Up<- ncol(Ucoords)/3

Un<- length(Uspecimen)

Uk<- 3

Uland<- arrayspecs(Ucoords, Up, Uk)

dim(Uland)

dimnames(Uland)[[3]]

dimnames(Uland)[[3]]<- rownames(Umydata)

plotAllSpecimens(Uland, mean=FALSE) #plots raw landmarks


#plot PCA

Ulna.gpa<- gpagen(Uland) #GPA alignment

UlnaPCA<-plotTangentSpace(Ulna.gpa$coords, groups=Utimebin, label = TRUE)

summary(UlnaPCA)

UlnaPCA23<- plotTangentSpace(Ulna.gpa$coords, groups=Utimebin, axis1=2, axis2=3,
label=TRUE)

UlnaPCA34<- plotTangentSpace(Ulna.gpa$coords, groups=Utimebin, axis1=3, axis2=4,
label=TRUE)

UlnaPCA45<- plotTangentSpace(Ulna.gpa$coords, groups=Utimebin, axis1=4, axis2=5,
label=TRUE)

UlnaPCscore<-UlnaPCA$pc.scores

UlnaPCscore


#writes as a space deliminated file for PAST
```

```
write.table(UlnaPCscore, file="Ulna time PC")


#########################################################################
######

#Femur

FEmydata<-read.csv("Historic femur.csv", header=TRUE, stringsAsFactors = FALSE)

FEmydata

FEspecimen<- as.matrix(FEmydata[,1])

FEtimebin<- as.factor(FEmydata[,2])

FEcoords<- as.matrix(FEmydata[, -c(1:2)])


#Convert coordinates to array

FEp<- ncol(FEcoords)/3

FEn<- length(FEspecimen)

FEk<- 3

FEland<- arrayspecs(FEcoords, FEp, FEk)

dim(FEland)

dimnames(FEland)[[3]]

dimnames(FEland)[[3]]<- rownames(FEmydata)

plotAllSpecimens(FEland, mean=FALSE) #plots raw landmarks


#plot PCA

Femur.gpa<- gpagen(FEland) #GPA alignment

FemurPCA<-plotTangentSpace(Femur.gpa$coords, groups=FEtimebin, label = TRUE)

summary(FemurPCA)

FemurPCA23<- plotTangentSpace(Femur.gpa$coords, groups=timebin, axis1=2,
axis2=3, label=TRUE)
```

```
FemurPCA34<- plotTangentSpace(Femur.gpa$coords, groups=timebin, axis1=3,
axis2=4, label=TRUE)

FemurPCA45<- plotTangentSpace(Femur.gpa$coords, groups=timebin, axis1=4,
axis2=5, label=TRUE)

FemurPCscore<-FemurPCA$pc.scores

FemurPCscore


#writes as a space deliminated file for PAST

write.table(FemurPCscore, file="femur time PC")


##########################################################################
#############

#Tibia

Tmydata<-read.csv("Historic tibia.csv", header=TRUE, stringsAsFactors = FALSE)

Tmydata

Tspecimen<- as.matrix(Tmydata[,1])

Ttimebin<- as.factor(Tmydata[,2])

Tcoords<- as.matrix(Tmydata[, -c(1:2)])


#Convert coordinates to array

Tp<- ncol(Tcoords)/3

Tn<- length(Tspecimen)

Tk<- 3

Tland<- arrayspecs(Tcoords, Tp, Tk)

dim(Tland)

dimnames(Tland)[[3]]

dimnames(Tland)[[3]]<- rownames(Tmydata)

plotAllSpecimens(Tland, mean=FALSE) #plots raw landmarks
```

```
#plot PCA

Tibia.gpa<- gpagen(Tland) #GPA alignment

TibiaPCA<-plotTangentSpace(Tibia.gpa$coords, groups=Ttimebin, label = TRUE)

summary(TibiaPCA)

TibiaPCA23<- plotTangentSpace(Tibia.gpa$coords, groups=Ttimebin, axis1=2, axis2=3,
label=TRUE)

TibiaPCA34<- plotTangentSpace(Tibia.gpa$coords, groups=Ttimebin, axis1=3, axis2=4,
label=TRUE)

TibiaPCA45<- plotTangentSpace(Tibia.gpa$coords, groups=Ttimebin, axis1=4, axis2=5,
label=TRUE)

TibiaPCscore<-TibiaPCA$pc.scores

TibiaPCscore


#writes as a space deliminated file for PAST

write.table(TibiaPCscore, file="Tibia time PC")


##########################################################################
#############

#Fibula

FImydata<-read.csv("Historic fibula.csv", header=TRUE, stringsAsFactors = FALSE)

FImydata

FIspecimen<- as.matrix(FImydata[,1])

FItimebin<- as.factor(FImydata[,2])

FIcoords<- as.matrix(FImydata[, -c(1:2)])


#Convert coordinates to array

FIp<- ncol(FIcoords)/3
```

```
FIn<- length(FIspecimen)

FIk<- 3

FIland<- arrayspecs(FIcoords, FIp, FIk)

dim(FIland)

dimnames(FIland)[[3]]

dimnames(FIland)[[3]]<- rownames(FImydata)

plotAllSpecimens(FIland, mean=FALSE) #plots raw landmarks


#plot PCA

Fibula.gpa<- gpagen(FIland) #GPA alignment

FibulaPCA<-plotTangentSpace(Fibula.gpa$coords, groups=FItimebin, label = TRUE)

summary(FibulaPCA)

FibulaPCA23<- plotTangentSpace(Fibula.gpa$coords, groups=FItimebin, axis1=2,
axis2=3, label=TRUE)

FibulaPCA34<- plotTangentSpace(Fibula.gpa$coords, groups=FItimebin, axis1=3,
axis2=4, label=TRUE)

FibulaPCA45<- plotTangentSpace(Fibula.gpa$coords, groups=FItimebin, axis1=4,
axis2=5, label=TRUE)

FibulaPCscore<-FibulaPCA$pc.scores

FibulaPCscore


#writes as a space deliminated file for PAST

write.table(FibulaPCscore, file="Fibula time PC")
```

G R Code for Multivariate Phylogenetic Signal and Evolutionary Tempo Analyses

```
setwd("")#user inputs working directory


#Load required packages
install.packages("geomorph", dependecies=TRUE)
install.packages("geiger", dependencies=TRUE)
library(geomorph)
library(geiger)



#Load phylogeny
tree<-read.tree("historic tree.phy")
plot(tree, cex=0.6)



##########################################################################
######

######################### Humerus Analysis
#####################################

Humerusdata<-read.csv("AK time humerus code.csv", header=TRUE, stringsAsFactors =
FALSE, row.names=1)
Humerusdata
Hlandmarks<-as.matrix(Humerusdata[,-c(1)])
Htime<-Humerusdata[,1, drop=FALSE]


#Match tip labels to data
tdH<-treedata(tree,Hlandmarks, sort=TRUE)
Hdata<-tdH$data
```

```
Htree<-tdH$phy

#Match tip labels of time to data
tdHT<-treedata(Htree,Htime, sort=TRUE)
Htimedata<-tdHT$data
Htimetree<-tdHT$phy
Htimef<-as.factor(Htimedata)



#align landmarks
Hcoords<- as.matrix(Hdata, drop=FALSE)
Hp<- ncol(Hcoords)/3
Hn<- length(Hdata)
Hk<- 3
Hland<- arrayspecs(Hcoords, Hp, Hk)
Hgpa<-gpagen(Hland)
HGPAcoords<-Hgpa$coords

Hcentroid<-Hgpa$Csize

####Phylogenetic Signal
#multivariate K test
HPS.shape <- physignal(A=Hgpa$coords,phy=Htree,iter=999)
summary(HPS.shape)
plot(HPS.shape)
```

```
####Evolutionary Rates Between the 2 times

names(Htimef)<-dimnames(HGPAcoords)[[3]]

Htimefa<-as.factor(Htimef)

Hrates<-compare.evol.rates(phy=Htree, A=HGPAcoords, gp=Htimefa, iter=999,
method="permutation")

summary(Hrates)



##########################################################################
######

######################### Radius Analysis
########################################

Radiusdata<-read.csv("AK time radius code.csv", header=TRUE, stringsAsFactors =
FALSE, row.names=1)

Radiusdata

Rlandmarks<-as.matrix(Radiusdata[,-c(1)])

Rtime<-Radiusdata[,1, drop=FALSE]


#Match tip labels to data

tdR<-treedata(tree,Rlandmarks, sort=TRUE)

Rdata<-tdR$data

Rtree<-tdR$phy


#Match tip labels of time to data

tdRT<-treedata(Rtree,Rtime, sort=TRUE)

Rtimedata<-tdRT$data

Rtimetree<-tdRT$phy

Rtimef<-as.factor(Rtimedata)
```

```
#align landmarks

Rcoords<- as.matrix(Rdata, drop=FALSE)

Rp<- ncol(Rcoords)/3

Rn<- length(Rdata)

Rk<- 3

Rland<- arrayspecs(Rcoords, Rp, Rk)

Rgpa<-gpagen(Rland)

RGPAcoords<-Rgpa$coords


Rcentroid<-Rgpa$Csize


####Phylogenetic Signal

#multivariate K test

RPS.shape <- physignal(A=Rgpa$coords,phy=Rtree,iter=999)

summary(RPS.shape)

plot(RPS.shape)


####Evolutionary Rates Between the 2 times

names(Rtimef)<-dimnames(RGPAcoords)[[3]]

Rtimefa<-as.factor(Rtimef)

Rrates<-compare.evol.rates(phy=Rtree, A=RGPAcoords, gp=Rtimefa, iter=999,
method="permutation")

summary(Rrates)
```

```
#########################################################################
######

########################## Ulna Analysis
########################################

Ulnadata<-read.csv("AK time ulna code.csv", header=TRUE, stringsAsFactors =
FALSE, row.names=1)

Ulnadata

Ulandmarks<-as.matrix(Ulnadata[,-c(1)])

Utime<-Ulnadata[,1, drop=FALSE]


#Match tip labels to data

tdU<-treedata(tree,Ulandmarks, sort=TRUE)

Udata<-tdU$data

Utree<-tdU$phy


#Match tip labels of time to data

tdUT<-treedata(Utree,Utime, sort=TRUE)

Utimedata<-tdUT$data

Utimetree<-tdUT$phy

Utimef<-as.factor(Utimedata)



#align landmarks

Ucoords<- as.matrix(Udata, drop=FALSE)

Up<- ncol(Ucoords)/3

Un<- length(Udata)

Uk<- 3

Uland<- arrayspecs(Ucoords, Up, Uk)
```

```
Ugpa<-gpagen(Uland)

UGPAcoords<-Ugpa$coords


Ucentroid<-Ugpa$Csize


####Phylogenetic Signal

#multivariate K test

UPS.shape <- physignal(A=Ugpa$coords,phy=Utree,iter=999)

summary(UPS.shape)

plot(UPS.shape)


####Evolutionary Rates Between the 2 time

names(Utimef)<-dimnames(UGPAcoords)[[3]]

Utimefa<-as.factor(Utimef)

Urates<-compare.evol.rates(phy=Utree, A=UGPAcoords, gp=Utimefa, iter=999,
method="permutation")

summary(Urates)



##########################################################################
######

########################## Femur Analysis
#########################################

Femurdata<-read.csv("AK time femur code.csv", header=TRUE, stringsAsFactors =
FALSE, row.names=1)

Femurdata

FElandmarks<-as.matrix(Femurdata[,-c(1)])

FEtime<-Femurdata[,1, drop=FALSE]
```

```
#Match tip labels to data
tdFE<-treedata(tree,FElandmarks, sort=TRUE)
FEdata<-tdFE$data
FEtree<-tdFE$phy

#Match tip labels of time to data
tdFET<-treedata(FEtree,FEtime, sort=TRUE)
FEtimedata<-tdFET$data
FEtimetree<-tdFET$phy
FEtimef<-as.factor(FEtimedata)

#align landmarks
FEcoords<- as.matrix(FEdata, drop=FALSE)
FEp<- ncol(FEcoords)/3
FEn<- length(FEdata)
FEk<- 3
FEland<- arrayspecs(FEcoords, FEp, FEk)
FEgpa<-gpagen(FEland)
FEGPAcoords<-FEgpa$coords

FEcentroid<-FEgpa$Csize

####Phylogenetic Signal
#multivariate K test
FEPS.shape <- physignal(A=FEgpa$coords,phy=FEtree,iter=999)
```

```
summary(FEPS.shape)

plot(FEPS.shape)


####Evolutionary Rates Between the 2 times

names(FEtimef)<-dimnames(FEGPAcoords)[[3]]

FEtimefa<-as.factor(FEtimef)

FErates<-compare.evol.rates(phy=FEtree, A=FEGPAcoords, gp=FEtimefa, iter=999,
method="permutation")

summary(FErates)



##########################################################################
######

######################### Tibia Analysis
########################################

Tibiadata<-read.csv("AK time tibia code.csv", header=TRUE, stringsAsFactors =
FALSE, row.names=1)

Tibiadata

Tlandmarks<-as.matrix(Tibiadata[,-c(1)])

Ttime<-Tibiadata[,1, drop=FALSE]


#Match tip labels to data

tdT<-treedata(tree,Tlandmarks, sort=TRUE)

Tdata<-tdT$data[-c(14),]

Ttree<-tdU$phy

Ttree<-drop.tip(Ttree, "USB3")
```

```
#Match tip labels of time to data
tdTT<-treedata(Ttree,Ttime, sort=TRUE)
Ttimedata<-tdTT$data
Ttimetree<-tdTT$phy
Ttimef<-as.factor(Ttimedata)


#align landmarks
Tcoords<- as.matrix(Tdata, drop=FALSE)
Tp<- ncol(Tcoords)/3
Tn<- length(Tdata)
Tk<- 3
Tland<- arrayspecs(Tcoords, Tp, Tk)
Tgpa<-gpagen(Tland)
TGPAcoords<-Tgpa$coords

Tcentroid<-Tgpa$Csize

####Phylogenetic Signal
#multivariate K test
TPS.shape <- physignal(A=Tgpa$coords,phy=Ttree,iter=999)
summary(TPS.shape)
plot(TPS.shape)

####Evolutionary Rates Between the 2 times
names(Ttimef)<-dimnames(TGPAcoords)[[3]]
```

```
Ttimefa<-as.factor(Ttimef)

Trates<-compare.evol.rates(phy=Ttree, A=TGPAcoords, gp=Ttimefa, iter=999,
method="permutation")

summary(Trates)
```

```
##########################################################################
######

########################## Fibula Analysis
#########################################

Fibuladata<-read.csv("AK time fibula code.csv", header=TRUE, stringsAsFactors =
FALSE, row.names=1)

Fibuladata

FIlandmarks<-as.matrix(Fibuladata[,-c(1)])

FItime<-Fibuladata[,1, drop=FALSE]


#Match tip labels to data

tdFI<-treedata(tree,FIlandmarks, sort=TRUE)

FIdata<-tdFI$data

FItree<-tdFI$phy


#Match tip labels of biome to data

tdFIT<-treedata(FItree,FItime, sort=TRUE)

FItimedata<-tdFIT$data

FItimetree<-tdFIT$phy

FItimef<-as.factor(FItimedata)
```

```
#align landmarks

FIcoords<- as.matrix(FIdata, drop=FALSE)

FIp<- ncol(FIcoords)/3

FIn<- length(FIdata)

FIk<- 3

FIland<- arrayspecs(FIcoords, FIp, FIk)

FIgpa<-gpagen(FIland)

FIGPAcoords<-FIgpa$coords


FIcentroid<-FIgpa$Csize


####Phylogenetic Signal

#multivariate K test

FIPS.shape <- physignal(A=FIgpa$coords,phy=FItree,iter=999)

summary(FIPS.shape)

plot(FIPS.shape)


####Evolutionary Rates Between the 2 times

names(FItimef)<-dimnames(FIGPAcoords)[[3]]

FItimefa<-as.factor(FItimef)

FIrates<-compare.evol.rates(phy=FItree, A=FIGPAcoords, gp=FItimefa, iter=999,
method="permutation")

summary(FIrates)
```

H R Code for Univariate Phylogenetic Signal Analysis

```
setwd("")#User enters working directory


install.packages("geiger",dependencies=TRUE )
```

```
install.packages("phytools",dependencies=TRUE )

library(geiger)
library(phytools)

#Load Phylogeny
tree<-read.tree("historic tree.phy")
plot(tree, cex=0.6)

#Load Data

#input limb proportions data
mydata<-read.csv("historic all bone centroid.csv", header=TRUE, row.names= 1)
mydata
humerus<-as.matrix(mydata[,1, drop=FALSE])
radius<-as.matrix(mydata[-c(18,20,22),2, drop=FALSE])
ulna<-as.matrix(mydata[-c(18,20,22),3, drop=FALSE])
femur<-as.matrix(mydata[,4, drop=FALSE])
tibia<-as.matrix(mydata[-c(25),5, drop=FALSE])
fibula<-as.matrix(mydata[-c(25),6, drop=FALSE])



#Convert to data frame
humerusdata<-as.data.frame(humerus)
radiusdata<-as.data.frame(radius)
```

```
ulnadata<-as.data.frame(ulna)

femurdata<-as.data.frame(femur)

tibiadata<-as.data.frame(tibia)

fibuladata<-as.data.frame(fibula)


#############################################################################

##########################Phylogenetic
Signal##############################

####Humerus####

#Match tip labels to data

tdHU<-treedata(tree,humerusdata, sort=FALSE)

dataHU<-tdHU$data

treeHU<-tdHU$phy


phylosig(treeHU, dataHU, method="K", test=TRUE, nsim=999)

phylosig(treeHU, dataHU, method="lambda", test=FALSE)


####Radius####

#Match tip labels to data

tdRA<-treedata(tree,radiusdata, sort=FALSE)

dataRA<-tdRA$data

treeRA<-tdRA$phy


phylosig(treeRA, dataRA, method="K", test=TRUE, nsim=999)

phylosig(treeRA, dataRA, method="lambda", test=FALSE)


####Ulna####
```

```
#Match tip labels to data
tdUL<-treedata(tree,ulnadata, sort=FALSE)
dataUL<-tdUL$data
treeUL<-tdUL$phy

phylosig(treeUL, dataUL, method="K", test=TRUE, nsim=999)
phylosig(treeUL, dataUL, method="lambda", test=FALSE)

####Femur####
#Match tip labels to data
tdFE<-treedata(tree,femurdata, sort=FALSE)
dataFE<-tdFE$data
treeFE<-tdFE$phy

phylosig(treeFE, dataFE, method="K", test=TRUE, nsim=999)
phylosig(treeFE, dataFE, method="lambda", test=FALSE)

####Tibia####
#Match tip labels to data
tdTI<-treedata(tree,tibiadata, sort=FALSE)
dataTI<-tdTI$data
treeTI<-tdTI$phy

phylosig(treeTI, dataTI, method="K", test=TRUE, nsim=999)
phylosig(treeTI, dataTI, method="lambda", test=FALSE)
```

```
####Fibula####

#Match tip labels to data

tdFI<-treedata(tree,fibuladata, sort=FALSE)

dataFI<-tdFI$data

treeFI<-tdFI$phy


phylosig(treeFI, dataFI, method="K", test=TRUE, nsim=999)

phylosig(treeFI, dataFI, method="lambda", test=FALSE)
```

Appendix VI: DNA Extraction and Concentration Quantification Protocol

Introduction

The protocol outlined below was used to extract DNA from both modern and historic (<150 years) samples. The methods differ for soft tissue and bone extractions and are separated, therefore, into two protocols.

Soft Tissue DNA Extraction

Materials

Reagents: All reagents and plastic consumables must be sterile (DNA and DNase free) and be of molecular biology grade or equivalent.

1. DNA lysis buffer (see Note 1)
    a. Sigma-Aldrich® 50 mM Tris-Cl, pH 8
    b. Sigma-Aldrich® 20 mM ethylenediaminetetraacetic acid (EDTA), pH 8
    c. Sigma-Aldrich® 2% sodium dodecyl sulfate (SDS)
2. Sigma-Aldrich® 3 M sodium acetate (NaOAc) (see Note 2)
3. ThermoScientific™ Proteinase K 20 mg/ml (see Note 3) from 25 mg/ml stock
4. ThermoScientific™ RNase A 1 mg/ml (see Note 4) from 10 mg/ml stock
5. Sigma-Aldrich® 5 mM dithiothreitol (DTT) (see Note 5)
6. Sigma-Aldrich® Phenol:chloroform:isoamyl 25:24:1 (PCI)
7. Sigma-Aldrich® Chloroform :isoamyl 24:1 (CI) equilibrated
8. 100% ethanol (EtOH)
9. DI H_2O

Methods

All extraction steps in this protocol should be conducted in a DNA clean room and gloves should be worn at all times. The protocol can be carried out at room temperature unless specified below. Steps 8-22 must be conducted in a fume hood.

1. Prior to DNA extraction mix DNA lysis buffer stock concentrations (see Note 1) following the protocol of Bello et al. (2001) (see Note 1).
2. Weigh approximately 25 mg of soft tissue per sample.
3. Place tissue in a labeled 2 ml capped tube and add 125 µl lysis buffer, 8.75 µl Proteinase K (20mg/ml), 5 µl RNase A (1mg/ml) (see Note 7), and 10 µl DTT (5mM).
4. Vortex each vial at speed 6 for 10 s.
5. Parafilm the lids of each 2 ml tube to prevent leaking.
6. Place tubes in an oven on a tube rotator (see Note 6) for 24 hours at 55°C.
7. After incubation, vortex each tube at speed 6 to ensure all tissue is degraded.
8. Place 125 µl of PCI into each 2 ml tube.

9. Vortex each tube at speed 6 for 10 s then centrifuge at 13,000 rpm for 5 min.
10. Remove the top aqueous layer (see Note 8) and place in a new 0.5 ml capped tube.
11. Repeat steps 8-10.
12. In the new 0.5 ml tube place 125 µl CI.
13. Vortex each tube at speed 6 for 10 s then centrifuge at 13,000 rpm for 3 min.
14. Remove the top aqueous layer (see Note 8) and place in a new 2 ml capped tube.
15. Add 12.5 µl 3 M NaOAc and 250 µl 100% EtOH.
16. Vortex each tube at speed 6 for 10 s and centrifuge at 13,000 rpm for 10 min to pellet the DNA.
17. Discard the supernatant (see Note 9).
18. Add 250 µl 70% EtOH.
19. Let sit for 30 s then discard the supernatant (see Note 9).
20. Repeat steps 18-19.
21. Leave lid open and let air dry for 20-30 min.
22. Elute each sample with 30 µl 10mM Tris-Cl, pH 8 or enough to reach a DNA concentration below 30 ng/µl (see Note 10).
23. Store DNA extracts in 2 ml tubes in a -20°C freezer.

Notes

1. Below is the protocol for making the stock concentrations of each lysis buffer reagent. 100 ml working stocks were then created by diluting stock concentrations with DI H_2O. All reagents can be mixed and stored at room temperature. I autoclaved each stock reagent.
    a. 50 mM Tris-Cl, pH 8
        i. In 500 ml flask add 7.57 g of Sigma-Aldrich® Trizma base and 125 ml of DI H_2O with a stir bar.
        ii. Once in solution, bring to 250 ml with DI H_2O
        iii. Bring pH to 8 by adding drops of HCl and measuring with a pH meter.
    b. 20 mM EDTA, pH 8
        i. In a 500 ml flask add 18.612 g of Sigma-Aldrich® EDTA powder and 250 ml of DI H_2O with a stir bar.
        ii. Bring pH to 8 by gradually adding NaOH pellets. Here 4.5 g of NaOH pellets were required.
        iii. Note the powder will not go into solution until the pH is 8.
    c. 2% SDS
        i. In a 250 ml flask, add 2 g of Sigma-Aldrich® SDS and 100 ml of DI H_2O with a stir bar.
        ii. Heat mixture on a medium heat setting until the powder is in solution.
        iii. When measuring the SDS it is recommended that a mask is worn, because the powder is light and can easily be inhaled.
2. 3 M NaOAc
    a. In 150 ml flask, add 40.824 g of Sigma-Aldrich® sodium acetate and 40 ml of DI H_2O with a stir bar.
    b. Once in solution, bring to 100 ml with DI H_2O
3. Proteinase K 20 mg/ml

    a. In a 2 ml capped tube place 800 µl of 25 mg/ml ThermoScientific™ Proteinase K stock and dilute with 200 µl DI H_2O.
    b. This will provide enough working stock for 8 extractions and should be made fresh each time to prevent de-activation of the Proteinase K.
4. RNase A 1 mg/ml
    a. In a 2 ml capped tube place 100 µl of 10 mg/ml ThermoScientific™ RNase A stock and dilute with 900 µl DI H_2O.
    b. This will provide enough working stock for 200 extractions
5. 5 mM DTT
    a. In a 250 ml flask add 0.07 g of Sigma-Aldrich® DTT powder and 100 ml of DI H_2O with a stir bar.
    b. From this stock, allocate 100 µl working stock.
6. RNase A must be kept on ice when working with other reagents.
7. Here a Fisher Scientific™ Isotemp incubator with rotisserie was used. The chosen tube rotator should allow tubes to invert completely. This allows the contents to mix thoroughly.
8. When removing top aqueous layer be sure to place pipette tip only in this top layer. Breaking the surface of the lower layer will contaminate the sample with partially digested tissue and molecules other than DNA.
9. When discarding the supernatant simply pour out contents of the tube.
10. If soft tissue is of good quality, DNA concentrations are often high (>200 ng/µl). In this case, first dilute with 30 µl 10mM Tris-Cl, pH 8, determine DNA concentration, then elute with an additional 250 µl 10mM Tris-Cl, pH 8.
11. Store 2 ml tubes with DNA extracts in -20°F freezer. Samples can be stored in -20°F freezer for duration of experiment (approximately 1 year), but long term storage should be in a -80°F freezer.

Bone Tissue DNA Extraction

Materials

Reagents: All reagents and plastic consumables must be sterile (DNA and DNase free) and be of molecular biology grade or equivalent. All can be mixed at room temperature.

1. 2-4% bleach
2. 50% bleach
3. 18 megaOhms (MΩ) H_2O from a Milli-Q Reference Water Purification System
4. Fisher Scientific Alconon™ Liquinox™ detergent
5. 100% EtOH
6. Liquid nitrogen
7. DNA lysis buffer (see Note 1)
    a. Sigma-Aldrich® 0.45 M EDTA, pH 8

    b. ThermoScientific™ Proteinase K 20mg/ml from 25 mg/ml stock
8. DNA binding buffer (see Note 2)
    a. Sigma-Aldrich® 6 M guanidine thiocyanate (GuSCN)
    b. Sigma-Aldrich® 300 µM NaOAc
9. DNA wash buffer
    a. 80% EtOH
10. DNA elution buffer (see Note 3)
    a. Sigma-Aldrich® 10 mM Tris
    b. Sigma-Aldrich® 0.1 mM EDTA, pH 8

Supplies:

1. Sterile weigh boats (sterilized using below protocol)
2. SPEX SamplePrep Small Grinding Vial Set (stainless steel impactor, end plug, polycarbonate center cylinder 6751C4)
3. Fisherbrand™ General-Purpose Extra-Long Forceps
4. Tin foil cut in 2x2 in squares (1 per sample)

All tools must be sterilized before use and between samples using the following protocol:

1. Wash in 2% Liquinox™ detergent and DI H_2O solution.
2. Sonicate in a 50% bleach solution for 5 min.
3. Soak in EtOH.
4. Place in oven (see Note 4) at 65°C until dry, approximately 15 min.

Methods

All bone extractions should be conducted in an aDNA clean room. Gloves, masks, hairnets, and HAZMAT suits should be worn during each step to prevent contamination. Extractions can be conducted at room temperature.

Bone powdering

1. Weigh 50 mg bone tissue per sample.
2. Place samples in a 5-15 ml lidded tube in a solution of 2-4% bleach and 18 MΩ water (see Note 5).
3. Vortex each tube at speed 6 for 10 s.
4. Allow samples to soak for 20 min.
5. Pour out bleach solution from each tube and rinse immediately with 18MΩ water. Repeat rinse steps until no bubbles remain.
6. Place each sample in a sterile weigh boat and allow to dry in a fume hood overnight (see Note 6).
7. Place dry samples in the SPEX SamplePrep Small Grinding Vial and insert a metal impactor.

8. Place impactor vials in a 6775 Freezer/Mill ® SPEX SamplePrep and program cycle: 5 min precool, 1-2 min grind, 15 impacts/s.
9. Once cycle is complete, place the impactor vials in an oven (see Note 4) at 65°C until defrosted and powder inside is dry.
10. Remove powder from the impactor vial in a 2 ml capped tube.
11. Reweigh all samples to ensure approximately 50 mg of bone tissue was retained. If less than 50 mg is retained, the reagent quantities in the below protocol must be modified accordingly.

Binding extraction protocol modified from Rohland (2012)

1. Prior to DNA extraction mix DNA lysis buffer (1:20 0.45 M EDTA and Proteinase K 20 mg/ml), DNA binding buffer (1:1 6 M GuSCN and 300 µM NaOAc), DNA wash buffer (4.7:1 100% EtOH and DI H_2O), and DNA elution buffer (1:1 10 mM Tris and 0.1 mM EDTA, pH 8).
2. In each 2 ml tube, containing samples place 1 ml of lysis buffer.
3. Parafilm each cap to prevent leaking.
4. Place tubes in an incubator on a tube rotator (see Note 7) for 24 hours at 56°C.
5. Centrifuge 2 ml tubes containing samples and lysis buffer at 13,000 rpm for 5 min.
6. Pour off contents of the supernatant into 15 ml tubes with 7 ml of binding buffer (see Note 8).
7. Place lids on 15 ml tubes tightly and parafilm to prevent leaking.
8. Wrap 15 ml tubes in foil to prevent light exposure (see Note 9).
9. Place 15 ml tubes on a nutator for 3 hours (see Note 10).
10. Connect disposable plastic funnel to a 2 ml spin column.
11. In a 50 ml tube place 5 ml of binding buffer (see Note 11).
12. Place the connected funnel and spin column in the 50 ml tube.
13. Pour the contents of the 15 ml tubes into the funnel, then cover the top with parafilm.
14. Centrifuge the 50 ml tubes at 30,000 rpm for 5 min (see Note 12).
15. Remove the spin columns and place in capless 2 ml tubes.
16. Wash each sample with 300 µl of wash buffer.
17. Centrifuge spin columns within the 2 ml tubes at 9,449 rpm for 30 s.
18. Pour out wash buffer in the 2 ml tube.
19. Repeat steps 20-22.
20. Place spin columns in a new capped 2 ml tube.
21. Elute samples with 40-65 µl of elution buffer (see Note 13) and allow to incubate at room temperature for 5 min.
22. Centrifuge at 12,000 rpm for 30 s.
12. Discard spin columns and store 2 ml tubes with DNA extracts in -20°F freezer. Samples can be stored in -20°F freezer for duration of experiment (approximately 1 year), but long term storage should be in a -80°F freezer.

Notes

1. DNA lysis buffer
    a. 0.45 M EDTA, pH 8
        i. In a 1 L flask add 83 g of Sigma-Aldrich® EDTA powder and 500 ml of DI H_2O with a stir bar.

ii. Bring pH to 8 by gradually adding NaOH pellets. Here 9 g of NaOH pellets were required.
iii. Note the powder will not go into solution until the pH is 8.

b. Proteinase K 20 mg/ml
i. In a 2 ml capped tube place 400 µl of 25 mg/ml ThermoScientific™ Proteinase K stock and dilute with 100 µl DI H_2O.
ii. This will provide enough working stock for 8 extractions and should be made fresh each time to prevent de-activation of the Proteinase K.

2. DNA binding buffer
   a. 6 M GuSCN
      i. In a 1 L flask, add 70.896 g of Sigma-Aldrich® GuSCN and 500 ml of DI H_2O.
   b. 300 µM NaOAc
      i. In a 150 ml flask, add 4 mg of Sigma-Aldrich® NaOAc and 40 ml of DI H_2O.
      ii. Once in solution, bring to 100 ml with DI H_2O
3. DNA elution buffer
   a. 10 mM Tris
      i. In a 15 ml capped tube, add 0.012 g of Sigma-Aldrich® Trizma base and 5 ml of DI H_2O with a stir bar.
      ii. Once in solution, bring to 100 ml with DI H_2O
   b. 0.1 mM EDTA, pH 8
      i. In a 150 ml flask add 3.72 g of Sigma-Aldrich® EDTA powder and 100 ml of DI H_2O with a stir bar.
      ii. Bring pH to 8 by gradually adding NaOH pellets. Here 1.8 g of NaOH pellets were required.
      iii. Note the powder will not go into solution until the pH is 8.
   c. Must be kept warm at 86°C
4. Here a ThermoScientific™ gravity convection oven was used, but any convection oven would be sufficient.
5. Place enough solution in each tube to entirely cover the specimen.
6. It is imperative the samples are dry prior to powdering or tissue will cake the inside of the impactor vial.
7. The incubator used here was a ThermoScientific™ compact incubator. The chosen tube rotator should allow tubes to invert completely. This allows the contents to mix thoroughly. Here a Boekel mini tube rotator was used.
8. When discarding the supernatant simply pour out contents of the tube.
9. Binding buffer must be kept in dark to prevent destabilization (Rohland, 2012; Rohland and Hofreiter, 2007).
10. The time left on the nutator is dependent on the quality of the samples. For historic and ancient bone 3 hours is sufficient.
11. This additional binding buffer prevents loss of sample in case the spin column detaches.
12. Gradually increase the speed of the centrifuge to prevent the spin columns from detaching.
13. The amount of elution buffer used will depend on the quality of DNA. Samples are first diluted with 40 µl 10mM Tris, and 0.1 mM EDTA, determine DNA

concentration, then if samples are greater than 30ng/µl elute with an additional 15µl of buffer.

DNA Concentration

Introduction

The protocol outlined below was used to measure the concentration of DNA in samples extracted from modern and historic (<150 years) tissue and from bone and soft tissue. It can also be applied to ancient bone samples. This protocol is specific to the ThermoFisher™ Qubit® Fluorometer.

Materials

Reagents: Reagents can be mixed at room temperature, however storage conditions vary by reagent. These are noted below.

1. Qubit® dsDNA HS Assay Kit
    a. Reagent
        i. Store at room temperature protected from light
    b. Buffer
        i. Store at room temperature
    c. Standard 1
        i. Store at -4°C
    d. Standard 2
        i. Store at -4°C

Supplies:

1. 0.5 ml thin-walled PCR tubes (see Note 1)
    a. Qubit® assay tubes

Methods

All extraction steps in this protocol should be conducted in a DNA clean room and gloves should be worn at all times. The protocol can be carried out at room temperature

1. Create master mix of 199 µl buffer plus 1 µl reagent per specimen plus an additional two samples which will act as calibration standards.
2. Place 195 µl of master mix into each sample assay tube plus the two standard assay tubes.

3. Add 5 µl DNA to each sample assay tube and 10 µl of standard 1 to an assay tube and 10 µl of standard 2 to another assay tube.
4. Allow samples and standards to incubate at room temperature for 2 min.
5. Vortex for 10 s at speed of 4.
6. Calibrate the Qubit® using standards 1 and 2. First select the desired assay, here I chose high sensitivity in case any of the extractions contain degraded DNA. The press read standard and insert standard 1. Once read, repeat with standard 2. When calibration is complete a Fluorescence vs. Concentration graph will appear.
7. Press run samples then select the sample volume. Here 5 µl of sample was used. Next chose an output of ng/µl.
8. Press read tube and continue until all samples are read.

Notes

1. Only thin-wall, clear 0.5-mL PCR tubes can be used in the Qubit® 3.0 Fluorometer. Other PCR tubes will prevent the Qubit® from detecting the fluorescent reagent.

References

Bello N, Francino O, Sánchez A. 2001. Isolation of genomic DNA from feathers. Journal of Veterinary Diagnostic Investigation 13(2):162-164.

Rohland N. 2012. DNA Extraction of Ancient Animal Hard Tissue Samples via Adsorption to Silica Particles. In: Shapiro B, Hofreiter M, editors. Ancient DNA Methods and Protocols. New York: Humana Press, Springer. p 21-28.

Rohland N, Hofreiter M. 2007. Ancient DNA extraction from bones and teeth. Nature Protocols 2(7):1756-1762.

Appendix VII: Simplex PCR Amplification of DNA Protocol

Introduction

The protocol outlined below was used for both modern and historic (<150 years) samples, although it can also be applied to ancient DNA. This protocol is appropriate for DNA extracted from either bone or soft tissue.

Materials

Reagents — All reagents and plastic consumables must be sterile (DNA and DNase free) and of molecular biology grade or equivalent.

1. Apex™ dNTPs of 100 mM combined and diluted in DNA free H_2O to yield a dNTP mix of 2.5 mM each dATP, dGTP, dTTP, and dCTP (see Note 1)
2. DNA polymerase and 10 X buffer (see Note 2)
3. 50 mM $MgCl_2$ (see Note 2)
4. Promega 10 mg/ml BSA
5. 100 µM stock concentration of forward and reverse primer (Table 1)
6. DNA free H_2O
7. 1X TBE buffer (see Note 3)
    a. Apex™ Tris
    b. Gentrox Boric acid
    c. Apex™ EDTA salt
8. 2% agarose gel (see Note 4)
    a. Apex™ general purpose LE agarose
    b. 1X TBE buffer
9. 6X loading dye (see Note 5)
    a. Sigma-Aldrich® molecular grade glycerol
    b. Apex™ 0.5M EDTA
    c. Fisher Scientific™ bromophenol blue
10. Apex™ low DNA 100 bp ladder
11. Apex™ 0.625 m/ml biotechnology grade Ethidium bromide (EtBr)

Methods

Primer Design

1. The DNA quality of each sample will differ such that the genes of some specimens can be amplified >1,000 bp per reaction while others will have to be amplified in fragments <300 bp.
2. Design a series of overlapping primers whose annealing temperatures do not vary by more than 3°C. This will allow primer sets to be combined when targeting larger amplicons.
3. Design primer sets that target between 100-300 bp and that overlap by 30-50 bp with the next set.
4. Design primers with >60% GC content to increase the likelihood of binding and amplifying the target region.
5. Primers were ordered from Sigma-Aldrich® as 0.025 µM dry custom oligos.

PCR Amplification

All PCR amplification must be conducted in a DNA clean room and can be done at room temperature. Gloves should be worn at all stages.

1. Prepare primers by diluting the 100 µM solutions into a 10 µM working stock.
2. Prepare a PCR master mix that includes all reagents except the DNA as outlined in Table 2. Prepare enough master mix for all samples, a negative control, and extra sample (see Note 6 and Note 7). Order of preparation does not matter, however, taq should be kept on ice during this step.
3. Aliquot 20 µl of the master mix into PCR strip tubes and then close all lids (see Note 8).
4. Add DNA template to each PCR tube individually, opening a single tube at a time. This prevents cross contamination. Fill the negative control last with 2 µl DNA free H_2O instead of DNA template.
5. Cycle PCR reactions as outlined in Table 3 on a Labnet International, Inc. MultiGene Optimax thermocycler. Annealing temperatures vary by primer set and extension times differ depending on the targeted amplicon size (see Note 9).

Agarose Gel Visualization

1. Prepare a 2% agarose gel using 1X TBE buffer. EtBr can be added directly to the gel or after staining (See Note 10). Please note EtBr is a mutagen and should only be handled with gloves within a fume hood.
2. Mix 1.5 µl 6X loading dye with 5 µl of PCR product.
3. Load each dyed product into an individual well, as well as a ladder at the end of each row.
4. Run out samples in an electrophoresis gel chamber for 30 min at 100 V. Here a Galileo bioscience system was used.
5. Image gels using UV light. Here a BioRad Gel Doc XR system was used for all imaging.
6. If bands are the expected length and the negative control is blank, continue to sequence cleaning. If they do not amplify, are faint, or the negative control is contaminated, modify PCR protocol (see Note 11).

Notes

1. Once mixed, dNTPs should be stored at -20°F. These should be mixed in small quantities to avoid excessive freezing and thawing, which results in the degradation of the nucleotides. Here, I allowed for two freeze thaw cycles for each mixture.
2. Both Fisher Scientific™ AmpliTaq Gold™ and Apex™ Taq were used in this protocol. Fisher Scientific™ AmpliTaq Gold™ was used in all reactions where specimens were extracted from bone tissue and DNA was, therefore, degrade. Apex™ Taq was used in all reactions where specimens were extracted from soft tissue.
3. 1X TBE buffer
    a. In a 1 L flask mix 10.8 g Tris, 5.5 g boric acid, and 0.74 g EDTA with a stir bar.
    b. Bring to 1 L with DI H_2O and allow to mix into solution.
    c. Can stored at room temperature.
4. 2% agarose gel

a. For an 80 well 2% agarose gel mix 1 g Apex™ general purpose LE agarose, and 50ml 1X TBE buffer in a 250 ml flask.
b. Cover flask with plastic wrap and poke a few holes in the top.
c. Microwave flask for 2 min on high or until all powder has gone into solution.
d. Use insulated gloves to remove flask from microwave.
e. Allow agarose to cool by sitting at room temperature or by placing in cool water (at this stage EtBr could be added if desired).
f. Once gel is cool to the touch but not solidified pour in sealed gel tray and add combs.
g. Allow to cool until solid and cloudy, then remove combs and place in electrophoresis buffer chamber.
h. Fill electrophoresis buffer chamber with 1X TBE buffer until fluid covers entire surface of the gel. The greater the amount of 1X TBE buffer that covers the gel, the longer samples will need to be run.

5. 6X loading dye
    a. In a 50 ml capped tube mix 12.5 ml Sigma-Aldrich® molecular grade glycerol, 10ml Apex™ 0.5 M EDTA, and 0.12 5g Fisher Scientific™ bromophenol blue.
    b. Bring to 50 ml with DNA free H_2O
    c. Must be stored in a refrigerator.
6. Additional sample accounts for any pipetting error and prevents the last sample from not having enough of the master mix.
7. For all DNA samples extracted from bone, Fisher Scientific™ AmpliTaq Gold buffer II was used in substitution of Apex™ Taq (Table 1). This is because AmpliTaq Gold is more successful in amplifying DNA that is degraded or damaged (Wales et al., 2014), which is often the case in bone samples (Adler et al., 2011). Concentrations of both taqs were equivalent.
8. PCR strip tubes with individual lids or individual PCR tubes work best and prevent cross contamination between samples.
9. When targeting differing amplicon lengths, extension times should be 30 s per 500 bp. Extension time for a 1400 bp amplicon, therefore, should be at least 90 s.
10. Addition of EtBr to agarose gels should be done in a fume hood. If EtBr is placed directly in the gel, it must be added when the gel has begun to cool but prior to it solidifying. This aids in preventing vaporization of the EtBr. Add 1 drop of EtBr for every 50 ml of agarose/TBE. The gel can then be imaged directly after running samples. Unused portions of the gel can be used at a later time, however, the gel should be wrapped in plastic wrap and stored in a labeled, lidded container in a refrigerator. The gel can also be stained with EtBr after samples have been run. For this protocol, place the gel in a lidded container with 1 L of DI H_2O or enough to cover the gel. Add 10 µl of EtBr for every liter of water. Let sit for 30 min before imaging. After imaging, rinse the gel in DI H_2O, removing the EtBr. Unused portions can then be wrapped in plastic wrap and stored in a refrigerator. All stained gels and liquids containing EtBr must be disposed of appropriately as chemical waste.
11. If PCR product does not amplify, rerun protocol with either a lowered annealing temperature, which will make the primers less specific in binding, or increase the extension time, which will allow for amplification of longer amplicons. If bands are faint, modify the PCR protocol by decreasing

annealing temperature or increasing the number of PCR cycles. If the negative control amplifies, test for contamination in reagents or replace all. Amplification in the negative control may also be caused by cross contamination. If all reagents are DNA free, take steps to prevent cross contamination by cleaning hands between samples and using filtered pipette tips.

Table 1. Gene Primer Sequences and Annealing Temperatures

Gene	Primer	Forward Sequence	Reverse Sequence	Annealing Temp C
12S	1	GCCTAGAAGAGTCACAAGAC	CACTGCTGTATCCCGTGG	60
	2	GAGCGGGCATCAGG	CGCCGTGAGCCTATTAATTC	52
	3	CGTGCCAGCCACC	GGCTGGGCATAGTGG	52
	4	CTCCAACAACACGATAGCTG	CGATTACAGAACAGGCTCC	60
	5	GGACTTGGCGGTGC	CATGGCCCTATTCAACTAAGC	58
	6	GGTCAAGGTGTAACCCATG	GGTGTAAGCCAGGTGC	58
16S	1	GCACCTGGCTTACACC	CATCATTCCCTTGCGGTAC	52
	2	CCAACTACCACGACATCC	CATAGGTAGCTCGTCTGG	50
	3	GCTACCTATGAGCAATCCAC	CTAAGCAAGGTTGTTTCCTTG	50
	4	CCTAACGTATCACTGGGC	CAGTGCCTCCAATACTGAG	52
	5	GCACAAGCTTATAACAGTCAACG	GGCCGTTAAACTAATGTCACTG	52
	6	CACAGGCGTGCAGTAAG	GTTAGACCTGGTTGGTGG	52
	7	GACGAGAAGACCCTATGGAG	GATAGCTGCTGCACCATC	54
	8	GACCTCGATGTTGGATCAG	CAATTACTGGGCTCTGCC	54
Dloop	1	CAACAGCCCCGCCATC	GTGRGGTGCACGGATGC	58
	2	CGTGCATTAATGGCTTGCC	GGATTGAGGACTTCCATGGC	58
	3	CGTGTACCTCTTCTCGCTC	GAAGGATAAGCCCAGCTACAAG	58
Cytb	1	CGAYYTACCTGCYCCATC	YAGGAACAGGCAGATGAAG	60
	2	YTCTTCATCTGCCTGTTCCTG	GCGAAGAATCGYGTTAGGGTAG	60
	3	CTGAGGAGGATTCTCGGTAGACAAGG	GGATTAGGAATAGGGCGCCTAGG	60
	4	CTAGGCGCCCTATTCCTAATC	CTGAGTGGGCGGAATATCAT	60
	5	CAATTRTCCCATTVCTYCATAC	RATGGCTGGCATRAGGAYTAG	60

Table 2. PCR Master Mix

Reagent	Volume (µl) per Sample	Final Concentration in Reaction
DNA free H_2O	11.30	1X
10X buffer	2.0	1X
50mM $MgCl_2$	0.8	2.0mM
BSA (20mg/ml)	1.0	1mg/ml
dNTPs (2.5mM each)	1.6	200µM
Forward primer (10 µM)	0.6	0.4µM
Reverse primer (10 µM)	0.6	0.4µM
Taq (5U/µl)	0.1	1.25U
Template (4-30 ng/µl)	2	

Table 3. PCR Cycle

Initial Denaturation	Denature	Anneal	Extension	Final Extension
	Repeat 35 cycles			
95°C	95°C	50-60°C	72°C	72°C
15 min	15 s	30 s	30-90 s	5 min

References

Adler CJ, Haak W, Donlon D, Cooper A. 2011. Survival and recovery of DNA from ancient teeth and bones. Journal of Archaeological Science 38(5):956-964.

Wales N, Andersen K, Cappellini E, Ávila-Arcos MC, Gilbert MTP. 2014. Optimization of DNA recovery and amplification from non-carbonized archaeobotanical remains. PLoS ONE 9(1):e86827.

Appendix VIII: PCR Cleaning and Sanger Sequencing Protocol

Introduction

The protocol outlined below was applied to PCR product amplified from both modern and historic (<150 years) samples and is appropriate for PCR product amplified from either bone or soft tissue extractions.

Materials

Reagents

All reagents and plastic consumables must be sterile (DNA and DNase free) and of molecular biology grade or equivalent.

1. Fisher Scientific™ Exonuclease 200 U/µl
2. Fisher Scientific™ Shrimp Alkaline Phosphate 1 U/µl
3. 1 µM forward and reverse primer (see Appendix # for primer design)
4. Sigma-Aldrich® 5 M Betaine
5. Fisher Scientific™ 5X Big Dye Buffer
6. Fisher Scientific™ Big Dye Terminator v3.1
7. Sigma-Aldrich® Superfine G-50 Sephadex
8. 18 megaOhms (MΩ) H_2O from a Milli-Q Reference Water Purification System

Supplies

1. EdgeBio Optima DTR™ 96-well plate kit (plate lid, waste tray, and collection tray)
2. FoilSeal™Sealing foil for PCR
3. 96 well PCR plate both skirted and non-skirted

Methods

All DNA cleaning and sequencing reactions must be conducted in a DNA clean room and can be done at room temperature. Gloves should be worn at all stages.

ExoSap Cleaning

1. Create master mix of Exonuclease and Shrimp Alkaline Phosphate (1:3) (ExoSap).
2. Aliquot 1-3 µl of ExoSap into PCR strip tubes (See Note 1) and then close all lids.
3. Add PCR product to each PCR tube individually, opening a single tube at a time. This prevents cross contamination.
4. Place samples in a Labnet International, Inc. MultiGene Optimax thermocycler for the cycle outlined in Table 1. Remove from thermocycler once it reaches 15°C.

Sequencing Reaction

1. To ensure adequate volume for both forward and reverse sequencing, as well as pipetting errors, create a sequencing master mix for twice the number of

samples plus one. The master mix consists of 2.55 µl DNA free H_2O, 2.0 µl betaine, 1.5 µl primer, 0.5 µl Big Dye buffer, 0.4 5µl Big Dye.
2. Aliquot 7µl of master mix into each well on a non-skirted PCR plate.
3. Aliquot 3µL ExoSap cleaned product into each well.
4. Cover plate with foil or with a FoilSeal™.
5. Place samples in a Labnet International, Inc. MultiGene Optimax thermocycler for the cycle outlined in Table 2 (see Note 4).

Sephadex Clean-up

1. Mix 3 g of Sephadex beads per 50 ml of 18 MΩ H_2O, ensuring beads are suspended.
2. Pipette 400 µl of Sephadex into the same number of wells as samples in an EdgeBio Optima DTR™ 96-well collection tray.
3. Weigh sample plate. Then fill balancing plate with equal weight of water (see Note 2).
4. Place both plates in centrifuge and spin at 2,500 rpm for 5 min.
5. Pour out waste tray and repeat steps 2-4 (see Note 3).
6. Add 20 µl of DNA free H_2O to the sequencing reactions of each sample and spin at 2,500 rpm for 2 min.
7. Replace catch plate on the EdgeBio Optima DTR™ 96-well plate with a skirted sequencing plate.
8. Add 30 µl of sequencing reaction product to each well containing Sephadex by pipetting directing over the column.
9. Weigh sample plate. Then fill balancing plate with equal weight of water (see Note 2).
10. Place both plates in centrifuge and spin at 2,500 rpm for 5 min.
11. Sample is now ready to be Sanger sequenced. For storage, seal sample with FoilSeal and place in refrigerator (see Note 4).

Notes

1. The amount of ExoSap differs depending on the quality of amplicon. If bands on the agarose gel were smeared or faint, increase the amount of ExoSap.
2. Plates must be within 1g or centrifuge will become unbalanced.
3. Often an additional centrifuge cycle at 2,500 rpm for 5 min is required to remove all remaining water.
4. After completion of sequencing reaction and Sephadex cleaning, samples CANNOT be frozen but should instead be stored in a refrigerator.

Table 1. ExoSap Cycle

37°C	80°C	15°C
15m	15m	∞

Table 2. Sequencing Reaction Cycle

Initial Denaturation	**Denature**	**Anneal**	**Extension**	**Final Extension**
	Repeat 44 cycles			
95°C	95°C	49°C	60°C	30°C
3 min	15 s	15 s	4 min	30 min

VITA

LEIGHA M LYNCH

Candidate for the Degree of

Doctor of Philosophy

Thesis: MITOCHONDRIAL AND SKELETAL LIMB EVOLUTION IN THE NORTH AMERICAN PINE MARTEN, *MARTES*

Major Field: Biomedical Sciences

Biographical:

Education:

Completed the requirements for the Doctor of Philosophy in Biomedical Sciences at Oklahoma State University, Stillwater, Oklahoma in May, 2018.

Completed the requirements for the Master of Science in Geosciences at East Tennessee State University, Johnson City, Tennessee in 2012.

Completed the requirements for the Bachelor of Science in Geology at Bowling Green State University, Bowling Green, Ohio in 2009.

Experience:

Graduate Teaching Assistant for Clinical Anatomy, BIOM 5116, at Oklahoma State University Center for Health Sciences from 2013 to 2016

Adjunct Professor for East Tennessee State University Department of Geosciences from 2012 to 2013.

Camp Manager and Field Assistant for Homestead Quarry through Oklahoma State University Center for Health Sciences in 2014 and 2015.

Field and Lab Assistant for the Gray Fossil Site through East Tennessee State University from 2012 to 2013.

Professional Memberships:

Sigma Xi, Geological Society of America, American Society of Naturalists, Paleontological Society, American Society of Mammalogists, Society for Integrative and Comparative Biology, Society of Vertebrate Paleontology, Don Sundquist Center of Excellence in Paleontology, and Southeastern Association of Vertebrate Paleontology